Posted
Acct
B
Ath

GEORGIA INSTITUTE OF TECHNOLOGY
OFFICE OF RESEARCH ADMINISTRATION

RESEARCH PROJECT INITIATION

Date: February 13, 1975

Project Title: Collaborative Research in Tribology

Project No: E-25-650

Principal Investigator: Dr. W. O. Winer

Sponsor: National Science Foundation

Agreement Period: From 1/1/75 Until 6/30/77

*24 months budget period plus 6 months for submission of required reports, etc.

Type Agreement: Grant No. ENG75-21002

Amount: $116,400 NSF
5,790 GIT (E-25-330)
$122,190 Total

Reports Required:

Annual Letter Technical, Fical Report

Sponsor Contact Person (s):

Administrative Matters
thru ORA
Mr. Gaylord L. Ellis
Grants Officer
National Science Foundation
Washington, D. C. 20550
(202) 632-5965

Assigned to: Mechanical Engineering

COPIES TO:

Principal Investigator	Library
School Director	Rich Electronic Computer Center
Dean of the College	Photographic Laboratory
Director, Research Administration	Project File
Director, Financial Affairs (2)	
Security-Reports-Property Office ✓	
Patent Coordinator	Other

RA-3 (6-71)

GEORGIA INSTITUTE OF TECHNOLOGY
OFFICE OF CONTRACT ADMINISTRATION

SPONSORED PROJECT TERMINATION

Date: May 8, 1978

Project Title: Collaborative Research in Tribology

Project No: E-25-650

Project Director: Dr. W. O. Winer

Sponsor: National Science Foundation

Effective Termination Date: 6/30/77

Clearance of Accounting Charges: 6/30/77

Grant/Contract Closeout Actions Remaining:

_ Final Invoice and Closing Documents
_X_ Final Fiscal Report
_ Final Report of Inventions
_ Govt. Property Inventory & Related Certificate
_ Classified Material Certificate
_ Other _____

Assigned to: Mechanical Engineering (School/Laboratory)

COPIES TO:

Project Director
Division Chief (EES)
School/Laboratory Director
Dean/Director—EES
Accounting Office
Procurement Office
Security Coordinator (OCA) ✓
Reports Coordinator (OCA)
Library, Technical Reports Section
Office of Computing Services
Director, Physical Plant
EES Information Office
Project File (OCA)
Project Code (GTRI)
Other _____

CA—4 (3/76)

E-25-650

COLLABORATIVE RESEARCH IN TRIBOLOGY

Sponsored by the National Science Foundation

ncipal Investigators

rbert S. Cheng
Northwestern University

ederick F. Ling
Rensselaer Polytechnic Institute

rd O. Winer
Georgia Institute of Technology

dustrial Advisory Board

bert L. Johnson, Chairman
NASA Lewis Research Center
Cleveland, Ohio 44135
216–433-4000, Ext. 464

bert L. Adamczak
Plans Office
AFWAL/XR
Wright-Patterson Air Force Base
Ohio 45433
513–255-3494

chard S. Fein
Texaco Research Center
P.O. Box 509
Beacon, New York 12508
914–831-3400

nald F. Hays
Engineering Mechanics Department
General Motors Corporation
12 Mile and Mound Roads
Warren, Michigan 48090
313–575-2927

uce W. Kelley
Caterpillar Tractor Company
Technical Center
Peoria, Illinois 61602
309–578-6620

orge H. Kitchen
Bell Telephone Laboratories, Inc.
Murray Hill, New Jersey 07974
201–582-2410

lter E. Littmann
The Timken Company
1835 Dueber Avenue, SW
Canton, Ohio 44706
216–453-4511, Ext. 305

n E. Mayer, Jr.
Scientific Research Staff
Ford Motor Company
P.O. Box 2053
Dearborn, Michigan 48120
313–322-9447

nton C. Moore
ias Turbine Division
General Electric Company
Building 53, Room 330
River Road
Schenectady, New York 12345
518–374-2211, Ext. 5-2186

leton N. Rowe
Mobil Research and Development Corp.
Box 1025
Princeton, New Jersey 08540
609–737-3000

vis B. Sibley
SKF Industries, Inc.
King of Prussia, Pennsylvania 19406
216–265-1900, Ext. 242

6 May 1976

Subject: First Year Report for NSF Project "Collaborative Research in Tribology"
Grants: No. ENG74-21002
No. ENG74-21181
No. ENG74-21330

Dr. Clifford J. Astill, Director
Solid Mechanics Program
Engineering Mechanics Section
Engineering Division
National Science Foundation
Washington, D.C. 20550

Dear Dr. Astill:

Enclosed please find our report of the first year of activity on the subject project. This report includes:

- Project Organizational Chart
- Summary of Research Efforts Conducted
- Professional Activities of Personnel
- Research Personnel Funded
- Industrial Advisory Board Members
- Industrial Advisory Board Meeting Minutes

During the first year of the project the principal investigators met five times for research coordination with the chairman of the Industrial Advisory Board. We also met with the Industrial Advisory Board in May and October 1975 and plan to meet with them again in May 1976. In addition to these formal meetings, there was considerable individual interaction between the principal investigators and the members of the Board. This included discussions and visits by some of us to industrial laboratories.

The original proposal was for three years but the funding commitment from NSF was for two years. The second year is expected to proceed as planned in the proposal. We hope to secure a continuation of the funding beyond the original two year NSF commitment. Please advise us as to the steps we should take for continuation.

We appreciate the support of the National Science Foundation for this project.

Very truly yours,

Herbert S. Cheng Frederick F. Ling Ward O. Winer

jed
Encl.

Department of Mechanical Engineering
Northwestern University
The Technological Institute
Evanston, Illinois 60201
312–492-3541

Department of Mechanical Engineering
Rensselaer Polytechnic Institute
Troy, New York 12181
518–270-6353

School of Mechanical Engineering
Georgia Institute of Technology
Atlanta, Georgia 30332
404–894-3270

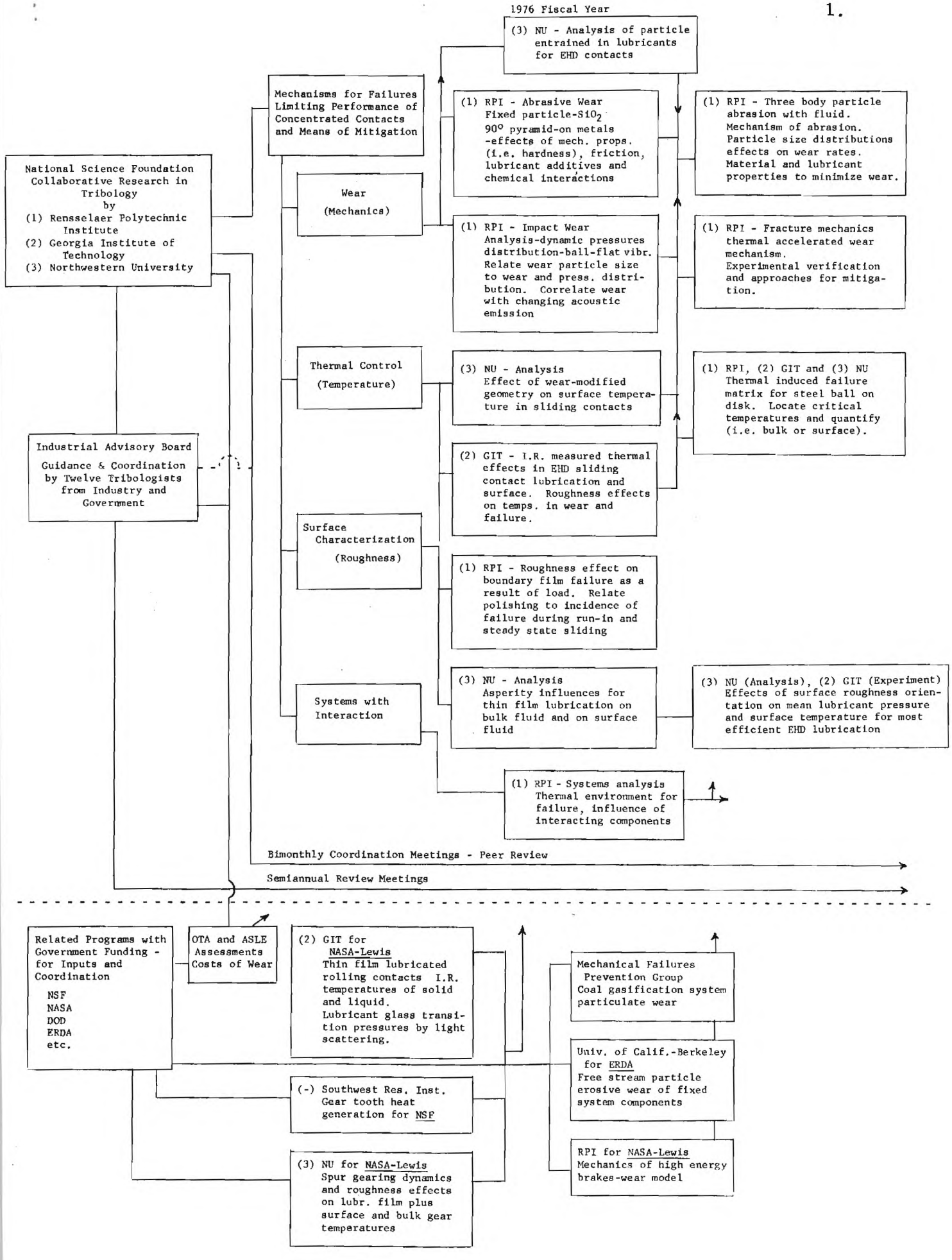
1976 Fiscal Year
(3) NU - Analysis of particle entrained in lubricants for EHD contacts
Mechanisms for Failures Limiting Performance of Concentrated Contacts and Means of Mitigation
(1) RPI - Abrasive Wear Fixed particle-SiO_2 90° pyramid-on metals -effects of mech. props. (i.e. hardness), friction, lubricant additives and chemical interactions
(1) RPI - Three body particle abrasion with fluid. Mechanism of abrasion. Particle size distributions effects on wear rates. Material and lubricant properties to minimize wear.
National Science Foundation Collaborative Research in Tribology by
(1) Rensselaer Polytechnic Institute
(2) Georgia Institute of Technology
(3) Northwestern University
Wear (Mechanics)
(1) RPI - Impact Wear Analysis-dynamic pressures distribution-ball-flat vibr. Relate wear particle size to wear and press. distribution. Correlate wear with changing acoustic emission
(1) RPI - Fracture mechanics thermal accelerated wear mechanism. Experimental verification and approaches for mitigation.
Thermal Control (Temperature)
(3) NU - Analysis Effect of wear-modified geometry on surface temperature in sliding contacts
(1) RPI, (2) GIT and (3) NU Thermal induced failure matrix for steel ball on disk. Locate critical temperatures and quantify (i.e. bulk or surface).
Industrial Advisory Board Guidance & Coordination by Twelve Tribologists from Industry and Government
(2) GIT - I.R. measured thermal effects in EHD sliding contact lubrication and surface. Roughness effects on temps. in wear and failure.
Surface Characterization (Roughness)
(1) RPI - Roughness effect on boundary film failure as a result of load. Relate polishing to incidence of failure during run-in and steady state sliding
Systems with Interaction
(3) NU - Analysis Asperity influences for thin film lubrication on bulk fluid and on surface fluid
(3) NU (Analysis), (2) GIT (Experiment) Effects of surface roughness orientation on mean lubricant pressure and surface temperature for most efficient EHD lubrication
(1) RPI - Systems analysis Thermal environment for failure, influence of interacting components
Bimonthly Coordination Meetings - Peer Review
Semiannual Review Meetings
Related Programs with Government Funding - for Inputs and Coordination
NSF
NASA
DOD
ERDA
etc.
OTA and ASLE Assessments Costs of Wear
(2) GIT for NASA-Lewis Thin film lubricated rolling contacts I.R. temperatures of solid and liquid. Lubricant glass transition pressures by light scattering.
Mechanical Failures Prevention Group Coal gasification system particulate wear
Univ. of Calif.-Berkeley for ERDA Free stream particle erosive wear of fixed system components
(-) Southwest Res. Inst. Gear tooth heat generation for NSF
RPI for NASA-Lewis Mechanics of high energy brakes-wear model
(3) NU for NASA-Lewis Spur gearing dynamics and roughness effects on lubr. film plus surface and bulk gear temperatures

SUMMARY OF RESEARCH EFFORTS CONDUCTED

Northwestern University

Entrained Particles in Lubricated Contacts

The objective of this task is to determine how effective is the elasto-hydrodynamic action of the lubricant in keeping the contaminants and the debris from entering the Hertzian region. It is an exploratory study of the motion of spheres in the inlet region of an EHD contact. Both the formulation of an analytical model as well as the design of an exploratory rig are well underway and the task should be finished on schedule.

Effect of Wear Modified Geometry on Transient Contact Temperature in Sliding Contacts

Failure of lubricated sliding contacts is related strongly to the surface temperature rise in the contact. Recent failure experiments have shown that the transient temperature in a lubricated sliding contact can increase unstably under certain conditions. This instability appears to be closely related to the change of surface geometry due to wear. The objectives of this task are: 1) to relate the frictional heating to a given surface roughness geometry; 2) to seek a wear model to predict the change of roughness geometry due to wear; and 3) to develop an analysis to determine the transient characteristics of contact temperature based on the models developed in (1) and (2). The development of this task is in the preliminary stage. Full progress must await more failure data in sliding contacts gathered at RPI and GIT.

Surface Roughness Effects on EHD Lubrication

This task is a continuation of a sustaining effort at NU on the effectiveness of EHD lubrication in the regime where a large part of the load is carried by asperities. A comprehensive lubrication analysis in this regime for

longitudinal roughness was accomplished jointly by NU and Thornton Research Centre in U.K. when H.S. Cheng was on a sabbatical leave at Thornton. Results show some very interesting and encouraging trends which agree very well with recent failure experiments conducted at Thornton. Based on the encouraging results, a major effort is launched recently at NU to extend the approach to include roughness of arbitrary orientations. The analysis should also be applicable to many other related tribological applications such as seals and metal rolling lubrication. This task should be completed by the end of 1976.

Morphological Study of Failure in Lubricated Sliding Contacts

In spite of the vast amount of literature available on failure in sliding contacts, the basic mechanism of the sliding failure in lubricated contacts is still not clear. In this task, an attempt is being made to study the sequential events at the incipient of sliding failure between a barrel and a cylinder. By the friction and temperature measurements and by the surface examination with SCM, one should be able to ascertain whether failure for a given condition is due to the breakdown of bulk lubricant film, oxide film, or the boundary surface film. The experimental rig has been completed and is ready for trial runs.

Effect of Variable Heat Transfer Coefficients on the Equilibrium Surface Temperature of Spur Gears

This task is an extension of a research previously sponsored by NASA at NU on EHD lubrication of spur gears. It was found that the most critical quantity governing failure modes in gears is the equilibrium surface temperature. In this task, the surface temperature analysis is refined to give an improved accuracy by incorporating a variable heat transfer coefficient in the radial direction. This task has been completed and is ready for publication.

SUMMARY OF RESEARCH EFFORTS CONDUCTED

Georgia Institute of Technology

The research conducted at Georgia Institute of Technology has been concerned with: a) the incipient scuffing failure of elastohydrodynamic contacts, b) surface roughness characterization, and c) the determination of the controlling lubricant rheological model in the elastohydrodynamic contact.

The results of research conducted under this grant have been the subject of three published papers and three additional invited presentations.

Elastohydrodynamic Contact Scuffing Failure Investigation

These studies are based on the assumption that the contact scuffing failure is temperature dependent. The emphasis has been on obtaining predictive relationships for the contact surface temperature as a function of the controlling independent parameters and on obtaining a relationship between surface temperature and wear rate. The capability for measuring film thickness, surface temperature, and traction in sliding and rolling contacts has been developed. Wear measurements have been made by both relocation profilometry and lubricant analysis for wear metals (ferrographic and spectrographic). Some of this work has been done in conjunction with a NASA grant to this laboratory.

The emphasis during the first year has been on sliding contacts. The apparatus for studying contacts with rolling components has been completed and preliminary data is being taken.

In the case of the sliding contacts considerable temperature and wear data has been taken under a wide variety of conditions typical of current engineering practice. Surface temperature measurements have been used to develop predictive equations which have been compared with the Blok-Jaegar-Archard flash temperature theories.

The effect of surface finish on wear and surface temperature in sliding contacts has been investigated. When the contact lambda ratio (ratio of the mean film thickness to the composite surface roughness) equals approximately one or less the surface temperature begins to fluctuate rapidly with time and wear of the metal surface occurs. The surface temperature time fluctuations are measured with an infrared detector and can be recorded for frequency analysis. The surface wear has been measured by both relocation profilometry of the surface and lubricant sample analysis (both ferrographic and spectrographic). These results clearly show that surface wear increases rapidly as the lambda ratio decreases below unity while the magnitude of the temperature fluctuation also increases. The wear data are a time integrated measurement for a defined experiment while the temperature fluctuation measurements are transient measurements of the instantaneous temperature during the duration of an experiment.

Spectral analysis of the temperature fluctuations and the surface profile before and after an experiment show that the fluctuations in temperature result from specific surface asperities interacting between the two surfaces. As these asperities interact they wear progressively and the magnitude of the temperature fluctuations decreases. At very low lambda ratios the asperities carry a significant portion of the load and the lubricant surrounding the asperity has a much lower pressure and temperature which is clearly seen in the temperature measurements.

Surface Roughness Characterization for Elastohydrodynamic Contact

In conjunction with the above-mentioned surface roughness temperature studies some interesting observations were made which are of practical significance. During low lambda ratio experiments the temperature fluctuations were recorded and subjected to spectral analysis. Surface profiles were also recorded before and after an experiment at the same location on the surface and

these were also subjected to spectral analysis. The surface finish was essentially isotropic and typical of good engineering practice. By these analyses it was found that although the surface roughness had a power spectra with a wide wavelength range of components, only a very narrow wavelength range was involved in the asperity interactions which caused the temperature fluctuations. The elastohydrodynamic contact acts as a mechanical filter on the surface roughness and is unaffected by surface roughness outside a narrow wavelength band. The significant band has wavelengths from about 1/2 to 2 times the Hertz diameter of the contact. It now appears clear that in essentially every application where surface finish is important, there will be a characteristic dimension which can be used to normalize the surface finish wavelength and to determine the significant components of the surface finish for the particular application. These results have important implications in the specification, measurement and production of surface finish. This work is currently being written for publication.

Lubricant Rheological Studies

The subject of lubricant rheology has long been of interest to this laboratory. Two projects on this subject have been part of the first year's effort under this grant. The earlier work in this laboratory on lubricant molecular degradation in elastohydrodynamic contacts was extended to study the degradation of a series of polymers which are of commercial importance in the automotive engine oil field. This work resulted in a paper recently presented to the American Chemical Society, and may be incorporated into a paper for the Society of Automotive Engineers next Spring.

The second activity relating to lubricant rheology is also supported by a grant from NASA and is concerned with the possible role of glass transition of the lubricant in the elastohydrodynamic contact. During this first year an

apparatus has been developed for measuring glass transitions as a function of pressure in two separate ways. One utilizes Brillouin light scattering and the other volume dilatometry. Preliminary data indicate the two methods correlate well and that many lubricants will go through a glass transition in elastohydrodynamic contacts under typical operating conditions. This field of investigation promises to be very fruitful and exciting, and may result in a significant contribution to the field of tribology.

Institutional Interaction

Program interaction currently exists on both the temperature/scuffing research and the surface roughness studies. Similar interaction is expected to develop in the lubricant rheology area as work progresses.

Identical lubricants have been secured for all three Institutions to conduct elastohydrodynamic experiments on the same material. Rensselaer Polytechnic Institute, as mentioned elsewhere in this report, is conducting steel-steel scuffing experiments under the same conditions as we are measuring temperature in the steel-sapphire system. Northwestern is measuring the effect of surface roughness on the film forming ability under similar conditions.

We are expanding our surface finish recording ability to provide Northwestern with a three dimensional mapping of surfaces on magnetic tape to be utilized in an elastohydrodynamic analysis of surface roughness-film thickness interactions. The surfaces to be recorded include typical surfaces used in our experiments as well as specifically tailored surfaces with different orientations.

SUMMARY OF RESEARCH EFFORTS CONDUCTED

Rensselaer Polytechnic Institute

Mechanism of Three Body Abrasion

Classic wear theory suggests that when abrasives, such as dirt, are contained in lubricant, fuel, or hydraulic fluid, and are trapped within a sliding contact, that the mechanism of wear will be either chip cutting or the breaking off of the ridges formed at the edge of the track. During the first year of this project this contention has been tested by detailed experimental and surface analytical investigations. It is concluded that wear does not occur in this manner. Rather, the particles (SiO_2) are trapped within the clearance and support the load. Sliding takes place between the SiO_2 particle and the metal surface. A film of metal is transfered to the SiO_2. Eventually the SiO_2 breaks up and is carried away by the fluid; it thus carries away the metal transfered to it. Accordingly, three body abrasion wear is seen to occur by a transfer mechanism. This suggests a variety of new approaches to abrasive wear reduction.

A report will soon be issued which documents this wear mechanism. During the second year attempts will be made to quantify this phenomena by determining the rate of transfer and the particle concentration.

Wear by Ductile Fracture

During the first year a study has been conducted of wear rates of copper base materials in unlubricated sliding. This study consisted of particle examinations and the measurement of wear rates as a function of generated interface temperatures. Particle examination showed that the wear particles were flat flakes whose dimensions were independent of operating temperature. Wear rates over the whole range of operating temperatures (26C to 1000C) could be predicted

by the following expression:

$$w = k \cdot \frac{T}{T_m - T} \quad .$$

Here T is the measured surface temperature and T_m, the melting point of the alloy in question. "k" is a function of the alloy. The particle shape and the correlation with temperature suggests a ductile fracture mechanism of wear. Theoretical considerations using principles of fracture mechanics have been used to establish wear rate behavior as a function of the parameters involved. Correlations are now being attempted.

Thermal Induced Failures

Previous research has indicated that surface failure in sliding does not have single parameter dependence but is a time related process in which a variety of events occur. As a part of the collaborative effort RPI has set up during the past year a test device with the necessary instrumentation to follow the progress of failure.

With this device we can measure as a function of time the following quantities:

(1) Friction

(2) Temperature of Surface

(3) Contact Resistance

(4) Induced Sonic Vibration

(5) Surface Roughness Profile

under a variety of operating conditions. These new techniques of friction analysis are expected to provide new insight into the failure processes. Specifically we expect to test the hypothesis, predicted analytically, that failure with non-transfering materials is a function not of the absolute surface temperature but rather the heat flux. That is failure will occur when the heat flux is sufficiently high to allow the failure to spread.

Roughness and Bearing Material Composition

For many years it has been known that certain materials are better bearing materials than others, even when hardness and differences in adhesion are accounted for. It has also been known that the better bearing materials polish to a smoother finish and thus allow hydrodynamic lubrication to be established sooner and at lower values of the operating parameters. A study has been underway for the past year to understand this effect and to isolate the critical material property involved. Research to date seems to indicate that the hard particles (e.g., Cu_3Sn in Bronze) are the determining factor. If the bearing material contains any phase harder than the shaft material, it will scratch (and roughen) the shaft. The shaft in turn roughens the bearing material. The steady state roughness is determined by the particle size and this roughness contributes to the hydrodynamic component of lubrication. Further confirmation is now underway using specially prepared materials with different shape and composition of particle additives.

Scratch Hardness and its Implications on Wear

Studies have been conducted determining the ability of single point tools of SiO_2 to scratch metals of different hardness and composition. It is found that the point scratch elimination is when the substrate is 1.2 x hardness of the tool. For SiO_2 this becomes 1200 Vickers. Contrary to expectations sliding indentations under lubricated conditions produces scratches of lower scratch depth. An analysis of the mechanical forces involved shows that this will be true under kinetic conditions while the reverse is true under static conditions.

PROFESSIONAL ACTIVITIES OF PERSONNEL

(1st Quarter 1975 - 1st Quarter 1976)

FREDERICK F. LING

Professional Activities

Chairman, Council, Mechanical Failure Prevention Group, National Bureau of Standards.
Chairman, Lubrication Division, American Society of Mechanical Engineers.
Member, Policy Board-Research, American Society of Mechanical Engineers.
Chairman, Panel on Fretting-Initiated Fatigue, National Materials Advisory Board, National Research Council, National Academy of Sciences - National Adacemy of Engineering.
Chairman, Seminar on Automobile/Spare Parts, Workshop on Wear Reduction, Congress of the United States Office of Technology Assessment, Washington, D.C., February 24, 1976.
Chairman, Educational Course on Technical Communications, American Society of Lubrication Engineers, to be held at the Annual Meeting, Philadelphia, Pennsylvania, May 12, 1976.
Chairman, Symposium on Prevention of Failures in Coal Conversion Systems, Mechanical Failure Prevention Group, Columbus, Ohio, April 21-23, 1976.

Publications

"Design of Pivots for Minimum Fretting," M.B. Peterson and F.F. Ling, North Atlantic Treaty Organization, Advisory Group for Aerospace Research and Development Proceedings, AGARD-CP-161 (1975).

"A Novel Method of Measuring Temperatures due to Sliding in Ultra-High Vacuum," J.D. Vasilakis and F.F. Ling, Space Tribology, European Space Agency, Neuilly, France, 87-100 (1975).

"Elastodynamic Response of Hollow Balls," F.F. Ling, C.Y. Chow and M.E. Rivera, American Society of Lubrication Engineers Transactions, 18, 105-115 (1975).

"Heat Effects in Rolling Contact," F.F. Ling, The Mechanics of the Contact between Deformable Bodies, A.D. de Pater and J.J. Valkev, eds., Delft University Press, 165-176 (1975).

Book

Fretting in Aircraft Systems, F.F. Ling, editor, North Atlantic Treaty Organization Advisory Group for Aerospace Research & Development AGARD-CP-161, 1975.

Invited Lectures

"A Novel Method of Measuring Temperatures due to Sliding in Ultra-High Vacuum," European Space Tribology Symposium, Frascati, Italy, April 9-11, 1975.

"Surface Mechanics and Wear," Advanced Research Projects Agency Workshop on Wear, LaJolla, California, July 15, 1975

Frederick F. Ling

Invited Lectures - cont'd.

"Failure Prediction -- Tribology," Advance Research Projects Agency Workshop on Automated Prognosis of Failure in Military Vehicles, Madison, Wisconsin, August 19, 1975.

"Surface Mechanics," Materials Engineering Seminar, Rensselaer Polytechnic Institute, Troy, New York, March 16, 1976.

MARSHALL B. PETERSON

Professional Activities

Special Congressional Employee, Consultant on Product Durability, Congress of the United States Office of Technology Assessment.
Member, Planning Committee, International Wear Conference, 1977.
Vice Chairman, International Solid Lubrication Conference, 1978.
Organizer of Naval Conference-Wear Control in Naval Aircraft, 1975.
Consultant, Naval Air Development Center, Application of New Technology to Naval Aircraft.
Member, Executive Committee, Lubrication Division, American Society of Mechanical Engineers, 1975-1978.
Editor, Proposed Wear Control Handbook, American Society of Mechanical Engineers, 1976-1978.

Invited Lectures

"Research in Wear," American Society of Metals, New York, N.Y., April 1975.

"Wear Control Techniques," American Society of Metals, Chicago, Illinois, April 1975.

"Ships Diagnostics Systems," Mechanical Failure Prevention Group Meeting, Los Angeles, California, April 1975.

"Wear of Cast Bronze Bearings," American Society of Lubrication Engineers Annual Meeting, May 1975.

"Wear Mechanisms," American Society of Mechanical Engineers, Rochester, New York, October 1975.

"Corrosion with Solid Film Lubrication," Mechanical Failure Prevention Group Meeting, Washington, D.C., October 1975.

"Cost of Wear/Ships Propulsion," Research Committee on Lubrication (ASME), Miami Beach, Florida, October 1975.

"Wear Testing Objectives," American Society for Testing Materials, New Orleans, La., November 1975.

"New Surface Treatments for Wear," Navy Wear Conference, December 1975.

"Wear Problems in Naval Aircraft," Navy Wear Conference, December 1975.

"Wear and Equipment Durability," Office of Technology Assessment Wear Conference, February 1976.

"Cost of Wear in Naval Aircraft," Office of Technology Assessment Wear Conference, February 1976.

Marshall B. Peterson

Invited Lectures - cont'd.

"Fundamentals of Solid Film Lubrication," American Society of Lubrication Engineers Annual Meeting, May 1976.

"Friction and Wear Tests," American Society of Lubrication Engineers Annual Meeting, May 1976.

"Parameter in Bronze Bearing Wear," American Society of Lubrication Engineers Annual Meeting, May 1976.

"A Study of Ice Friction," Gordon Research, June 1976.

WARD O. WINER

Honors and Awards

1. 1975 ASME Melville Award, (W. O. Winer, D. M. Sanborn, and V. Turchina) for the best original paper presented before the American Society of Mechanical Engineers.

2. 1975 Georgia Tech Chapter of Sigma Xi Award for Sustained Research Contributions in Engineering, (W. O. Winer).

3. 1975 Georgia Tech Chapter of Sigma Xi Research Award for a Junior Faculty Member in Mechanical Engineering (D. M. Sanborn).

4. 1975 Georgia Tech Chapter of Sigma Xi Award for Advising the Best M.S. Thesis in Engineering (D. M. Sanborn).

Professional Activities:

W. O. Winer:
Secretary, Lubrication Division, American Society of Mechanical Engineers
Chairman, Finance Committee, American Society of Mechanical Engineers, Research Committee on Lubrication, Wear Control Handbook Project
Member, Research Committee on Lubrication, American Society of Mechanical Engineers
Member, Conference Planning Committee, American Society of Mechanical Engineers/American Society of Lubrication Engineers, Lubrication Conference
Chairman, Advanced Seminar on Elastohydrodynamic Lubrication, American Society of Lubrication Engineers, May 1975.
Participating Delegate from the United States to the International Research Group on the Wear of Engineering Materials, under the Sponsorship of OECD.

Publications:

"Traction of Elastohydrodynamic Contacts with Thermal Shearing Flow", Trans. ASME, Journal of Lubrication Technology, Vol. 97, No. 3, 1975, pp. 424-429, (J. Jakobsen and W. O. Winer).

"Dissipative Heating Effects and End Corrections for Viscous Newtonian Flow in High Shear Stress Capillary Viscometry", Trans. ASME, Journal of Lubrication Technology, Vol. 97, No. 3, 1975, pp. 424-278, (J. Jakobsen and W. O. Winer).

Ward O. Winer

Publications (continued)

"High Shear Stress Behavior of Some Representative Lubricants", Trans. ASME, Journal of Lubrication Technology, Vol. 97, No. 3, 1975, pp. 479-485, (J. Jakobsen and W. O. Winer).

"Viscosity-Pressure Measurements for Several Lubricants to 5.5 x 10^8 N/m^2 (8 x 10^4 psi) and 149 C (300F) Trans. ASLE, Vol. 97, 1975, (W. R. Jones, R. L. Johnson, D. M. Sanborn and W. O. Winer).

"The Viscous Lubrication of Rolling and Sliding Rigid Cylinders", ASME Transactions, Journal of Lubrication Technology, Vol. 97F, No. 2, April 1975, pp. 180-186, (S. F. Carlson and W. O. Winer).

"Dynamics of Roller Bearings Considering Elastohydrodynamic Forces" (M. A. Molina-Combita, and D. M. Sanborn and W. O. Winer), Proceedings, Japanese Society of Lubrication Engineers/American Society of Lubrication Engineers Joint International Meeting, Tokyo, Japan, June 1975, pp. 9-16, Vol. II.

"Molecular Degradation of Lubricants in Sliding Elastohydrodynamic Contacts", Trans. ASME, Journal of Lubrication Technology, Vol. 97, No. 3, 1975, pp. 390-397, (D. L. Walker and D. M. Sanborn and W. O. Winer).

"Prediction of Traction in Sliding EHD contacts" (R. K. Kunz and W. O. Winer, presented at 1975 ASME/ASLE Lubrication Conference, Miami, Florida, October 1975 and to be published Transactions, ASME).

"Infrared Temperature Mapping in Elastohydrodynamics Lubrication", (V. K. Ausherman, H. S. Nagaraj, D. M. Sanborn and W. O. Winer, presented at ASME/ASLE Lubrication Conference, Miami, Florida, October 1975, and to be published in Trans. ASME, J.O.L.T.).

"Chemical Effects in Contact Fatigue: Part III - Load-Life Exponent, Life Scatter, and Overall Analysis", (W. E. Littmann, B. W. Kelley, W. J. Anderson, R. S. Fein, E. E. Klaus, L. B. Sibley and W. O. Winer, ASME Paper No. 75-Lub-45, to be published in Trans. ASME JOLT).

"Lubricant Properties in Thin Lubricating Films", (D. M. Sanborn and W. O. Winer, presented at ACS Meeting, New York City, April 1976).

"Fluid Film Bearing Housing Design for a Hot Ambient Environment", (with J. D. McHugh, and G. D. Robson, ASME Paper No. 76-GT-93, presented at ASME Gas Turbine Conference, New Orleans, March 1976).

Ward O. Winer

Technical Reports

"Bearings and Seals Investigation No. 2 Bearing with Air Cooled Housing in Model MS 7000 Gas Turbine", The General Electric Company, Large Gas Turbine Division, July 1975 (W. O. Winer, D. M. Sanborn, S. V. Shelton and S. Bair).

"Investigations of Lubricant Rheology as Applied to Elastohydrodynamic Lubrication", NASA CR-134882, August 1975 (W. O. Winer, D. M. Sanborn, R. K. Kunz, H. S. Nagaraj).

Invited Lectures (W. O. Winer)

"Temperature Measurements in Sliding Elastohydrodynamic Contacts - The Detection of Transition Phenomena", Rensselaer Polytechnic Institute, Applied Mechanics Seminar Series, May 1, 1975.

"Basic Concepts of Elastohydrodynamic Lubrication", Advanced Seminar in Elastohydrodynamic Lubrication, ASLE Annual Meeting, Atlanta, Georgia, May 5, 1975.

"Recent Developments in Tribology and Rheology Research at the Georgia Institute of Technology", ASME Research Committee on Lubrication, May 9, 1975, Atlanta, Georgia.

"Some Recent Developments in Infrared Temperature Measurements in Elastohydrodynamics Contacts", OECD International Research Group on the Wear of Engineering Materials, June 13, 1975, Tokyo, Japan.

"Tribology at Georgia Tech", Georgia Tech Sigma Xi lecture, March 11, 1976.

"Lubricant Properties in Thin Lubricating Films", Symposium on Lubricant Properties in Thin Lubricating Films Presented before the Division of Petroleum Chemistry of the American Chemical Society, New York City, April 4-9, 1976.

"Design and Testing of a Bearing Housing for High Temperature Applications", Meeting of the Power Generation Council of American Society of Lubrication Engineers, May 11, 1976, Philadelphia, Pennsylvania (with J. D. McHugh and G. Robson).

"Some Recent Developments in Infrared Temperature Measurements in Elastohydrodynamic Contacts", International Research Group on the Wear of Engineering Materials, Paris, France, April, 1976 (given by G. Solomon for W. O. Winer in absentia).

"The Wear Control Handbook Project of the Research Committee on Lubrication of American Society of Mechanical Engineers", Workshop on Wear Reduction, Congress of the United States Office of Technology Assessment, Washington, D. C., February 23-25, 1976.

Ward O. Winer

Invited Lectures (Continued)

"The Role of Glass Transition in Concentrated Contacts", The Gordon Research Conference on Friction, Lubrication and Wear, New London, New Hampshire, June 14-18, 1976.

HERBERT S. CHENG

Publications

"Pressure Perturbation in EHD Contacts Due to an Ellipsoidal Asperity," Journal of Lubrication Technology, Transactions of the American Society of Mechanical Engineers, 98, 8-15 (1976); with L.S.H. Chow.

"The Effect of Surface Roughness on the Average Film Thickness Between Lubricated Rollers," Journal of Lubrication Technology, Transactions of the American Society of Mechanical Engineers, 98, 117-125 (1976); with L.S.H. Chow.

"Transient Effect of Lubricant on Elastohydrodynamic Film Thickness," NASA CR-2669, also presented at a Symposium on Thin-Film Lubrication sponsored by American Chemical Society; with K.L. Wang.

"Thesis Topics in Tribology-II," to appear in the July issue of Journal of Lubrication Technology, Transactions of the American Society of Mechanical Engineers; with member of ASME Research Committee on Lubrication.

"Elastohydrodynamic Lubrication of Circumferentially Ground Rough Disks," submitted to American Society of Lubrication Engineers for presentation at the 1976 ASLE/ASME Joint Lubrication Conference; with A. Dyson.

Sabbatical Leave

1 April - 21 September 1975	Thornton Research Fellow at Thornton Research Centre, Chester, England

Invited Lectures and Seminar

"Recent Developments in Elastohydrodynamic Lubrication," invited lecture at Durham University, Durham, U.K., July 1975.

"Effect of Surface Roughness on EHD Lubrication," invited lecture at Thornton Research Centre, Chester, U.K., August 1975.

"Effects of Roughness Orientation on Film Thickness in EHD Contacts," seminar, Imperial College, Limits of Lubrication Conference, July 1975.

Visitations

Cambridge University with Dr. K.L. Johnson, July 1975.

Reading University with Professor Hirst, July 1975.

Glasgow University with Professor J. Lamb, August 1975.

Leicester University with Dr. J.F. Archard, June 1975.

Leeds University with Professor D. Dowson, September 1975.

University of Lyon with Professor M. Godet, August 1975.

RESEARCH PERSONNEL FUNDED

Georgia Institute of Technology

Ward O. Winer, Professor and Principal Investigator
David M. Sanborn, Associate Professor
Scott Bair, Research Engineer
M. Alsaad, Ph.D. candidate
H. Nagaraj, Ph.D. candidate
R.K. Kunz, Ph.D. candidate
plus two undergraduates on an hourly basis

Northwestern University

Herbert S. Cheng, Professor and Principal Investigator
David Durkee, Ph.D. candidate
Nadir Patir, Ph.D. candidate

Rensselaer Polytechnic Institute

Frederick F. Ling, Professor and Principal Investigator
Marshall B. Peterson, Senior Research Scientist & Manager, Institute for Wear Control Research
S. Frank Murray, Research Engineer
Henry A. Scarton, Assistant Professor
Ting-Long Ho, Postdoctoral Associate
Robert S. Pozniakas, Graduate Assistant
William J. Renault, Graduate Assistant
Ted Bolszio, Student Technician
Mary C. Herbert, Student Technician

INDUSTRIAL ADVISORY BOARD

Robert L. Johnson, Chairman

Robert L. Adamczak

Richard S. Fein

Donald F. Hays

Bruce W. Kelley

George H. Kitchen

P. M. Ku

Walter E. Littmann

John E. Mayer, Jr.

Clinton C. Moore

Carleton N. Rowe

Lewis B. Sibley

COLLABORATIVE RESEARCH IN TRIBOLOGY

Sponsored by the National Science Foundation

cipal Investigators

bert S. Cheng
orthwestern University

derick F. Ling
ensselaer Polytechnic Institute

d O. Winer
eorgia Institute of Technology

ustrial Advisory Board

bert L. Johnson, Chairman
ASA Lewis Research Center
leveland, Ohio 44135
16—433-4000, Ext. 464

bert L. Adamczak
lans Office
FWAL/XR
right-Patterson Air Force Base
hio 45433
13—255-3494

hard S. Fein
exaco Research Center
O. Box 509
eacon, New York 12508
14—831-3400

nald F. Hays
ngineering Mechanics Department
eneral Motors Corporation
2 Mile and Mound Roads
arren, Michigan 48090
13—575-2927

ce W. Kelley
atepillar Tractor Company
echnical Center
eoria, Illinois 61602
09—578-6620

rge H. Kitchen
ell Telephone Laboratories, Inc.
urray Hill, New Jersey 07974
01—582-2410

ter E. Littmann
he Timken Company
335 Dueber Avenue, SW
anton, Ohio 44706
16—453-4511, Ext. 305

n E. Mayer, Jr.
cientific Research Staff
ord Motor Company
O. Box 2053
earborn, Michigan 48120
13—322-9447

ton C. Moore
as Turbine Division
eneral Electric Company
uilding 53, Room 330
River Road
chenectady, New York 12345
18—374-2211, Ext. 5-2186

leton N. Rowe
obil Research and Development Corp.
ox 1025
rinceton, New Jersey 08540
09—737-3000

vis B. Sibley
KF Industries, Inc.
ing of Prussia, Pennsylvania 19406
16—265-1900, Ext. 242

July 15, 1975

TO: Members, Industrial Advisory Board

FROM: Chairman, Industrial Advisory Board

SUBJECT: Minutes of Meeting

Enclosed are the Minutes of the first meeting of the Industrial Advosory Board held May 8, 1975, at Georgia Institute of Technology, Atlanta, Georgia.

Robert L. Johnson

Enclosure

Department of Mechanical Engineering
Northwestern University
The Technological Institute
Evanston, Illinois 60201
312—492-3541

Department of Mechanical Engineering
Rensselaer Polytechnic Institute
Troy, New York 12181
518—270-6353

School of Mechanical Engineering
Georgia Institute of Technology
Atlanta, Georgia 30332
404—894-3270

May 13, 1975

MEMORANDUM FOR RECORD

FROM: Chairman, Industrial Advisory Board

SUBJECT: NSF Grant Program on Collaborative Research in Tribology

The Industrial Advisory Board for the National Science Foundation sponsored program on Collaborative Research in Tribology had its first meeting at Georgia Institute of Technology on May 8, 1975 from 2:00 to 4:30 pm. The program plans for the three collaborating institutions were discussed with reference to the original proposal. Copies of that proposal were distributed to members of the IAB. Professor H. Cheng was in Great Britain, therefore his activities were described by Professor Winer.

The proposal and program followed the Tribology Workshop at Georgia Institute of Technology in October 1973. The program was funded by the NSF on March 1 retroactive to January 1, 1975 for the first two years of the proposed three-year program. It is anticipated that a productive program would be further funded after the initial two-year period. Some discussion considered the communication of results from the program to possible industrial application and with basic NSF sponsorship to possible expanded support by other government organizations, industries and research associations.

A press release announcing the grant was distributed on April 7, 1975 and should appear in a number of technical journals. The format for program stationary was displayed and approved by those present.

The program priorities are centered on Mechanical Contact Failure. Georgia Tech will emphasize the thin film lubrication transitions between elastohydrodynamic and boundary lubrication measuring critical fluid conditions and properties. Northwestern University activities are analytical

treating inlet heating phenomena, surface roughness effects and load zone flash temperature effects for correlation with Georgia Tech's experimental measurements. Rensselaer Polytechnic Institute plans were presented by Professor F. F. Ling and M. B. Peterson; they are presently studying the origin of wear failure. It is clear that abrasive wear and impact wear merit careful study. Mr. Peterson indicated the impact wear phenomena would be studied on the basis of fracture mechanics.

The Board discussed the very great industrial importance of abrasive wear, the many publications on problems and the lack of fundamental understanding that has impeded the scientific solution of problems. This Chairman mentioned that the OECD sponsored International Research Group on Wear of Engineering Materials is also anticipating expanded activities on abrasive wear under Professor Helge Christensen of Norway. The work of Professor J. Ledocq of Mons on abrasive wear test methods was described. The Basic Fluid Power Research Institute at Oklahoma State University was reported to be a source of lubricant sample analyses for particulates at reasonable costs ($11/sample).

The RPI documentation of failures is looked to for providing clarified real problem definitions delineating the needs for unplanned maintenance and showing how improved planning may be achieved. It is intended that the results of experimental studies should be effectively modeled for convenient use.

Considerations of the Board for additional areas of emphasis developed the view that the vendors now supply critical design information to machine designers and accordingly the options to those designers are limited. Expanded objective tribological information for designers is a high priority need. The Board agreed that there are many tasks for consideration that

cannot be economically justified by machine builders but which are important to technical progress; these include:

1. An assessment of the economic impact of tribology on our nation and functional industries showing the primary troublesome components and indicating the costs of such wear and failure in energy and materials and hence the importance of sustained tribology programs; cooperation with other interested organizations (e.g., ASLE, ASME, ASTM, MFPG, etc.) in such studies.

2. Specific modification of the bearing materials to reduce skidding wear damage in high-speed, rolling-element bearings.

3. Improved quantitive method of defining and measuring surface topography (roughness, waviness, micro-geometry, etc.) on a three-dimensional basis recognizing that computerized profile tracing devices lack needed sensitivity, are laborious to use for three-dimensional information and cannot be used with many parts from operating machinery. More convenient and significant approaches should be sought.

4. Elastomeric lip seals are commonly misapplied, and it was agreed that the present program might develop the optimum material property requirements for achieving EHD lubrication at the lip-shaft interface. Elastomer compounders might be able to achieve improved materials if they have the needed properties defined.

The foreign scholar program was briefly discussed and the IAB members were asked to suggest candidates. The writer has suggested Professor J. Ledocq (Belgium) and Dr. Daniel Berthe (France) as potential candidates. Their interests, training and youth suggest their participation would be technically significant and enhance U.S. relations with significant elements of the European technical community.

The next meeting of IAB will be at the time of the 1975 ASLE/ASME Lubrication Conference in Miami Beach next October with details of the meeting to be developed between the Principal Investigators and the Chairman.

151

Robert L. Johnson

cc:
Prof. W. O. Winer
Prof. F. F. Ling
Mr. M. B. Peterson

Final Distribution:
Attendees
R.L. Adamczak
C.N. Rowe
W.E. Littmann
C.C. Moore
R.S. Fein
L.B. Sibley
D.F. Hays
W.O. Winer
F.F. Ling
M.B. Peterson
R.L. Johnson
B.W. Kelley
G.H. Kitchen
J.E. Mayer, Jr.

COLLABORATIVE RESEARCH IN TRIBOLOGY

Sponsored by the National Science Foundation

cipal Investigators

bert S. Cheng
orthwestern University

lerick F. Ling
nsselaer Polytechnic Institute

d O. Winer
orgia Institute of Technology

strial Advisory Board

ert L. Johnson, Chairman
ASA Lewis Research Center
veland, Ohio 44135
6-433-4000, Ext. 464

rt L. Adamczak
ns Office
WAL/XR
ight-Patterson Air Force Base
io 45433
3-255-3494

rd S. Fein
kaco Research Center
. Box 509
con, New York 12508
-831-3400

ld F. Hays
ineering Mechanics Department
eral Motors Corporation
Mile and Mound Roads
ren, Michigan 48090
-575-2927

W. Kelley
apillar Tractor Company
hnical Center
ria, Illinois 61602
-578-6620

e H. Kitchen
Telephone Laboratories, Inc.
ray Hill, New Jersey 07974
-582-2410

E. Littmann
Timken Company
5 Dueber Avenue, SW
on, Ohio 44706
-453-4511, Ext. 305

E. Mayer, Jr.
ntific Research Staff
Motor Company
Box 2053
born, Michigan 48120
-322-9447

n C. Moore
Turbine Division
eral Electric Company
ling 53, Room 330
er Road
nectady, New York 12345
-374-2211, Ext. 5-2186

n N. Rowe
Research and Development Corp.
1025
eton, New Jersey 08540
737-3000

. Sibley
Industries, Inc.
of Prussia, Pennsylvania 19406
265-1900, Ext. 242

12 December 1975

TO Members, Industrial Advisory Board

FROM Chairman, Industrial Advisory Board

SUBJECT Record of October 23, 1975 Meeting

Enclosed is my interpretive record of our October 23, 1975 meeting at the Carillon Hotel in Miami Beach, Florida. Your comments or corrections can become part of the record for our next meeting in the spring. Please advise me of any critical comments that may influence the course of the investigations at your earliest convenience. The investigators intend to be responsive to the IAB.

Best regards.

Robert L. Johnson
Chairman

jed
encl.

Department of Mechanical Engineering
Northwestern University
The Technological Institute
Evanston, Illinois 60201
312-492-3541

Department of Mechanical Engineering
Rensselaer Polytechnic Institute
Troy, New York 12181
518-270-6353

School of Mechanical Engine
Georgia Institute of Technolo
Atlanta, Georgia 30332
404-894-3270

MEMORANDUM FOR RECORD

FROM Chairman, Industrial Advisory Board

SUBJECT Collaborative Research in Tribology--Meeting of Industrial Advisory Board, Miami Beach, Florida, October 23, 1975

The dinner meeting convened from 5:00 p.m. to 10:00 p.m. at the Carillon Hotel with all Principal Investigators, Mr. M.B. Peterson and all members of the IAB present except Drs. Adamzcak and Fein.

The record memorandum by the Chairman dated May 13, 1975 on the IAB meeting of May 8, 1975 at the Georgia Institute of Technology was accepted as an adequate record of that meeting.

The Chairman announced he had retired from NASA-Lewis and accepted an appointment as an Adjunct (non-resident) Professor of Mechanical Engineering at Rensselaer Polytechnic Institute. In that position it will be possible for even more direct interaction with the studies of this program than could be achieved from the NASA base. It has been the considered opinion of the Principal Investigators that such direct participation can improve the interaction and direction of the program to achieve complementary objectives and approaches.

A report was read (Attachment A) on the ad-hoc meeting of September 10, 1975 at NASA-Lewis of representative Tribologists with Dr. E. Passaglia of NBS and the Congressional Office of Technology Assessment.

Dr. Passaglia concurred in the substance of Attachment A. He added that his actions in seeking workshops on Costs of Wear and Corrosion had needed approvals and detailed plans are moving forward. Socialogical and economic as well as engineering aspects assessing the state of technology are being integrated into the planning. Guidance will be sought on:

(1) The irreducible cost with present technology of wear (also corrosion) in representative industries.

(2) The actual cost in the various industries (i.e. how closely is the irreducible cost approached).

(3) Is the best wear (also corrosion) control technology being applied and if not what are the obstacles to its application?

(4) What would be the net economic effect of using the best wear (also corrosion) control measures available with present technology? The workshop will have an advisory or steering committee representing consumer products like appliances and automobiles and industrial equipment like heavy construction machines, railroad rolling stock, metal cutting machines (lathes, etc.), aircraft, and military and ordnance machines.

Questions for workshop consideration can deal with materials substitution, design changes, maintenance (including education of mechanics), etc. Attempts will be made to identify critical components that fail in industry because of wear. For example, 180 million automobile tires wear out or fail each year. What would be the means and the economic impact of extending automobile lives by 8 percent?

In response to Dr. Passaglia's inquiry, it was agreed that IAB members will participate as requested in planning the workshop insofar as possible.

Professors Winer, Cheng, Ling and Mr. Peterson discussed the respective collaborative efforts. A summary of Collaborative Project Number 1 as prepared by Professor Winer is Attachment B.

A summary of Collaborative Project Number 2 is Attachment C.

There was concern by members of the IAB expressed by Kelley, Sibley and others that the objectives and approach including working postulates are not sufficiently clear in the discussion presented; that all the system thermodynamic factors (time, temperatures, pressures, environment, etc.) must be carefully documented and relevant to real problems. M. Peterson emphasized that failures are rate processes with bulk temperatures and area interactions with wear rate and surface temperatures to predict failure and understand transient effects.

General concern was evident that data made available from other programs (e.g. those sponsored by NASA, AF, ONR, Industrial Organizations, etc.) at the collaborating institutions and elsewhere be identified and factored into the overall program concept. Professor Cheng indicated that

data from Southwest Research Institute will be used in his ongoing efforts. The collaborative experimental program of the OECD sponsored International Research Group on Wear of Engineering Materials on critical surface failure conditions was also considered potentially useful for analytical efforts.

Project 3 on the effects of particulates in tribological systems was considered to have dominant practical importance that merits more concentration of effort. Mr. Peterson mentioned some maintenance survey efforts that indicated 80 percent of maintenance of ship equipment results from particulate and contamination effects in wear, corrosion, and erosion. He mentioned the experimental configuration of 3 line contacts (cylinders) against a flat was to be used and initial studies consider hardness independent of chemistry or metallurgy. The relevance of friction to wear in specific systems will be shown and the use of additives to increase friction and to react with particulates as well as particulate size distribution on wear will be explored. Professor Cheng will analyze the role of particulates in the EHD inlet region.

Project 4 is a sample exploratory area including the system interactions for a tribological component. The influences of traction on EHD contacts will be considered.

With regard to Project 5, concern was expressed by the Chairman that our physical methods for surface characterization were inadequate as well as inconvenient as a basis for interpretive analytical studies in Project 2 and elsewhere. Improved methods of quantifying surface topography are urgently needed.

A 6th area for study is the thermal environment in mechanical systems.

Group discussions emphasized the practical importance of abrasive wear, types of lubricants, temperatures, shear stability and degradation of the lubricants. The rubbing failure of tapered roller end contact areas was emphasized as a critical problem where bulk thermal influence dominates failure as Professor Cheng's recent analyses suggest.

The next meeting of the entire Industrial Advisory Board will be at the time of the ASLE Annual Meeting in Philadelphia, May 10-14, 1976. In the interim, Board members are encouraged to relate specific concerns and suggestions to the Principal Investigators or the Chairman. It is anticipated that periodic specific collaborative meetings of the investigators will be planned.

September 10, 1975 - Lewis Research Center
Meeting on Cost of Wear by an Ad Hoc Group

A meeting was held at the NASA-Lewis Research Center on September 10, 1975 to provide an interface with American wear expertise for Dr. Elio - Passaglia. Dr. Passaglia is from the National Bureau of Standards and is now on assignment to the Materials Section of the Congressional Office of Technical Assessment. That Office under (former Congressman) Emilio Daddario had been asked by Senator Tunney's Special Subcommittee on Science, Technology and Commerce to make an assessment of the national costs of corrosion and wear. In the course of discussing other matters, Fred Ling informed Dr. Passaglia as to the similar American Society of Lubrication Engineers O & O Committee activities in progress on the cost of wear. At Fred's suggestion the writer telephoned Dr. Passaglia and an opportunity for him to meet with interested wear experts was arranged; the background for and ASLE activities were also discussed. Accordingly, the September meeting included representation from ASLE's O & O as well as Government Liaison Committees, the ASME Research Committee on Lubrication, the Industrial Advisory Board as well as participants in the National Science Foundation Collaborative Research Program on Tribology at RPI, Georgia Tech and Northwestern, the NASA-Lewis Research Center and the Mechanical Failures Prevention Group. A number of the individuals present represented several activities; the group included F.F. Ling, R. Torrens, M.B. Peterson, A. Morrow, D. Hays, W. Winer, C.C. Moore, L.P. Ludwig, H.E. Sliney, D.H. Buckley, Dr. Passaglia and the writer.

Dr. Passaglia indicated that responsibility for pursuing the corrosion and wear assessment had been assigned to him. He was seeking to learn the opportunities for materials conservation by control of the wasteage processes of corrosion and wear. In his view the task was a large one requiring contractual efforts and was considering a RFP (Request for Procurement) with O.T.A. funding. He would seek to learn what is not being done with present technology that could be accomplished to minimize materials shortage and waste. What the severities of the corrosion and wear problem are in regard to our economy should be determined. Further, what can be done by legislation to reduce such problems as by tax consideration to encourage improved

maintenance or improving education on related matters. Should products be labeled for life cycle costs considering whether design for longer life merits these increased costs, etc.

The O.T.A. program RFP is in the formulative stage. It will likely concentrate on classes of products from the 5 digit S.I.C. code for (a) consumer and (b) capital goods that represent the major consumers of steel. Categories of capital goods mentioned were (1) fabricated metal buildings, (2) metal tanks factory produced and field erected, (3) agricultural tractors, (4) power cranes, draglines and shovels, (5) freight cars, (6) lathes, etc., (7) harvesting machines and parts, and (8) military ships. The group suggested that the impact of foreign markets could be important in these categories and should be considered. Pennock and Yager of Battelle were reported to have surveyed household appliances. It was also felt that Caterpillar had made a study of the life factors for construction equipment. An interesting comment was that 60 million automobile mufflers were replaced in 1972 because our technology is more concerned with just cost rather than durability. Poor packaging was a contributing cost with a large proportion of materials having to be reprocessed before use.

Dr. Passaglia indicated a Corrosion Workshop to explore those costs was to be organized by Roger Staley. The economic slowdown in the U.S. has quieted down the Congressional pressures for materials conservation but pressures will increase as business conditions improve. The Federated Materials Societies have substantial interest in these activities and the methods of accounting for corrosion costs are being developed.

A workshop on wear funded by O.T.A. was considered to be a forward step before proceeding with the study RFP. Open discussion by a body concerned with both the technical and economic aspects. The scheduled and unscheduled costs need to be pursued to learn how such costs can be reduced. Also, the national economic consequences of extending the lives of products like automobiles need be considered. Dr. Passaglia plans to leave the O.T.A. in November and by that time would like to have a workshop planned. It was

felt that such a workshop could be organized in 4 months; that it was prudent to delay the O.T.A. RFP until after the workshop. It would then be the responsibility of Dr. Passaglia's successor. The workshop should delineate (1) poor lubrication and maintenance practices that contribute to wear costs, (2) technology breakthroughs needed and anticipated, (3) design for repairability and recycling of materials, (4) export considerations, (5) legislative actions that can minimize problems.

Dr. Passaglia thanked the group for a clarifying discussion. He proposes to review this approach for technical assessment and to call on the contacts established for assistance in developing a workshop. A course of action will be determined by his office (O.T.A.).

Robert L. Johnson

B

Collaborative Project No. 1: "Failure Processes in Concentrated Sliding Contacts"

It is assumed that surface initiated failures in sliding concentrated contacts are related to the contact temperatures. On this project we will attempt to relate measured contact temperatures, calculated or predicted contact temperatures and surface failure. The objective is to develop engineering design criteria to be used so the designer can avoid surface initiated failures.

In this project surface and lubricant temperatures are being measured by the infrared radiation technique at Georgia Tech. The independent variables in the study include Hertz pressure (up to 300,000 psi), sliding speed (0.1 to 10 m/s), composite surface roughness (0.011 μm to 0.381 μm rms) for lambda ratios (λ= mean film thickness divided by composite surface roughness) ranging from one quarter to two. The contact system is 52100 steel against sapphire with a naphthenic mineral oil (no additives) as the lubricant. Considerable data has already been collected including conditions where unsteady temperature flashes associated with asperity interactions have been observed. However, no failures of the lubrication of the contact have been produced.

The efforts at Northwestern are concerned with the mathematical modeling of the system in an attempt to first predict the surface temperatures measured and then to develop a suitable design criteria.

The efforts at RPI are concerned with an experimental system similar in geometry to that at Georgia Tech but having steel on steel surfaces and capable of much higher loads and speeds. They are trying to induce failures and observe wear in these surfaces with operating variables similar to those used at Georgia Tech. They will also be concerned with examining the design criteria developed at Northwestern.

C

Collaborative Project No. 2:

"Effect of Surface Roughness Orientation on Scuffing Failures in Thin-film EHD Contacts"

Both the fatigue and scuffing failure tests of EHD contacts have indicated that the failure conditions are influenced markedly by the orientation of the surface roughness ridges with respect to the sliding or rolling motion. If the ridges run transversely to the motion, fatigue life and scuffing loads are higher than the conditions where the ridges run longitudinally to the motion. It is believed that the difference in tolerance to failure is due to the EHD lubrication process as influenced by the surface roughness and its orientation. The objectives of this project are: (1) to analyze qualitatively how is the EHD lubrication process affected by the presence of the transverse or longitudinal ridges; (2) to confirm the analytical findings by measurement of film thickness and surface temperature in a steel roller and sapphire flat rig; and (3) to run scuffing failure tests in a simple sliding rig between two steel contacts.

The efforts at Northwestern are concerned first with the development of a series of analyses to predict the mean separation, hydrodynamic pressure, asperity contacting pressure and surface temperatures in the inlet half region of the contact. This first task will indicate the effectiveness of lubrication in terms of statistically mean quantities, but it most likely will not reveal the nature of scuffing mechanism. The second task is aimed at understanding the scuffing mechanism. This will be achieved by studying the local lubrication process near an ellipsoidal asperity when it slides across the contact, or micro-EHD.

C

It is hoped the detailed knowledge of film and temperature at the microlevel will reveal the lubrication breakdown mechamism which initiates the scuffing failure.

At Georgia Tech., efforts for this project are concentrated in two areas. First, the statistics of surface geometry for initial as well as run-in surfaces will be analyzed by a surface analyzing routine currently being developed at Georgia. In this technique, the surface topography is recorded on tape by a Bendix surface profilometer and processed automatically by a digital computer to produce the desirable surface parameter needed for the elastohydrodynamic analysis at Northwestern. Second, the measurement of film thickness using the optical technique and contact temperature by infrared radiation for the case of longitudinal as well as transversed roughness will be carried out at Georgia Tech. with a roller on flat rig.

The efforts at RPI are concerned with the scuffing failure tests with a system similar in geometry to that at Georgia Tech. but having steel on steel surfaces and capable of much higher loads and speeds. It is hoped that by correlating the analytical findings with the failure tests, one can arrive at a more firm design criteria against scuffing failures.

E 25-650

Final

COLLABORATIVE RESEARCH IN TRIBOLOGY

NSF GRANT ENG 74–21002

By

Ward O. Winer
Principal Investigator

March 1978

GEORGIA INSTITUTE OF TECHNOLOGY
SCHOOL OF MECHANICAL ENGINEERING
ATLANTA, GEORGIA 30332

1978

GEORGIA INSTITUTE OF TECHNOLOGY
School of Mechanical Engineering
Atlanta, Georgia

COLLABORATIVE RESEARCH IN TRIBOLOGY

NSF Grant ENG 74-21002

Ward O. Winer
Principal Investigator

March, 1978

SUMMARY

The research conducted under NSF Grant ENG 74-21002 has been concerned with a) the failure of, b) the surface roughness characterization of, and c) the lubricant rheological properties in highly loaded lubricated contacts. The results of this research have been the subject of nine published papers, several invited lectures, two Ph.D. theses, and two M.S. degree theses. The research concerned with incipient scuffing and surface roughness characterization was carried out in collaboration with Professor H. S. Cheng of Northwestern University and Professor F. F. Ling of Rensselaer Polytechnic Institute.

The incipient scuffing failure study was directed toward determining the temperatures occurring in lightly loaded contacts during severe operation. It was found that, although the final massive failure appears to be a stochastic process with no particular limiting temperature, localized wear and surface asperity interaction occurs when the film thickness to surface roughness ratio is approximately one. Considerable wear can take place in this mode without failure of the contact. Temperatures in the range of 300 to 600C were observed during apparently steady state operation of the contact. Temperatures as high as 1100 to 1300C were observed during localized scuffing of the contact. The scuffing was, only to a limited extent, repeatable. This study suggests that the concept of a limiting flash temperature which predicts surface failure, as proposed by the Blok-Jaegar-Archard theories, may not be valid.

The surface roughness characterization was done in conjunction with surface temperature fluctuation measurements. The surface roughness which is important to an EHD contact is that roughness with wavelengths in the range of one half to four times the Hertz contact dimension in the direction of motion. Surface typography with wavelengths considerably shorter or considerably longer than this range tend not to be involved in the wear processes which occur when the asperities of the two surfaces come in contact. This finding has considerable implication with respect to surface geometry specification and production in manufacturing technology, and for the influence of that surface geometry on component surface life.

The research into the rheological properties of the lubricants found that the viscoelastic or glass transition phenomenon in lubricants is important. It was shown that many of today's lubricants undergo a viscoelastic transition when in elastohydrodynamic contacts. This work is being continued to determine not only further transition properties but also the large strain rheological response of the material in the glassy state.

In summary, it is believed that significant contributions have been made in all three areas of research. Considerable understanding has been gained with respect to the behavior of the elastohydrodynamic contacts and the behavior of lubricants in them.

TECHNICAL SUMMARY

OF RESEARCH EFFORTS CONDUCTED

The research conducted at Georgia Institute of Technology has been concerned with: a) the incipient scuffing failure of elastohydrodynamic contacts, b) surface roughness characterization and its influence in elastohydrodynamic contacts, and c) the determination of the controlling lubricant rheological model in the elastohydrodynamic contact.

The results of research conducted under this grant have been the subject of nine published papers and five invited presentations. (One copy of each preprint accompanies this report.)

Elastohydrodynamic Contact Scuffing Failure Investigation

These studies were based on the assumption that the contact scuffing failure is temperature dependent. The emphasis was on obtaining predictive relationships for the contact surface temperature as a function of the controlling independent parameters and on obtaining a relationship between surface temperature and wear. The capability for measuring film thickness, surface temperature, and traction in sliding and rolling contacts was developed. Wear measurements were made by both relocation profilometry and lubricant analysis for wear metals (ferrographic and spectrographic). Some of this work has been done in conjunction with a NASA grant to this laboratory.

In the case of the sliding contacts considerable temperature and wear data were taken under a wide variety of conditions typical of current engineering practice. Surface temperature measurements were used to

develop predictive equations which were compared with the Blok-Jaegar-Archard flash temperature theories. Although the temperature trends with operating parameters were as expected from these theories, the measured values were in general lower than predicted (maximum measured was about equal the average predicted values). This is reasonable because in the theoretical models all energy dissipation and transport processes are assumed to occur within the EHD contact whereas in the actual physical system there is additional energy transport from the solid because of the fluid surrounding the contact.

Massive scuffing was not observed under what would be considered severe conditions (Hertz pressure of 3 GPa and sliding speeds of 10 m/s) with fully flooded contacts. Although average surface temperatures of 300C and extensive asperity interaction between the surfaces was observed. Local scuffing did occur in these contacts when the lubricant was removed and starvation occurred. However, even under these conditions the surface integrity was surprisingly good. The scuffing was stochastic, local and persistant. The onset of the scuffing was not predictable with time, the scuffing was localized to one small region on the circumference of the moving surface and persisted at this location for many traverses of the surface.

The effect of surface finish on wear and surface temperature in sliding contacts was investigated. When the contact lambda ratio (ratio of the mean film thickness to the composite surface roughness) equals approximately one or less the surface temperature fluctuates rapidly with time and wear of the metal surface occurs. The surface temperature

fluctuations were measured with an infrared detector and recorded for frequency analysis. The surface wear was measured by both relocation profilometry of the surface and lubricant sample analysis (both ferrographic and spectrographic). These results show that surface wear increases rapidly as the lambda ratio decreases below unity and the magnitude of the temperature fluctuations also increase. The wear data are a time integrated measurement for a defined experiment while the temperature fluctuation measurements are transient measurements of the instantaneous temperature during the duration of an experiment.

Spectral analysis of the temperature fluctuations and the surface profile before and after an experiment showed that the fluctuations in temperature result from specific surface asperities interacting between the two surfaces. As these asperities interact they wear progressively and the magnitude of the temperature fluctuations decreases. At very low lambda ratios the asperities carry a significant portion of the load and the pressure of the lubricant surrounding the asperity is reduced. This is reflected in reduced surface temperatures in the vicinity of the asperities.

In conclusion this portion of the research provided considerable knowledge with respect to surface temperature prediction, the role of surface roughness, and the nature of scuffing. But the prediction and clear understanding of scuffing itself remains illusive.

Surface Roughness Characterization for Elastohydrodynamic Contacts

In conjunction with the above-mentioned surface roughness temperature studies some interesting observations were made which are of practical

fluctuations were measured with an infrared detector and recorded for frequency analysis. The surface wear was measured by both relocation profilometry of the surface and lubricant sample analysis (both ferrographic and spectrographic). These results show that surface wear increases rapidly as the lambda ratio decreases below unity and the magnitude of the temperature fluctuations also increase. The wear data are a time integrated measurement for a defined experiment while the temperature fluctuation measurements are transient measurements of the instantaneous temperature during the duration of an experiment.

Spectral analysis of the temperature fluctuations and the surface profile before and after an experiment showed that the fluctuations in temperature result from specific surface asperities interacting between the two surfaces. As these asperities interact they wear progressively and the magnitude of the temperature fluctuations decreases. At very low lambda ratios the asperities carry a significant portion of the load and the pressure of the lubricant surrounding the asperity is reduced. This is reflected in reduced surface temperatures in the vicinity of the asperities.

In conclusion this portion of the research provided considerable knowledge with respect to surface temperature prediction, the role of surface roughness, and the nature of scuffing. But the prediction and clear understanding of scuffing itself remains illusive.

Surface Roughness Characterization for Elastohydrodynamic Contacts

In conjunction with the above-mentioned surface roughness temperature studies some interesting observations were made which are of practical

significance. During low lambda ratio experiments the temperature fluctuations were recorded and subjected to spectral analysis. Surface profiles were also recorded before and after an experiment at the same location on the surface and these were also subjected to spectral analysis. The surface finish had no preferred orientation and was typical of good engineering practice. By these analyses it was found that, although the surface roughness had a power spectra with a wide wavelength range of components, only a very narrow wavelength range was involved in the asperity interactions which caused the temperature fluctuations. The elastohydrodynamic contact acts as a mechanical filter on the surface roughness and is unaffected by surface roughness outside a narrow wavelength band. The significant band has wavelengths from about 1/2 to 2 times the Hertz diameter of the contact. It now appears clear that in many applications where surface finish is important, there will be a characteristic dimension which can be used to normalize the surface finish wavelength and to determine the significant components of the surface finish for the particular application. These results have important implications in the specification, measurement and production of surface finish.

Lubricant Rheological Studies

The subject of lubricant rheology has long been of interest to this laboratory. Two projects on this subject have been part of the research effort under this grant.

The earlier work in this laboratory on lubricant molecular degradation in elastohydrodynamic contacts was extended to study the degradation

of a series of polymers which are of commercial importance in the automotive engine oil field. This study showed that the polymers were extensively degraded in the high energy dissipation field of the EHD contact. They have almost no influence on contact traction and very little influence on the film thickness developed. Because only a minute fraction of the total lubricant in an automotive engine passes through EHD contacts, the permanent degradation of the bulk engine oil is less than that which has gone through an EHD contact. For this reason the EHD results did not correlate well with engine studies. The EHD simulator would, however, be a good bench test to screen polymers for their tendency to mechanically degrade. This work resulted in a paper presented to the American Chemical Society.

The second activity relating to lubricant rheology was jointly supported by a grant from NASA and was concerned with the possible role of glass transition of the lubricant in the elastohydrodynamic contact. Facilities were developed for measuring glass transition as a function of pressure in two separate ways. One utilizes Brillouin light scattering and the other volume dilatometry. Data obtained on several lubricants demonstrate that many lubricants will go through a glass transition in elastohydrodynamic contacts under typical operating conditions.

The light scattering experiments were to pressures of 0.4 GPa while dilatometry measurements were made to 1.4 GPa. When the transition data is related to EHD conditions it is clear that many current lubricants in typical contacts undergo a transition in rheological response to solidlike behavior. This is borne out by EHD data in the literature on the same materials. The observed EHD behavior can be explained

in terms of the glass transition measurements. As a result of these observations a program of studying the shear rheological response of these materials in the glassy state has been started. A limiting shear stress type behavior has been observed. These glassy state studies have lead to several papers and invited lectures and will continue. The findings are believed to have significant impact on the field of EHD in general and traction drive development in particular.

Institutional Interaction

Program interaction exists on the temperature/scuffing research, the surface roughness studies and the lubricant rheology areas.

Identical lubricants were secured for all three Institutions to conduct elastohydrodynamic experiments on the same material. Rensselaer Polytechnic Institute conducted steel-steel scuffing experiments under the same conditions as were used to measure surface temperatures in the steel-sapphire system. Northwestern has been measuring the effect of surface roughness on the film forming ability under similar conditions.

We provided Northwestern with a three dimensional mapping of surfaces on magnetic tape to be utilized in an elastohydrodynamic analysis of surface roughness-film thickness interactions. The recorded surfaces include typical surfaces used in our experiments as well as specifically tailored surfaces with different orientations.

MISCELLANEOUS ACTIVITIES

During the course of this grant the principal investigator was invited to present lectures and visit laboratories in Europe (September 1977). During that trip, which was funded on this grant, the principal investigator presented papers at the Leeds-Lyon Symposium on Surface Roughness Effects in Lubrication; at INSA (University of Lyon) in Lyon, France. During that meeting he also chaired a technical session. In the first few days of October, the author also attended the Eurotrib meeting sponsored by the International Council on Tribology at Dusseldorf. He presented an invited review paper on "Direct Surface Temperature Measurement by Infrared Radiation in EHD, and the Correlation with the Blok Flash Temperature Theory",. During the approximately one month trip to Europe for these two lectures, the principal investigator also acted as an external examiner for three Master's Theses in the field of lubrication at INSA (University of Lyon). He also visited and conducted research discussions with colleagues at the University of Cambridge, University of Leicester, and BAMM in West Berlin.

During the course of this grant, the Georgia Institute of Technology hosted three visiting foreign scholars whose trips were in part supported by the grant. The three scholars who visited our laboratory for varying amounts of time (two to four days) were:

Dr. Horst Czichos (10-13 June 1976)
BAMM
D-1 Berlin 45
Unter den Eichen 82
West Germany

Dr. Lou Rozeanu (20-22 June 1976)
Technion-Israel Institute of Technology
Haifa, Israel

Dr. A. Dyson (30 September and 1 October 1976)
Shell Thornton Research Center
P.O. Box #1
Chester, England

Professor H. Blok, University of Delft, was also invited and expected to visit in September of 1976 but due to personal problems cancelled at the last minute.

RESEARCH PERSONNEL

Winer, Ward O.	Professor, Principal Investigator
Sanborn, David M.	Associate Professor, Faculty Associate
Bair, Scott	Research Engineer

Graduate Students

Alsaad, Mohammed	Ph.D. granted September 1976 Research contributions in the area of the light-scattering study of glass transition and glassy state in lubricating oils Thesis title: "Lubricant Rheology in the Glassy State"
Nagaraj, H.S.	Ph.D. granted December 1976 Research contributions in the area of infrared temperature measurements in EHD films Thesis title: "Thermal Phenomena in Elastohydrodynamic Contacts"
Kunz, Richard K.	M.S.M.E. granted December 1974 Research contribution in the area of analytical treatment of surface temperatures and tractions in EHD lubrication Thesis title: "Thermal and Traction Behavior in an Elastohydrodynamic Contact"
Khemka Vijay	M.S.M.E. granted January 1978 Research contributions in the area of shear viscoelastic transitions at atmospheric pressures Thesis title: "Viscoelastic Transition of Lubricants"

Undergraduate Research Assistants

Bacon, Doris	January 1977 - assistance in dielectric measurements
Barrington, J.	June 1976 - assistance in dielectric measurements

C. Technical Papers (Continued)

6. "Direct Surface Temperature Measurement by Infrared Radiation in EHD, and the Correlation of the Blok Flash Temperature Theory", presented at Eurotrib 77 World Tribology Conference, and to be published in WEAR (H.S. Nagaraj, D. M. Sanborn and W. O. Winer).

7. "The Effect of Surface Roughness on Surface Temperature Fluctuations in EHD Contacts", presented at Leeds-Lyons Conference, September 1977, and to be published in the Proceedings of Leeds-Lyon Conference (H.S. Nagaraj, D. M. Sanborn and W. O. Winer).

8. "Surface Temperature Measurements in Rolling and Sliding EHD Contacts", to be published in ASLE Trans. (H. S. Nagaraj and W. O. Winer).

9. "Effects of Load, Speed, and Surface Roughness on Sliding EHD Contact Temperatures", Journal of Lubrication Technology, Vol. 99, No. 2, April 1977 (H. S. Nagaraj, D. M. Sanborn and W. O. Winer).

PUBLICATIONS ACKNOWLEDGING NSF

A. Student theses completed and published
(for investigation completed under Grant GK-31154)

1. Alsaad, Mohammed A., Ph.D.
"Lubricant Rheology in the Glassy State"
September 1976

2. Nagaraj, H.S., Ph.D.
"Thermal Phenomena in Elastohydrodynamic Contacts"
December 1976

3. Kunz, R. K., M.S.M.E.
"Thermal and Traction Behavior in an Elastohydrodynamic Contact"
December 1974

4. Khemka, Vijay K., M.S.M.E.
"Viscoelastic Transition of Lubricants"
January 1978

C. Technical Papers

1. "Lubricant Properties in Thin Lubricating Films", American Chemical Society, Division of Petroleum Chemistry Preprints, Vol. 21, No. 1, 1976, pp. 57-67 (D. M. Sanborn, W. O. Winer).

2. "Light-Scattering Study of the Glass Transition in Lubricants", presented at the ASME/ASLE Lubrication Conference, Kansas City, Missouri, October 1977 and to be published Trans. ASME, Journal of Lubrication Technology, ASME Paper No. 77-Lub-15 (M. A. Alsaad, F. D. Medina and D. C. O'Shea and W. O. Winer).

3. "Asperity Interactions in EHD Contacts", presented at the ASME/ASLE Lubrication Conference, Kansas City, Missouri, October 1977 and to be published Trans. ASME, Journal of Lubrication Technology, ASME Paper No. 77-Lub-19 (H.S. Nagaraj, D. M. Sanborn and W. O. Winer).

4. "Glass Transitions in Lubricants: Its Relation to EHD Lubrication", presented at the ASME/ASLE Lubrication Conference, Kansas City, Missouri, October 1977 and to be published Trans. ASME, Journal of Lubrication Technology, ASME Paper No. 77-Lub-3 (M. A. Alsaad, S. Bair, D. M. Sanborn and W. O. Winer).

5. "Glass Transitions in Lubricants: Its Relation to Elastohydrodynamic Lubrication (EHD)", Bulletin of the Japan Petroleum Institute, Vol. 19, No. 1, May 1977 (M. Alsaad, S. Bair, D. M. Sanborn and W. O. Winer).

PREPRINTS

Symposia

Symposium on Advanced Processes for Oil Refining, Etc.

Co-Chairmen: [illegible]

Symposium on Sulfur in Stored Chemicals (Joint with Division of Fuel Chemistry)

Co-Chairmen: [illegible]

Papers from Chicago Meeting, August 29-Sept. 3, 1976

AMERICAN CHEMICAL SOCIETY 1876-1976

DIVISION OF PETROLEUM CHEMISTRY, INC.
American Chemical Society

New York, N.Y.
April 4-9, 1976

Volume 21, No. 2
Advance Copy

1. Presented at The Division of Petroleum Chemistry, Inc. American Chemical Society, New York Meeting, 4-9 April 1976

(1) Low, M. J. D., and Coleman, I., Spectrochim. Acta, 22, 369 (1966).
(2) Allen, C. M., Draughis, E., Glaeser, W. A., Alexander, C. A., and Jakobsen, R. J., Technical Report, AFAPL-TR-73-121, Vol. 11, Battelle Columbus Laboratories, January 1975.
(3) Lauer, J. L., and Peterkin, M. E., Developments in Applied Spectroscopy, Vol. 10, New York, Plenum Press, 1972.
(4) Hirst, W., and Moore, A. J., Proc. Roy. Soc. London A, 344, 403 (1975).
(5) Lauer, J. L., and Peterkin, M. E., Trans. ASME, J. of Lubrication Technology, 97, 145 (1975).
(6) Foord, C. A., Wedeven, L. D., and Westlake, F. J., J. Institution of Mechanical Engines, 184, Part 1, 1970.
(7) Goldblatt, I. L., ASLE Trans., 16, No. 2, 150 (1973).
(8) Jones, W. R., NASA TN D-7804, October 1974.
(9) Jones, W. R., Private Communication, November 11, 1975.
(10) Turchina, V., Sanborn, D. M., and Winer, W. O., Trans. ASME, J. of Lubrication Technology, Series F, 96, No. 3, 464 (July 1974).

AMERICAN CHEMICAL SOCIETY
NEW YORK MEETING, APRIL 4-9, 1976

LUBRICANT PROPERTIES IN THIN LUBRICATING FILMS

By

D. M. Sanborn and W. O. Winer
School of Mechanical Engineering, Georgia Institute of Technology, Atlanta, Georgia 30332

INTRODUCTION

The lubrication of highly loaded machine elements (gears, cams, etc.) frequently result in lubricant films less than 3 μm thick. These thin lubricant films are subjected to pressures to 3 GN/m^2, shear stresses to 0.2 GN/m^2 and shear rates in excess of 10^6 s^{-1}. Lubrication under these conditions is referred to as elastohydrodynamics lubrication (EHD). These conditio result in mechanical energy dissipation rates in the lubricant of up to 0.2 TW/kg which causes both high temperature and irreversible molecular degradation. Temperatures of the lubricant film have been measured by an infrared technique (1) and have been found to be as high as 300°C

This paper describes a technique for obtaining a lubricant sample from a highly loaded sliding elastohydrodynamic contact which simulates machine elements such as cams and gears. The samples are analyzed for irreversible changes in rheological properties by measuring the viscosity and in some cases measuring the molecular weight distribution.

Automotive engine lubrication with multi-grade motor oils containing high polymers is one area where irreversible polymer degradation is important. Several studies have been reported where attempts were made to develop a bench test which simulated actual engine perform The measure used to evaluate the bench test was the correlation of the results of the bench test with those of automobile fleet tests on a standard set of blended oils. A review of this program through 1974 was presented by Steward and McMillan (2). Although a bench test has the advanta of requiring a small sample and short testing time compared to fleet testing, the bench test doe not always subject the lubricant to the combined conditions of high pressure and high shear stre which occur in the highly loaded elastohydrodynamic contacts in an engine. The bench test described in this paper overcomes this disadvantage except that although the temperatures in the c tact can be high for the short time, the lubricant is in the contact ($\leq$ 1.0 ms), the average bulk temperature of the sample is low (40°C) and the test lasts only two hours or less. However, in engine test the bulk oil temperature is typically 125°C and the test may last for up to 25 hours. This can result in some oxidative increases in oil viscosity to counteract the viscosity decrease resulting from mechanical shear degradation.

The objective of this study was to subject a variety of fluids to conditions that are found in elastohydrodynamic lubrication and to determine the extent of the molecular degradation. T fluids were subjected to peak pressures of 1 GN/m^2 and shear rates of 10^6 to 10^7 s^{-1} in an elastohydrodynamic simulator. Samples of the fluid were collected for low shear rate viscosit measurements. In those cases where data was available the viscosity average molecular weigh of the sheared sample was also determined (3,4). In a few cases the molecular weight distribu tions of the sheared and unsheared samples were obtained and compared.

Test Lubricants

The lubricants selected for examination were chosen so that a wide range of molecular weights and fluid types could be tested. They are listed in Tables IA and IB.

As representative examples of the hydrocarbon type fluids, a paraffinic base oil (P1) a three solutions of high molecular weight polyalkylmethacrylate (PAMA) were chosen. Two of these solutions used a PAMA additive with a viscosity average molecular weight (MW_v) of 560, atomic units (au) with concentrations of 4 percent and 8 percent, P2 and P3 respectively. The third solution used a PAMA additive with a MW_v of 1,650,000 au and a concentration of 4 perce (P6). In this manner variations with concentration and MW could be studied. The paraffinic b oil with an average MW of 404 was also tested as a control.

Four synthetic fluids were also tested. A commercially available silicone diffusion pu fluid (S5) with a MW of 546 au was tested because of its very narrow MW distribution which pe mitted small changes in MW to be detected. Another commercially available silicone lubricat which had a bimodal MW distribution centered around molecular weights of 10,000 and 47,000 tested (S6). In addition, a sebacate diester (MW = 426) (S1) and a modified polyphenyl ether (MW = 425) (S2) were examined.

TEST FLUIDS

Designation	Fluid Description*
P1	Paraffinic base oil (R-320-12)
P2	P1 + 4 percent polyalkylmethacrylate (PL-4521)
P3	P1 + 8 percent polyalkylmethacrylate (PL-4521)
P6	P1 + 4 percent polyalkylmethacrylate (PL-4523)
S1	Diester-bis-2-ethyl hexyl sabacate (PL-5159)
S5	Pentaphenyltrimethyltrisiloxane (DC-705)
S6	Dimethylsiloxane (DC-200)
S9	Modified Polyphenyl Ether (MCS-418)

*Manufacturer's designation is shown in parentheses.

In addition, Table IB shows a series (ARO) of twelve oils, which were formulated for the ASTM shear stability program using all the commercially available chemical types of polymeric viscosity index (VI) improvers available in 1970. (There were originally 13 oils in the ARO series but Oil No. 104 was not available to us.) All the ARO oils were blended with the same batch of detergent-inhibitor package and used a combination of two base stocks from the same refinery. The base stock ratios and polymer concentrations were adjusted so that the finished oil viscosities at 98.9°C (210°F) and -17.8°C (0°F) were comparable for the SAE 10W/40 oils (ARO 101 through 113). The two SAE 10W/30 oils (ARO 111 and 112) were also blended to be comparable at 98.9°C (210°F) and -17.8°C (0°F). The SAE 20W/20 (ARO 113) was blended without a V.I. improver to serve as a control oil. More information on the ARO Test oils can be found in Stewart and McMillan (2).

TABLE IB

ARO TEST FLUIDS

ARO Oil No.	V.I. Improver Type	SAE Viscosity Grade	98.9 Viscosity $m/s^2 \times 10^6$	37.8 Viscosity $m/s^2 \times 10^6$	-17.8 Viscosity $ns/m^2 \times 10^3$
101	Polymethacrylate-1	10W/40	15.08	86.33	2040
102	Polymethacrylate-2	10W/40	15.03	85.92	2030
103	Polyisobutylene	10W/40	14.98	97.91	1970
105	Vinyl Copolymer	10W/40	14.87	83.94	1930
106	Polyacrylate	10W/40	14.96	76.27	1940
107	Polyalkylstyrene	10W/40	15.14	97.26	2000
108	Olefin terpolymer	10W/40	14.96	104.84	1880
109	Styrene polyester	10W/40	15.23	90.53	1940
110	Olefin copolymer-2	10W/40	15.01	104.26	1950
111	Polymethacrylate-1	10W/30	10.97	66.31	2020
112	Polyisobutylene	10W/30	11.03	74.88	2100
113	None	20/20W	6.72	48.54	2600

EXPERIMENTAL

The experimental equipment is a modification of the apparatus used to study elastohydrodynamic film thickness, traction (5,6) contact temperatures by infrared radiation (7,8) and lubricant sampling (9). Further details of the apparatus relating to each of the measurements cited can be found in those references.

The equipment is shown schematically in Figure 1. The sliding elastohydrodyramic point contact is formed by rotating a 31.8 mm-dia. steel sphere which is loaded against a sapphire disk. The sphere has a surface finish of 0.038 μm. Optical interference techniques were used to

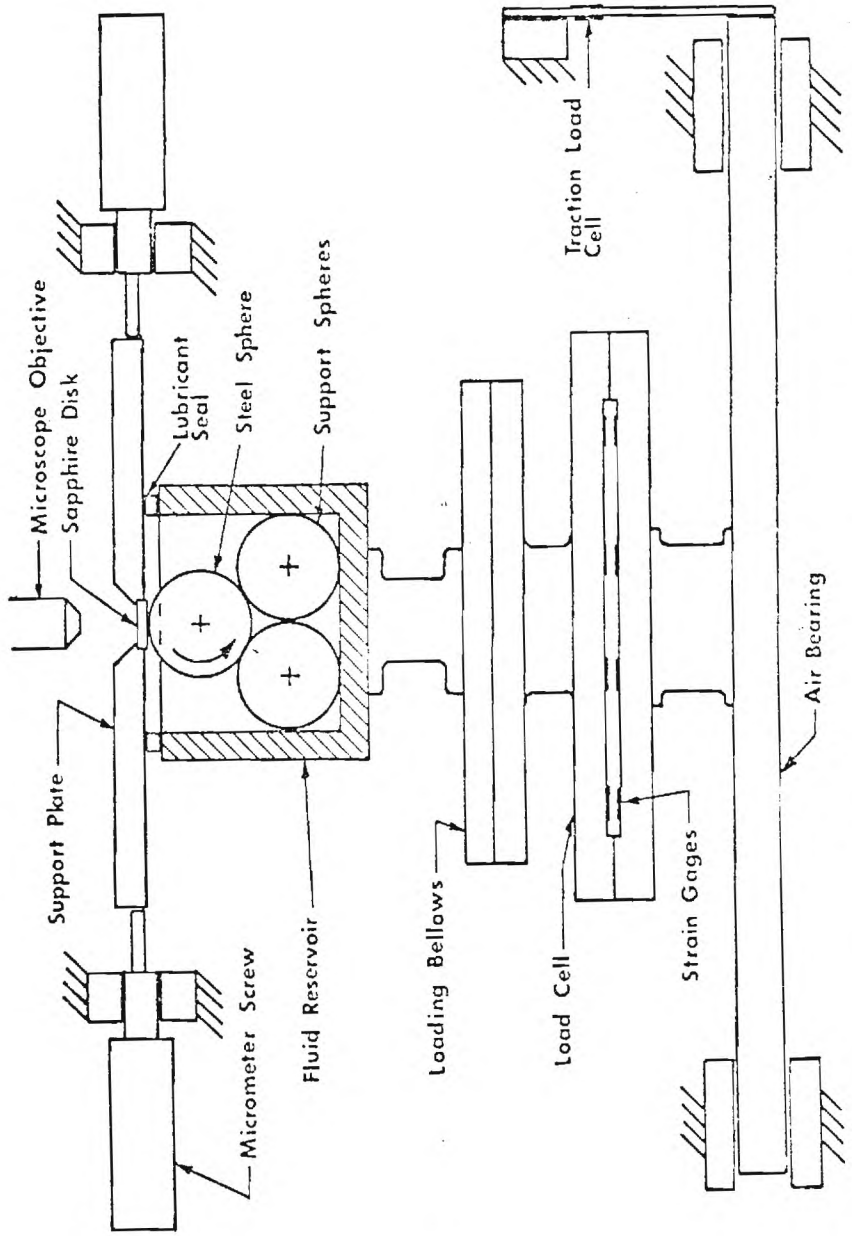

Figure 1. Schematic Diagram of the Experimental Equipment

TEST FLUIDS

Designation	Fluid Description*
P1	Paraffinic base oil (R-320-12)
P2	P1 + 4 percent polyalkylmethacrylate (PL-4521)
P3	P1 + 8 percent polyalkylmethacrylate (PL-4521)
P6	P1 + 4 percent polyalkylmethacrylate (PL-4523)
S1	Diester-bis-2-ethyl hexyl sabacate (PL-5159)
S5	Pentaphenyltrimethyltrisiloxane (DC-705)
S6	Dimethylsiloxane (DC-200)
S9	Modified Polyphenyl Ether (MCS-418)

*Manufacturer's designation is shown in parentheses.

In addition, Table IB shows a series (ARO) of twelve oils, which were formulated for the ASTM shear stability program using all the commercially available chemical types of polymeric viscosity index (VI) improvers available in 1970. (There were originally 13 oils in the ARO series but Oil No. 104 was not available to us.) All the ARO oils were blended with the same batch of detergent-inhibitor package and used a combination of two base stocks from the same refinery. The base stock ratios and polymer concentrations were adjusted so that the finished oil viscosities at 98.9°C (210°F) and -17.8°C (0°F) were comparable for the SAE 10W/40 oils (ARO 101 through 113). The two SAE 10W/30 oils (ARO 111 and 112) were also blended to be comparable at 98.9°C (210°F) and -17.8°C (0°F). The SAE 20W/20 (ARO 113) was blended without a V.I. improver to serve as a control oil. More information on the ARO Test oils can be found in Stewart and McMillan (2).

TABLE IB

ARO TEST FLUIDS

ARO Oil No.	V.I. Improver Type	SAE Viscosity Grade	98.9 Viscosity $m/s^2 \times 10^6$	37.8 Viscosity $m/s^2 \times 10^6$	-17.8 Viscosity $ns/m^2 \times 10^3$
101	Polymethacrylate-1	10W/40	15.08	86.33	2040
102	Polymethacrylate-2	10W/40	15.03	85.92	2030
103	Polyisobutylene	10W/40	14.98	97.91	1970
105	Vinyl Copolymer	10W/40	14.87	83.94	1930
106	Polyacrylate	10W/40	14.96	76.27	1940
107	Polyalkylstyrene	10W/40	15.14	97.26	2000
108	Olefin terpolymer	10W/40	14.96	104.84	1880
109	Styrene polyester	10W/40	15.23	90.53	1940
110	Olefin copolymer-2	10W/40	15.01	104.26	1950
111	Polymethacrylate-1	10W/30	10.97	66.31	2020
112	Polyisobutylene	10W/30	11.03	74.88	2100
113	None	20/20W	6.72	48.54	2600

EXPERIMENTAL

The experimental equipment is a modification of the apparatus used to study elastohydrodynamic film thickness, traction (5,6) contact temperatures by infrared radiation (7,8) and lubricant sampling (9). Further details of the apparatus relating to each of the measurements cited can be found in those references.

The equipment is shown schematically in Figure 1. The sliding elastohydrodyramic point contact is formed by rotating a 31.8 mm-dia. steel sphere which is loaded against a sapphire disk. The sphere has a surface finish of 0.038 μm. Optical interference techniques were used to

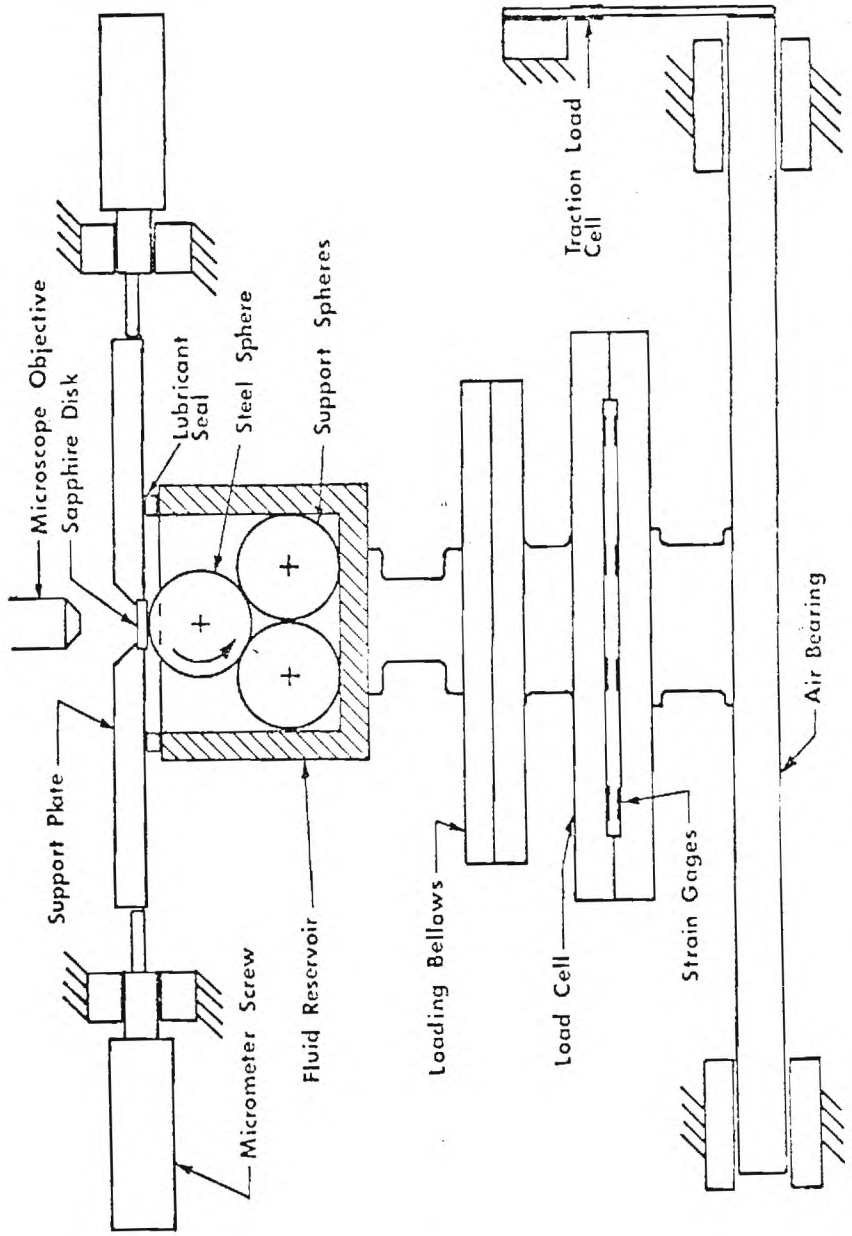

Figure 1. Schematic Diagram of the Experimental Equipment

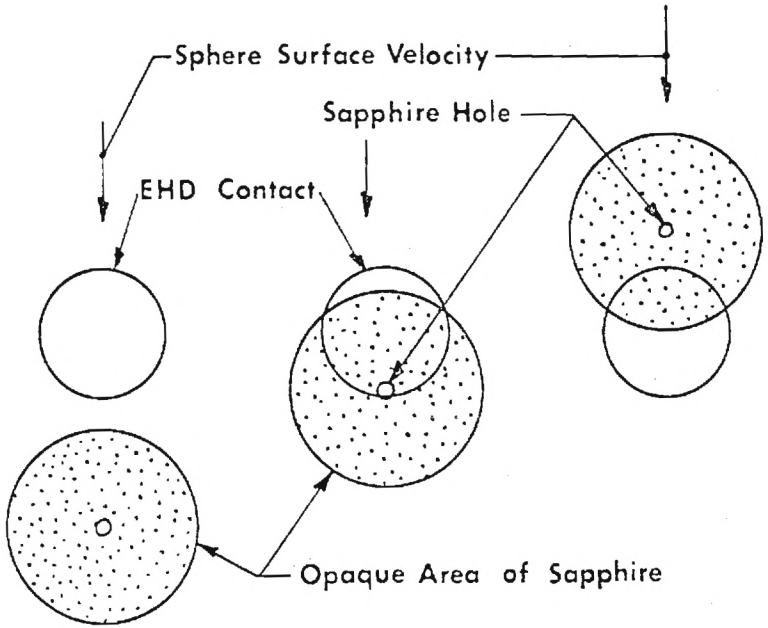

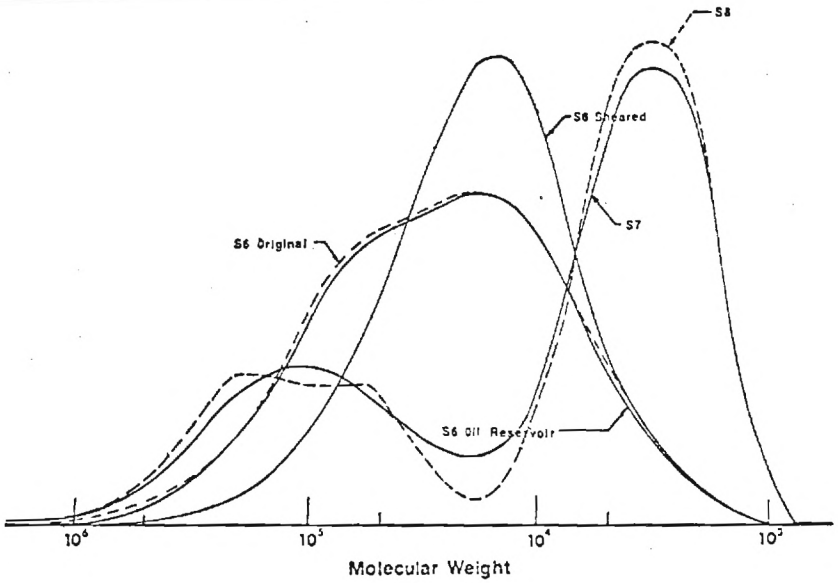

Figure 3. Molecular Weight Distribution, Fluids S6, S7, And S8

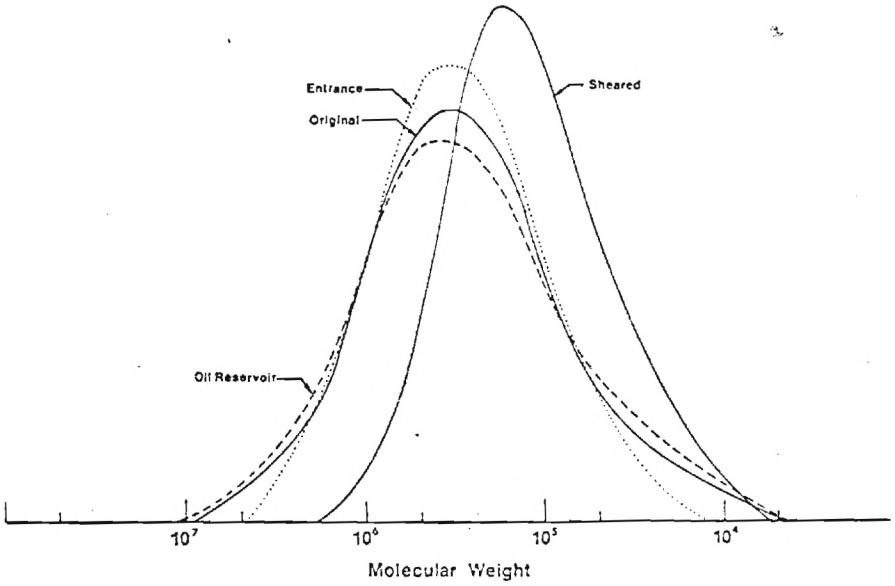

Figure 4. Molecular Weight Distribution, Fluid P2

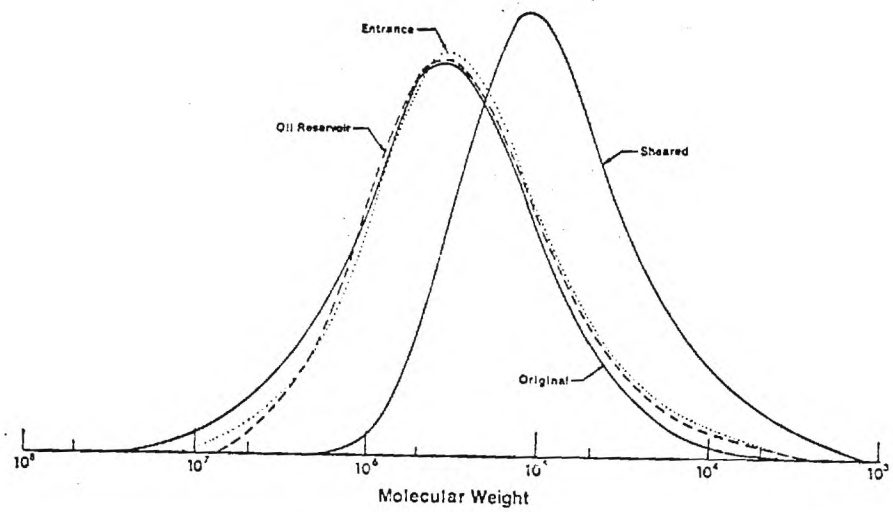

Figure 5. Molecular Weight Distribution, Fluid P3

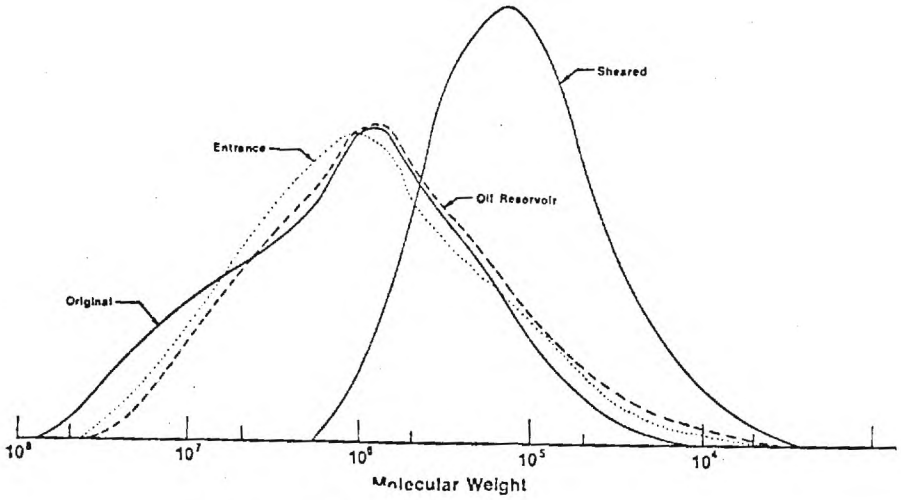

Figure 6. Molecular Weight Distribution, Fluid P6

The surface temperature of the steel sphere at the center of the EHD contact was measured by replacing the optical microscope with an infrared microdetector. The details of that technique can be found in reference (8).

The technique used for extracting a lubricant sample from the contact entrance and exit involved introducing a hole in the sapphire flat into the desired region. This orifice was then allowed to fill up with the lubricant. Most of the data was taken using a sapphire disk 7.87 mm in dia., 1.52 mm thick and with a conical hole having a minimum diameter of approximately 50 μm at the oil interface. A micrometer screw adjustment mechanism (Figure 1) allowed the orifice in the sapphire to be positioned at the desired location. Both the hole and EHD contact could be observed through the microscope.

Figure 2 shows the orifice in the sapphire in relation to the EHD contact. The dark area surrounding the minimum hole diameter is a result of the conical shape of the orifice. When the orifice was moved up to the exit edge of the contact, the flow of lubricant into the cone could be observed. When a sufficient amount of oil had collected on the sapphire, two 10^{-6} m^3 samples were extracted using disposable syringes. In order to compare changes in molecular weight and viscosity, samples were also taken from the fluid reservoir and the original sample container.

TABLE II

ELASTOHYDRODYNAMIC OPERATING CONDITIONS

Fluid	μ_0 (25°C) NS/m^2	Load N	Speed m/s	h_c μm	TC	Contact* Surface Temperature C
P1	0.052	65	2.36	0.22	0.035	
P2	0.112	67	2.34	0.25	0.033	
P3	0.274	67	2.34	0.31	0.032	
P6	0.240	67	2.34	0.25	0.038	
S1	0.017	67	2.34	0.09	0.024	
S5	0.175	69	1.45	0.43	0.068	
S6	0.931	69	2.41	0.25	0.027	
S9	0.056	67	2.34	0.30	0.042	
ARO 101	(a)	53.38	1.52	0.19	0.042	64
ARO 102		53.38	1.52	0.16	0.042	75
ARO 103		53.38	1.52	0.19	0.048	77
ARO 105		53.38	1.52	0.16	0.046	78
ARO 106		53.38	1.52	0.20	0.053	83
ARO 107		53.38	1.52	0.19	0.048	77
ARO 108		53.38	1.52	0.18	0.049	74
ARO 109		53.38	1.52	0.20	0.051	72
ARO 110		53.38	1.52	0.19	0.049	74
ARO 111		53.38	1.52	0.20	0.051	90
ARO 112		53.38	1.52	0.18	0.048	73
ARO 113		53.38	1.52	0.23	0.053	79

(a) See Table IB.
* at the center of contact

The experimental conditions for each test are given in Table II. Also listed are the centerline film thickness, the traction coefficient (TC) and, for the ARO oils, the sphere surface temperature in the center of the contact. Table III is a summary of the average conditions experienced by the fluid in the EHD contact. An average shear rate $\dot{\gamma}$ is determined from the relative velocity of the bearing surfaces divided by the film thickness. The average shear stress τ is calculated by dividing the traction force by the contact area. The energy dissipation rate per unit volume (E) is given by the product of the shear stress and the shear rate. Finally, the energy dissipation rate per kg of lubricant ($\dot{\epsilon}$) is determined by dividing E by the lubricant density.

A variety of techniques were used to analyze the samples obtained from the EHD contact. The viscosity of most of the fluids was measured in a microcapillary. In a few cases molecular weight distributions were also obtained. The micro-capillary was made from a glass tube with a capillary section 60 mm long by 75 μm inside diameter. The capillary was used in a constant

Measurements were highly repeatable in both flow directions through the capillary. As a check on the procedure, the viscosities of samples of an unsheared fluid were determined using both the microcapillary and standard capillary viscometers. Good agreement was found. The MW-viscosity correlation proposed by Barry (3) was then used to determine MW from the micro capillary results for the siloxanes while the relation proposed by Wright and Crouse (4) was used for the PAMA solutions.

TABLE III

ENERGY DISSIPATION

Fluid	$\dot{\gamma} \times 10^{-6}$ s^{-1}	$\tau \times 10^{-6}$ N/m^2	$E \times 10^{-12}$ W/m^3	$\dot{\epsilon} \times 10^{-12}$ W/kg
P1	10.7	25.2	287	0.33
P2	9.4	24.8	211	0.25
P3	7.5	23.0	184	0.21
P6	9.3	27.4	257	0.31
S1	25.0	17.3	459	0.50
S5	3.4	49.0	176	0.16
S6	9.5	19.5	196	0.20
S9	7.8	30.2	251	0.21
ARO 101	8.0	26.5	212	0.26
ARO 102	9.5	26.5	252	0.30
ARO 103	8.0	30.3	242	0.29
ARO 105	9.5	29.1	276	0.33
ARO 106	7.6	33.5	255	0.31
ARO 107	8.0	30.3	242	0.29
ARO 108	8.4	31.0	260	0.32
ARO 109	7.6	32.2	245	0.30
ARO 110	8.0	31.0	248	0.30
ARO 111	7.6	32.2	245	0.30
ARO 112	8.4	30.3	255	0.31
ARO 113	6.6	33.5	221	0.27

In addition to the microcapillary measurements, molecular weight distributions were obtained for the higher polymers (P2, P3, P6) and silicones (S5, S6) using gel permeation chromatography (GPC).

RESULTS

All but two of the lubricants exhibited permanent changes in viscosity as a result of being sheared in the EHD contact. Three others had less than 5 percent permanent change in viscosity. All five of the fluids with little permanent change in viscosity were fluids with no high polymer constituents. They all had average molecular weights of less than 600. In two of these cases the viscosity increased (S1 - 4.3% and S9 - 0.7%) apparently as a result of the degradation products causing a slight increase in viscosity. In all other cases the fluids had some high molecular weight polymer components and the permanent reduction in viscosity ranged up to 75% while the reduction in average molecular weight ranged up to 91%. These results are shown in Table IV.

With the low MW silicone fluid S5, no degradation was detectable. This fluid was tested by the manufacturer using a gas chromatograph. Silicone fluid S6 exhibited marked degradation after shearing in the EHD contact. Both viscosity and GPC measurements were made on this fluid. The permanent viscosity loss was found to be 56.1 percent. The results of the GPC tests are shown in Figure 3. The location at which each sample was extracted is noted on the figure. There is virtually no change in the molecular weight distribution (MWD) between the original fluid and the sample taken from the oil reservoir; however, there is marked change after the fluid has passed through the EHD contact. The viscosity loss was calculated from the MW found with the GPC and was found to be 61.4 percent.

Two additional silicones (S7 and S8), were specifically blended to give an indication of a limiting MW for degradation but were not successfully tested. Although a fluid film could be

and the sphere with subsequent scratching of both in most cases. Figure 3 shows the MWDs for these two fluids and by comparison with the unsheared samples of fluid S6, it can be seen that they have a greater concentration of high MW fractions and are more disperse in makeup.

TABLE IV

EXPERIMENTAL RESULTS

Fluid	$\Delta\mu$[1] @ 98.96%	Mol. wt. Unsheared Sample	ΔMW[2] %
P1	1.6[3]	404	0
P2	42.3	5.6×10^5 (5)	72.3 (5)
P3	61.0	5.6×10^5 (5)	80.2 (5)
P6	73.6	1.65×10^6 (5)	91.2 (5)
S1	-4.3[3]	426	0
S5	0	546	0
S6	56.1[4]	2.6×10^4	
S9	-0.7[3]	422	-0.4
ARO 101	43.8		
ARO 102	44.8		
ARO 103	37.0		
ARO 105	38.1		
ARO 106	9.8		
ARO 107	12.0		
ARO 108	57.1		
ARO 109	30.0		
ARO 110	47.6		
ARO 111	34.5		
ARO 112	32.8		
ARO 113	0		

1) $\Delta\mu = \frac{\mu_o - \mu_s}{\mu_o} \times 100$; $\mu_o \equiv$ unsheared viscosity; $\mu_s \equiv$ sheared sample viscosity

2) $MW = \frac{MW_o - MW_s}{MW_o} \times 100$; $MW_o \equiv$ average molecular weight of original sample; $MW_s \equiv$ average molecular weight of sheared sample

3) indicates data at 38°C

4) indicates data at 25°C

5) molecular weight of polymer only

A slight increase in viscosity and MW (as determined from gas chromatography by the manufacturer) was found in the sheared samples of fluid S9, the modified polyphenyl ether. However, these changes were both within experimental error. A small amount of a low boiling point substance was found in all of the samples except the original fluid. It is thought that this might be an indication of some degradation.

Fluid S1, the diester, exhibited a marked increase in viscosity, 4.3 percent, however, neither IR spectroscopy, gas chromatography nor mass spectroscopy could detect any change in the composition of the fluid. The increase in viscosity is typical of what has been found in extended service conditions (10).

The paraffinic base oil P1 was tested in a cone and plate viscometer and a 1.6 percent decrease in viscosity was found. However, this is within the experimental error (± 2%) of this particular instrument. Because of its low MW, the other analytical techniques mentioned above were not used to establish a molecular weight distribution.

The permanent viscosity decreases in the PAMA solutions, fluids P2, P3, and P6, were found to be extreme, up to 70 percent. In fact, the viscosities of these solutions were reduced almost to the viscosity of the base oil (P1). The molecular weight distributions for the polymers in these three solutions were obtained by the manufacturer using GPC and are shown in Figures 4-6. It can be seen that only a small amount of shearing takes place in the oil reservoir and the entrance region of the EHD contact.

Table V includes the viscosity loss at 98.6°C for the ARO fluids as measured in this study along with the viscosity loss for these fluids in a series of automobile fleet tests. The fleet test

mobiles with conventional engine designs and 3) the Institute of Petroleum Fleet A consists of data from a European Fleet of automobiles with a common sump for the engine and transmission. The European Fleet A with common sump for transmission and engine results, as expected, in more severe lubricant degradation because the transmission gearing subjects the lubricant to more EHD contacts. However, the permanent viscosity loss after the 1500 mile (2414 km) fleet test is still not as large as that occurring in the EHD bench test reported here.

TABLE V

VISCOSITY LOSS (cSt.) AT 98.9°C OF ARO OILS IN EHD SIMULATOR EXPERIMENT COMPARED TO AUTOMOTIVE FLEET TESTS

ARO No.	EHD Simulator	U.S. Six-Fleet Average	European Fleets A	B
101	6.61	1.64	3.38	2.02
102	6.73	3.03	4.73	3.18
103	5.54	1.75	4.54	--
105	5.67	4.06	--	4.06
106	1.47	3.85	--	3.78
107	1.82	2.17	--	2.25
108	8.54	2.37	6.07	--
109	4.57	0.04	3.17	--
110	7.14	0.34	3.59	0.55
111	3.78	0.67	-	--
112	3.62	0.74	--	--
113	0	-0.31	--	--

It is clear from the results shown in Table V that the EHD simulator experiment causes more severe permanent degradation in the polymer blends than that occurring in an automotive engine. A least squares linear regression between the viscosity loss in the laboratory experiment and the fleet tests produce correlation coefficients of only 0.17 when the U.S. Six-Fleet average is used and 0.57 when compared to the European fleet A which had the common sump for transmission and engine. There are several possible reasons for this poor correlation. They include the fact that the sample from the EHD contact has not been diluted as would occur in the engine test, the EHD sample had not been subjected to the oxidative environment which the engine sample had been subjected to, and that the EHD conditions used in the laboratory experiment may have been more severe than those occurring in the engine.

It has further been suggested that the EHD contact inlet flow may segregate out the larger polymer molecules resulting in a change of concentration as well as molecular weight distribution in the sample collected from the EHD contact. However, this seems unlikely because the areas under the GPC curves of the original and sheared samples are essentially the same suggesting that the polymer concentration has not changed. This point needs further clarification however.

RESULTS

A significant change in viscosity was found in fifteen of the twenty lubricants tested, with a maximum decrease of seventy-three percent. Changes in average molecular weight of the polymer were also found with a maximum decrease of ninety percent. This large amount of degradation indicates that the EHD contact may be the primary source of molecular degradation occurring in lubricants. The permanent viscosity loss also may explain the disagreement that has been reported between experimental data and theoretical predictions of film thickness for high MW fluids (5, 11).

The non-Newtonian behavior of certain fluids under high shear conditions has previously been given as the reason for the lack of agreement between theory and experiment in EHD lubrication. For the hydrocarbon solutions tested in this study, this lack of agreement can be explained by permanent degradation of the fluid. In a previous publication (5), the authors determined an apparent viscosity loss S by estimating an effective viscosity μ_e which would bring the film thickness data for high MW fluids into agreement with data for Newtonian fluids. This apparent viscosity is defined by

$$S = 1 - \frac{\mu_o}{\mu_o}$$

VI lists these values for the fluids which were studied in both works. The correlation is apparent. The quantitative differences are partially explained by the fact that the base viscosities were measured at different temperatures. Also, in the degradation studies, samples were extracted from near the contact centerline. The samples have, therefore, been subjected to the highest shear stresses in the EHD contact. The apparent viscosity loss determined on the basis of film thickness correlations would be influenced by degradation in the contact inlet, which has shear stresses somewhat lower than the maximum expected near the contact center. It is generally believed that the viscosity in the inlet zone of an EHD contact controls the film thickness of the contact. The correlation shown in Table VI suggests that there may be significant carryover of the fluid on the ball surface causing the inlet to be very dependent on fluid already sheared in the contact.

TABLE VI

APPARENT AND PERMANENT VISCOSITY LOSSES

Fluid	S (10)	S_p
P1	0.00	0.02
P2	0.26	0.42
P3	0.54	0.61
P6	0.63	0.74
S1	0.00	-0.04

Based on the ARO oil series EHD data compared to fleet data, the EHD conditions to which the oils were subjected in this study were more severe and caused more permanent degradation than occurs in a typical automotive engine. This is true even when the lubricant is used in the transmission as well.

CONCLUSIONS

Thin film elastohydrodynamic contacts cause extensive molecular degradation in lubricants with constituents having molecular weights above 10^4. Materials with molecular weights below 600 appear to undergo no significant molecular changes in the EHD contacts.

ACKNOWLEDGMENT

The authors are indebted to Mr. Anders G. Larson of the Chalmers University of Technology, Gothenberg, Sweden for assistance in taking some of the data.

LITERATURE CITED

(1) Ausherman, V., Nagarag, H., Sanborn, D. M., and Winer, W. O., "Infrared Temperature Mapping in Elastohydrodynamic Lubrication", ASME Paper No. 75-Lub-13 (to be published in ASME Trans., J. Lubrication Technology.

(2) Stewart, R. M., and McMillan, M. L., SAE Paper No. 75058, Feb. 1975.

(3) Barry, A. J., J. Applied Physics, 17, 1020 (1946).

(4) Wright, W. A., and Crouse, W. W., I and EC Product Research and Development, 3, 153 (June, 1964).

(5) Sanborn, D. M., and Winer, W. O., Trans. ASME, J. Lubrication Technology, 93, 262 (1971).

(6) Sanborn, D. M., and Winer, W. O., Trans. ASME, J. Lubrication Technology, 93, 342 (1971).

(7) Turchina, A. V., Sanborn, D. M., and Winer, W. O., Trans. ASME, J. Lubrication Technology, 96, 464 (1974).

(8) Ausherman, V. K., Nagaraj, H. S., Sanborn, D. M., and Winer, W. O., ASME Paper No. 75-Lub-13 (to be published in ASME Trans., J. of Lubrication Technology).

(9) Walker, D. L., Sanborn, D. M., and Winer, W. O., Trans. ASME, J. of Lubrication Technology, 97, 390 (1975).

(10) Gunderson, R. C., Hart, A. W., ed. "Synthetic Lubricants", Reinhold, New York, 1962.

(11) Dyson, A., and Wilson, A. R., Proc. of the Institution of Mechanical Engineers, 180, Pt. 3K, 97 (1965-66).

2. Presented at the ASME/ASLE Lubrication Conference
Kansas City, Missouri, October 1977 (ASME Paper No.
77-Lub-15)

LIGHT-SCATTERING STUDY OF THE GLASS TRANSITION IN LUBRICANTS

by

Mohammed A. Alsaad* and Ward O. Winer
School of Mechanical Engineering

Fernando D. Medina** and Donald C. O'Shea
School of Physics

Georgia Institute of Technology, Atlanta, Georgia 30332

ABSTRACT

The sound velocity of four lubricants has been measured as a function of temperature and pressure using Brillouin scattering. A change in slope of the velocity as a function of temperature or pressure allowed the determination of the glass transition temperature and pressure. The glass transition data were used to construct a phase diagram for each lubricant. The data indicate that T_g increased with pressure at a rate which ranged from 120 to 200 C/GPa. The maximum pressure attained was 0.69 GPa and the temperature range was from 25 to 100 C.

*Current address: Khaledeyah, P.O. Box 17013, KUWAIT.

**Current address: Physics Department, Northeastern University, Boston, Massachusetts 02115.

Introduction

The mechanical behavior of a lubricant as it passes through an elastohydrodynamic (EHD) contact has been assumed by many workers to be viscous in nature. The proposition that this behavior might not be that of a viscous liquid but an elastic solid was first presented by Smith [1] in 1960. The results of Johnson and Roberts [2] and Johnson and Cameron [3] indicate a change in physical properties of the lubricants at high pressures. The physical state of lubricating oils in EHD contacts is important because it influences the two most important dependent variables of an EHD contact: the film thickness and the traction.

Most lubricating oils contain linear and highly branched hydrocarbons as well as ring structures. Thus, a lubricant can display both a glass transition temperature (T_g) and a phase transition. [4] The glass transition temperatures at atmospheric pressure were measured by the technique of Differential Scanning Calorimetry (DSC) [5] for two lubricating oils: naphthenic base oil designated as N1 and five ring polyphenyl ether, 5P4E. The glass transition temperatures obtained were -59 C for N1 and -21 C for 5P4E. Possibly because these values are low compared to the operating temperatures in a typical EHD contact, the occurrence of the glass transition phenomena and the existence of the glassy state in the contact have received little attention to date [6,7]. However, because of the fact that the glass transition temperature increases with pressure [8,9], and because of the existence of high pressures in the EHD contacts, the glass transition temperature can be greater than the operating temperature in the contact. According to McKinny [8], the glass transition is an isoviscous state. The change

in temperature with pressure required to maintain constant viscosity [10] indicates that the glass transition temperature would increase with pressure at a rate ranging from 75 to 300 C/GPa for typical lubricants. Thus it would be expected that lubricants will be in the glassy state in an EHD contact with average pressure of 0.70 GPa or higher at room temperature.

The glass transition temperature of four lubricants was determined [5] as a function of pressure using the light scattering technique. A transition diagram for each lubricant is constructed and can be used to determine if a lubricating oil behavior, under the operating conditions of pressure, temperature and characteristic rate of the EHD contact, can be expected to be glasslike or liquidlike.

Light Scattering Theory

When a laser beam passes through a transparent medium, a small portion of the light is scattered in all directions due to the optical inhomogeneities in the medium. The inhomogeneities are the result of fluctuations of the dielectric constant brought about by fluctuations of the density of the medium due to random thermal motion of the molecules [11]. Those fluctuations in the dielectric constant can be separated into entropy fluctuations at constant pressure and pressure fluctuations at constant entropy. The adiabatic pressure fluctuations can be described by means of plane sound waves of thermal origin propagating in all directions. The interaction of a light wave of wave length λ with the sound waves in a media with refracture index n leads to Brillouin scattering of light by sound waves of a particular wavelength, Λ, in the direction given by the scattering angle θ and

satisfying the Bragg condition:

$$2 \Lambda \sin \theta/2 = \frac{\lambda}{n} \quad . \tag{1}$$

Moreover, as a consequence of the movement of the sound waves, the frequency of the incident light is altered by the Doppler effect with respect to the original value, ω_o. This effect was first predicted by Brillouin [12] as

$$\omega_B = 2(nV \sin \theta/2)/\lambda \tag{2}$$

which can be written as

$$V = \frac{\omega_B \lambda}{2n \sin \theta/2} \quad . \tag{3}$$

Equation (3) shows that the sound velocity, V, can be determined if monochromatic light strikes the material and the frequency shift, ω_B, of the scattered light is measured for a fixed scattering angle.

In recent years, Brillouin scattering has been used in the study of polymers above and below the glass transition temperature. A change in slope of the velocity as a function of temperature or pressure, like density or specific heat, defines the glass transition and has been observed by many workers [13-17]. The change in the temperature and pressure coefficients of the sound velocity indicating the occurrence of glass transition was observed in all lubricants investigated in this study.

Experimental Technique

The schematic arrangement of the basic components of the light

scattering experiment is shown in Figure 1a and consists of an argon ion laser having a power of about 200 mw in single mode operation at $\lambda = 0.5145$ μm, a high pressure scattering cell* (Figure 1b) containing the lubricant sample to be investigated, and a detector which permits the spectroscopic analysis of the scattered light. The scattered light is collimated by a lens and analyzed by a Fabry-Perot interferometer operating in triple pass geometry. The ring pattern from the interferometer is focused on a screen which has a pinhole in front of a photomultiplier tube (PMT), so that only the center frequency of the ring pattern is detected. One of the Fabry-Perot plates is attached to three piezoelectric stacks and can be swept in and out, thus changing the frequency that passes through the pinhole. The output signal from the PMT can be processed by a standard counting system and stored in a multichannel analyser. The multichannel analyser was triggered off the Rayleigh line to avoid broadening that results from drifts of the incident laser frequency relative to the interferometer pass frequency. The spectrum can also be plotted on an X-Y recorder and/or punched on paper tape.

The high pressure equipment consists of a scattering cell which was used to pressures of 0.69 GPa, a strain gage pressure transducer, a hand pump, and a 9:1 area ratio intensifier.

The four lubricants investigated were: naphthenic base oil (N1), N1 blended with 2.2 percent high molecular weight polybutane (N2), polyphenyl either (5P4E), and cycloaliphatic hydrocarbon (MCS-1218).

*Designed by W. B. Daniels of the University of Delaware.

These oils were selected because they represent typical commercially available lubricants and research materials of current interest in the field of EHD lubrication. The fluids were passed through a millipore filter which substantially reduced parasitic light scattering and made it possible to obtain the Brillouin spectra. More detailed descriptions of the oils can be found in Appendix A.

Experimental Procedure and Data Reduction Technique

Two standard procedures were adopted to form the glass of the materials investigated. In formation history A, the glass was formed by pressurizing the samples at room temperature from atmospheric pressure until the glassy state was reached. Brillouin spectra were taken at pressure intervals of about 0.02 to 0.03 GPa. The spectra were taken 20 minutes after the pressure change was imposed. In formation history B, the pressure was increased from atmospheric to a reference pressure while the sample temperature was increased such that it remained in the liquid state. When a temperature of about 15C above the assumed glass transition for the corresponding pressure was reached, the pressure and temperature were kept constant for about 30 minutes. The sample was then cooled at constant pressure and frequency spectra were recorded at 2 or 3 C intervals. Twenty minutes were allowed for the temperature ot reach equilibrium before each spectrum was recorded.

This procedure was repeated at different pressures. The sample temperature was changed by controlling the voltage input to a resistance heater tape wrapped around the intensifier-cell assembly which was enclosed in an oven. The temperature was measured with a copper-constantan thermocouple in conjunction with a direct reading

digital thermometer referenced to an ice bath. The temperature was controlled to better than $\mp$ 0.1 C.

All spectra were recorded at a fixed scattering angle of 90^{o}. Light scattering results of the naphthenic base oil (N1) were selected to explain the data reduction technique. Results of other experimental oils investigated were obtained in a similar manner and only their transition diagrams will be reported in this paper.

The Brillouin spectrum of N1 recorded at 0.277 GPa and 24.4C (History A) is shown in Figure 2. It is typical in general appearance of all spectra obtained. The Fabry-Perot Plate separation was 0.40 cm corresponding to a free spectral range of 37.5 GHz. The frequency shift was determined from the position of the Brillouin peaks and the sound velocity was calculated from equation (3). The refractive index needed in equation (3) was measured as a function of temperature by using a precision Abbe "60" refractometer (sodium D, lim, λ = 0.5896 μm). Since it was not possible to measure the variation of the refractive index with pressure, it was assumed that $\frac{dn}{dP}$ for all experimental oils investigated has a constant value of 2.9×10^{-4} per MN/m^2. This value was estimated from information available in the literature [6] for 5P4E. Any other estimate for $\frac{dn}{dP}$ will only shift the velocity of sound up or down without changing the location of the glass transition.

Experimental Results

Figure 3 shows the variation of the frequency shift and the sound velocity with pressure for N1 (History A). The sound velocity and frequency shift increase with increasing pressure and a change in the slope is apparent at 0.474 GPa. This change of slope represents the glass transition [13-15,17]. Results obtained by History B at

different constant formation pressures are shown in Figure 4. The sound velocity increases as the temperature is decreased and a change in slope is observed for each formation pressure. The two portions of the sound velocity curves of Figures 3 and 4 were fit by least square regression to straight lines and were solved for their intersection to determine the glass transition. Figure 4 shows that T_g shifted to a higher value as the formation pressure was increased. The glass formation temperature-pressure combinations resulted in the transition diagram in Figure 5. Also included in this figure are the transition diagrams of the other experimental fluids obtained by the data reduction technique discussed above.

The glass transition temperatures and pressures for each oil were least square fitted to a straight line and the expressions obtained are given in Table 1. They show that the rate of increase of T_g with pressure for N1 has the lowest value (120 C/GPa) while that of MCS-1218 has the largest value (200 C/GPa). The glass transition data obtained by History A are also shown in Figure 5 but were excluded from the fit due to the different history by which the glass was formed. However, in general, the transition obtained by History A falls on or near the transition line obtained by History B.

Figure 5 also shows the effect of the viscosity-index improver blended with the naphthenic base oil on the glass transition behavior of the blend relative to the base oil. The glass transition pressure at room temperature for the blend occurred at 0.438 GPa compared with .475 GPa obtained for the base oil. The glass transition temperature for N2 occurred at 7.5C higher than that of N1 at 0.69 GPa. As seen

from Table 1, the rate of increase of T_g with pressure increased by about 10 percent from 120 to 134 C/GPa.

The velocity of sound in the temperature and pressure ranges investigated was 2300 to 3400 m/s for N1 and N2 fluids, 2200 to 2900 m/s for 5P4E and 2600 to 3500 m/s for MCS-1218. This data can be used to determine the secant bulk modulus

$$\text{sound velocity} = (\text{modulus/density})^{1/2}$$

The velocity of sound as a function of pressure for 5P4E at comparable temperatures and history A where consistently about 3 to 4% higher than those reported by Dill et al. [6].

Table 1. Least-square Expressions for the Glass Transition Temperature as a Function of Pressure for Experimental Lubricants Based on Formation History B. T_g in C and P_g in GPa.

Experimental Lubricants	Range of Measurements GPa	Least Square Expression for T_g
5P4E	0.16 - 0.41	$T_g = -4.74 + 182.9\ I_g$
MCS-1218	0.16 - 0.46	$T_g = -4.66 + 197.4\ I_g$
N1	0.46 - 0.70	$T_g = -32.79 + 120.8\ P_g$
N2	0.43 - 0.70	$T_g = 033.40 + 134.5\ P_g$

Error Analysis

The uncertainties in the absolute value of the sound velocity which arise from the uncertainties in the scattering angle θ, the frequency shift ω_B and the refractive index n are not of great concern in the present work as the absolute value of the sound velocity is not our main concern. The quantity of interest is the intersection of the sound velocity versus temperature or pressure curves in the liquid and glassy regions which represents the glass transition for the material. This quantity is not strongly influenced by any of the above uncertainties. In obtaining all frequency spectra for each experimental fluid at different constant formation pressures, the position of the scattering cell remained fixed and a single separation distance of the Fabry-Perot mirrors was chosen to cover the expected frequency range of the calculated velocities. This arrangement ensured that the error in the calculated velocities due to the uncertainties mentioned above for each constant formation pressure is the same for all other pressures. The influence of the above errors on the measurements is to shift the velocity-temperature or the velocity-pressure curves to higher or lower velocities without changing the location of the glass transition temperature or pressure.

The error in the location of T_g and P_g is the most important uncertainty in this work. A statistical method giving the confidence limits of the abscissa of the intersection of two linear regressions is described in Reference [18]. This method can be used to determine the confidence limits on T_g using the liquid and the glassy linear regression expressions of the form

$$V = a + b\,T \qquad (4)$$

Using the equal variance assumption, the confidence limit, ΔT_g, is equal to the difference of the two roots of the following quadratic equation

$$A\,T_g^2 + B\,T_g + C = 0 \qquad (5)$$

where the coefficients A, B, and C are given in Reference [18]. The 95 percent confidence limits of T_g were calculated for all lubricants investigated ΔT_g ranged from a low of 0.7 to 1.1 C for N_1 to a high of from 0.7 to 3.6 C for 5P4E.

Conclusions

Light scattering is a useful technique in determining the transition between the liquid-like and solid-like behavior of materials. The glass transition obtained for N1 is in good agreement (within 5 to 8C) with glass transition measurements from PVT technique [19-20].

These data also show that lubricants in an EHD contact can exist in a glassy state at relatively high temperatures if the operating pressures are high. Therefore the rheological behavior in the glassy state will play a significant role in determining the rheological behavior of lubricants in EHD contacts and may offer a basis for selecting lubricants for specific EHD applications.

Acknowledgments

This research was supported by NASA Grant Number NSR-11-002-133 and NSF Grant Number END 74-21002.

Nomenclature

P	=	Press (GN/m^2 or GPa)
P_g	=	Glass Transition Pressure (GN/m^2 or GPa)
T	=	Temperature (C)
Tg	=	Glass Transition Temperature (C)
V	=	Velocity of Sound (m/sec.)
n	=	Refractive index
θ	=	Scattering Angle
λ	=	Wavelength of Incident Light (μm)
Λ	=	Wavelength of Sound in the Medium (μm)
ω_o	=	Frequency of Incident Light (GHz)
ω_B	=	Frequency Shift or Brillouin Shift (GHz)

References

1. Smith, F. W., "Lubricant Behavior in Concentrated Contact - Some Rheological Problems," ASLE Transaction, 3, 18, 1960.

2. Johnson, K. L., and Roberts, K. D., "Observation of Viscoelastic Behavior of an EHD Lubricant Film," Proc. Roy. Soc. Lond. A-337, 217, 1974.

3. Johnson, K. L., and Cameron, R., "Shear Behavior of Elastohydrodynamic Oil Films at High Rolling Contact Pressures," Proc. Inst. Mech. Engrs., 182, Pt. 1, 307, 1967/68.

4. Noel, F., "Thermal Analysis of Lubricating Oils," Thermonica Act. 4, 377, 1972.

5. Alsaad, M. A., "Light Scattering Study of the Glass Transition and the Glassy State in Lubricating Oils," Ph.D. Thesis, Georgia Institute of Technology, Atlanta, Georgia, August 1976.

6. Dill, J. F., Drake, P. W. and Litovitz, T. A., "The Study of Viscoelastic Properties of Lubricants Using High Pressure Optical Techniques", ASLE, 18(3), 202, 1975.

7. Lauer, J. L. and Peterkin, M. E., "Traction and Film Temperature as Related to the Glass Transition and Freezing", ASLE Preprint No. 77AM-1A-3.

8. McKinny, J. E., and Goldstein, M., "PVT Relationship for Liquid and Glassy Poly (Vinyl Acetate)," Journal of Research of the NBS-Physics and Chemistry, 78A, 331, 1974.

9. Haward, R. N., The Physics of Glassy Polymers, Wiley and Sons, Inc., New York, 1961.

10. ASME Pressure-Viscosity Report, I, II, A Report Prepared by the ASME Research Committee on Lubrication, New York, ASME, 1953.

11. Fabelinskil, I. L., Molecular Scattering of Light, Plenum Press, New York, 1968.

12. Brillouin, L., Ann. Phys. (Paris), 17, 88, 1922.

13. Stevens, J. R., Jackson, D. A., and Champion, J. V., "Evidence for Ordered Regions in Poly(n-butyl) Methacrylate from Light Scattering Studies," Molecular Physics, 29(6), 1893, 1975.

14. Coakley, R. W., Mitchell, R. S., Stevens, J. R., and Hunt, J. L., "Rayleigh-Brillouin Light Scattering Studies on Atactic Polystrena," A Paper Presented at the American Physical Society Conference, Atlanta, Georgia, April, 1976.

15. Jackson, D. A., Pentecost, H. T. A., and Powels, J. G., "Hypersonic Absorption in Amorphous Polymers by Light Scattering," Molecular Physics, 23(2), 425, 1972.

16. Juang, Y., and Wang, C., "Brillouin and Rayleigh Scattering in Polybutadiene," 61, 1868, 1974.

17. Mitchell, R. S., and Guillet, J. E., "Brillouin Scattering in Amorphous Polymeric Solid," J. Polym. Sci.: Polym. Phys. Ed., 12, 713, 1974.

18. Filliben, J. J., and McKinny, J. E., "Confidence Limits for the Abscissa of Intersection of Two Linear Regressions", J. Res. Nat. Bur. Stand. (U.S.), 76B (Math. Sci.), 179, 1972.

19. Winer, W. O., and Sanborn, D. M., "Investigations of Lubricant Rheology as Applied to Elastohydrodynamic Contacts," NASA CR-2837, Sept. 1976.

20. Alsaad, M. A., Bair, S., Sanborn, D. M., and Winer, W. O., "Glass Transition in Lubricants - Its Relationship to EHD Lubrication", ASME paper to be presented at ASLE-ASME Lubrication Conference, October 3-5, 1977, Kansas City, Missouri.

APPENDIX A

DESCRIPTION OF EXPERIMENTAL FLUIDS

The following table summarizes the oils investigated and gives characteristic data for each oil.

Symbol	Description
5P4E	Polyphenyl Ether
MCS-1218	Cycloaliphatic Hydrocarbon
N1	Naphthenic Base Oil R-620-15
N2	N1 + 2.2 percent Polybutane LF-5346

Fluid Characterization

Symbol:	5P4E	
Type:	Five-ring Polyphenyl Ether	
Source:	Monsanto Company	
Properties:	Viscosity at 37.7 C, m^2/s	363×10^{-6}
	Viscosity at 98.8C, m^2/s	13.1×10^{-6}
	Density at 22C, Kg/m^3	1205
	Density at 37.7C, Kg/m^3	1190
	Flash Point, C	288
	Pour Point, C	4
	Refractive Index at 24C	1.6309
Symbol:	MCS-1218	
Source:	Monsanto Company	
Type:	Cycloaliphatic Hydrocarbon	

Properties:	It is a combination of two components each have a molecular weight less than 1000.	
	Viscosity at 37.7C, m^2/s	1418×10^{-6}
	Viscosity at 98.8C, m^2/s	18.37×10^{-6}
	Density at 24C, Kg/m^3	9400
	Refractive Index at 24C	1.5114
Symbol:	N1	
Source:	Sun Oil Company	
Type:	Naphthenic Base Oil R-620-15	
Properties:	Viscosity at 37.7C, m^2/s	24×10^{-6}
	Viscosity at 98.8C, m^2/s	3.728×10^{-6}
	Viscosity Index (ASTM D-2270)	-13
	Flash Point, C	157
	Pour Point, C	- 43
	Density at 20C, Kg/m^3	9157
	Average Molecular Weight	305
	Refractive Index at 24C	1.5033
Symbol:	LF 5346, used as additive in lubricant N1	
Type:	Polybutane in oil solution	
Source:	American Oil Company	
Properties:	Density at 25C, Kg/m^3	8656
	Viscosity at 37.7C, m^2/s	8041×10^{-6}
	Viscosity at 98.8C, m^2/s	637×10^{-6}
	Viscosity Index	123.5
	Flash Point, C	205
	Dilute Oil Content, percent	80
	Dilute Oil Viscosity at 37.7C, m^2/s	18×10^{-6}

Weight Average Molecular Weight of the Polymer	50,000

The percent additive reported above (2.2 percent by volume) is the percent polymer in the final solution.

LIST OF FIGURES

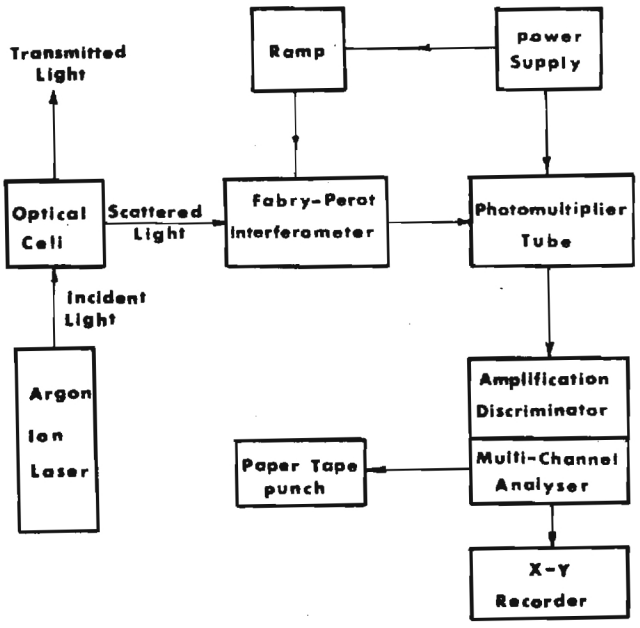
Transmitted Light
Ramp
power Supply
Optical Cell
Scattered Light
Fabry-Perot Interferometer
Photomultiplier Tube
Incident Light
Argon Ion Laser
Amplification Discriminator
Paper Tape punch
Multi-Channel Analyser
X-Y Recorder

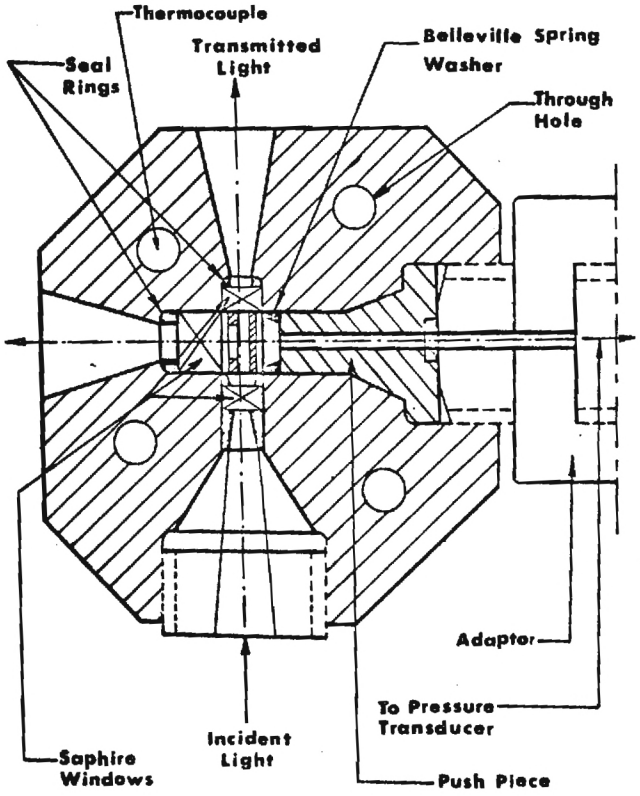
Thermocouple
Transmitted Light
Belleville Spring Washer
Seal Rings
Through Hole
Adaptor
To Pressure Transducer
Incident Light
Saphire Windows
Push Piece

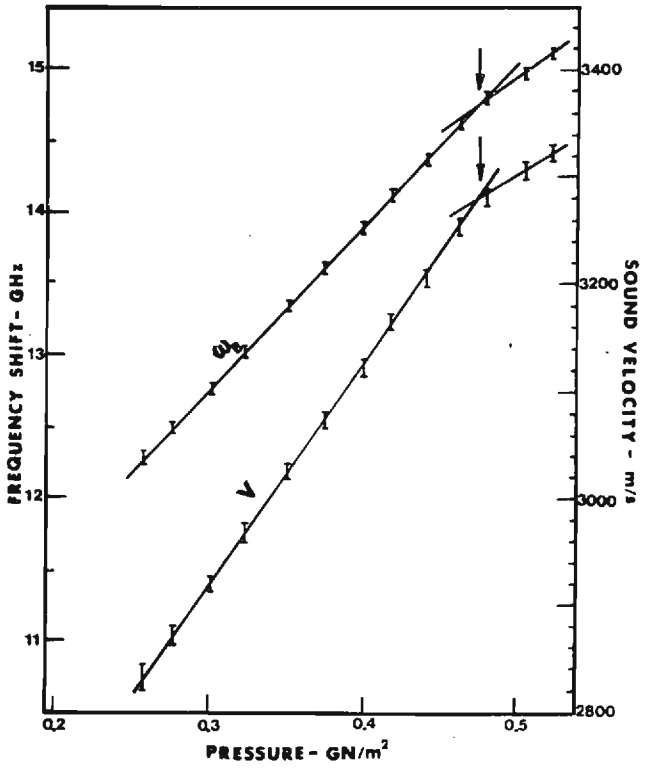
15
14
13
12
11
FREQUENCY SHIFT - GHz
3400
3200
3000
2800
SOUND VELOCITY - m/s
0,2
0,3
0,4
0,5
PRESSURE - GN/m²
ω
V

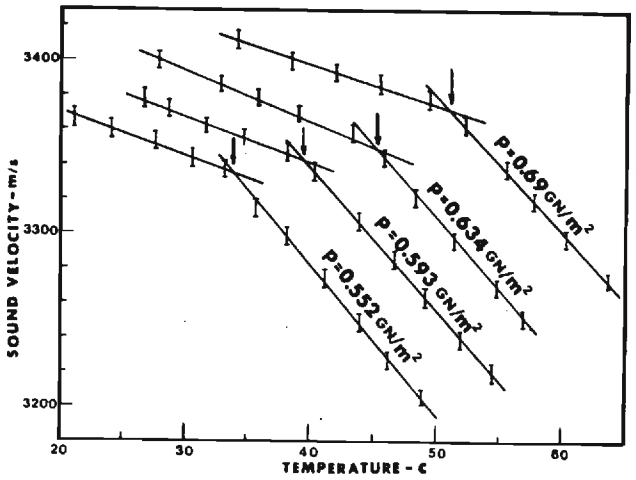
3400
3300
3200
SOUND VELOCITY - m/s
20
30
40
50
60
TEMPERATURE - C
P=0.69 GN/m²
P=0.634 GN/m²
P=0.593 GN/m²
P=0.552 GN/m²

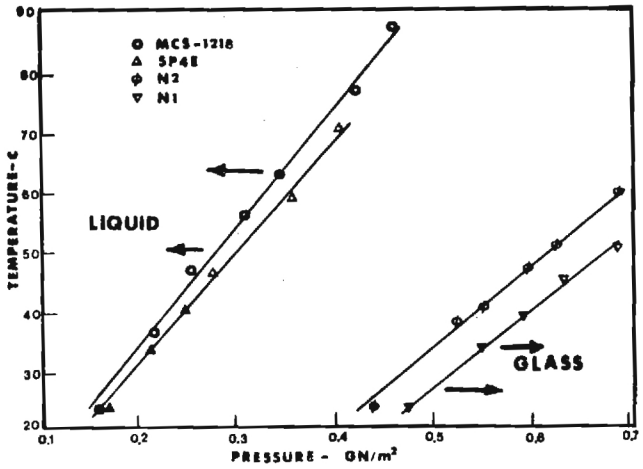
MCS-1218
SP4E
N2
N1
LIQUID
GLASS
TEMPERATURE - C
PRESSURE - GN/m²
90
80
70
60
50
40
30
20
0.1
0.2
0.3
0.4
0.5
0.6
0.7

3. Presented at the ASME/ASLE Lubrication Conference
Kansas City, Missouri, October 1977
(ASME Paper No. 77-Lub-19)

ASPERITY INTERACTIONS

IN EHD CONTACTS

by

H. S. Nagaraj
Graduate Student

D. M. Sanborn
Associate Professor

W. O. Winer
Professor

Georgia Institute of Technology
School of Mechanical Engineering

April, 1977

Revised

ABSTRACT

Infrared temperature measurements, Ferrographic analysis and surface profilimetry were used to monitor asperity interactions in a sliding EHD point contact. The contact temperature and surface profile signals obtained both before and after a run-in period are compared in the frequency domain by means of a Fourier analyzer. The interaction of surface asperities is accompanied by the presence of a high frequency component in the infrared signal. It is also shown that only a relatively narrow band of wavelengths of the surface profile spectrum are relevant in the interaction process.

NOMENCLATURE

C	Autocorrelation function
d	Hertzian Contact diameter, m
h_c	Film thickness at Contact Center, m
ℓ	Length, m
$P_{Avg.}$	Average Hertz pressure, N/m^2
P_{EHD}	Average Fluid pressure, N/m^2 (EHD Load divided by contact area)
P_H	Peak Hertz pressure, N/m^2
T_b	Ball Surface temperature, C
V_s	Sliding velocity, m/s
W_{EHD}	Portion of Load carried by EHD film, N
x	Distance along surface, m

β	Length shift in computing autocorrelation function, m
β^*	Correlation distance, m
θ	Inclination of the asperity flank with the mean surface, rad
Λ	h_c/σ
λ	wavelength, m
σ	Surface roughness, rms or Ra, m
σ_θ	Tangent of θ

INTRODUCTION

Because of imposed changes in operating load and speed, machine elements designed to run under full EHD lubrication usually experience some operation in the partial EHD regime. In this mode of lubrication the total load is shared between the EHD fluid film and the contacting asperities. Depending on operating conditions and surface characteristics, the partial EHD lubrication may be stable, resulting in an improved surface, or unstable resulting in a surface which can no longer be used.

This paper examines the stable situation. Its purpose is to show the usefulness of the infrared signal emitted from the EHD contact in detecting asperity interaction.

EXPERIMENTAL EQUIPMENT AND TECHNIQUE

A schematic diagram of the apparatus used in the EHD simulation is shown in Figure 1. The equipment has capabilities for measuring the lubricant film thickness, traction force and both contact surface and film temperatures. The EHD contact was formed using a 31.8 mm diameter AISI 52100 steel ball rotating and loaded against a flat stationary sapphire disk.

Steel balls of two different roughness values (.075 and .38 μm Ra) have been used to study the effects of surface roughness. The balls have no preferential roughness pattern. A relatively smooth ball (.011 μm Ra) has also been used extensively in this laboratory. However, because of limitations in load and speed available in the EHD simulator, it was not possible to produce noticeable surface alteration with this surface even to Hertz pressures and sliding velocities of 1.5 GPa and 12.7 m/s.

A consequence of requiring relatively rough surfaces for this investigation is the absence of an optical interference fringe pattern. This makes optical film thickness data impossible to obtain, which in turn precludes the determination of an average film temperature. Thus only ball surface temperatures are measured. However, this is not a major limitation of the study since the surface temperature is of primary importance in predicting contact failure.

The ball surface temperatures are deduced from the output of an infrared microdetector having a spot size resolution of 38 μm and a time response of 8 μs [1-3]. In order to have a common reference temperature for all the test runs which formally generate different

amounts of heat, the lubricant reservoir was maintained at about 15°C above ambient by circulating the test lubricant through a heat exchanger. In all results reported here, the temperatures are the maximum moving surface temperature values in the EHD contact.

A typical experiment involved taking a new ball cemented to a drive shaft and placing it in a surface profilimeter to obtain an initial surface profile. The analog voltage signal was recorded on magnetic tape. The specimen was then placed in the EHD simulator and subjected to the desired operating conditions. The AC signal from the infrared detector was recorded during running both at the beginning and end of the run-in experiment. The ball was then removed and another surface profile recording was made. The magnetic tape recordings of the temperature and surface profile data were used as input to a Fourier Analyzer to transform the signals from the time domain to the frequency domain.

During some of the experiments, a fresh lubricant sample was used and a Ferrogram was obtained of the lubricant sample taken after run-in [4]. The purpose of the Ferrographic analysis was to determine the concentration and size distribution of debris in the lubricant sample.

The fluid used throughout this investigation is a naphthenic base oil designated N1 in previous studies [1-5]. A complete description is given in the appendix of reference [5].

EXPERIMENTAL RESULTS

The recording of the profilometer trace was transferred to a Fourier Analyzer. The first step in an analysis performed by this instrument is an A/D conversion. After analysis of the digital representation of the input signal, the results may be printed and/or a D/A conversion can be made and the results plotted or displayed on a CRT.

Figure 2a shows the surface profile of the unused ball having an initial surface roughness of 0.38 μm Ra obtained using the 0.76 mm cut-off wavelength of the instrument. The trace represents the signal after the A/D and D/A conversions and is an excellent replica of the original signal plotted by the profilometer. The distance along the ball surface is shown in terms of the Hertzian contact diameter, d. For the conditions of steel on sapphire at 1.24 GPa peak Hertz pressure, the calculated contact diameter is 0.43 mm.

Figure 2b shows the same ball after running for 24 minutes in the simulator. The profile traces shown in Figure 2 were taken in the direction of the sliding motion. No attempt was made to measure the profile at precisely the same location on the ball surface. The traces taken are of sufficient length that they should be representative of any position within the wear trace. On the basis of previous results [3], the conditions of 1.24 GPa and V_s = 1.02 m/s should result in a value of $\Lambda < 1$ based on the unused ball surface roughness and the film thickness for a .011 μm Ra operating at the same conditions. The parameter Λ is the ratio of contact film thickness to composite surface roughness with the value $\Lambda < 1$ indicating that asperity interaction should

be expected. Comparing the two traces in Figure 2, it is apparent that the 24 minute run-in period has resulted in a smoother surface. The final roughness is .25 μm Ra which results in $\Lambda \simeq .4$. The 15.9 mm radius of curvature of the ball surface can also be seen.

The primary function of the Fourier Analyzer is to perform the Fast Fourier Transform (FFT) on the time varying input signal. A convenient way of displaying the amplitudes of the component terms in Fourier series is through the power spectrum. The input to the analyzer is a time varying voltage. After the A/D conversion, the FFT results in a complex amplitude for each of the 127 (plus a constant) terms used in the series for this equipment. Each of these terms is assigned a pair of channels in the analyzer. The frequency range, and therefore, frequency increment can be selected. The frequency assigned to two adjacent pairs of channels differs by a constant. The resulting plot of the power spectrum is linear in the independent variable frequency. The value of the ordinate at each center frequency (channel) is the product of the complex amplitude for that frequency and its conjugate. The units are, therefore, V^2 versus Hz. The D/A conversion makes the plotted results appear to be continuous, but all of the data processing was done digitally in terms of the coefficients of the first 127 terms of the Fourier series.

Although the results are plotted on a linear frequency scale, this is not a convenient representation for this study. This is due to the fact that the frequency is influenced by the profilometer stylus scanning speed and differences between magnetic tape recording and play-back speeds. In order to remove these effects, the abscissa has

been changed to read wavelength. The unit of wavelength selected is d, the Hertz contact diameter of 0.43 mm. The power spectra of the profiles shown in Figure 2 are given in Figure 3.

The first four channels (0-3) were cleared prior to plotting. This is because these are related to gross ball curvature and waviness. These values are so large compared to the values in higher channels (see insert), that a plot would show only the very low frequency components. Therefore, only components having wavelengths <3d have been plotted. In comparing the power spectra for the unused and run-in ball surface profiles, note the factor of two change of scale in Figure 3a versus 3b. The most apparent contrast is the reduction of the components having wavelengths <2d. Comparing the tabular data in Figure 3, it appears that roughness components having wavelengths >2d remain essentially unchanged after the 24 minute run-in period. The nine percent difference in DC level can be attributed to slight differences in signal amplification in obtaining the two surface profiles. The most drastic change occurs for a wavelength of one Hertz diameter. This component has been reduced by more than a factor of eight.

It has been shown previously [3] that asperity interaction can significantly alter the DC level of the ball surface temperature. In the DC mode of operation, the frequency response of the detector is 400 Hz. From surface profile measurements it has been determined that only a single asperity occupies the detector's field of view (~38 μm diameter) at any one time. However, at 1.0 m/s sliding velocity the asperity resident time in the field of view is only 40 μs. The DC mode, therefore, yields only a time averaged value. In the AC mode of operation the system can

detect such temperature transients since it has a response time of 8 μs. An important consequence of operating in the AC mode, however, is that the reference signal is absent. Instead, the instrument will produce a voltage difference proportional to the variation in target radiation emitted. Through an independent experiment, using an external chopper, it has been determined that the variation indicated in the AC mode is centered on the signal received in the DC mode. From this information a plot of time-averaged surface temperature along with the maximum and minimum values can be obtained.

Figure 4 shows a plot of the ball surface temperature at the contact center as a function of Hertz pressure. The plot shown was constructed using the DC mode data at five different Hertz pressures. In addition, the AC mode was used at the four highest Hertz pressure levels. As is shown in Figure 4, the AC data shows no fluctuation about the DC level at P_H = 1.05 GN/m^2, but shows an increasing amount of fluctuation as the pressure in increased. The upper and lower curves represent the range of temperatures detected. It is believed that the peak values represent individual asperity intereactions. Figure 4 also shows the significance of the parameter Λ in predicting the onset of asperity interaction.

The AC signal from the infrared detector recorded during the run-in process was also subjected to Fourier analysis. However, in order to eliminate noise in the detector signal, a 20 KHz, 3dB filter was used during data acquisition. The noise remaining below 20 GHz had a peak power of about $5 \times 10^{-6} V^2$ whereas the detector signal had a power content on the order of $10^{-4} V^2$. Furthermore, the sampling

technique used by the Fourier Analyzer tends to average out the random noise while enhancing the signal.

Figure 5 shows a normalized histogram of the AC signal from the detector obtained at the beginning of the run-in period (Figure 5a) and after running for eight minutes (Figure 5b). The figure shows that the voltage distributions appear to be Gaussian. Secondly, it is apparent that the amount of dispersion is decreased by the run-in process. It is interesting that both the high and low extremes in temperature signal have been eliminated as the asperity peaks were removed. The symmetry of the fluctuations supports the argument advanced previously [3] that the peak in the temperature fluctuation signal is due to local heating at an asperity; whereas the minimum signal occurs directly after this maximum and is due to the relatively low local pressure in the region following an asperity.

Figure 6 shows the power spectra for the same IR detector signals as used for Figure 5. The abscissa has been replotted in terms of wavelength in units of d (Hertz diameters). It is apparent from Figure 6 that the run-in process results in a significant reduction in power at all wavelengths. In both spectra, the peak occurs near $\lambda = 2d$, although the run-in process has reduced the peak magnitude by more than a factor of three. It should be noted that the detector signal was also filtered to remove frequency components less than 500 Hz. This corresponds to wavelengths which are greater than 5d (see Figure 6). The power spectrum decreases very rapidly for $2 < \lambda \leq 5d$, therefore, the reduction shown in Figure 6a is not due to filtering.

A Ferrographic analysis of the lubricant sample was made following selected experiments [4]. The purpose of the analysis was to independently show a correlation between wear debris in the lubricant and the presence of the AC temperature fluctuations. The correlation was confirmed by the analysis. Also, the reliability of the parameter Λ in predicting the onset of interaction was confirmed.

In Ferrographic analysis, solid particles are precipitated from the lubricant by a magnetic field as it flows slowly over a substrate. Particles are precipitated from the oil at a rate depending on size and magnetic permeability. The resulting Ferrogram yields the size distribution and concentrations of particles in the oil sample. Using special precautions to avoid lubricant contamination by particles other than contact wear debris, 30 mℓ samples were taken for experiments at various Hertz pressures and 1 m/s sliding. Knowing the approximate film thickness and surface roughnesses for each of these conditions, the Ferrogram results can be interpreted in terms of the Λ parameter.

Optical density measurements were made on each Ferrogram at several different locations: entry, 54, 50, 40, 30, 20, and 10 mm. In addition, a composite or representative density was determined by averaging the several different readings. A plot of composite Ferrogram density for each test as a function of initial Λ ratio appears in Figure 7. The large and very rapid increase in particle density at low Λ values is evident. The transition to the high wear regime occurs as the Λ ratio approaches 1. This is in agreement with the findings of other investigators. Tallian [6] has shown that the onset of surface distress occurs at a Λ value of about 1.5. Czichos [7] reports that the change

from a full EHD film to continuous asperity contact occurs as Λ decreases from 2.5 to 0.7. In Figure 7, at Λ values greater than 2, a composite particle density of between 1 and 2 percent is observed. Since a full film should be present at these higher Λ ratios, little wear should take place. Therefore, these density readings represent the background or contaminant particle density for this set of experiments.

The importance of the parameter Λ in predicting asperity interaction is clearly shown in Figure 7. The onset of asperity interactions predicted by the occurrence of surface temperature fluctuations correlates very well with the results of the Ferrographic analysis. The calculation of the Λ value was based on a profilimeter roughness cut-off of 0.76 mm, which is reasonably close to 2d recommended value (discussed below).

Average traction coefficients for comparable tests measured at a steady state bath temperature of $40^{o}C$ appear in Figure 8. As one would expect, fairly constant traction values (0.061 to 0.062) were observed for all tests at Λ ratios greater than 1.5 where a full EHD film existed. As asperity interactions increased as Λ decreased below one, the traction values also increased, as expected. No abrupt traction increases or transitions were observed which would have signaled a boundary film failure or a catastrophic failure mode.

Microscopic examination of the wear debris generated during these studies showed that essentially all of the metallic wear particles, regardless of the initial surface roughness, were composed of small asymmetric thin (metallic) flakes. These flakes were typically less

than 10 μm in major dimension and no more than 1.5 μm thick. On the ferrograms, these particles are typically arranged in strings due to the magnetic field generated by the ferrograph.

DISCUSSION OF RESULTS

An autocorrelation function of the surface profile data shown in Figures 2 and 3 was obtained using the Fourier Analyzer. In addition to the power spectrum, the autocorrelation function can be useful in describing the surface profile. In fact, Whitehouse and Archard [8] and Peklenik [9] suggest the description of a real surface in terms of only σ, the rms roughness, and β^*, the correlation distance. Briefly, the autocorrelation function is obtained by comparing a time varying signal, in this case the surface profile measurement, with a replica of itself where the replica is shifted an amount $\beta(0 \leq \beta \leq \infty)$ along the surface. The autocorrelation function $C(\beta)$ therefore, depends on β and is obtained from

$$C(\beta) = \frac{1}{\ell}\int_0^{\ell} a(x)a(x + \beta)dx \qquad (1)$$

where $a(x)$ is the amplitude of the surface profile trace at a distance x along the surface. For a truly random signal, $C(\beta)$ will be a maximum at $\beta = 0$. If the signal is periodic, $C(\beta)$ will peak whenever β is a multiple of the wavelength. If a Gaussian distribution of surface roughness amplitudes is considered, equation 1 results in an exponential autocorrelation function when normalized such that $C(0) = 1.0$,

$$C(\beta) = \exp\ (-\beta/\beta^*) \qquad (2)$$

Therefore, when $\beta = 2.3\beta^*$, $C(\beta) = 0.10$. The value 0.10 has been arbitrarily set by Whitehouse and Archard as being sufficiently small that two points on the surface may be regarded as being independent. This

follows from the fact that when the autocorrelation function $C(\beta)$ is close to unity, two points on the surface β distance apart are strongly interdependent. However, when $C(\beta)$ attains values close to zero, two points on the surface β distance apart are weakly correlated and therefore essentially independent. The correlation distance $2.3\beta^*$ can also be viewed as roughly being equal to the spacing between equal sized asperities. The power spectrum is the inverse Fourier transform of the autocorrelation function, or

$$P(\omega) = \int_{-\infty}^{\infty} C(t)e^{-i\omega t}dt \qquad (3)$$

Substituting equation (2) into (3) results in

$$\begin{aligned} P(\omega) &= 0.5 \quad \text{for} \quad \lambda_s = 1/\omega = \beta^* \\ P(\omega) &\simeq 0 \quad \text{for} \quad \lambda_s = 1/\omega < 0.1\beta^* \qquad (4) \\ P(\omega) &\simeq 1 \quad \text{for} \quad \lambda_s = 1/\omega > 10\beta^* \end{aligned}$$

The wavelength β^* can therefore be thought of as a dividing point between those surface wavelength components having significant amplitudes and the shorter wavelengths which do not. Whitehouse and Archard have shown the model to be in good agreement with a large number of real surface profiles.

Figure 9 shows the autocorrelation function for the unused and run-in ball surfaces shown in Figure 2. The position shift β is shown in terms of the Hertz diameter d. If the Whitehouse-Archard model is applied to the data in Figure 9, the value of β^* can be found from

$C(2.3\beta^*) = 0.1\ C(0)$. The correlation distance β^* is .17d (74μm) for the unused ball and .33d (142μm) for the run-in surface. It is apparent that the exponential model of equation (2) can only be used for $\beta \leq 2.3\beta^*$. The further increase in $C(\beta)$ implies that the profile is not truly random, but has strong periodic components with wavelengths > d. This can also be seen from the power spectra shown in Figure 3.

Figure 9 shows that the correlation distance has doubled as a result of the run-in process. From equation (2), a doubling of β^* implies that two points on the surface must be taken twice as far apart after run-in to be considered independent. Because of the interrelationship between the power spectra and autocorrelation function, if the surfaces were in fact random, the half power point would be shifted to a wavelength twice the value of that for the unused surface. This is the case when the high frequency components are reduced much more than the low frequency components (see Figure 3). This is also consistent with the notion of independent points. Consider, for example, a surface comprised of only two wavelength components 2d and 0.2d. When the 0.2d wavelength component is present, the autocorrelation function would have a value of 1.0 for $\beta = 2nd$ where n is an integer. However, it would also have sizeable peaks for $\beta = 0.2nd$ (with drops to near zero midway between). After run-in, however, the 0.2d wavelength component will be substantially reduced. Assuming it to be eliminated, the $C(\beta)$ now peaks only once every $\beta = 2nd$ and reaches zero half way between the peaks. If the correlation distance is defined as the ten percent point, it is apparent that this distance must be increased if high frequency components are reduced or eliminated. The change in the

autocorrelation function as shown in Figure 9 is what would be expected as a result of the run-in process.

Based on the results shown in Figures 3 and 6, the authors believe that the methods presently used to determine acceptable levels of the R_a or rms surface roughness may not be the most appropriate. For example, the true rms value of the surface shown in Figure 2a (unused rough ball) is equal to the square root of the integral of the power spectrum (Figure 3a) over all wave lengths ($0 \leq \lambda \leq \infty$). However, the finite limits of integration must be chosen. The profilimeter uses an upper limit of .76 mm (through electrical fitering) for averaging purposes and has a lower limit set by the stylus radius of 13 μm. If one assumes that the absence of surface temperature fluctuations is indicative of negligible asperity interaction then as far as asperity interaction is concerned, one can determine the significant wavelengths of the surface profile. For example, Figure 6a shows that the temperature spectral power content during asperity interaction drops to less than ten percent of its peak value for the wavelengths $\lambda \leq d/4$. However, Figure 3a shows that there are significant roughness components down to at least $\lambda = .08d$ (the power content is essentially the square of the amplitude). The same figures show that the major components for both the roughness profile and the temperature signal are in the range $\frac{1}{2}d \leq \lambda \leq 3d$. Therefore, whereas the roughness wavelength in the range $\frac{1}{2}d \leq \lambda \leq 3d$ are obviously important in causing temperature fluctuations, wavelengths shorter than d/4 appear to have little or no effect. Based on the power reduction to ten percent of its maximum value, the lower bound for rms determination should be $\lambda \simeq d/4$. The

upper limit is set at $\lambda = 2d$ because the temperature signal drops off rapidly for $\lambda > 2d$ even though there are roughness components present with wavelengths greater than 2d (see Figure 3).

On the basis of the data taken, it appears that the rms surface roughness to be used in a calculation of $\Lambda(\Lambda = h/\sigma)$ should consider only wavelengths in the range $d/4 \leq \lambda \leq 2d$. For this experiment, d = 0.43 mm the applicable range is then $.11 \leq \lambda \leq .86$ mm. A roughness of about .38 μm Ra was obtained using the profilimeter with limits of about $.013 \leq \lambda \leq .76$ mm. By integrating the power spectrum of surface profile between the limits of $.11 \leq \lambda \leq .86$ mm, and taking the square root, the rms value was .53 μm. This higher rms value is believed to be due to significant power in the range $.76 \leq \lambda \leq .86$ mm and the natural difference between rms and Ra roughness measurements. The profilimeter also has available cutoffs at .25 mm and .067 mm. The use of either of these values would correspond to rms integration limits of $.030d \leq \lambda \leq .58d$ and $.030d \leq \lambda \leq .18d$ respectively. Since the desired range is $.25d \leq \lambda \leq 2d$, the resulting rms values would not be reliable in predicting surface interaction.

In addition to the possibility of getting a value of surface roughness which cannot reliably predict performance, the fact that wavelengths shorter than 0.25d do not appear to be significant might have an economic impact. For example, under conditions in which the Hertz diameter is relatively large, the final stages in a lapping or polishing process may not be important.

Most of the cases studies in this investigation fall into the

category of partial EHD lubrication wherein the load is shared by the hydrodynamic film and surface asperities. The influence of this normal load sharing on the surface temperature is shown in Figure 4. It is believed that the upper curve in Figure 4 corresponds to temperatures developed directly at the site of an interacting asperity. Also, the lower curve in the same figure corresponds to the temperature of the fluid pocket (relatively low pressure region) in the neighborhood following an asperity. It can be seen from Figure 4 that the temperature of the fluid pocket (lower curve) increases up to a certain value of peak Hertz pressure (P_H), reaches a maximum, and then decreases with further increase in P_H. This can be explained as follows; even though the total load on the contact is increased, beyond a certain load, the average fluid pressure begins to decrease because the asperities share an increasing portion of the total load. In order to determine the exact proportional of the total load shared by the asperities, normal load sharing calculations were performed using Tallian's approach [10,11]. An approximate statistical description of the surface is used for the medium rough ball.

Table I shows the calculated value of the portion of load carried by the EHD film (W_{EHD}) and the corresponding average fluid pressure (P_{EHD}) at various normal loads for two different asperity slopes (σ_θ). The area of fluid pockets is assumed to be equal to the Hertzian area. This assumption is valid since the area of the contacting asperities is indeed small [12]. The assumed rms slopes of asperities (σ_θ), represent their typical values. It can be seen (Table I) that

the average fluid pressure increases with the normal load up to a certain value, reaches a maximum (depending on σ_θ), and then decreases with further increase in normal load.

Figure 10 shows a plot of average fluid pressure versus peak Hertz pressure for the medium rough ball at a sliding velocity of 1.0 m/s, corresponding to the results shown in Table I. The dotted line corresponds to conditions when the entire load is supported by the EHD film. At low values of Hertz pressure, the Λ ratio is greater than one and therefore, the entire load is supported by the EHD film. As the Hertz pressure is increased, Λ decreases below one and the curve falls below the dotted line. The influence of the asperity slopes is apparent at this stage. With further increase in P_H, the average fluid pressure reaches a peak and then starts decreasing. Even though the exact value of σ_θ for the medium rough ball was not measured, the two values of .035 ($\theta = 2^o$) and .122 ($\theta = 7^o$) appear to be in a reasonable range and therefore direct comparisons can be made.

Table I. Normal Load Sharing Between Asperities and the EHD Film. (Medium rough ball: .076 μm R_a, Fluid N1, V_s = 1.0 m/s, V_{sa} = 0)

				σ_θ = .035		σ_θ = .122	
W N	P_H GPa	P_{avg} GPa	Λ	W_{EHD} N	P_{EHD} GPa	W_{EHD} N	P_{EHD} GPa
8.9	.52	.35	4.3	8.89	.348	8.86	.347
18	.65	.44	3	17.8	.435	17.7	.433
25	.74	.49	2.5	25.2	.489	24.7	.479
40	.86	.57	2	39.0	.559	36.8	.527
67	1.02	.68	1.5	62.4	.636	54.3	.552
215	1.51	1.00	1	192	.900	153	.715
222	1.52	1.02	.8	191	.876	142	.649
253	1.59	1.06	.6	208	.872	144	.602
294	1.67	1.11	.4	228	.866	146	.556
307	1.70	1.13	.3	234	.857	146	.536

CONCLUSIONS

Changes in the surface profile and EHD contact temperatures have been measured and analyzed. The existence of high frequency temperature fluctuations is found to be due to surface asperity interactions. Ferrographic analysis of the lubricant sample supports this argument.

It appears that the EHD contact behaves like a mechanical filter. Only a relatively narrow band of surface roughness wavelengths appears to be important in the process of asperity interaction. The size of the EHD contact, therefore, has a direct influence on the selection of the optimum surface finishing technique for a machine element.

The experimental results of the roughness, temperature and Ferrographic measurements support one another and theoretical predictions. In addition, the transition from full to partial EHD as monitored by these measurements can be accurately predicted using a properly evaluated Λ value.

ACKNOWLEDGMENTS

This research was supported by NASA-Lewis (NGR-11-002-133) and the National Science Foundation (ENG 74-21002). The continuing encouragement of and helpful discussions with Dr. L. Wedeven of NASA-Lewis are greatly appreciated. Also, the efforts of Mr. William Jones of NASA-Lewis in obtaining the Ferrograms of the lubricant samples is appreciated. Finally, the authors also wish to thank Mr. Scott Bair of Georgia Tech for the design and construction of much of the necessary equipment.

REFERENCES

1. Turchina, V., Sanborn, D. M., and Winer, W. O., "Temperature Measurements in Sliding Elastohydrodynamic Point Contacts", Trans. ASME, Journal of Lubrication Technology, Vol. 96, 1974. pp. 464-471.

2. Ausherman, V. K., Nagaraj, H. S., Sanborn, D. M., and Winer, W. O., "Infrared Temperature Mapping in Elastohydrodynamic Lubrication", Trans. ASME, Journal of Lubrication Technology, Vol. 98, Series F, No. 2, April 1976, pp. 236-243.

3. Nagaraj, H. S., Sanborn, D. M., and Winer, W. O., "Effect of Load, Speed and Surface Roughness on Sliding EHD Contact Temperatures", Trans. ASME, Journal of Lubrication Technology, Paper No. 76-Lub-23, presented at the Joint ASME-ASLE Lubrication Conference, Boston, Massachusetts, October 1976.

4. Jones, W. R., and Nagaraj, H. S., and Winer, W. O., "Ferrographic Analysis of Wear Debris Generated in a Sliding EHD Contact", to be published in ASLE Transactions 1977.

5. Sanborn, D. M., Winer, W. O., "Fluid Rheological Effects in Sliding Elastohydrodynamic Point Contacts with Transient Loading: I - Film Thickness", Trans. ASME, Journal of Lubrication Technology, Vol. 93, pp. 262-271, 1971.

6. Tallian, T. E., "On Competing Failure Modes in Rolling Contacts", ASLE Trans., Vol. 10, 1967, pp. 418-439.

7. Czichos, H., "Influence of Asperity Contact Conditions on Failure of Sliding Elastohydrodynamic Contacts", to be published in Wear Magazine, 1976.

8. Whitehouse, D. J. and Archard, J. F., "The Asperities of Random Surfaces of Significance in their Contact", Proc. Roy. Soc. Lond. A., 316, 97-121, 1970.

9. Peklenik, J., "New Developments in Surface Characterization and Measurements by Means of Random Process Analysis", Proc. Inst. Mech. Engr., Vol. 182, Pt. 3K, 1967-1968.

10. Tallian, T. E., "The Theory of Partial Elastohydrodynamic Contacts", Wear, Vol. 21, 1972, pp. 49-101.

11. Tallian, T. E., Author's Comments on "The Theory of Partial Elastohydrodynamic Contacts", Wear, Vol. 24, 1973, pp. 255-258.

12. Greenwood, J. A., and Williamson, J. B. P., "Contact of Nominally Flat Surfaces", Proc. Roy. Soc. Lond., Vol. 295, Ser. A., pp. 300-319, 1966.

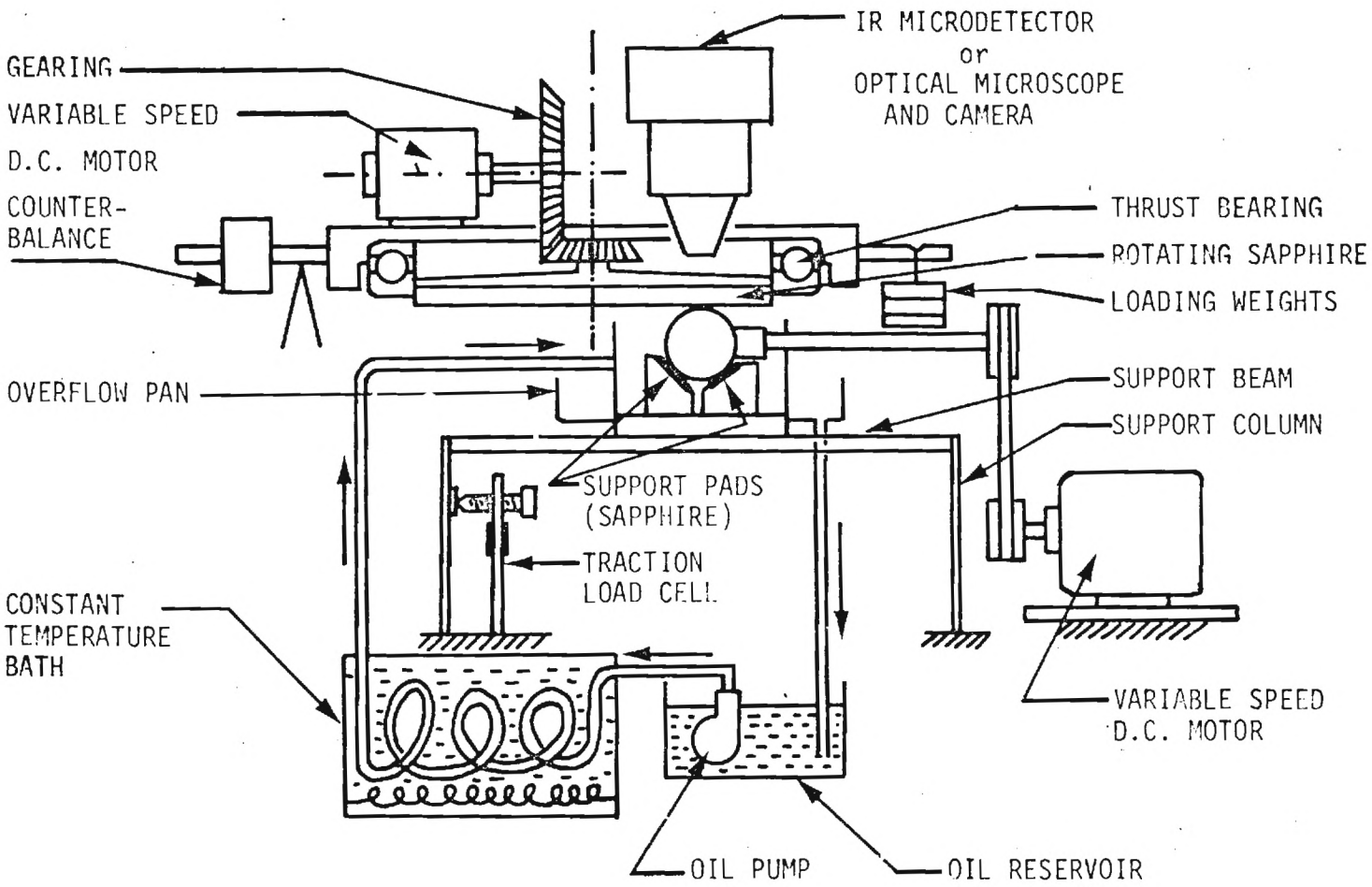

Figure 1. Schematic of the Combined Rolling and Sliding EHD Contact Simulator.

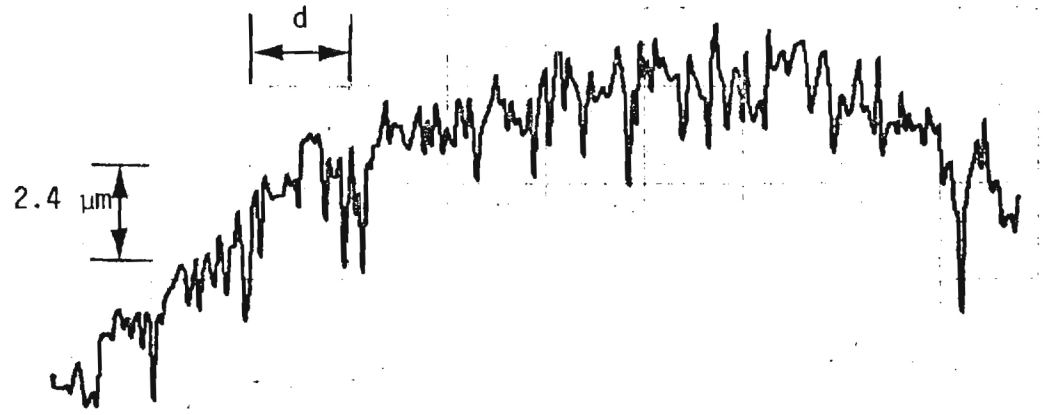

a) Unused ball surface (.38 µm Ra roughness).

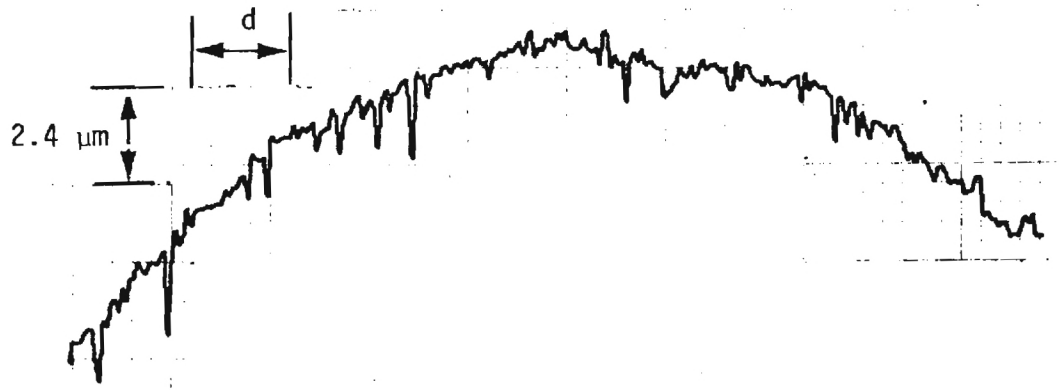

b) Ball surface after running 24 minutes (.25 µm Ra roughness).

Figure 2. Surface Profiles in Direction of Sliding (P_H = 1.24 GN/m^2, V_s = 1.02 m/s, Hertz Diameter d = 0.43 mm, pure sliding).

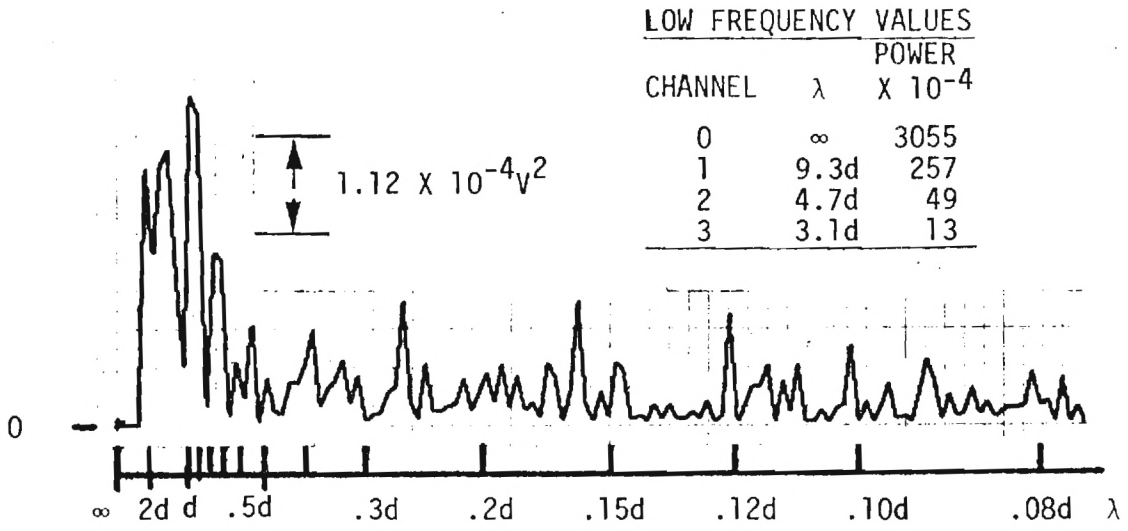

a) Unused ball surface.

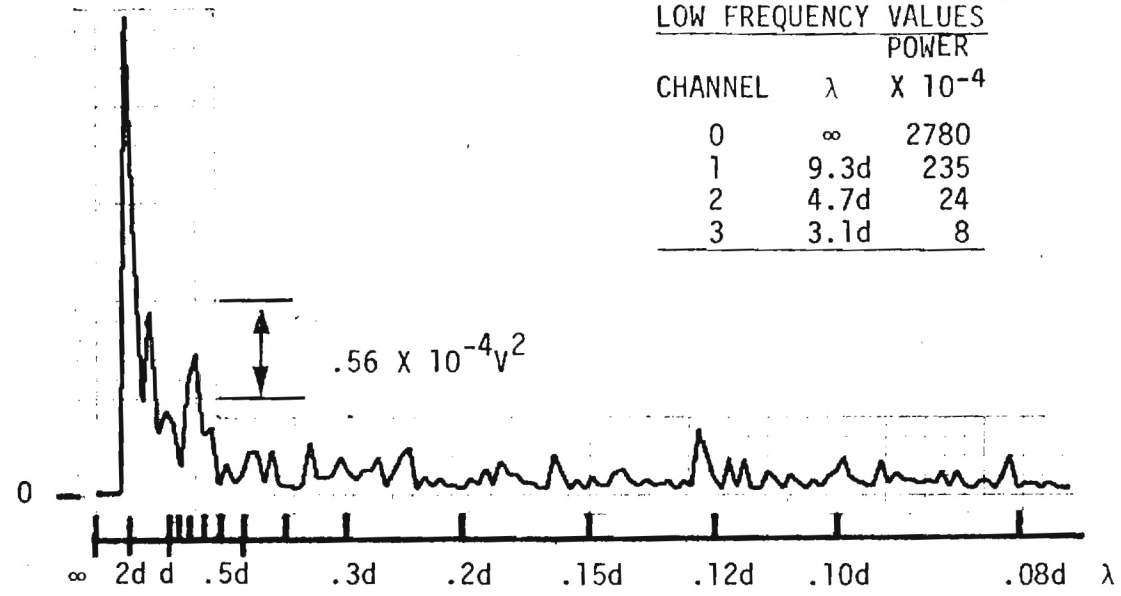

b) Ball surface after running 24 minutes.

Figure 3. Power Spectra of the Surface Profiles (P_H = 1.24 GN/m^2, V_s = 1.02 m/s, Hertz diameter d = 0.43 mm, pure sliding.)

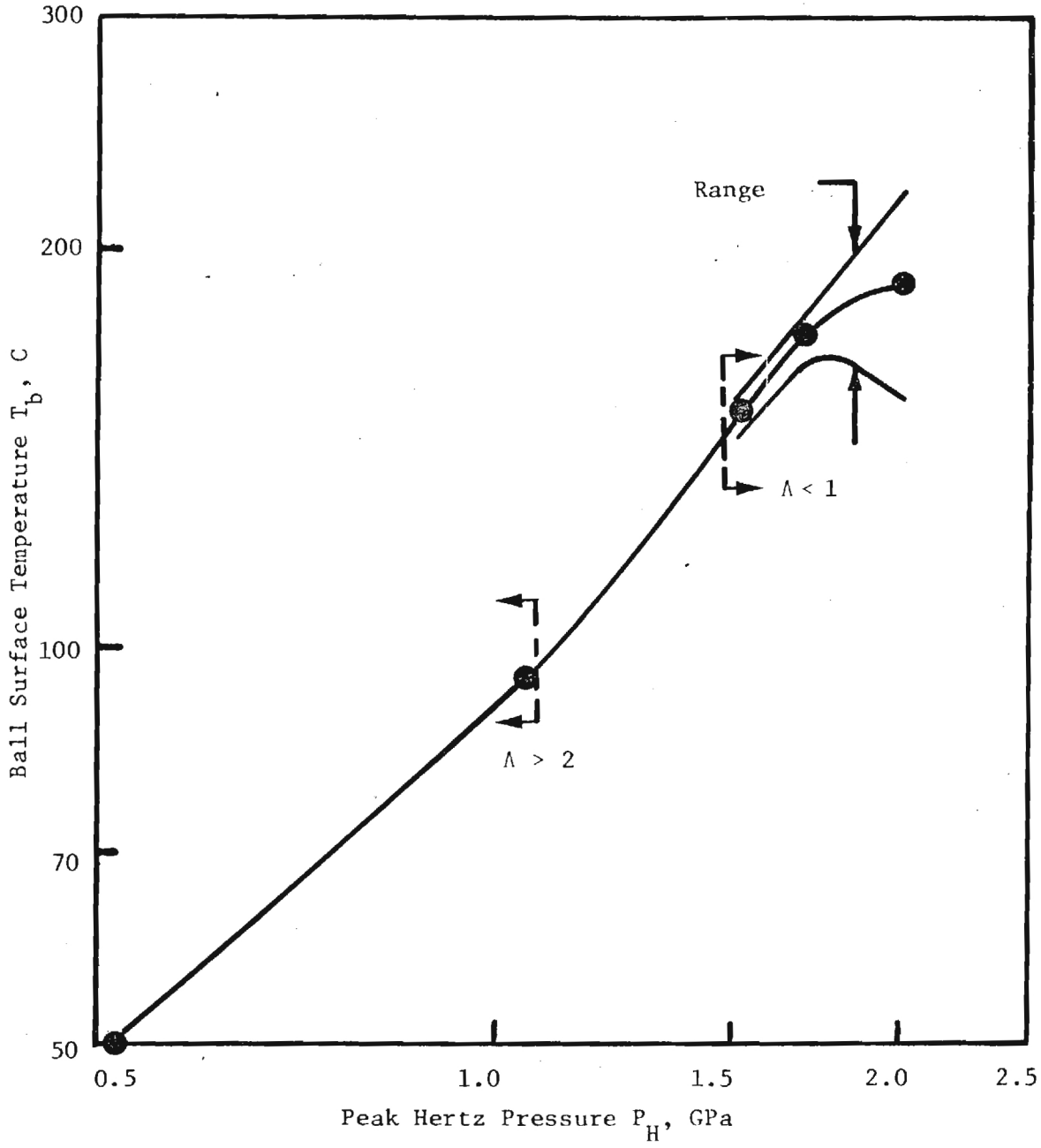

Figure 4. Average Value and Range of Ball Surface Temperature Fluctuation versus Peak Hertz Pressure (Medium Rough Ball: .076 μm R_a, Fluid N1, V_s = 1.0 m/s, V_{sa} = 0).

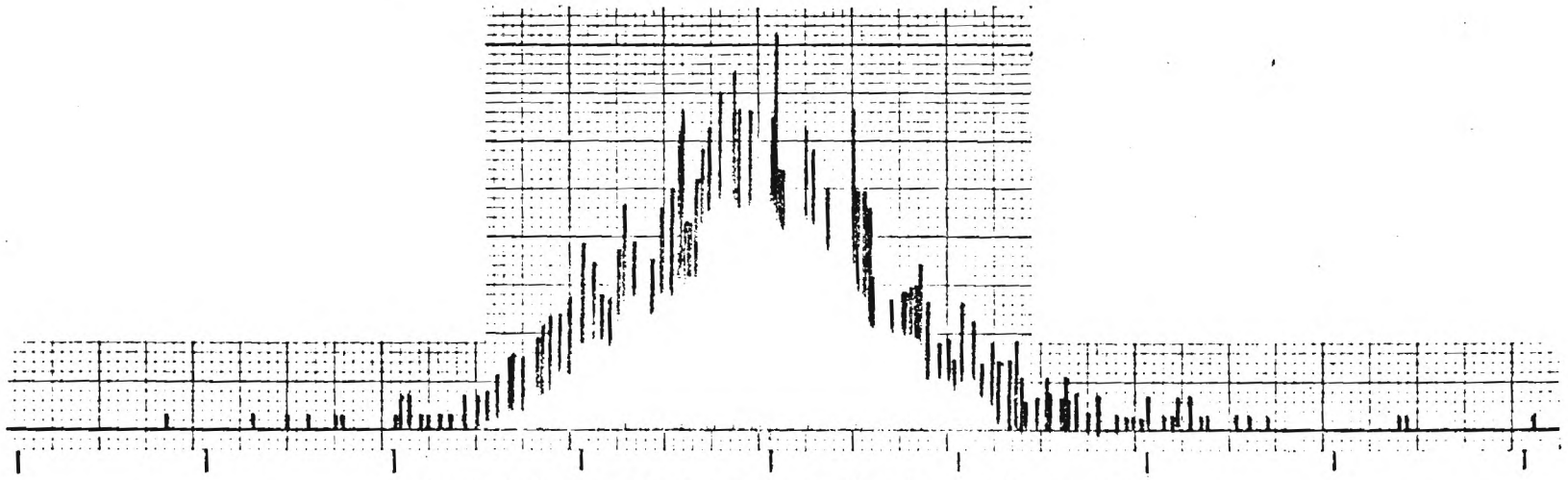

a) Initial Ball Surface Radiation Fluctuations.

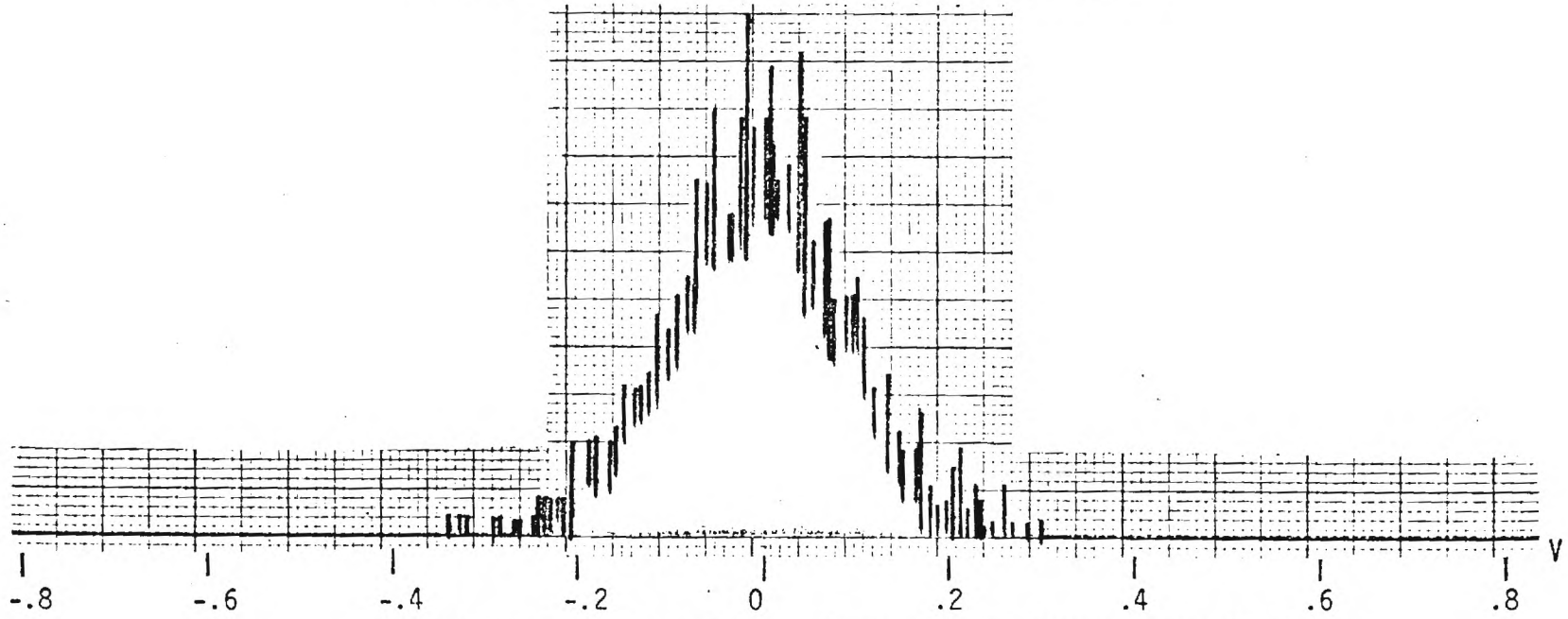

b) Ball Surface Radiation Fluctuations after Running 8 Minutes.

Figure 5. Normalized Histograms of Ball Surface Radiation Fluctuations (.38 μm R_a initial roughness, P_H = 1.24 GN/m^2, V_s = 1.02 m/s, Hertz diameter d = 0.43 mm, pure sliding).

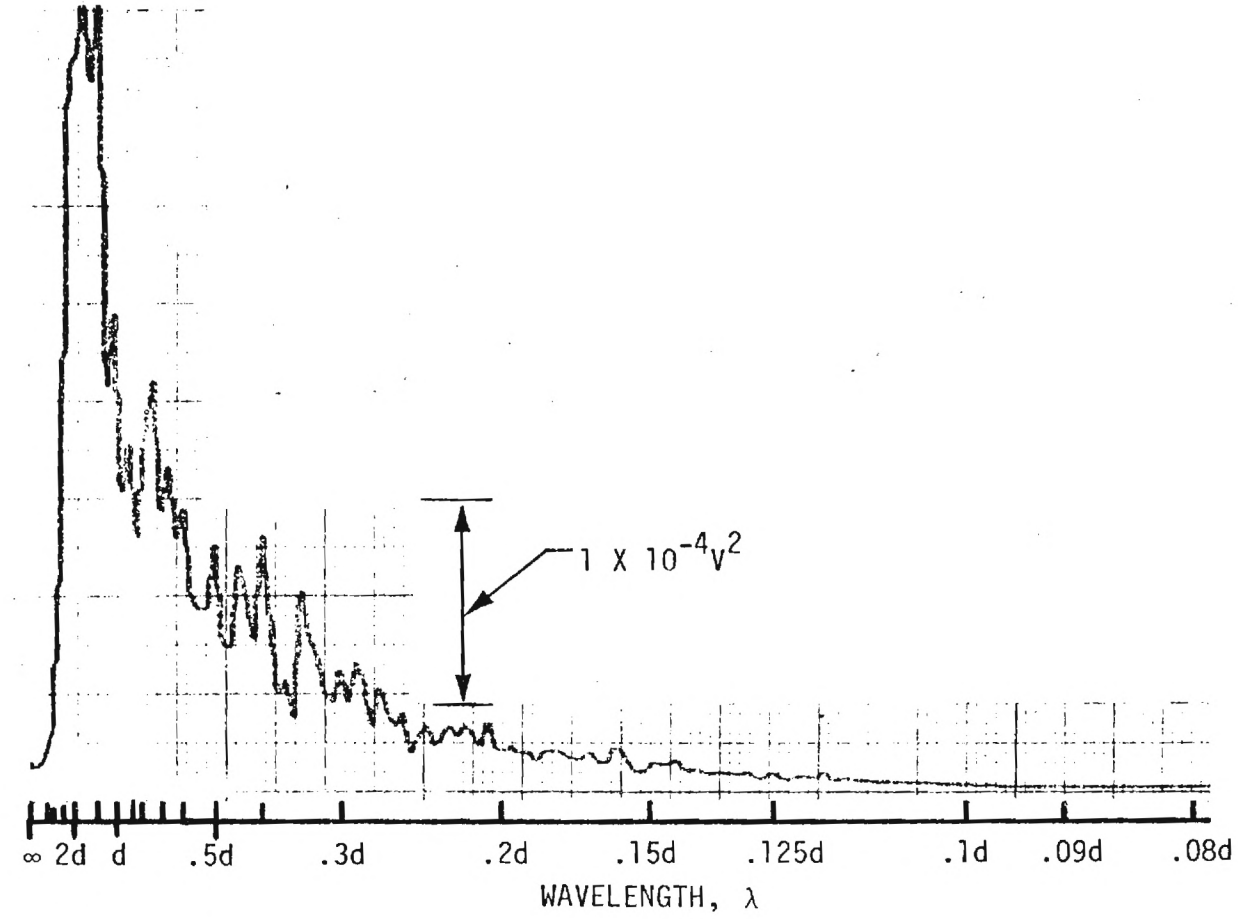

a) Ball Surface Temperature Fluctuations at Start of Run-in.

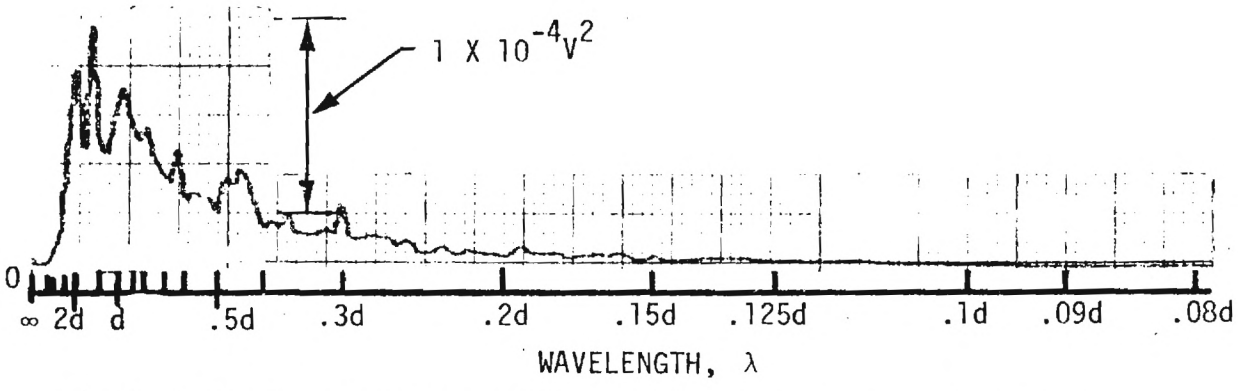

b) Ball Surface Temperature Fluctuations after 8 Minutes Run-in.

Figure 6. Power Spectra of Ball Surface Temperature Fluctuations (.38 μm Ra initial roughness, P_H = 1.24 GN/m^2, V_s = 1.02 m/s, Hertz diameter = 0.43 mm, pure sliding).

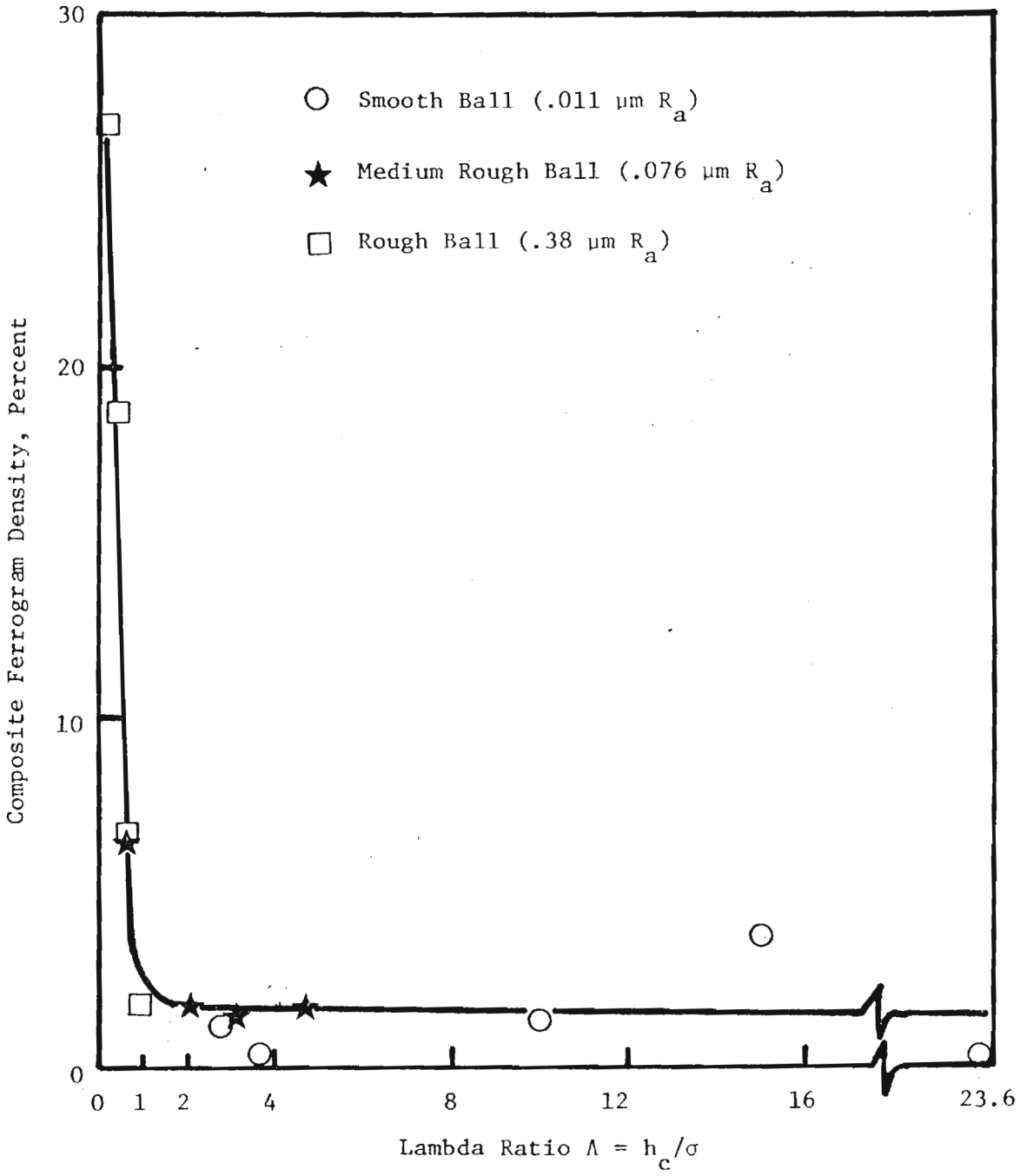

Figure 7. Composite Ferrogram Density versus Lambda Ratio.

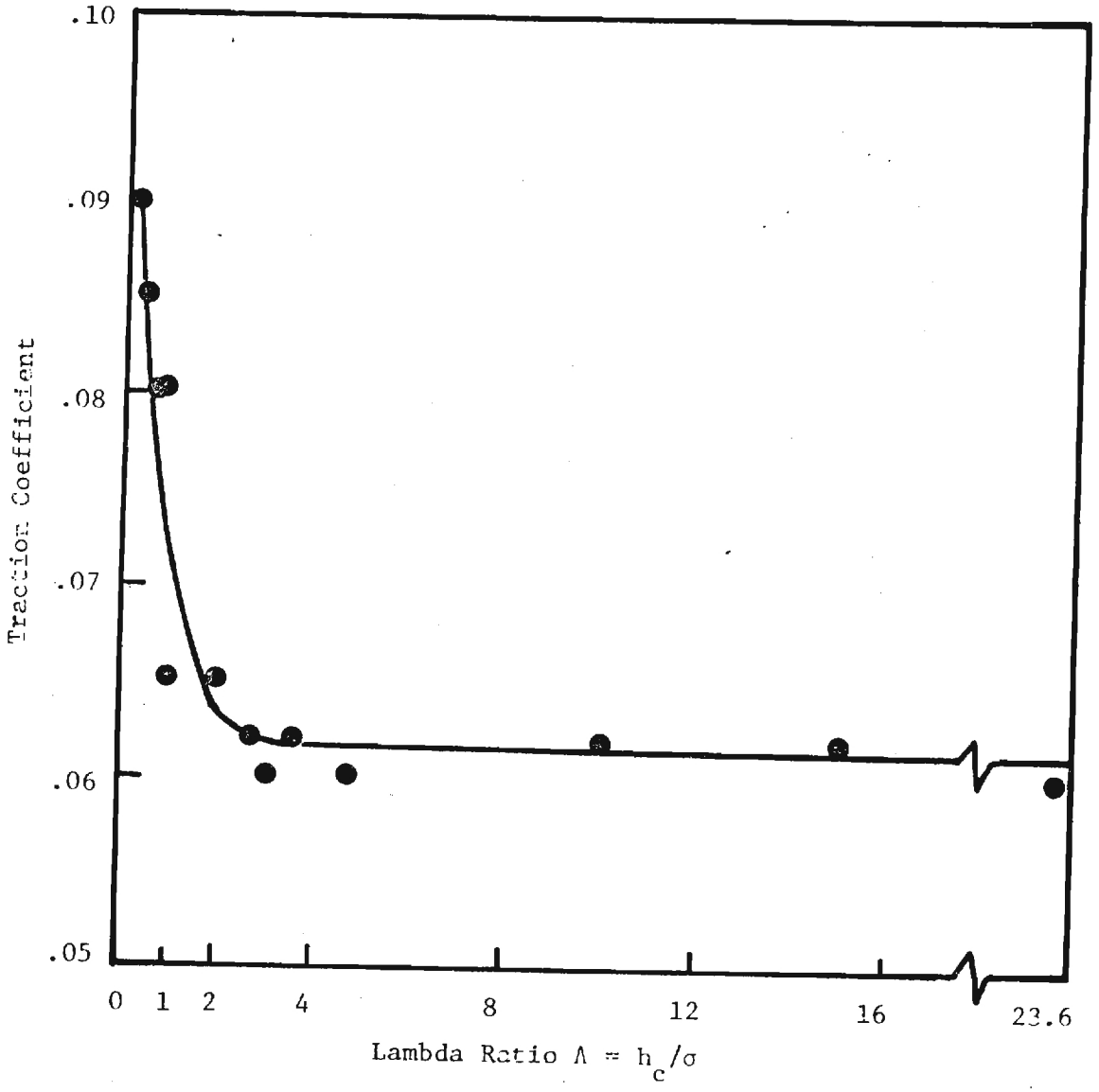

Figure 8. Coefficient of Friction versus Lambda Ratio.

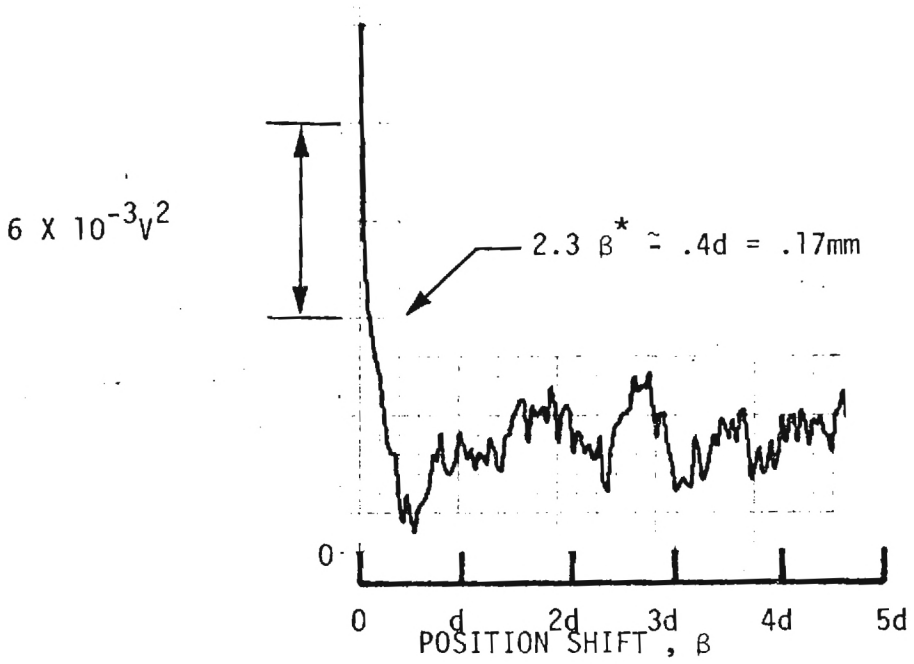

a) Unused ball surface (.38 μm Ra roughness).

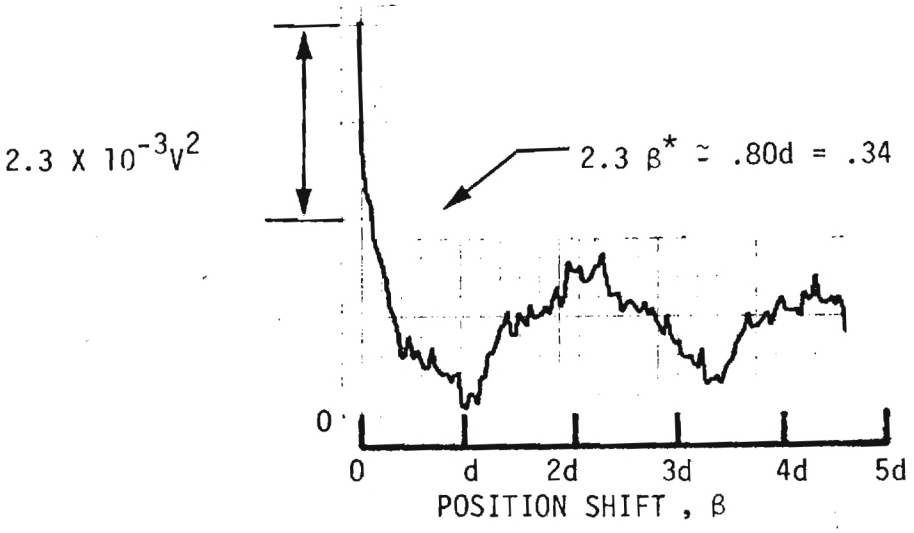

b) Ball surface after running 24 minutes. (.25 μm R_a roughness)

Figure 9. Autocorrelation Functions of the Surface Profiles. (λ > 3d not included, P_H = 1.24 GN/m^2, V_S = 1.02 m/s, Hertz diameter d = 0.43 mm, pure sliding)

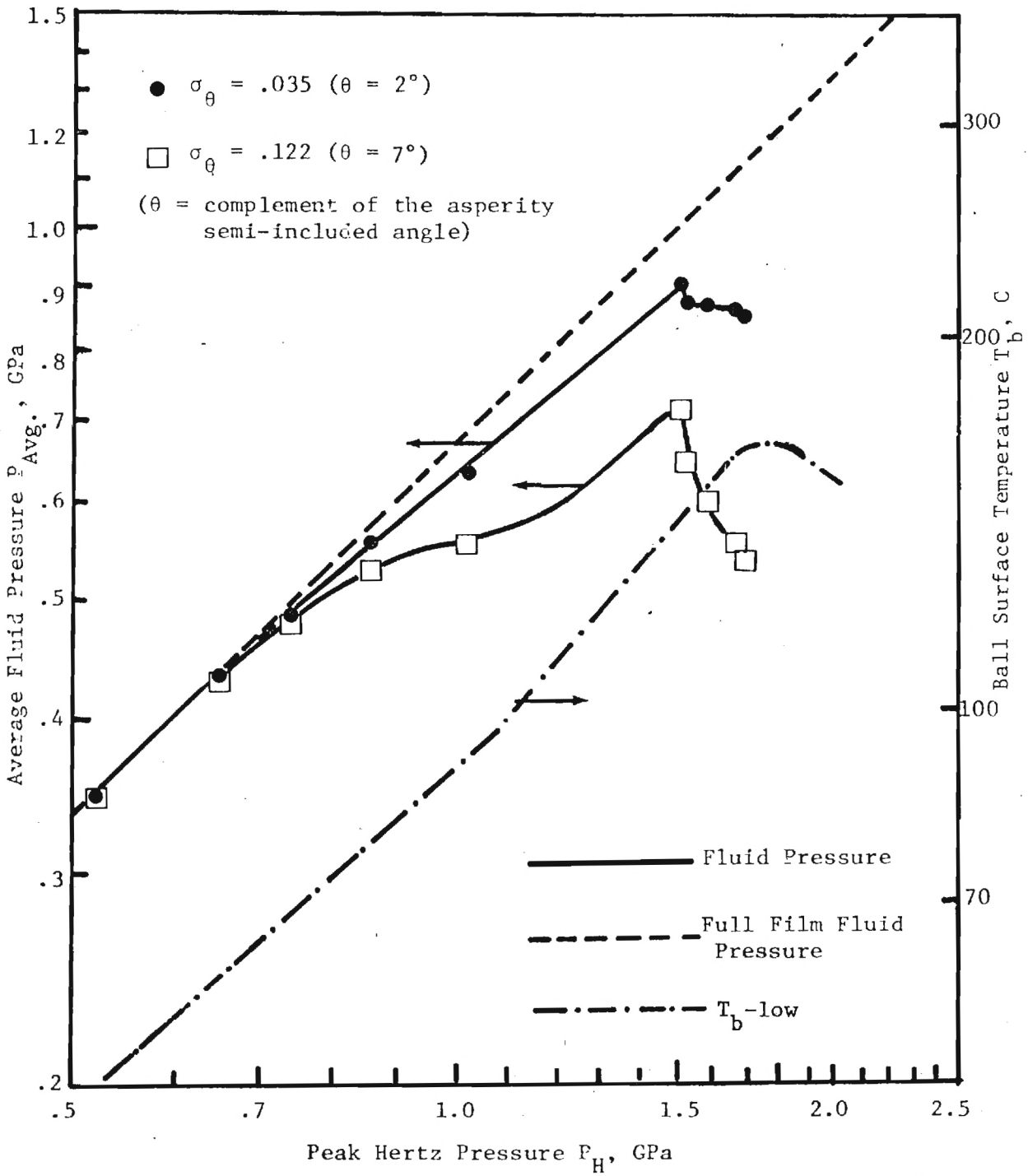

Figure 10. Average Fluid Pressure versus Peak Hertz Pressure under Partial EHD Conditions (Medium Rough Ball: .076 μm R_a, Fluid N1, V_s = 1.0 m/s, V_{sa} = 0).

inted in U.S.A.

4. Presented at the ASME/ASLE Lubrication Conference
Kansas City, Missouri, October 1977
(ASME Paper No. 77-Lub-3)

Paper No.
77-Lub-3

an ASME publication

$3.00 PER COPY $1.50 TO ASME MEMBERS

M. Alsaad[1]
Research Fellow.

S. Bair
Research Engineer.

D. M. Sanborn
Associate Professor.

W. O. Winer
Professor.

School of Mechanical Engineering,
Georgia Institute of Technology,
Atlanta, Ga.

Glass Transitions in Lubricants: Its Relation to Elastohydrodynamic Lubrication (EHD)

A preliminary investigation into the possible role of glass transition and glassy state behavior of lubricants in EHD contacts is reported. Measurements of the glass transition of lubricants as a function of pressure by two methods are presented along with a discussion indicating possible implications of the results to EHD lubrication.

A. Introduction

A preliminary investigation into the possible role of glass transition and glassy state behavior of lubricants in EHD contacts is reported. Measurements of the glass transition of lubricants as a function of pressure by two methods are presented along with a discussion indicating possible implications of the results to EHD lubrication.

The proposition that the mechanical behavior of lubricants in EHD contacts might not be that of a viscous liquid but of an elastic solid was first presented by Smith [1][2] in 1960. The results of Johnson and Roberts [2], and Johnson and Cameron [3] suggest that the lubricant film responds as an elastic solid under the conditions of pressure, temperature and shear rate of their EHD experiments.

Lubricating oils contain linear and highly branched hydrocarbons. Thus a lubricating oil can display both a glass transition which is associated with the noncrystallized (nonlinear hydrocarbons) part of the lubricant oil and a phase transition which is associated with the wax in the oil (linear hydrocarbons). Regardless of the wax content in a given oil, the glass transition temperature remains unchanged [4]. When comparing the conditions to which a lubricant is subjected in a typical EHD contact to available glass transition data, it appears quite likely that many lubricants are in or near the glassy state. This appears to be certain for some bulk polymers and polymer solutions and may also be true for low molecular weight hydrocarbons. If in or near the glassy state, the solid-like behavior and ultimate mechanical properties of the lubricant may be the controlling material characteristics in the large strain and large strain rate conditions that exist in EHD.

A preliminary review of the literature of the physics of glassy solids indicates that the stress and strain occurring in EHD contacts exceed the ultimate stress and strain in many materials. The work performed in our laboratory on the molecular degradation of lubricants in EHD contacts clearly demonstrates that yielding on a molecular level does occur in these applications [5, 6]. The infinitesimal strain work of Lamb [7] and Litovitz and Dill [8] are important in determining the extent to which the lubricant is in the glassy state, but, it seems to us, the important material properties are the ultimate or large strain properties and not the linear viscoelasticity properties.

In the early stages of this research, glass transition temperatures at atmospheric pressure were measured by the technique of Differential Scanning Calorimetry (DSC) for two lubricating oils: naphthenic base oil R-620-15, designated as N1 and five ring polyphenyl ether, 5P4E (more detailed fluid identifications are given in the Appendix). Glass transition temperatures were −59 C for N 1 sample and −21 C for 5P4E. Probably because these values are low compared to the operating temperatures in a typical EHD contact, the occurrence of the glass transition phenomenon and the existence of the glassy state in the contact were not investigated earlier by other researchers in this field. However, because of the fact that the glass transition temperature increases with pressure, and because of the existence of high pressures in the EHD contacts, the glass transition temperature can be greater than the operating temperature in the contact. The ASME Pressure-Viscosity-Report [9] was used to obtain an estimate of the variation of T_g with pressure. The solidification points indicated in the ASME report were assumed to be approximate glass transition points. Since these are reported as pressures at several different temperatures, they permit an estimate of the change of glass transition

[1] Present address: Assistant Professor, Kuwait University, College of Engineering and Petroleum, Mechanical Engineering Department, Kuwait.

[2] Numbers in brackets designate References at end of paper.

Contributed by the Lubrication Division of THE AMERICAN SOCIETY OF MECHANICAL ENGINEERS for representation at the ASLE-ASME Joint Lubrication Conference, Kansas City, Mo., October 3–5, 1977. Manuscript received by the Lubrication Division May 2, 1977; revised manuscript received July 14, 1977. Paper No. 77-LUB-3.
Copies will be available until June, 1978.

temperature with pressure. Also, according to McKinny and Goldstein [10], the glass transition is an isoviscous state. This is apparently because the glass transition represents a constant relaxation time for a given process and the relaxation time is essentially proportional to the viscosity. The change in temperature with pressure required to maintain constant viscosity gives results that are consistent with the results based on solidification. Based on this approach for typical lubricants, the glass transition temperature increases with pressure at a rate ranging from 80 to 350 C/GPa. Thus it would be expected that some lubricants will be in the glassy state in an EHD contact with average pressures of 0.7 GPa or higher at room temperature. It also would be expected that many lubricants are in the glassy state for a significant portion of the time they are in the contact.

The temperatures and pressures at which glass transition occurs and the mechanical properties of the lubricant in the glassy state may influence the two most important dependent operating variables of an EHD contact: the film thickness and the traction. Since the relaxation time of a material in the glassy state is long compared to the residence time in the contact, it is possible that once in the glassy state, the lubricant will remain in the glassy state on the moving surface while the surface moves from one EHD contact to the next. This may happen in spite of the fact that the pressure causing the glassy state formation has been removed. It is also possible that the glassy lubricant does not have time to flow while in the EHD contact but cleaves somewhere in the film so that solid layers of lubricant adhere to the contact surfaces and slide upon each other or the lubricant may undergo large strain like a ductile solid subjected to large stresses.

Therefore the glass transition temperature as a function of pressure is a significant material property of lubricants. The mechanical and thermal properties of a substance in the glassy state are known to be functions of the glass transition temperature and the history of how the material enters the glassy state.

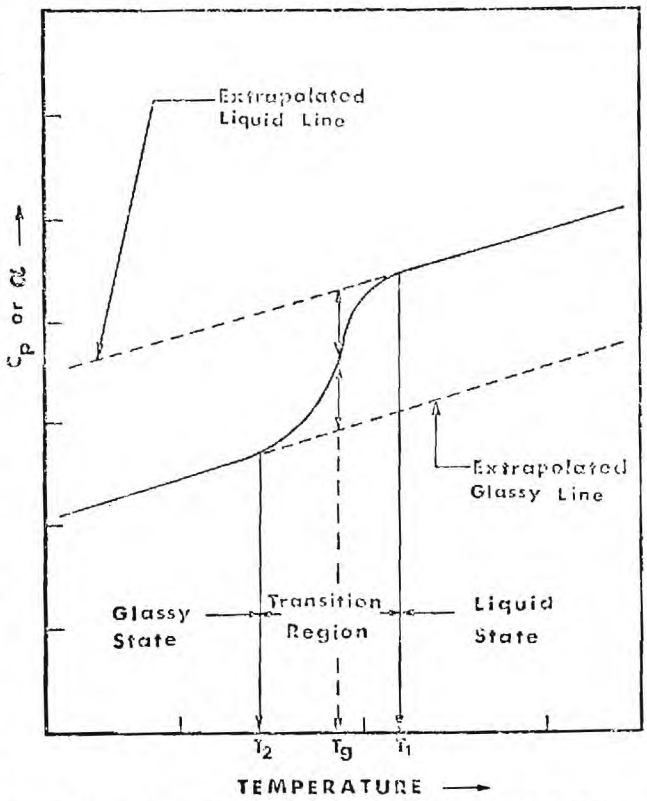

Fig. 1 Thermal expansion coefficient or specific heat for a typical glassy material

B. Glass Transition Temperature and the Glassy State

Glass transition is characterized by certain experimental observations which occur while the imposed environment of the material is changing. Commonly experiments are performed for isobaric cooling or isothermal compression of the material. As the temperature is reduced in the liquid region, the material contracts and the viscosity increases. If the material is capable of crystallization, a point will be reached where crystallization starts. If crystallization does not occur or can be avoided, the viscosity will continue to increase until some level of 10^7–10^{12} Pas is reached [11, 12, 13, 14]. At this point, the material becomes rigid and the thermal expansion coefficient falls by about one-half to one-third of its value in the melt or liquid state as shown in Fig. 1.

Glass transition is also accompanied by a change in the specific heat, c_p, isothermal compressibility, β, and other properties. It corresponds to a change in slope of a plot of specific volume versus temperature as shown in Fig. 2. Thus glass transition phenomena are characteristic of any liquid which can be supercooled to a sufficiently low temperature without crystallization.

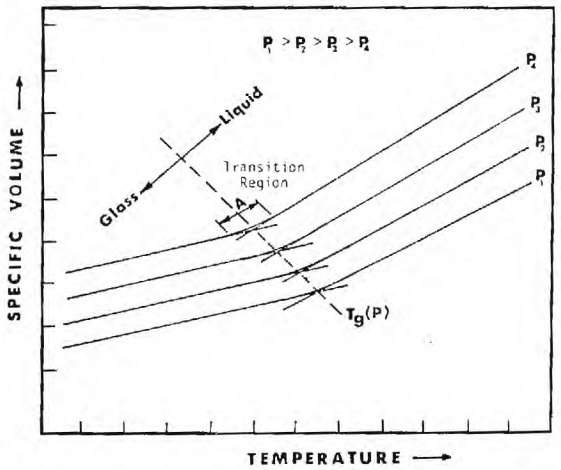

Fig. 2 Typical plot of specific volume versus temperature for a glassy material at different formation pressures

Glass transition phenomena are often referred to as apparent second-order transitions since they are characterized by a discontinuous change in the secondary thermodynamic quantities. These changes occur over a range of temperatures and are not strictly discontinuous. Ferry [14] and Haward [15] show that glass transition phenomena are not second-order thermodynamic transitions since at T_g the substance is not in thermodynamic equilibrium. This is due to the slowness of molecular rearrangements at this temperature. Absence of thermodynamic equilibrium is part of the definition of the glassy state.

Below T_g, the degree of order will appear fixed and will not vary with temperature or pressure during the time of experimental observation. Because of this, the structural degrees of freedom are said to be frozen-in and therefore, the structural contribution to α, c_p and β are absent in the glassy state.

The effect of pressure on T_g is shown in Fig. 2. The glass transition temperature shifts upward as the pressure is increased. The increase in T_g with pressure will be sufficient to maintain an isoviscous state. A sufficiently high pressure can induce a transition from the liquid state to the glassy state without requiring a decrease in the temperature.

The transition temperature of a material is a function of the imposed rate of change of the material's environment, and for a series of constant rate experiments, the transition temperature curve is a constant relaxation time curve. The characteristic time of the experiment is dependent on the observation time employed in the experiment. An approximate value of the relaxation time of the material when transition occurs is the observation time employed in the experiment. The range in the relaxation time of the material as it goes through the transition from liquid to glass is from about 0.1 to 10^2

times the observation time. In the transition region the material exhibits both viscous and elastic behavior relative to the process. The range of the transition region is indicated in Figs. 1 and 2.

As a result of the nonequilibrium state, the thermodynamic history of a glass forming liquid has considerable influence on the structure, the transition and the properties in the glassy state. The rate of the imposed environmental change effects the transition point and the properties of the glassy substance. Glass transition can be reached by isobaric cooling, isothermal compression, an imposed rate change or a combination of these changes on the material. For example, the influence of the rate of cooling, K, on the shift of the glass transition temperature of poly(vinyl acetate) has been studied over a wide range of rates by Kovacs [16]. The volume-temperature response obtained from different constant rates of cooling of a glass-forming substance is shown in Fig. 3. Since decreasing the rate of cooling increases the effective experimental time, the glass transition temperature will be shifted to lower values. Matsouka and Maxwell [17] studied the effect of rate of compression on the compressibility curves of polysterene at 121 C. Their results indicate that glass transition pressure, P_g, shifts to lower values when a greater rate of pressure application is employed. If the pressure is increased slowly, the molecules of the material will have enough time to rearrange and the glass transition will take place at a higher pressure. On the other hand, if the rate of pressurization is increased, the time for any structural changes is smaller and the glass transition occurs at a lower pressure.

The influence of thermodynamic history on glass transition of poly(vinyl acetate) was studied by McKinney and Goldstein [10] by using three different thermodynamic histories: variable formation history (isobaric cooling at different pressures), and two constant formation histories (cooling at atmospheric pressure or 80 MPa (800 bar) followed by pressure changes in the glassy state).

Several techniques are employed for the determination of the glass transition temperature such as dilatometry [10, 12, 18], differential scanning calorimetry [4, 19, 20], thermomechanical analysis (TMA) and dielectric [21, 22] and light-scattering techniques [23–36]. Depending on the technique used, various methods exist for specifying the glass transition temperature within the transition region. The usual dilatometric technique is to cool the liquid at a constant rate and extrapolate the linear portions of the volume-temperature relation above and below the transition region to their intersection. The temperature at this intersection [10] is taken as the glass transition temperature as shown in Fig. 2. If T_g is measured by the change in the expansion coefficient or the specific heat, then T_g is taken as the mid-point in the step-change as measured from the extensions of the glass and liquid base lines as shown in Fig. 1. While the choice is somewhat arbitrary, and other authors have suggested alternate techniques, the above methods are the most commonly used. Because of these different ways of defining T_g for different experiments, and because of the different inherent rates and histories in the different experiments, different glass transition temperatures may be measured on the same material in different experiments.

The first step in the study of the importance of the glassy state in EHD contacts is to determine if the lubricant is in or near the glassy state while in an EHD contact. This requires the determination of the glass transition temperature as a function of pressure and rate at observation times comparable to that of an EHD contact for typical lubricants. From these data, a phase diagram showing the liquid and the glassy states for the lubricant can be constructed. Based on the temperatures and pressures in the contact inferences can then be made regarding the state of the lubricant in the contact.

C. Experimental Technique

The glass transition temperature as a function of pressure based on two different techniques—light scattering and volume dilatometry—is reported. The two techniques are complimentary because the observation times are similar (about 200s) but the characteristic rates of the experiments are quite different—($10^{-2}s^{-1}$ for dilatometry and $10^{-10}s^{-1}$ for light scattering). Therefore as the material approaches the amorphous glassy state in the case of the volumetric experiment the material is a viscous liquid while in the light scattering it is behaving as an elastic liquid.

1. Light-Scattering Method. The basic concepts of the light-scattering technique and the description of experimental equipment used for measuring the glass transition temperature are discussed in detail in [35, 36]. The theory of the interaction of the coherent laser light and sound waves (or Debye thermal elastic waves [37]) is not new and is presented elsewhere [38]. The interaction of light waves and sound waves is referred to as Brillouin scattering [39]. The technique is basically one in which the frequency shift of the incident light scattered off the elastic waves is a measure of the sound velocity in the material.

The sound velocity changes continuously with temperature and pressure. A change in the slope of the sound velocity as a function of temperature and/or pressure defines the glass transition in a manner similar to that associated with other property changes. Fig. 4 shows the variation of the sound velocity and frequency shift with temperature for atactic polystyrene [28] where a change of slope is clearly observed at the glass transition temperature.

The dependence of the velocity of sound on the density, ρ, is seen

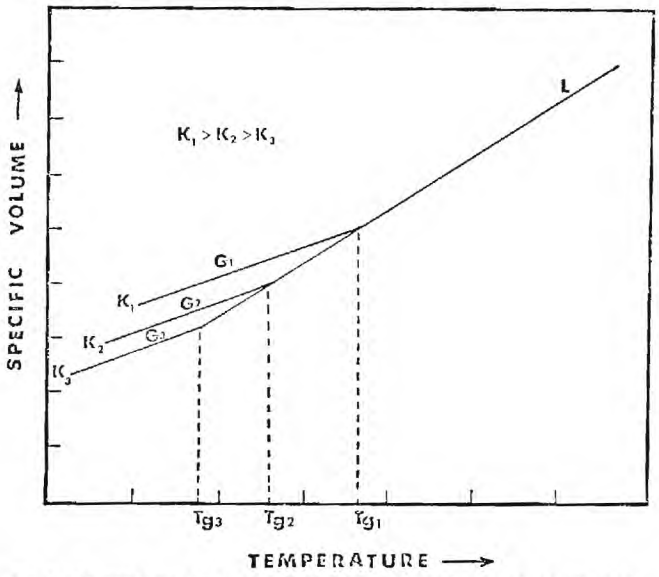

Fig. 3 Dependence of the glass transition temperature on the cooling rate, K_i. L = liquid and G = glass

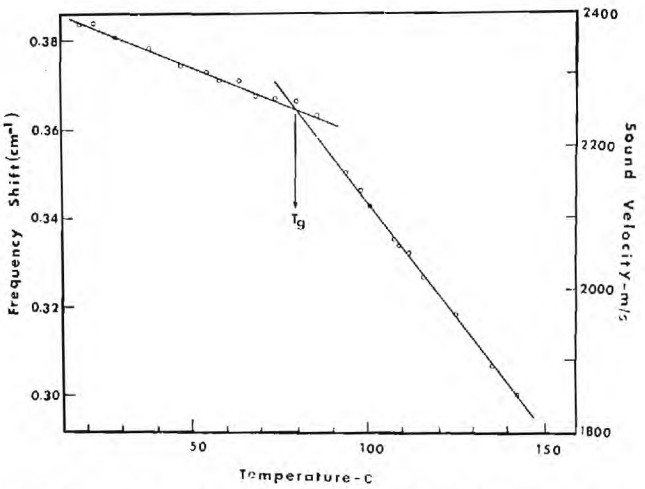

Fig. 4 The variation of the Brillouin frequency shift and the sound velocity with temperature at atmospheric pressure for atactic polystyrene [28]

through the relation

$$V = (M/\rho)^{1/2} \tag{1}$$

where M represents the appropriate modulus of elasticity which is a function of the density. Since the density appears explicitly in the above relation, it is clear that a change must appear in the slope of the velocity-temperature and velocity-pressure curves at the glass transition. A comparison of volume-temperature data with velocity-temperature data taken from literature [31] is consistent with the above observation. However, the expansion coefficient of polystyrene is 2.2×10^{-4} °C^{-1} for $T < T_g$ and 5×10^{-4} °C^{-1} for $T > T_g$ while the velocity coefficient is 8×10^{-4} °C^{-1} for $T < T_g$ and 14×10^{-4} for $T > T_g$ which shows that the dependence of velocity on density is chiefly through the strong dependence of the modulus on density and only to a lesser extent through the explicit appearance of density.

The experimental equipment[3] used in the light scattering experiment consisted of an argon ion laser (λ = 5.45A), a high pressure sample scattering cell, a triple pass Fabry-Perot interferometer, a photomultiplier tube and signal analyzing equipment. Detailed discussions of the apparatus can be found in references [35, 36]. The sample cell was capable of sustaining pressures to 0.66 GPa.

2. Dilatometry Method. As mentioned in the introduction, dilatometry can be used to measure the glass transition at long observation times. In many respects volume dilatometry is both conceptually and experimentally less complicated than the light scattering method for determining glass transition. Dilatometry is inherently a low rate process. A change in rate shifts the glass transition in a known manner. Therefore, dilatometry data is significant in that any temperature-pressure combination placing the material in the glassy-state by dilatometry measurements will indicate glass formation in an EHD contact because of the shorter observation time in the EHD contact.

Dilatometry measures the relative volume of the material as a function of temperature and pressure. The compressibility and thermal expansion coefficients of the material differ in the liquid and glass regions and the glass transition is defined by this change as discussed in the introduction and shown in Figs. 1, 2, and 3.

Three dilatometers were constructed, one of which is shown schematically in Fig. 5. The three devices were made to cover different pressure ranges. Both the isobaric cooling and isothermal compression experiments had observation times on the order of 10^2s to 10^3s.

3. Glass Formation History. Because of the dependence of the glass properties on formation history, two standard procedures were adopted to form the glass of the materials investigated. They are shown schematically in Fig. 6. In both formation histories the transition was measured by progressing from the liquid state to the glassy state. The two histories were isobaric cooling (history A) or isothermal compression (history B) while passing through the transition.

In the case of light-scattering experiments using formation history A the pressure was increased from atmospheric to a reference pressure in the liquid region. At the same time, the sample temperature was increased at a rate of 6.1 mC/s (22C per hour) to about 17 C above its assumed glass transition temperature. At this point the pressure and temperature were kept constant for about 30 minutes. The sample was then cooled at constant pressure and frequency spectra were taken at 2.8C (5 F) intervals. Twenty minutes was allowed for the temperature to reach equilibrium before each spectrum was recorded. Hence, experimental measurements were started in the liquid state and the glassy state was reached by decreasing the temperature at constant pressure as shown in Fig. 6. This procedure was repeated at different constant pressures and, therefore, the structure of the glass formed varies with the formation pressure. In the second formation history (history B), the glass was formed by pressurizing the sample at room temperature from atmospheric pressure until the glassy state

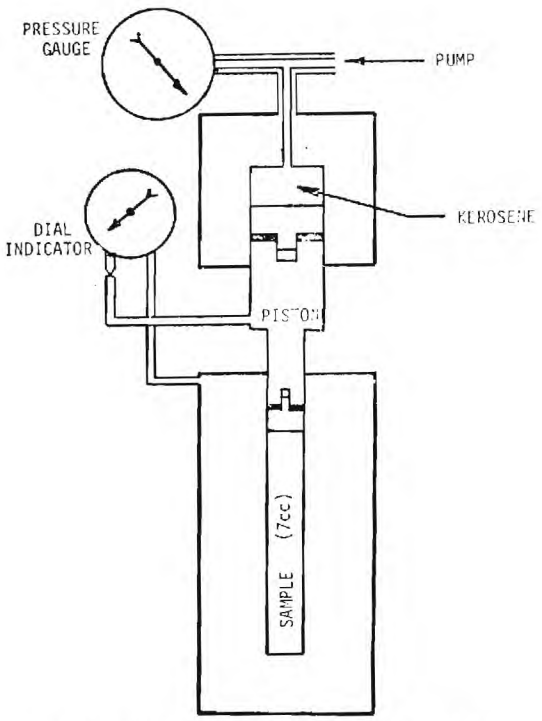

Fig. 5 High pressure dilatometer (.13 to 1.2 GPa)

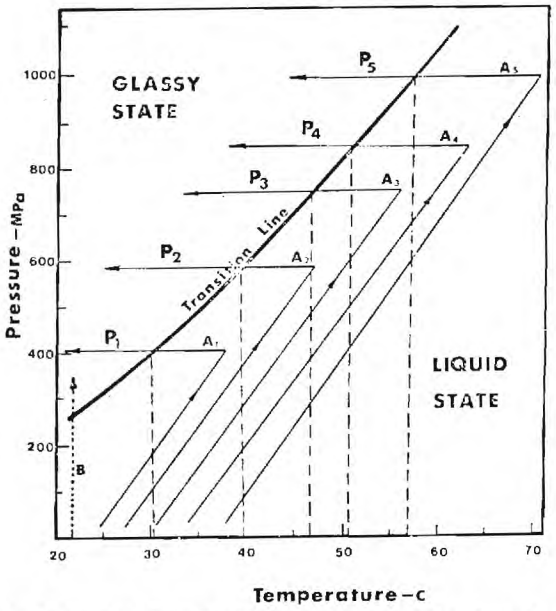

Fig. 6 Schematic of formation histories used to form the glass. A_i and B represent constant formation histories at pressure P_i and room temperature, respectively

was reached. Frequency spectra for this case were taken at pressure intervals of about 20 to 27 MPa (3000 to 4000 psi). Again up to twenty minutes was allowed for the sample to reach equilibrium before the spectra were recorded.

The formation histories in the dilatometry experiments were similar in that the material was always taken from the liquid state into the glassy state. For elevated pressure experiments this required heating and pressurizing in the liquid region well above the glass transition to some starting pressure and temperature from which the isobaric cooling or isothermal compression would start. As the experiment

[3] The assistance of Drs. D. C. O'Shea and F. D. Medina of the Georgia Tech Physics Department for the use of their light scattering equipment and guidance in this work is gratefully appreciated.

progressed the relative specific volume would be obtained as a function of temperature or pressure and the intersection of the curves in the liquid and glassy regions would define the glass transition.

D. Experimental Results

Seventeen lubricants have been investigated to date by the volumetric method and two by light scattering. The materials are listed in Tables 1 and 2. More detailed material descriptions can be found in Appendix A.

1. **Light-Scattering Experiments.** The light-scattering measurements result in a frequency shift of the laser light employed and a measure of the longitudinal speed of sound both as a function of temperature or pressure. Typical results for 5P4E are shown in Fig. 7, for history B (isothermal compression). From this figure, it is seen that the sound velocity and the frequency shift increase with increasing pressure and a change in the slope is apparent at 0.17 GPa (24,700 psi) corresponding to a velocity of sound of 2658 m/s. This change of slope represents the glass transition. The velocities on each side of the transition region can be represented by linear functions of pressure. The two sections of Fig. 7 were each fit by least squares regression to a linear expression. The intersection of these lines are interpreted [28–34] as occurring at the glass transition pressure.

Similar results for history A experiments (isobaric cooling) for 5P4E are shown in Fig. 8. The sound velocity increases as the temperature is decreased. At the transition region the dependence of sound velocity on temperature changes. This change of slope of the temperature coefficient of the sound velocity was observed at all formation pressures. Once again, the two portions of the sound velocity curves were fit by least square regression to straight lines. 5P4E was subjected to formation history A at a total of six formation pressures. The resulting material behavior is shown in Fig. 9.

The least square expressions for both portions of the velocity-temperature curves were solved for their intersection to determine

Table 1 Experimental fluids [a] in volumetric glass transition experiments

5P4E(b)	XRM-177-F4
N1[b], N2	DN 600
P1	FN 2961
MCS 460	S2-Polybutene
MCS 1218	S1-Diester
Sanotrac 50	S3-DC200-Blend I
Formulated Advanced Ester	DC 200-50

[a] Detailed descriptions are given in Appendix A.
[b] Measurements also made by light-scattering.

Table 2 Fluids for which no transition was observed by the volumetric method in the indicated temperature and pressure ranges (isothermal compression)

Sample	Maximum pressure (GPA)	Temperature (°C)
DIESTER (S1)	1.13	−3.3
DC 200 BLEND II	[a] .61	7.2
DC 200 − 50 (S3)	[b] .92	21.1
ADVANCED ESTER	[b] 1.07	16.9

[a] Displacement limited
[b] Piston seized

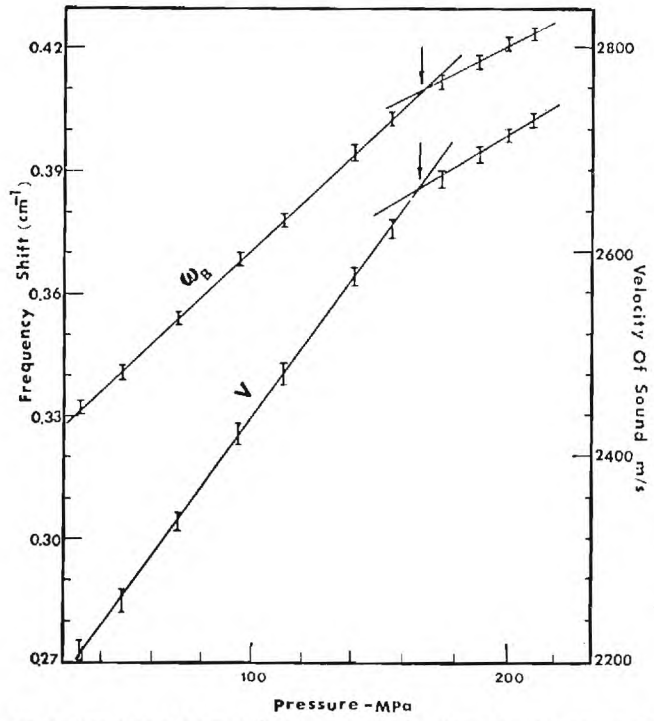

Fig. 7 Variation of frequency shift and velocity of sound with pressure at 24.4C (76F) for 5P4E Fluid (history B). Arrows indicate glass transition

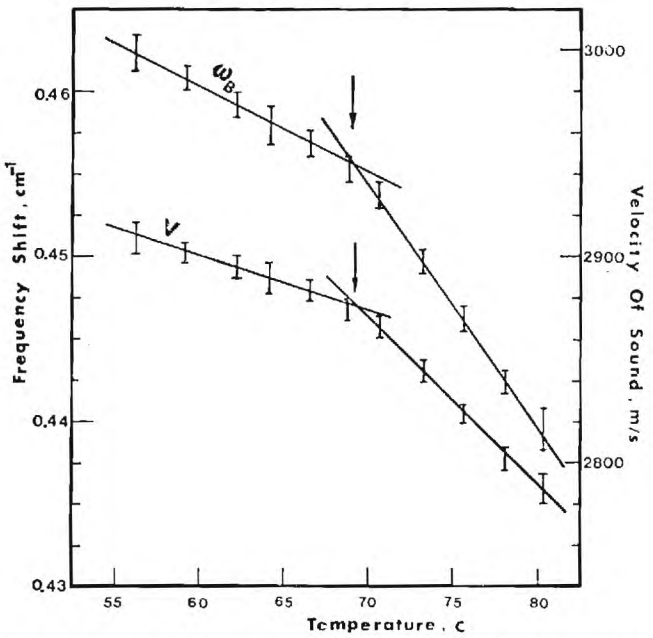

Fig. 8 Variation of frequency shift and velocity of sound with temperature at 0.40 GPa (59,000 psi) for 5P4E (history A). Arrows indicate glass transition

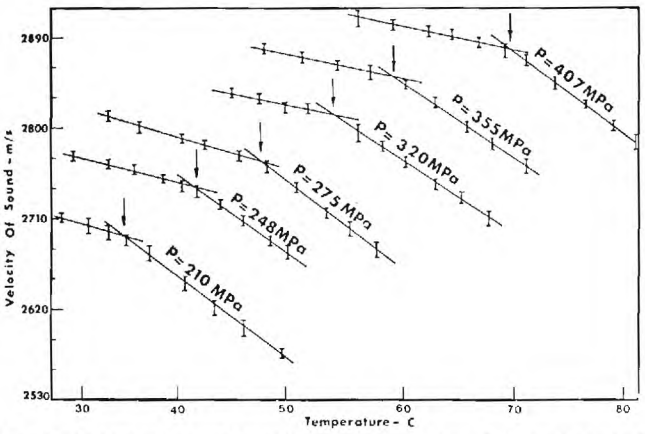

Fig. 9 Velocity of sound dependence on temperature at different constant pressures for 5P4E fluid (history A). Arrows indicate T_g

the glass transition temperature at each formation pressure. The glass formation temperature-pressure combinations result in the phase diagram shown in Fig. 10. The glass transition temperatures and pressures were least square fit with a straight line. The expression obtained is given by

$$T_g = 0.183\, P_g - 4.74$$

with T_g in C and P_g in MPa. The glass transition temperature at 24.4C (76F) by history B was excluded from the fit due to the different history by which the glass was formed. However, in general, the transition obtained by history B fell near the line obtained by history A.

2. **Dilatometry Experiments.** The dilatometry experiments give a change in slope of specific volume as a function of temperature or pressure. That change of slope defines the glass transition and permits construction of a liquid-glass phase diagram similar to Fig. 10 which was constructed from the light-scattering data.

Experiments have been completed on the materials shown in Table 1. The phase diagram for 5P4E obtained with the volumetric method compared with that from the light-scattering is shown in Fig. 11. The reason for the difference in the data from the two techniques is believed to be pressure measurement error in the light-scattering experiment. The difference is small, however, relative to the temperature and pressure ranges a material is subjected to in an EHD contact. Therefore, if 5P4E is subjected to a temperature-pressure combination in an EHD contact which is to the right of the dilatometry curve on this phase diagram, the material will be in the glassy state in the EHD contact. These data suggest that 5P4E would be in the glassy state in most EHD applications. Fig. 12 contains similar comparisons for material N1. The same comments made regarding 5P4E are applicable to N1.

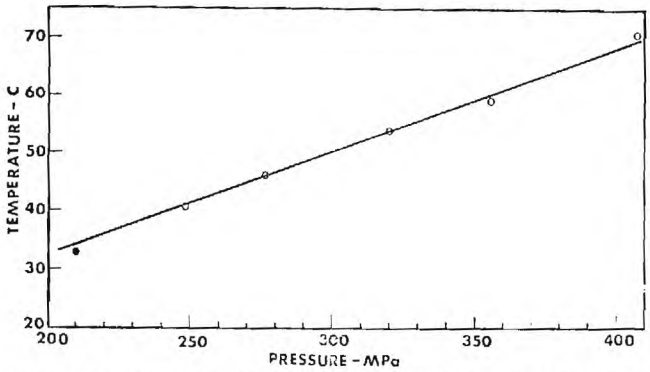

Fig. 10 Phase diagram for 5P4E fluid based on light scattering experiment. dT_g/dP = 183 C/GPa. History A(○). History B(●)

Fig. 13 contains phase diagram data for several materials based on the isothermal compression measurements. The variation in glass forming tendencies of the materials is large. However, the typical mineral oil based lubricants studied have very similar glass forming characteristics as shown in Fig. 14.

Typical transition regions for the compression experiments are shown in Figs. 15 and 16. Because the observation time in these experiments was approximately five minutes the glass transition point is where the material relaxation time is approximately five minutes and the transition region represents the changes in relaxation time (τ_m) from about one tenth that value on the liquid end to about 10^2 times that on the glassy end ($0.5 \leq \tau_m \leq 500$ minutes). In this region the material exhibits both viscous and elastic behavior relative to this experiment. In the liquid region the relaxation time is much less than 0.5 minute and the material can be treated as a viscous liquid in this process. In the glassy region the relaxation time is greater than 500 minutes and the material can be treated as a solid in this process.

Table 2 lists those materials which were studied but for which no glass transition was observed for the volumetric experiments in the pressure and temperature range studied. This implies that the relaxation times of these materials were much less than one half minute in the pressure and temperature range of observation.

3. **Two Additional Experiments.** Glass transition is accompanied by changes in all the physical properties of the material including very large changes in viscosity. In the past, glass transition has been defined as the point at which the viscosity of the material reaches a high value (e.g. 10^{11}Ns/m^2).Because the approximate shear rates and shear stresses to which the material is subjected in an EHD contact are not consistent with such high viscosities, while the temperatures and pressures indicate it is in the glassy state, two simple shearing

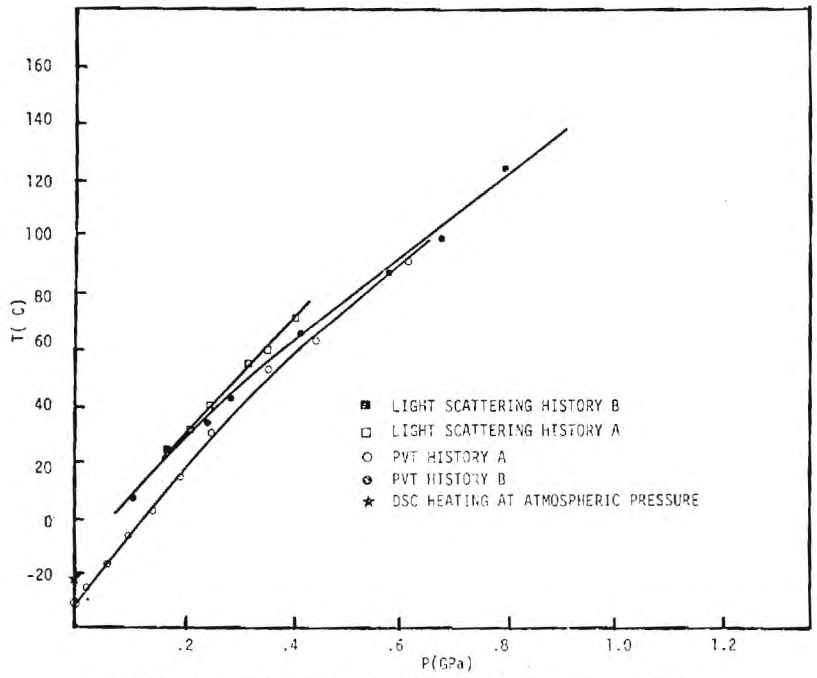

Fig. 11 Comparison of glass transition of 5P4E by various methods

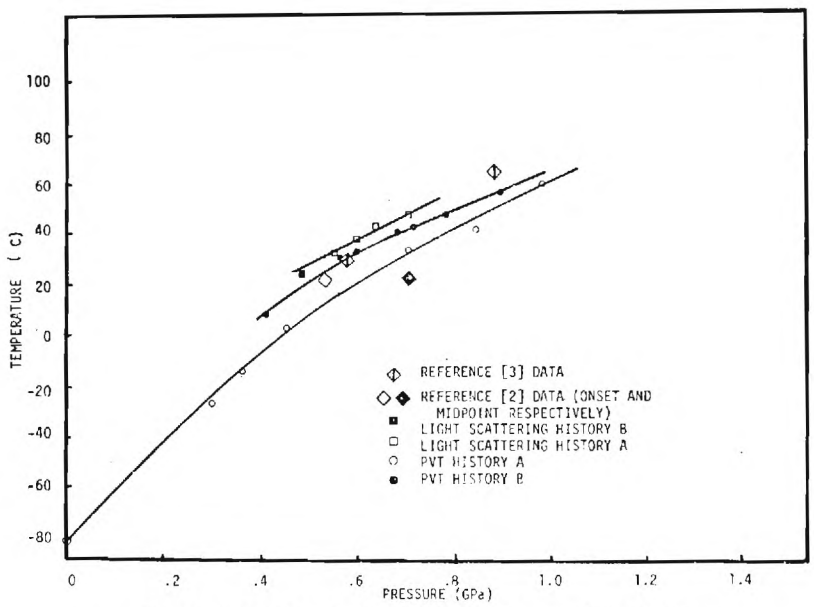

Fig. 12 Comparison of glass transition of N1 by various methods

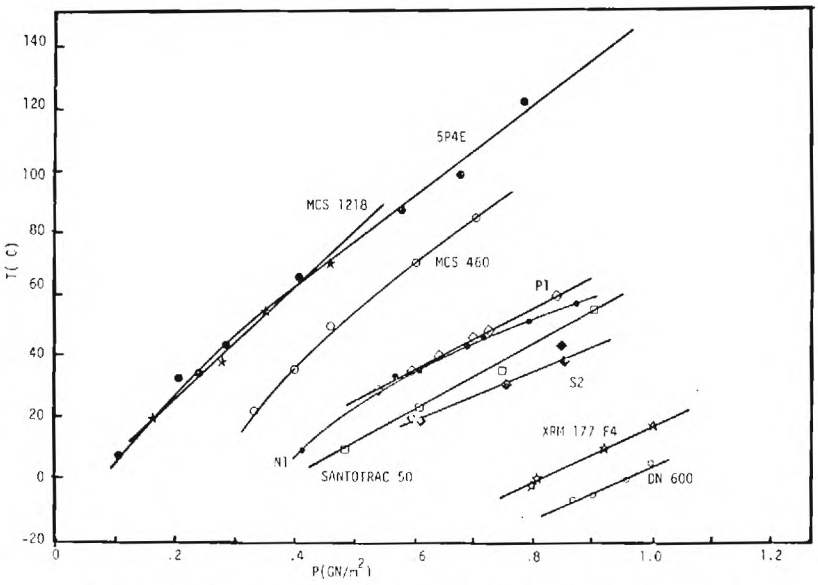

Fig. 13 Glass transition by isothermal compression from liquid (dilatometry)

experiments were conducted. Both were conducted in a concentric cylinder device. In one experiment the torque (shear stress) was measured continuously at constant shear rate (0.43 s^{-1}) while the 5P4E sample was cooled continuously. In the second experiment a crude indication of the ultimate shear strength of the material in the glassy state was obtained.

The viscosity measurement experiment was conducted in a Haake concentric cylinder viscometer and the results are shown in Fig. 17. As expected the viscosity increases rapidly with decreasing temperature but the trend begins to change substantially as the glass transition temperature is approached. The glass transition temperature as measured by differential scanning calorimetry is −23C and is marked on the figure. The shear stress limit of the instrument is about 3.5 kPa. As the temperature continues to decrease below the glass transition temperature the material effectively becomes a rigid solid.

Once in the glassy state the material has solid-like properties such as sound velocity, thermal expansion coefficient, specific heat, etc., and might also be expected to have an ultimate yield shear strength. To get an estimate of this property at atmospheric pressure, a concentric cylinder device was constructed with a sample outer diameter of 16 mm, inner diameter of 13 mm and length of 16 mm. The outer cylinder could be held firm and the inner cylinder turned with a torque wrench when the sample was cooled below its glass transition temperature. A thermocouple was inserted into the sample through the inner cylinder and the device cooled by liquid nitrogen. The torque required to break the inner cylinder loose was then an estimate of the yield shear strength of the material. The data are shown in Table 3. These results suggest that yield behavior of the material in the glassy state should be studied in conjunction with the study of material behavior in EHD contacts.

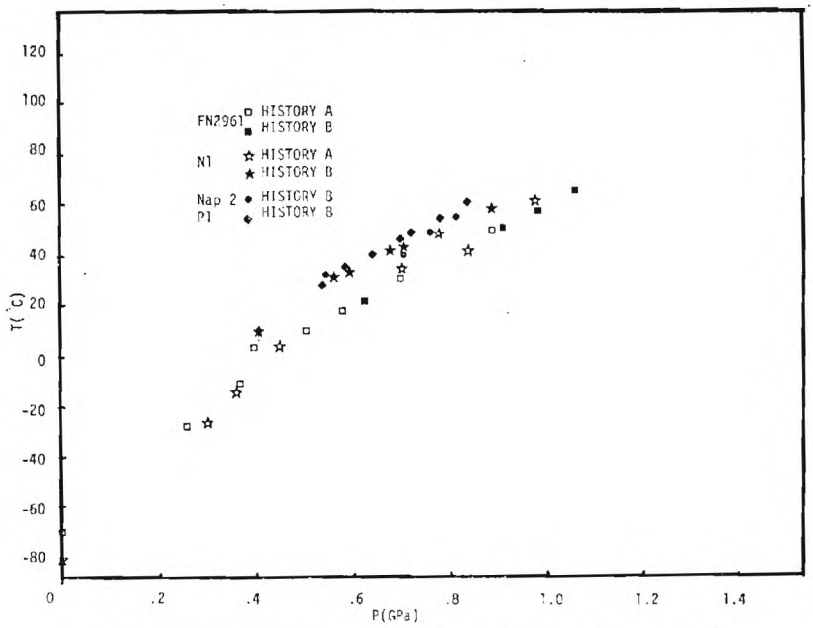

Fig. 14 Glass transition of various hydrocarbon oils determined by dilatometry

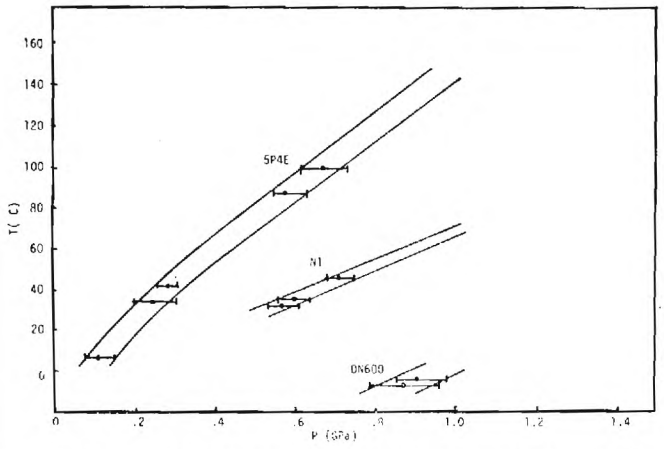

Fig. 15 Dispersion region in isothermal compression by dilatometry

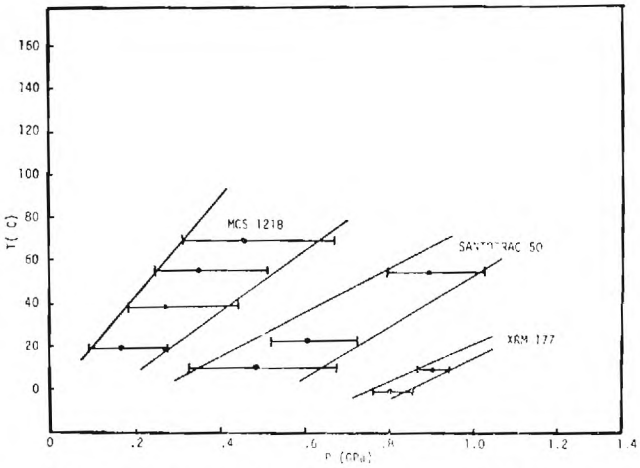

Fig. 16 Dispersion region in isothermal compression by dilatometry

E. Discussion of Results

1. Pressure Dependence of Glass Transition Temperatures in Lubricants. The glass transition results presented suggest that glass transition phenomena and rheological behavior in the glassy state are important for some lubricants in some EHD applications.

The volumetric experiments covered the widest range of pressure and temperature. As seen in Fig. 12 for N1 at low formation pressures (up to about 0.45 GPa), the transition temperature is a linear function of pressure with a slope of about 190 C/GPa. Above 0.45 GPa, the slope decreased gradually and the glass transition relation became linear again above 0.55 GPa with a slope of about 100 C/GPa.

The glass transition temperature for N1 at atmospheric pressure was also determined by the volumetric measurements and has a value of −81 C. This value is lower than that obtained by the DSC measurements by about 22 C. The decrease in T_g is due to the different cooling rates (28 C/hr for the volumetric measurements and 1220 C/hr for the DSC measurements) and the different formation history used in each technique.

The volumetric and light scattering transition data for 5P4E are shown in Fig. 11 and have behavior similar to that discussed above for N1.

Table 3 Approximate yield shear strength at atmospheric pressure

Fluid	T	T_g	$\simeq \tau$ yield, MPa
5P4E	−60C	−23C	5.38
N1	$<T_g$	−62C	3.24
XRM	$<T_g$	N.A.	2.96

2. Relationship of Glass Transition to EHD Conditions. To obtain an impression of the relationship between glass transition for various lubricants and conditions in EHD contacts, Figure 18 has been prepared. Fig. 18 contains the liquid-glass transitions for three lubricants as measured by the volumetric technique. The three lubricants selected represent a wide range of behavior with respect to glass transition. Above and to the left of each curve is the liquid region for the material for low rate (long observation time) processes. To the right and below each curve is the glassy region. Based on limited measurements on three other hydrocarbon base oils the curve for N1

is an adequate first approximation for nonpolymer containing hydrocarbon base oils. Also indicated in Fig. 18 are the approximate ranges of pressure in the inlet and the Hertzian zones of an EHD contact. The approximate temperature ranges are also marked for an inlet temperature of about 20 C based on the IR temperature measurements made in this laboratory [35]. What this heuristic depiction shows is that glass transition most probably occurs in many practical applications of EHD contacts with many existing lubricants. The higher the contact pressure the more likely the transition to the glassy state, particularly with rolling and low slip ratio contacts. The glass transition and glassy state behavior are most likely to effect traction but may also effect film thickness if the transition occurs in the inlet zone. The above clearly suggests the phenomena of glass transition occurs in EHD and its effects may be observable in EHD data already available.

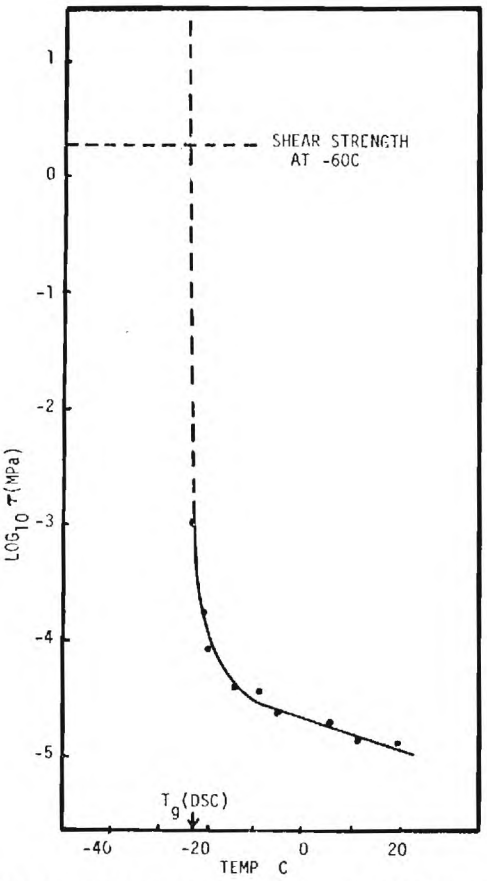

Fig. 17 Shear stress between concentric cylinders for 5P4E cooled at 2.75 C/min., shear rate $\dot{\gamma} = .434\ s^{-1}$

2(a) EHD Traction Data. Johnson and Cameron [3] measured the traction transmitted by an elastohydrodynamic film in a rolling contact with low sliding speeds and near isothermal conditions. From the traction measurements, the variation in apparent viscosity of their oil[4] with pressure and temperature is shown in Fig. 19. The variation of the apparent viscosity with pressure shows a marked change above 10^3 Pas. The authors [3] remarked that it is tempting to suppose that this change indicates a change in physical properties of the oil at high pressure. To test their remarks, the linear sections of Fig. 19 were extrapolated to obtain an intersection. Pressures of about 0.57 and 0.88 GPa were obtained at 30 and 70C, respectively. These intersection points fall near the glass transition lines of N1 fluid as shown in Fig. 12. The fact that the intersection points correspond to the measured glass transition points support the authors' [3] remark.

2(b) EHD Side Thrust Data. Johnson and Roberts [2] devised a rolling-contact experiment with a small amount of twist. Because of certain kinematic characteristics of their contact, no side thrust will be transmitted if the lubricant behavior is that of a liquid. If the material behaves like a solid, some side thrust will be observed. Fig. 20 is a plot of the relative side thrust as a function of contact pressure. This transition in the behavior of their oil[5] is similar to that of specific heat or expansion coefficient of a material passing through a glass transition as discussed earlier. This observation raises the question of whether the behavior shown in Fig. 20 is the result of a glass transition. The onset of solid like behavior occurs at about 0.5 GPa and 23C which is plotted on Fig. 12. When the technique for determining

[4] Shell Vitra 76 similar to N1 but of higher viscosity.
[5] Shell Vitra 76 similar to N1 but of higher viscosity.

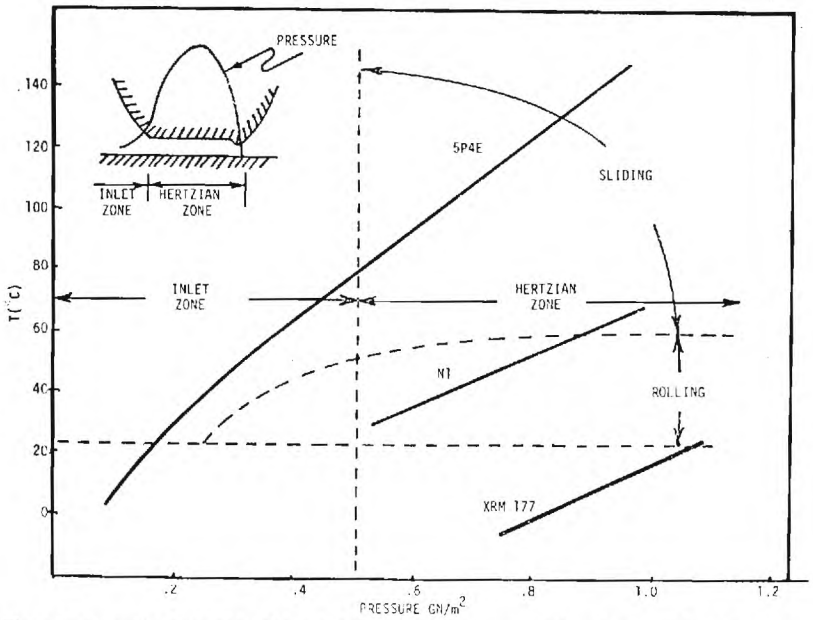

Fig. 18 Heuristic estimates of the relationship between conditions in an EHD contact and glass-liquid phase diagram of some lubricants (lubricant supply temperature about 20C)

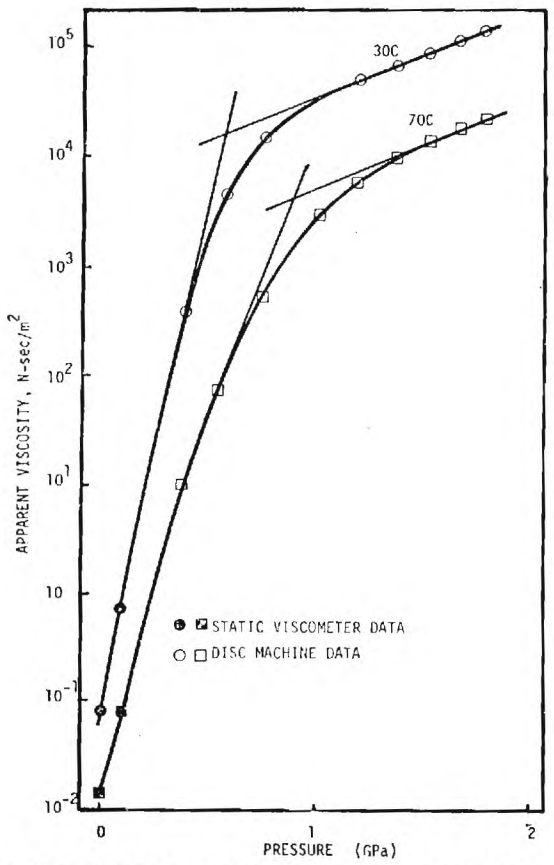

Fig. 19 The variation of apparent viscosity with pressure and temperature [3]

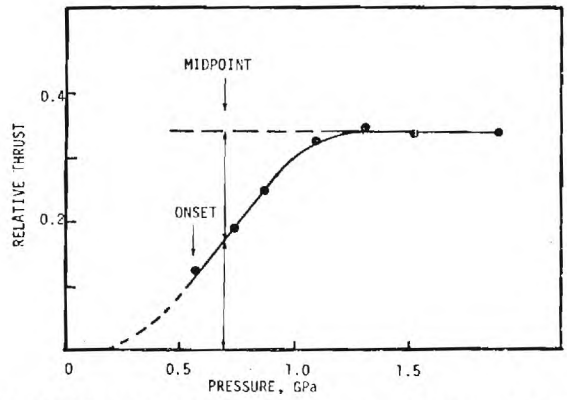

Fig. 20 Variation of the relative side thrust with contact pressure at 23C and 0.1 m/s [2]

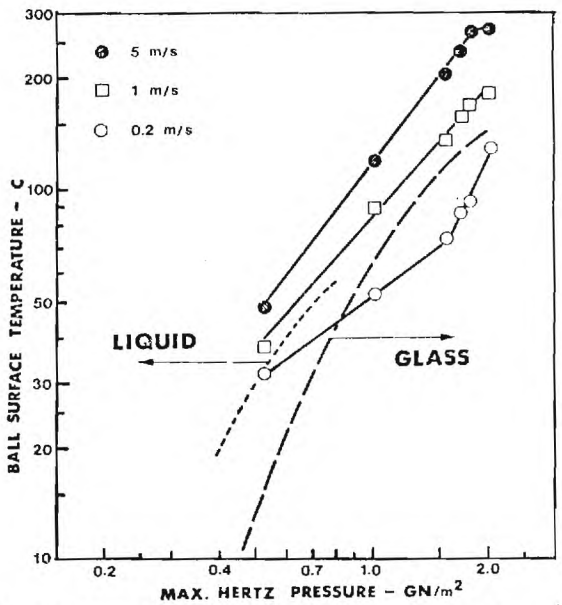

Fig. 21 The physical state of N1 lubricant in the center of a sliding contact at various speeds and Hertz pressures (reference [9]) - - - - - - and — — represent the light-scattering and the volumetric glass transition lines, respectively

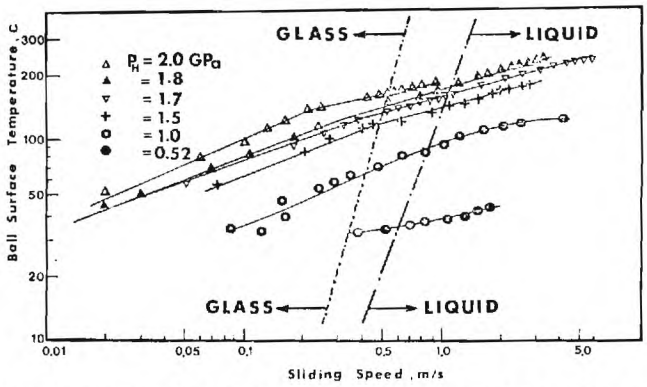

Fig. 22 The physical state of N1 lubricant in the center of a sliding contact at various speeds and Hertz pressures - - - - - and - - - represent the light-scattering and the volumetric glass transition lines

the glass transition temperature for such a physical behavior was used, a midpoint transition pressure (see Fig. 12) of about 0.7 GPa was obtained at 23C. These values of pressure are seen to fall in the transition and glassy regions of Fig. 12. This result agrees with Johnson and Roberts' conclusion that a transition from viscous to solid behavior occurred above a contact pressure of about 0.5 GPa.

2(c) EHD Temperature Measurements. Fluid and ball surface temperature distributions in a sliding and rolling contact have been measured in this laboratory [35, 40, 41]. Fig. 21 is a plot of the ball surface temperature at the contact center versus maximum Hertz pressure at three sliding speeds. Fig. 22 shows the ball surface temperature versus sliding speed at different Hertz pressures. Because both figures have temperature and pressure plotted, we can include the glass transition lines obtained by the light-scattering and volumetric measurement techniques. As shown in these figures, the lubricant near the ball surface is in the glassy state at a sliding speed of 0.2 m/s. At higher sliding speeds, the glassy state exists only at high pressures. This result was expected since a sliding contact generates frictional heat and thus the temperature levels in the contact are relatively high.

The above discussion indicates the existence of the glassy state in sliding EHD contacts at relatively low speeds or sufficiently high pressures.

Ball surface temperature distributions for fluid N1 at different slide-to-roll ratios ($\Sigma = 2\,(u_2 - u_1)/(u_2 + u_1)$) are shown in Fig. 23(35). The speed ratio, Σ, ranged from zero (pure rolling) to 2.0 (simple sliding) at a constant Hertzian pressure of 1 GPa and at constant rolling speed of 0.75 m/s. Based on the measured temperatures, assumed Hertzian pressure distributions, and the glass transition data, it can be estimated what portion of the fluid in contact with the ball surface will be in the glassy or liquid states. The portions are shown in the bar diagrams included in Fig. 23. The lubricant near the ball

surface is in the glassy state for all speed ratios except that of $\Sigma = 2.0$. At sufficiently low speed ratios, the glassy state occupies all the contact area. This result shows that the lubricant N1 is in the glassy state in a rolling/sliding contact and the glass can occupy all the contact area at low slide-to-roll speed ratios.

F. Conclusions

The glass transition temperatures of lubricants increase sufficiently with pressure to cause glass transition in EHD contacts with many typical lubricants. The glass transition behavior of lubricants of current interest varies considerably. Some, for example 5P4E, undergo glass transition at room temperature at about 0.14 GPa while bis-2-ethyl hexyl sebacate did not undergo a glass transition down to −3C and up to 1.1 GPa.

It appears that EHD data already available in the literature are consistent with the glass transition observations reported here. Glass transition of lubricants can be expected to influence both the EHD traction and the film thickness depending on the location of the transition in the contact.

The results of the study reported here clearly suggest that further research into the glass transition of lubricants, rheological behavior of lubricants in the glassy state and further verification of glass transition in EHD contacts are needed. Analytical modeling of the mechanics of EHD contacts with glassy lubricants should be pursued. Also the study of the relationship of chemical structure to glass transition may be useful in future lubricant formulation.

Acknowledgment

The authors wish to acknowledge the support of the National Science Foundation (ENG 74-21002) and the National Aeronautics and Space Administration, Lewis Laboratory (NSG 3106) for supporting this program.

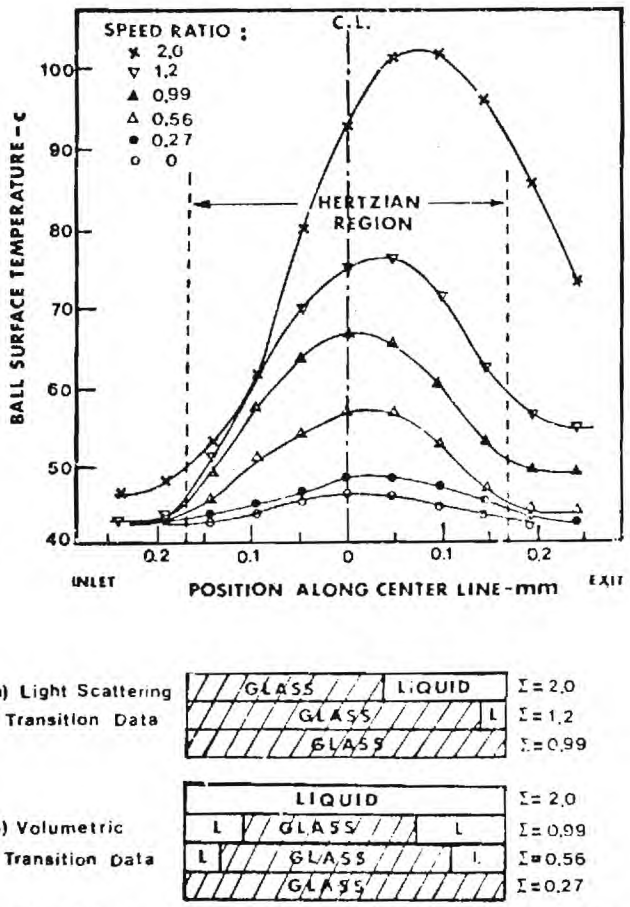

Fig. 23 Ball surface temperature distribution along the contact center line at constant Hertzian pressure of 1.0 GPa and constant rolling speed of 0.75 m/s. (*a*) and (*b*) represent the physical state of the lubricant in the contact area as determined by the light scattering and volumetric transition data, respectively

References

1 Smith, F. W., "Lubricant Behavior in Concentrated Contact—Some Rheological Problems", *ASLE Transaction*, Vol. 3, 1960, p. 18.

2 Johnson,, K. L., and Roberts, A. D., "Observation of Viscoelastic Behavior of an EHD Lubricant Film", *Proc. Roy. Soc. Lond. A-337*, 1974, p. 217.

3 Johnson, K. L., and Cameron, R., "Shear Behavior of Elastohydrodynamic Oil Films at High Rolling Contact Pressures," *Proc. Inst. Mech. Engrs.*, Vol. 182, Pt. 1, 1967–1968, p. 307.

4 Noel, F., "Thermal Analysis of Lubricating Oils," *Thermonica Act.*, Vol. 4, 1972, p. 377.

5 Walker, D. L., Sanborn, D. M., and Winer, W. O., "Molecular Degradation of Lubricants in Sliding Elastohydrodynamic Contacts," JOURNAL OF LUBRICATION TECHNOLOGY, TRANS-ASME, Series F, Vol. 97, No. 3, pp. 390–397.

6 Sanborn, D. M., and Winer, W. O., "Lubricant Properties in Thin Lubricating Films," *American Chemical Society, Division of Petroleum Chemistry Preprints*, Vol. 21, No. 1, 1976, pp. 57–67.

7 Lamb, John, "Experimental Linear Viscoelastic Measurements for Liquids," *ACS Symposium on Lubricant Properties in Thin Lubricating Films*, Apr. 1976. (to be published).

8 Dill, J. F., Drake, P. W., and Litovitz, T. A., "The Study of Viscoelastic Properties of Lubricants Using High Pressure Optical Techniques," *ASLE, 18* Vol. 3, 1975, p. 202.

9 *ASME, Pressure-Viscosity Report, I, II*, A Report Prepared by the ASME Research Committee on Lubrication, New York, ASME, 1953.

10 McKinny, J. E., and Goldstein, M., "PVT Relationships for Liquid and Glassy Poly(Vinyl Acetate)," *Journal of Research of the NBS-Physics and Chemistry*, Vol. 78A, 1974, p. 331.

11 Turnbull, D., *Contemp. Phys.* Vol. 10, 1969, p. 473.

12 Gee, G., "The Glassy State in Polymers," *Contemp. Phys.*, Vol. 11, No. 4.

13 Harrison, G., *The Dynamic Properties of Supercooled Liquids*, Academic Press, New York, 1976.

14 Ferry, J. D., *Viscoelastic Properties of Polymers*, New York, Wiley, 1961.

15 Haward, R. N., *The Physics of Glassy Polymers*, New York, Wiley.

16 Kovacs, A. J., *J. Polym. Sci.*, Vol. 30, 1958, p. 131.

17 Matsuaka, S., and Maxwell, B., *J. Poly. Sci.*, Vol. 32, 1958, p. 131.

18 Yourtee, J. B., and Cooper, S. L., "Properties of Densified Amorphous Polystyrene," *J. Appl. Poly. Sci.*, Vol. 18, 1974, p. 897.

19 Greet, R. J., and Turnbull, D., "Glass Transition in 0-Terphenyl," *J. Chem. Phys.*, Vol. 46, No. 4, 1967.

20 Barrall, II, E. M., Porter, R. S., and Johnson, J. F., "Heat of Transition for Some Cholesteryl Esters by Differential Scanning Calorimetry," *J. Phys. Chem.*, Vol. 71, No. 5, 1967, p. 1224.

21 Johari, G. P., and Goldstein, M., "Viscous Liquids and the Glass Transition," *J. Chem. Phys.*, Vol. 55, No. 9, 1971, p. 4245.

22 Yano, O., and Wada, Y., "Dynamic and Dielectric Relaxations of Polysterene Below the Glass Temperature," *J. Poly. Sci.*, Vol. 9, Part A2, 1971, p. 669.

23 Rank, D. H., Kiess, E. M., and Fink, U., "Brillouin Spectra of Viscous Liquids," *J. Opt. Soc. Am.*, Vol. 56, No. 2, 1966, p. 103.

24 Pinnow, D. A., Candau, S. J., LaMacchia, I. T., and Litovitz, T. A., "Brillouin Scattering: Viscoelastic Measurements in Liquids," *J. Acoust. Soc. Am.*, Vol. 43, 1968, p. 13.

25 Rank, D. H., Kiess, E. M., Fink, U. and Wiggins, T. A., *J. Opt. Soc. Am.*, Vol. 54, 1964, p. 1286.

26 Cummins, H. Z., and Gammon, R. W., "Rayleigh and Brillouin Scattering in Liquids: The Landau-Placzek Ratio," *J. Chem. Phys.*, Vol. 44, No. 7, 1966, p. 2785.

27 Stevens, J. R., Jackson, D. A., and Champion, J. V., "Evidence for Ordered Regions in Poly(n-butyl) Methacrylate from Light Scattering Studies," *Molecular Physics*, Vol. 29, No. 6, 1975, p. 1893.

28 Coakley, R. W., Mitchel, R. S., Stevens, J. R., and Hunt, J. L., "Rayleigh-Brillouin Light Scattering Studies on Atactic Polystrene," A paper presented at the American Physical Society Conference, Atlanta, Georgia, Apr. 1976.

29 Jackson, D. A., Pentecost, H. T. A., and Powels, J. G., "Hypersonic Absorption Amorphous Polymers by Light Scattering", *Molecular Physics*, Vol. 23, No. 2, 1972, p. 425.

30 Romberger, A. B., Eastman, D. P., and Hunt, J. L., "Evidence for Structure in Plastics from Light Scattering," *J. Chem. Phy.*, Vol. 51, No. 9, 1969, p. 3723.

31 Work, Richard N., "On the Discontinuity in the Temperature Coefficient of the Velocity of Ultra Waves in Polymeric Materials," *J. Appl. Phys.*, Vol. 27, No. 7, 1956, p. 69.

32 Mitchell, R. S., and Guillet, J. E., "Brillouin Scattering in Amorphous Polymeric Solid," *J. Polymer Sci.: Polymer Phys. Ed.*, Vol. 12, 1974, p. 713.

33 Friedman, E. A., Ritger, A. J., and Andrews, R. D., "Brillouin Scattering Near the Glass Transition of Polymethyl Methacrylate," *J. Appl. Phys.*, Vol.

40, No. 11, 1969, p. 4243.
34 Fabelinskii, I. L., *Molecular Scattering of Light*, Plenum Press, New York, 1968.
35 Sanborn, D. M., and Winer, W. O., "Investigations of Lubricant Rheology as Applied to Elastohydrodynamic Lubrication," NASA CR No. 2837, Sept. 1976.
36 Alsaad, M., "Light-Scattering Study of the Glass Transition and the Glassy State in Lubricating Oils," PhD thesis, Georgia Institute of Technology, 1976.
37 Debye, P., *Ann. Physik*, Vol. 39, 1912, p. 789.
38 Brillouin, L., *Ann. Phys.*, Paris, Vol. 17, 1922, p. 88.
39 Landau, L., and Placzek, G., *Z. Phys. Sowjetunion*, Vol. 5, 1934, p. 172.
40 Ausherman, V. K., Nagaraj, H. S., Sanborn, D. M., and Winer, W. O. "Infrared Temperature Mapping in Elastohydrodynamics Lubrication," JOURNAL OF LUBRICATION TECHNOLOGY, TRANS. ASME, Series F, Vol. 98, No. 2, 1976, pp. 236–243.
41 Nagaraj, H. S., Sanborn, D. M., and Winer, W. O., "Effects of Load, Speed and Surface Roughness on Sliding EHD Contact Temperatures," JOURNAL OF LUBRICATION TECHNOLOGY TRANS. ASME, Series F, Vol. 99, No. 2, Apr. 1977, p. 254.

APPENDIX A

Description of experimental fluids

The following table summarizes the oils investigated in this research and gives characteristic data for each oil.

Experimental Fluids

Symbol	*Description*
5P4E	Polyphenyl Ether
MCS-1218	Cycloaliphatic Hydrocarbon
MCS-460	Synthetic Hydrocarbon
Santotrac 50	Cycloaliphatic Hydrocarbon Traction Fluid plus additive
N1	Naphthenic Base Oil R-620-15
P1	Paraffinic Base Oil R-620-12
Nap 2	Napthenic Base Oil R-620-16
FN 2961	Super Refined Napthenic Mineral Oil
XRM-177-F4	Synthetic Paraffinic Hydrocarbon plus anti-wear additive
DN-600	Polyalkyl Aromatic
S1	Diester
DC-200-Blend II	Dimethylsiloxane Blend
S3-DC-200-50 Advanced Ester	Dimethylsiloxane
S2	Polybutene LF-5193

Fluid Characterization

Symbol:	5P4E	
Type:	Five-ring Polyphenyl Ether	
Source:	Monsanto Company	
Properties:	Viscosity at 37.8C, m^2/s	363×10^{-6}
	Viscosity at 98.9C m^2/s	13.1×10^{-6}
	Density at 22.2C, Kg/m^3	1.205×10^3
	Density at 37.8C, Kg/m^3	1.19×10^3
	Flash Point, C	288
	Pour Point, C	4.4
Symbol:	MCS-1218	
Source:	Monsanto Company	
Type:	Cycloaliphatic Hydrocarbon	
Properties:	It is a combination of two components each have a molecular weight less than 1000.	
	Viscosity at 37.8C, m^2/s	1418×10^{-6}
	Viscosity at 98.9C, m^2/s	18.37×10^{-6}
	Density at 23.9C, Kg/m^3	0.94×10^3
Symbol:	MCS-460	
Source:	Monsanto Company	
Type:	Synthetic Hydrocarbon	
Properties:	Viscosity at 37.8C m^2/s	37.2×10^{-6}
	Viscosity at 98.9C m^2/s	4.0×10^{-6}
	Viscosity at 148.9C m^2/s	1.9×10^{-6}
	Pour Point	−29 to −32C
	Density 25C Kg/m^2	$.9327 \times 10^3$
Symbol:	Santotrac 50	
Source:	Monsanto Company	
Type:	Synthetic Cycloaliphatic Hydrocarbon Traction Fluid	
Properties:	Viscosity at 37.8C m^2/s	$.34 \times 10^{-4}$
	Viscosity at 98.9C m^2/s	$.056 \times 10^{-4}$
	Pour Point C	−37
	Density at 37.8C	$.889 \times 10^3$ Kg/m^3
	Flash Point C	163
	Fire Point C	174
	Specific Heat at 37.8C J/Kg·K	0.51
	Additive package includes: Antiwear (zinc dialkyl dithiophosphate), Oxidation inhibitor Antifoam, VI Improver (Polymethacrylate).	
Symbol:	N1	
Source:	Sun Oil Company	
Type:	Naphthenic Base Oil R-620-15	
Properties:	Viscosity at 37.8C, m^2/s	24×10^{-6}
	Viscosity at 98.9C, m^2/s	3.728×10^{-6}
	Viscosity Index (ASTM D-2270)	−13
	Flash Point, C	157
	Pour Point	−43
	Density at 20C, gm/cc Kg/m^3	0.9157×10^3
	Average Molecular Weight	305
Symbol:	P1	
Source:	Sun Oil Company	
Type:	Paraffinic Base Oil	
Properties:	Viscosity at 37.8C m^2/s	33.74×10^{-6}
	Viscosity at 98.9C m^2/s	5.402×10^{-6}
	Density at 25C Kg/m^3	$.8602 \times 10^3$
	V.I. (ASTM D-2270)	103
	Pour Point C	−15
	Average molecular weight	404
Symbol:	Nap 2	
Source:	Sun Oil Company	
Type:	Napthenic Base Oil R-620-16	
Properties:	Viscosity at 37.8C m^2/s	114.2×10^{-6}
	Viscosity at 98.9C m^2/s	8.076×10^{-6}
	Viscosity Index (D2270)	<0
	Density at 20C Kg/m^3	$.9303 \times 10^3$
	Average Molecular Weight	357
	Refractive Index	1.5173
	Pour Point C	−23
Symbol:	FN 2961	
Source:	Humble Oil and Refining Company	
Type:	Super Refined Napthenic Mineral Oil	
Properties:	Viscosity at 37.8C m^2/s	78.08×10^{-6}
	Viscosity at 98.9C m^2/s	8.238×10^{-6}
	Viscosity at 148.9C m^2/s	3.3×10^{-6}
	Density at 15.6C Kg/m^3	$.887 \times 10^3$
	Pour Point C	−34
Symbol:	XRM-177-F4	
Source:	Mobil	
Type:	Synthetic Paraffinic Hydrocarbon plus antiwear additive	
Properties:	Viscosity at 37.8C Ns/m^2	376×10^{-3}
	Viscosity at 98.9C Ns/m^2	31.6×10^{-3}
	Pour Point C	< −40
	Density 37.8C Kg/m^3	$.8389 \times 10^{-3}$
Symbol:	DN-600	
Source:	Continental Oil Company	
Type:	Polyalkyl Aromatic	
Properties:	Viscosity at 37.8C m^2/s	30×10^{-6}
	Viscosity at 98.9C m^2/s	5.0×10^{-6}
	Viscosity at 148.9C m^2/s	2.3×10^{-6}

	Density at 37.8C Kg/m^3	0.851×10^3
	Pour Point C	−60
	Specific Heat at 37.8C J/Kg C	1624
Symbol:	S1-Diester	
Source:	Rohm and Haas Company	
Type:	Diester-Plexol 201 bis-2-ethyl hexyl sebecate (PL 5159)	
Properties:	Viscosity at −53.9C m^2/s	7988×10^{-6}
	Viscosity at 37.8C m^2/s	12.75×10^{-6}
	Viscosity at 98.9C m^2/s	3.32×10^{-6}
	Cloud Point (ASTM D-2500)	below −54C
Symbol:	DC-200-Blend II	
Source:	Dow Corning Corporation	
Type:	Dimethylsiloxane Blend E1923-49	
Properties:	Viscosity at 25C m^2/s	1060×10^{-6}
	Molecular Weight (GPC)	160,000
	Component Viscosities:	
	50×10^{-6} m^2/s	75%
	$11{,}000 \times 10^{-6}$ m^2/s	12%
	$330{,}000 \times 10^{-6}$ m^2/s	13%
Symbol:	S2	
Source:	American Oil Company	
Type:	Polybutene LF-5193	
Properties:	Viscosity at −17.8C m^2/s	$18{,}836 \times 10^{-6}$
	Viscosity at 37.8C m^2/s	109×10^{-6}
	Viscosity at 98.9C m^2/s	10.6×10^{-6}
	Density at 25C Kg/m^3	0.8443×10^3
	V.I. (ASTM D-2270)	87
	Polymer Number Average molecular weight	409
Symbol:	S3-DC-200-Blend II	
Source:	Dow Corning Corporation	
Type:	Dimethylsiloxane DC-200	
Properties:	Viscosity at 37.8C m^2/s	82.6×10^{-6}
	Viscosity at 98.9C m^2/s	33.1×10^{-6}
	Density at 25C Kg/m^3	$.968 \times 10^3$
	Molecular Weight (Average)	7,000
Symbol:	Advanced Ester	
Source:	Shell Oil Company	
Type:	Based on Pentaerythritol (Aeroshell Turbine Oil 555 Base Oil)	
Properties:	Viscosity at 37.8C m^2/s	25.8×10^{-6}
	Viscosity at 98.9C m^2/s	5.1×10^{-6}
	Viscosity at 148.9C m^2/s	2.3×10^{-6}
	Density at 37.8C Kg/m^3	$.979 \times 10^3$

Printed in U. S. A.

5. Published in Bulletin of The Japan Petroleum Institute
Vol. 19, No. 1, May 1977

Glass Transitions in Lubricants: Its Relation to Elastohydrodynamic Lubrication (EHD)

M. Alsaad, S. Bair, D. M. Sanborn, and W. O. Winer

Reprinted from
BULLETIN OF THE JAPAN PETROLEUM INSTITUTE
Volume 19, No. 1, May, 1977

SCIENTIFIC PAPER

Glass Transitions in Lubricants: Its Relation to Elastohydrodynamic Lubrication (EHD)*

*by M. Alsaad**, S. Bair***, D. M. Sanborn***, and W. O. Winer****

1 Introduction

A preliminary investigation into the possible role of glass transition and glassy state behavior of lubricants in EHD contacts is reported. Preliminary results of the glass transition of lubricants as a function of pressure by two methods are presented along with a discussion indicating possible implications of the results to EHD lubrication.

The proposition that the mechanical behavior of lubricants in EHD contacts might not be that of a viscous liquid but of an elastic solid was first presented by Smith[2] in 1960. The results of Johnson and Roberts[3], and Johnson and Cameron[4] suggest that the lubricant film responds as an elastic solid under the conditions of pressure, temperature and shear rate of their EHD experiments.

Lubricating oils contain linear and highly branched hydrocarbons. Thus, a lubricating oil can display both a glass transition which is associated with the non-crystallized (non-linear hydrocarbons) part of the lubricant oil and a phase transition which is associated with the wax in the oil (linear hydrocarbons). Regardless of the wax content in a given oil, the glass transition temperature remains unchanged[5]. When comparing the conditions to which a lubricant is subjected in a typical EHD contact to available glass transition data, it appears quite likely that the lubricant is in or near the glassy state. This appears to be certain for some bulk polymers and polymer solutions and may also be true for low molecular weight hydrocarbons. If in or near the glassy state, the solidlike behavior and ultimate mechanical properties of the lubricant may be the controlling material characteristics in the large strain and large strain rate conditions that exist in EHD.

A preliminary review of the literature of the physics of glassy solids indicates that the stress and strain occurring in EHD contacts exceed the ultimate stress and strain in many materials. The work performed in this laboratory on the molecular degradation of lubricants in EHD contacts clearly demonstrates that yielding on a molecular level does occur in these applications[6],[7]. The infinitesimal strain work of Lamb[8] and Litovitz and Dill[9] are important in determining the extent to which the lubricant is in the glassy state, but, it seems to us, the important material properties are the ultimate or large strain properties and not the linear viscoelasticity properties.

In the early stages of this research, glass transition temperatures at atmospheric pressure were measured by the technique of Differential Scanning Calorimetry (DSC) for two lubricating oils: naphthenic base oil R–620–15, designated as Nl and five ring polyphenyl ether, 5P4E (more detailed fluid identifications are given in the Appendix). Glass transition temperatures were −59°C for N–1 sample and −21°C for 5P4E. Probably because these values are low compared to the operating temperatures in a typical EHD contact, the occurrence of the glass transition phenomenon and the existence of the glassy state in the contact were not investigated earlier by other researchers in this field. However, because of the fact that the glass transition temperature increases with pressure, and because of the existence of high pressures in the EHD contacts, the glass transition temperature can be greater than the operating temperature in the contact. The ASME Pressure-Viscosity-Report[10] was used to obtain an estimate of the variation of T_g with pressure. The solidification points indicated in the ASME report were assumed to be approximate glass transition points.

* Received Feb. 18. 1977.
This article is condensed from a NASA Contract Report (1) and was in part presented at the Gordon Conference on Friction, Lubrication and Wear, New London, New Hampshire, USA, June 1976.

** Present address: Kuwait University, College of Engineering and Petroleum, Mechanical Engineering Department, P. O. Box 5969, Kuwait.

*** School of Mechanical Engineering, Georgia Institute of Technology, Atlanta, Georgia, U.S.A.

Since these are reported as pressures at several different temperatures, they permit an estimate of the change of glass transition temperature with pressure. Also, according to McKinny and Goldstein[11], the glass transition is an isoviscous state. This is apparently because the glass transition represents a constant relaxation time for a given process and the relaxation time is essentially proportional to the viscosity. The change in temperature with pressure required to maintain constant viscosity gives results that are consistent with the results based on solidification. Based on this approach for typical lubricants, the glass transition temperature increases with pressure at a rate ranging from 80 to 350 C/GPa. Thus, it would be expected that some lubricants will be in the glassy state in an EHD contact with average pressures of 0.7 GPa or higher at room temperature. It also would be expected that many lubricants are in the glassy state for a significant portion of the time they are in the contact.

The temperatures and pressures at which glass transition occurs and the mechanical properties of the lubricant in the glassy state may influence the two most important dependent operating variables of an EHD contact: the film thickness and the traction. Since the relaxation time of a material in the glassy state is long compared to the residence time in the contact, it is possible that once in the glassy state, the lubricant will remain in the glassy state on the moving surface while the surface moves from one EHD contact to the next. This may happen in spite of the fact that the pressure causing the glassy state formation has been removed. It is also possible that the glassy lubricant does not have time to flow while in the EHD contact but cleaves somewhere in the film so that solid layers of lubricant adhere to the contact surfaces and slide upon each other or the lubricant may undergo large strain like a ductile solid subjected to large stresses.

Therefore, the glass transition temperature as a function of pressure is a significant material property of lubricants. The mechanical and thermal properties of a substance in the glassy state are known to be functions of the glass transition temperature and the history of how the material enters the glassy state.

2 Glass Transition Temperature and the Glassy State

Glass transition is characterized by certain experimental observations which occur while the imposed environment of the material is changing. Commonly experiments are performed for isobaric cooling or isothermal compression of the material. As the temperature is reduced in the liquid region, the material contracts and the viscosity increases. If the material is capable of crystallization, a point will be reached where crystallization starts. If crystallization does not occur or can be avoided, the viscosity will continue to increase until some level of 10^7-10^{12} Pas is reached[12~15]. At this point, the material becomes rigid and the thermal expansion coefficient falls by about one-half to one-third of its value in the melt or liquid state as shown in **Fig. 1**.

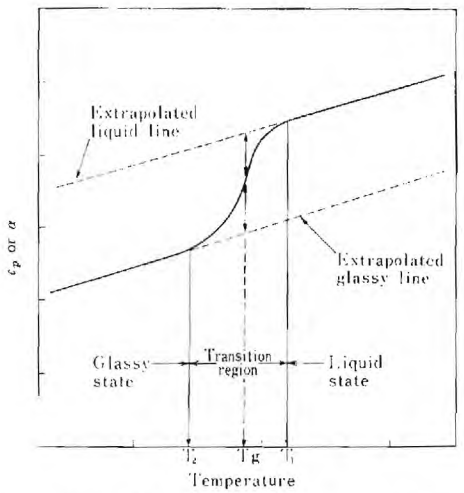

Fig. 1 Thermal Expansion Coefficient or Specific Heat for a Typical Glassy Material

Glass transition is also accompanied by a change in the specific heat, c_p, isothermal compressibility, β, and other secondary properties. It corresponds to a change in slope of a plot of specific volume versus temperature as shown in **Fig. 2**. Thus, glass transition phenomena are characteristic of any liquid which can be supercooled to a sufficiently low temperature without crystallization.

Glass transition phenomena are often referred to as apparent second-order transitions since they are characterized by a discontinuous change in the secondary thermodynamic quantities. These changes occur over a range of temperatures and are not strictly discontinuous. Ferry[15] and Haward[16] showed that glass transition phenomena are not second-order thermodynamic transitions since at T_g the substance is not in thermodynamic equilibrium. This is due to the slowness of molecular rearrangements at this temperature.

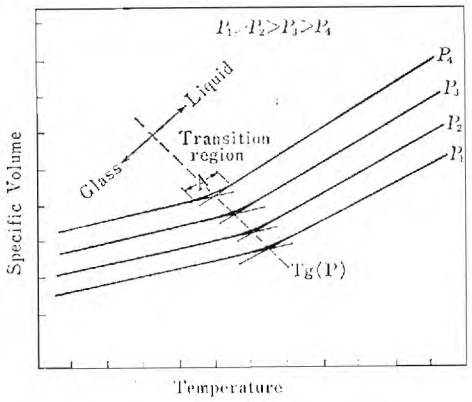

Fig. 2 Typical Plot of Specific Volume Versus Temperature for a Glassy Material at Different Formation Pressures

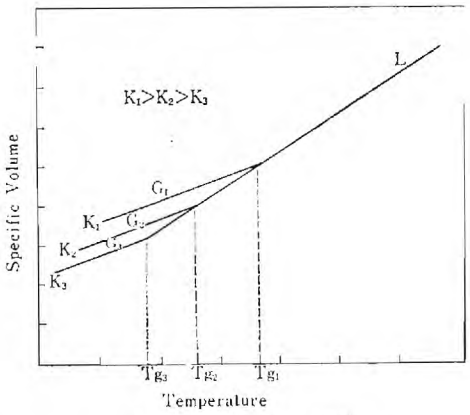

L=Liquid and G=Glass

Fig. 3 Dependence of the Glass Transition Temperature on the Cooling Rate, K_i

Absence of thermodynamic equilibrium is part of the definition of the glassy state.

Below T_g, the degree of order will appear fixed and will not vary with temperature or pressure during the time of experimental observation. Because of this, the structural degrees of freedom are said to be frozen-in and therefore, the structural contribution to α, c_p and β are absent in the glassy state.

The effect of pressure on T_g is shown in **Fig. 2**. The glass transition temperature shifts upward as the pressure is increased. The increase in T_g with pressure will be sufficient to maintain an isoviscous state. A sufficiently high pressure can induce a transition from the liquid state to the glassy state without requiring a decrease in the temperature.

The transition temperature of a material is a function of the imposed rate of change of the material's environment, and for a series of constant rate experiments, the transition temperature curve is a constant relaxation time curve. The characteristic time of the experiment is dependent on the observation time employed in the experiment. An approximate value of the relaxation time of the material when transition occurs is the observation time employed in the experiment. The range in the relaxation time of the material as it goes through the transition from liquid to glass is from about 0.1 to 10^2 times the observation time. In the transition region the material exhibits both viscous and elastic behavior relative to the process. The range of the transition region is indicated in **Figs. 1** and **2.**

As a result of the non-equilibrium state, the thermodynamic history of a glass forming liquid has considerable influence on the structure, the transition and the properties in the glassy state. The rate of the imposed environmental change effects the transition point and the properties of the glassy substance. Glass transition can be reached by isobaric cooling, isothermal compression, an imposed rate change or a combination of these changes on the material. For example, the influence of the rate of cooling, K, on the shift of the glass transition temperature of poly(vinyl acetate) has been studied over a wide range of rates by Kovacs[17]. The volume-temperature response obtained from different constant rates of cooling of a glass-forming substance is shown in **Fig. 3**. Since decreasing the rate of cooling increases the effective experimental time, the glass transition temperature will be shifted to lower values. Matsuoka and Maxwell[18] studied the effect of rate of compression on the compressibility curves of polystyrene at 121°C. Their results indicate that glass transition pressure, P_g, shifts to lower values when a greater rate of pressure application is employed. If the pressure is increased slowly, the molecules of the material will have enough time to rearrange and the glass transition will take place at a higher pressure. On the other hand, if the rate of pressurization is increased, the time for any structural changes is smaller and the glass transition occurs at a lower pressure.

The influence of thermodynamic history on glass transition of poly(vinyl acetate) was studied by McKinney and Goldstein[11] by using three different thermodynamic histories: variable formation history (isobaric cooling at different pressures), and two constant formation histories [cooling at atmospheric pressure or 80 MPa (800 bar) followed by pressure changes in the glassy state].

Several techniques are employed for the determination of the glass transition temperature such as dilatometry[11),13),19)], differential scanning calorimetry[5),20),21)], thermomechanical analysis (TMA) and dielectric[22),23)] and light-scattering techniques[24)~36)]. Depending on the technique used, various methods exist for specifying the glass transition temperature within the transition region. The usual dilatometric technique is to cool the liquid at a constant rate and extrapolate the linear portions of the volume-temperature relation above and below the transition region to their intersection. The temperature at this intersection[11)] is taken as the glass transition temperature as shown in **Fig. 2**. If T_g is measured by the change in the expansion coefficient or the specific heat, then T_g is taken as the mid-point in the step-change as measured from the extensions of the glass and liquid base lines as shown in **Fig. 1**. While the choice is somewhat arbitrary, and other authors have suggested alternate techniques, the above methods are the most commonly used. Because of these different ways of defining T_g for different experiments, and because of the different inherent rates and histories in the different experiments, different glass transition temperatures may be measured on the same material in different experiments.

The first step in the study of the importance of the glassy state in EHD contacts is to determine if the lubricant is in or near the glassy state while in an EHD contact. This requires the determination of the glass transition temperature as a function of pressure and rate at observation times comparable to that of an EHD contact for typical lubricants. From these data, a phase diagram showing the liquid and the glassy states for the lubricant can be constructed. Based on the temperatures and pressures in the contact inferences can then be made regarding the state of the lubricant in the contact.

3 Experimental Technique

The glass transition temperature as a function of pressure based on two different techniques—light scattering and volume dilatometry—is reported. The two techniques are complimentary because the observation times are similar (about 200 s) but the characteristic rates of the experiments are quite different—(10^{-2} s^{-1} for dilatometry and 10^{-10} s^{-1} for light scattering). Therefore as the material approaches the amorphous glassy state in the case of the volumetric experiment the material is a viscous liquid while in the light scattering it is behaving as an elastic liquid.

3.1 Light-Scattering Method

The basic concepts of the light-scattering technique and the description of experimental equipment used for measuring the glass transition temperature are discussed in detail in Ref. 2), 3). The theory of the interaction of the coherent laser light and sound waves (or Debye thermal elastic waves[37)]) is not new and is presented elsewhere[38)]. The interaction of light waves and sound waves is referred to as Brillouin scattering[39)]. The technique is basically one in which the frequency shift of the incident light scattered off the elastic waves is a measure of the sound velocity in the material.

The sound velocity changes continuously with temperature and pressure. A change in the slope of the sound velocity as a function of temperature and/or pressure defines the glass transition in a manner similar to that associated with other property changes. **Fig. 4** shows the variation of the sound velocity and frequency shift with temperature for atactic polystyrene[29)] where a change of slope is clearly observed at the glass transition temperature.

The dependence of the velocity of sound on the density, ρ, is seen through the relation

$$V=(M/\rho)^{1/2} \qquad (1)$$

where M represents the appropriate modulus of elasticity which is a function of the density. Since the density appears explicitly in the above relation, it is clear that a change must appear in the slope of the velocity-temperature and velocity-pressure curves at the glass transition. A com-

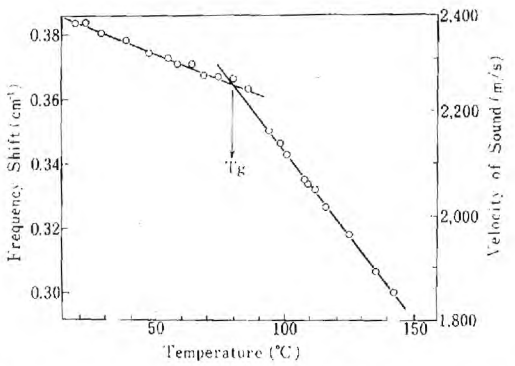

Fig. 4 The Variation of the Brillouin Frequency Shift and Velocity Sound of with Temperature at Atmospheric Pressure for Atactic Polystyrene[29)]

parison of volume-temperature data with velocity-temperature data taken from literature[32] is consistent with the above observation. However, the expansion coefficient of polystyrene is 2.2×10^{-4} °C^{-1} for $T<T_g$ and 5×10^{-4}°C^{-1} for $T>T_g$ while the velocity coefficient is 8×10^{-4}°C^{-1} for $T<T_g$ and 14×10^{-4} for $T>T_g$ which shows that the dependence of velocity on density is chiefly through the strong dependence of the modulus on density and only to a lesser extent through the explicit appearance of density.

The experimental equipment*[1] used in the light scattering experiment consisted of an argon ion laser (λ=5.45 A), a high pressure sample scattering cell, a triple pass Fabry-Perot interferometer, a photomultiplier tube and signal analyzing equipment. Detailed discussions of the apparatus can be found in references[1),36]. The sample cell was capable of sustaining pressures to 0.66 GPa.

3.2 Dilatometry Method

As mentioned in the introduction, dilatometry can be used to measure the glass transition at long observation times. In many respects volume dilatometry is both conceptually and experimentally less complicated than the light scattering method for determining glass transition. Dilatometry is inherently a low rate process. A change in rate shifts the glass transition in a known manner. Therefore, dilatometry data is significant in that any temperature-pressure combination placing the material in the glassy-state by dilatometry measurements will indicate glass formation in an EHD contact because of the shorter observation time in the EHD contact.

Dilatometry measures the relative volume of the material as a function of temperature and pressure. The compressibility and thermal expansion coefficients of the material differ in the liquid and glass regions and the glass transition is defined by this change as discussed in the introduction and shown in **Figs. 1, 2** and **3**.

Three dilatometers were constructed, one of which is shown schematically in **Fig. 5**. The three devices were made to cover different pressure ranges. Both the isobaric cooling and isothermal compression experiments had observation times on the order of 10^2 s to 10^3 s.

*1 The assistance of Drs. D. C. O'Shea and F. D. Medina of the Georgia Tech Physics Department for the use of their light scattering equipment and guidance in this work is gratefully appreciated.

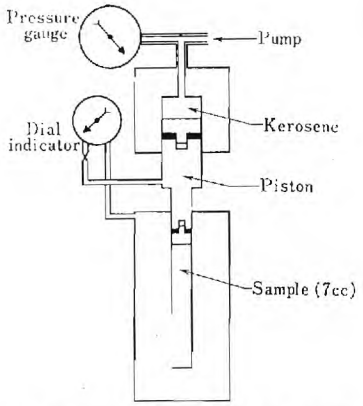

Fig. 5 High Pressure Dilatometer (0.13 to 1.2 GPa)

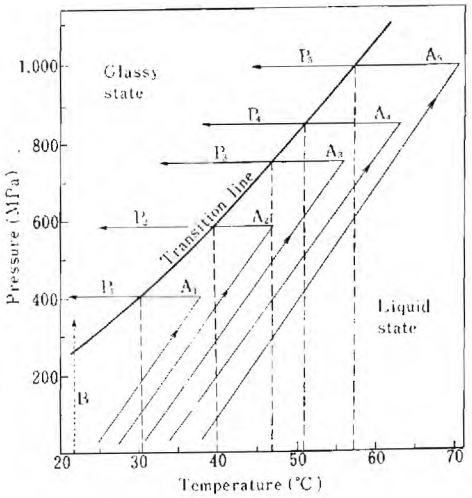

Fig. 6 Schematic of Formation Histories Used to Form the Glass. A_i and B Represent Constant Formation Histories at Pressure P_i and Room Temperature Respectively

3.3 Glass Formation History

Because of the dependence of the glass properties on formation history, two standard procedures were adopted to form the glass of the materials investigated. They are shown schematically in **Fig. 6**. In both formation histories the transition was measured by progressing from the liquid state to the glassy state. The two histories were isobaric cooling (history A) or isothermal compression (history B) while passing through the transition.

In the case of light-scattering experiments using formation history A the pressure was increased from atmospheric to a reference pressure in the liquid region. At the same time, the sample temperature was increased at a rate of 6.1 mC/s (22 °C per hour) to about 17°C above its assumed glass transition temperature. At this point the

pressure and temperature were kept constant for about 30 minutes. The sample was then cooled at constant pressure and frequency spectra were taken at 2.8°C (5°F) intervals. Twenty minutes was allowed for the temperature to reach equilibrium before each spectrum was recorded. Hence, experimental measurements were started in the liquid state and the glassy state was reached by decreasing the temperature at constant pressure as shown in **Fig. 6**. This procedure was repeated at different constant pressures and, therefore, the structure of the glass formed varies with the formation pressure. In the second formation history (history B), the glass was formed by pressurizing the sample at room temperature from atmospheric pressure until the glassy state was reached. Frequency spectra for this case were taken at pressure intervals of about 20 to 27 MPa (3,000 to 4,000 psi). Again up to twenty minutes was allowed for the sample to reach equilibrium before the spectra were recorded.

The formation histories in the dilatometry experiments were similar in that the material was always taken from the liquid state into the glassy state. For elevated pressure experiments this required heating and pressurizing in the liquid region well above the glass transition to some starting pressure and temperature from which the isobaric cooling or isothermal compression would start. As the experiment progressed the relative specific volume would be obtained as a function of temperature or pressure and the intersection of the curves in the liquid and glassy regions would define the glass transition.

4 Experimental Results

Seventeen lubricants have been investigated to date by the volumetric method and two by light scattering. The materials are listed in **Tables 1** and **2**. More detailed material descriptions can be found in Appendix A.

Table 1 Experimental Fluids* in Volumetric Glass Transition Experiments

5P4E[2]	XRM-177-F4
N1[2], N2	DN 600
P1	FN 2961
MCS 460	S2-Polybutene
MCS 1218	S1-Diester
Santotrac 50	S3-DC200-Blend I
Formulated Advanced Ester	DC 200-50

* Detailed descriptions are given in Appendix A.
** Measurements also made by light-scattering.

Table 2 Fluids for Which No Transition was Observed by the Volumetric Method in the Indicated Temperature and Pressure Ranges (Isothermal Compression).

Sample	Maximum Pressure (GPA)	Temperature (°C)
Diester (S1)	1.13	−3.3
DC 200 Blend II	**0.61	7.2
DC 200—50 (S3)	*0.92	21.1
Advanced ester	*1.07	16.9

* Piston Seized.
** Displacement Limited.

4.1 Light-Scattering Experiments

The light-scattering measurements result in a frequency shift of the laser light employed and a measure of the longitudinal speed of sound both as a function of temperature or pressure. Typical results for 5P4E are shown in **Fig. 7**, for history *B* (isothermal compression). From this figure, it is seen that the sound velocity and the frequency shift increase with increasing pressure and a change in the slope is apparent at 0.17 GPa (24,700 psi) corresponding to a velocity of sound of 2,658 m/s. This change of slope represents the glass transition. The velocities on each side of the transition region can be represented by linear functions of pressure. The two sections of **Fig. 7** were each fit by least squares regression to a linear expression of the form

$$V = A + BP$$

where V is in m/s and P in MPa. The intersection of these lines are interpreted[29)~35)] as occur-

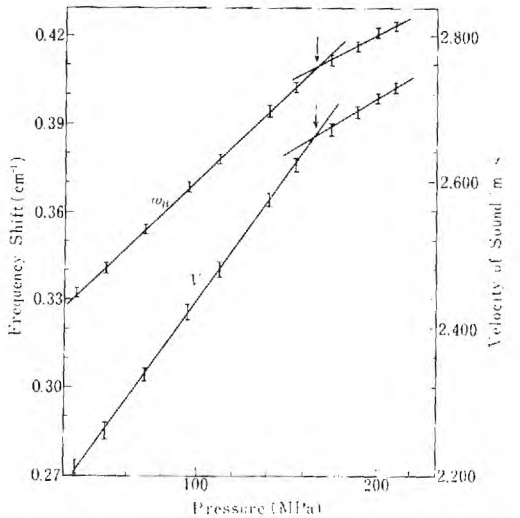

Fig. 7 Variation of Frequency Shift and Velocity of Sound with Pressure at 24.4°C (76°F) for 5P4E Fluid (History B). Arrows Indicate Glass Transition

Table 3 Least-Square Expressions for Sound Velocity, Temperatures and Sound Velocity at Transition for Different Constant Pressures: 5P4E History A.

Formation Pressure, MPa	Range of Measurements °C	Least-square Expression for Sound Velocity	Glass Transition Temperature (T_g) °C	Sound Velocity at T_g, m/s
210	48—27	$V_L=2961-7.99T$ $V_g=2798-3.15T$	34	2,692
248	49—27	$V_L=3043-7.49T$ $V_g=2856-2.88T$	41	2,739
276	58—32	$V_L=3138-7.94T$ $V_g=2903-2.88T$	46	2,769
321	68—43	$V_L=3172-6.79T$ $V_g=2942-2.43T$	53	2,812
355	72—46	$V_L=3259-6.95T$ $V_g=3015-2.48T$	59	2,848
407	82—54	$V_L=3410-7.60T$ $V_g=3032-2.23T$	70	2,875

ring at the glass transition pressure. The least square expression obtained for each section of the velocity-pressure curve shown in **Fig. 7** is

$$V_L=2{,}098+156.3\,P$$

and

$$V_g=2{,}397+72.87\,P$$

Solving these two equations for their intersection, one obtains

$$P_g=170.3 \text{ MPa and } V=2{,}658 \text{ m/s}.$$

Similar results for history B experiments (isobaric cooling) for 5P4E are shown in **Fig. 8**. The sound velocity increases as the temperature is decreased. At the transition region the dependence of sound velocity on temperature changes. This change of slope of the temperature coefficient of the sound velocity was observed at all formation pressures. Once again, the two portions of the sound velocity curves were fit by least square regression to straight lines of the form

$$V=a+b\,T$$

where V in m/s and T in C. 5P4E was subjected to formation history A at a total of six formation pressures. The resulting material behavior is shown in **Table 3** and **Fig. 9**.

The least square expressions for both portions of the velocity-temperature curves were solved for their intersection to determine the glass transition temperature at each formation pressure. The glass formation temperature-pressure combinations result in the phase diagram shown in **Fig. 10**. The glass transition temperatures and pressures were least square fit with a straight line. The expression obtained is given by

$$T_g=0.183\,P_g-4.74$$

with T_g in C and P_g in MPa. The glass transition temperature at 24.4°C (76°F) by history B

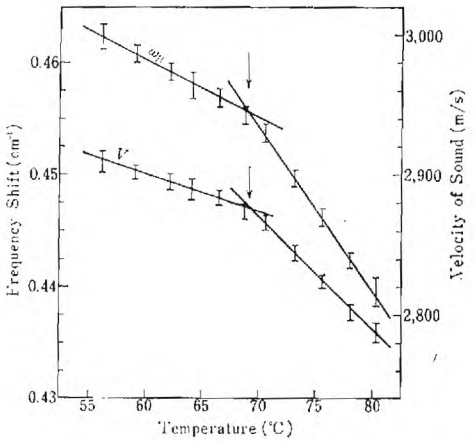

Fig. 8 Variation of Frequency Shift and Velocity of Sound with Temperature at 0.40 GPa (59,000 psi) for 5P4E (History A). Arrows Indicate Glass Transition

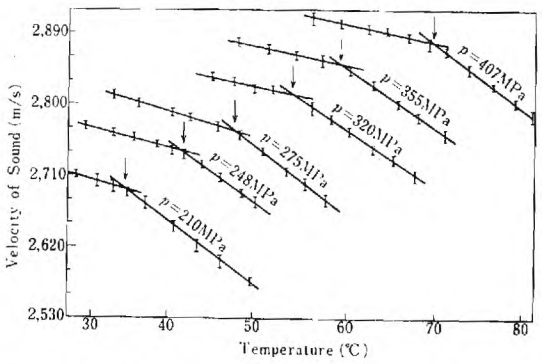

Fig. 9 Velocity of Sound Dependence on Temperature at Different Constant Pressure for 5P4E Fluid (History A). Arrows Indicate T_g

was excluded from the fit due to the different history by which the glass was formed. However, in general, the transition obtained by History B fell near the line obtained by History A.

4.2 Dilatometry Experiments

The dilatometry experiments give a change in

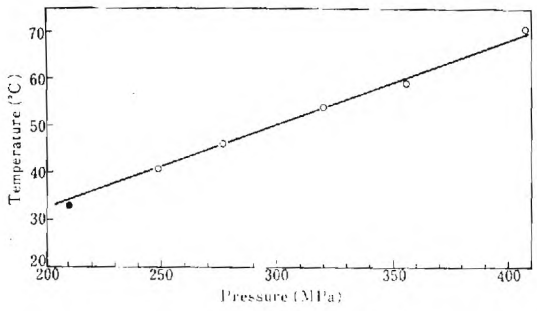

History A (○). History B (●). $\frac{dT_g}{dP}$=183°C/GPa.

Fig. 10 Phase Diagram for 5P4E Fluid Based on Light-Scattering Experiment

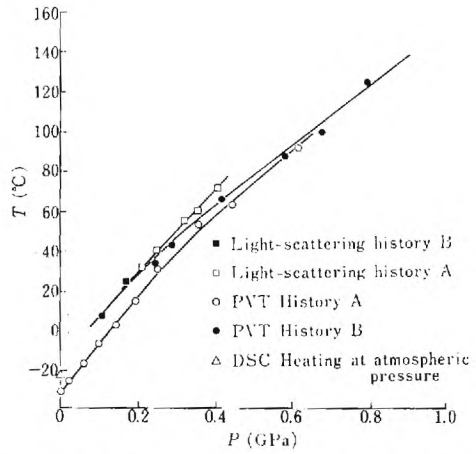

Fig. 11 Comparison of Glass Transition of 5P4E by Various Methods

slope of specific volume as a function of temperature or pressure. That change of slope defines the glass transition and permits construction of a liquid-glass phase diagram similar to **Fig. 10** which was constructed from the light-scattering data.

Experiments have been completed on the materials shown in **Table 1**. The phase diagram for 5P4E obtained with the volumetric method compared with that from the light-scattering is shown in **Fig. 11**. The reason for the difference in the data from the two techniques is believed to be pressure measurement error in the light-scattering experiment. The difference is small, however, relative to the temperature and pressure ranges a material is subjected to in an EHD contact. Therefore, if 5P4E is subjected to a temperature-pressure combination in an EHD contact which is to the right of the dilatometry curve on this phase diagram, the material will be in the glassy state in the EHD contact. These data suggest that 5P4E would be in the glassy state in most EHD applications. **Fig. 12** contains similar

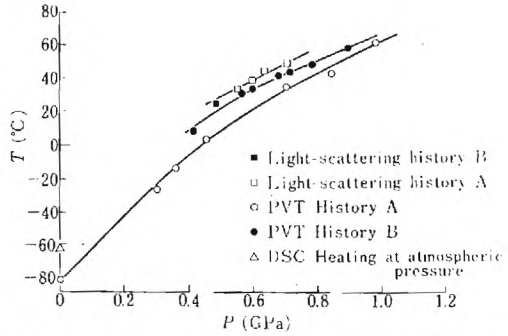

Fig. 12 Comparison of Transition of N1 by Various Methods

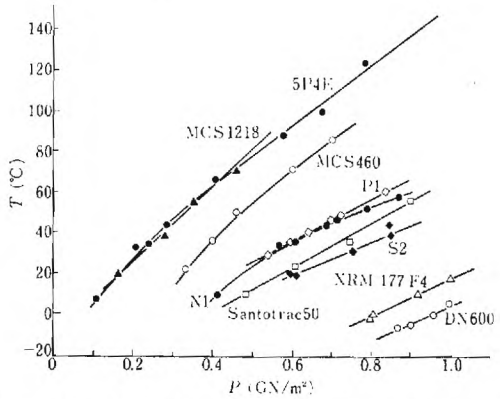

Fig. 13 Glass Transition by Isothermal Compression from Liquid (Dilatometry)

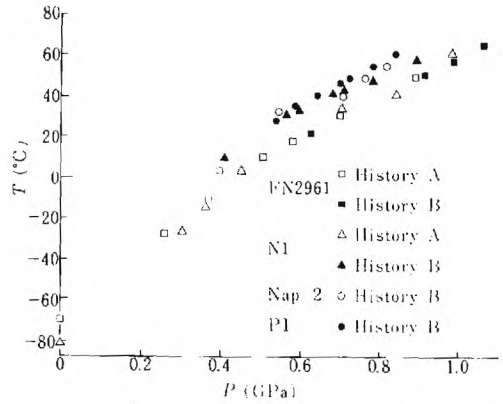

Fig. 14 Glass Transition of Various Hydrocarbon Oils Determined by Dilatometry

comparisons for material N1. The same comments made regarding 5P4E are applicable to N1.

Fig. 13 contains phase diagram data for several materials based on the isothermal compression measurements. The variation in glass forming tendencies of the materials is large. However, the typical mineral oil based lubricants studied have very similar glass forming characteristics as shown in **Fig. 14**.

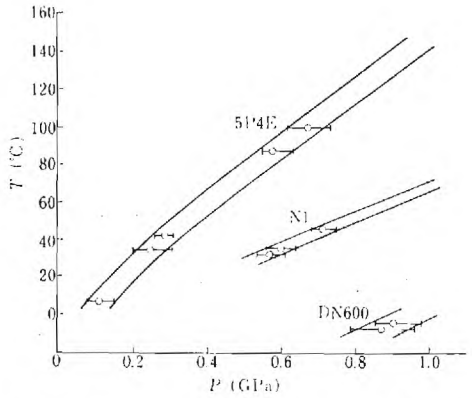

Fig. 15 Dispersion Region in Isothermal Compression by Dilatometry

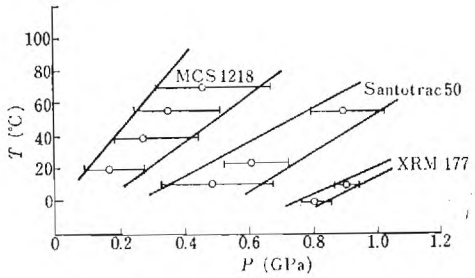

Fig. 16 Dispersion Region in Isothermal Compression by Dilatometry

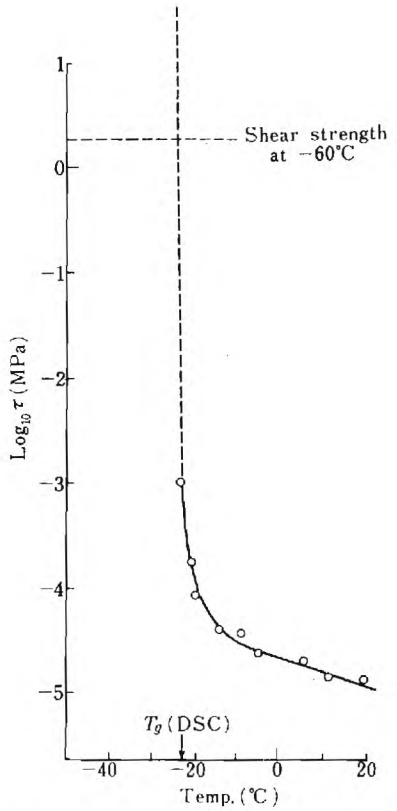

Fig. 17 Shear Stress between Concentric Cylinders for 5P4E Cooled at 2.75°C/min., Shear Rate $\gamma = 0.435\ s^{-1}$

Typical transition regions for the compression experiments are shown in **Figs. 15** and **16**. Because the observation time in these experiments was approximately five minutes the glass transition point is where the material relaxation time is approximately five minutes and the transition region represents the changes in relaxation time (τ_m) from about one tenth that value on the liquid end to about 10^2 times that on the glassy end ($0.5 \leq \tau_m \leq$ 500 minutes). In this region the material exhibits both viscous and elastic behavior relative to this experiment. In the liquid region the relaxation time is much less than 0.5 minute and the material can be treated as a viscous liquid in this process. In the glassy region the relaxation time is greater than 500 minutes and the material can be treated as an elastic solid in this process.

Table 2 lists those materials which were studied but for which no glass transition was observed for the volumetric experiments in the pressure and temperature range studied. This implies that the relaxation times of these materials were much less than one half minute in the pressure and temperature range of observation.

4.3 Two Additional Experiments

Glass transition is accompanied by changes in all the physical properties of the material including very large changes in viscosity. In the past, glass transition has been defined as the point at which the viscosity of the material reaches a high value (e. g. 10^{11} Ns/m^2). Because the approximate shear rates and shear stresses to which the material is subjected in an EHD contact are not consistent with such high viscosities, while the temperatures and pressures indicate it is in the glassy state, two simple shearing experiments were conducted. Both were conducted in a concentric cylinder device. In one experiment the torque (shear stress) was measured continuously at constant shear rate (0.43 s^{-1}) while the 5P4E sample was cooled continuously. In the second experiment a crude indication of the ultimate shear strength of the material in the glassy state was obtained.

The viscosity measurement experiment was conducted in a Haake concentric cylinder viscometer and the results are shown in **Fig. 17**. As expected the viscosity increases rapidly with decreasing temperature but the trend begins to change substantially as the glass transition temperature is approached. The glass transition temperature as measured by

Table 4 Approximate Yield Shear Strength at Atmospheric Pressure

Fluid	T	T_g	$\simeq\tau$ Yield, MPa
5P4E	−60°C	−23°C	5.38
N1	$<T_g$	−60°C	3.24
XRM	$<T_g$	N.A.	2.96

differential scanning calorimetry is −23°C and is marked on the figure. The shear stress limit of the instrument is about 3.5 kPa. As the temperature continues to decrease below the glass transition temperature the material effectively becomes a rigid solid.

Once in the glassy state the material has solid-like properties such as sound velocity, thermal expansion coefficient, specific heat, etc., and might also be expected to have an ultimate yield shear strength. To get an estimate of this property at atmospheric pressure, a concentric cylinder device was constructed with a sample outer diameter of 16 mm, inner diameter of 13 mm and length of 16 mm. The outer cylinder could be held firm and the inner cylinder turned with a torque wrench when the sample was cooled below its glass transition temperature. A thermocouple was inserted into the sample through the inner cylinder and the device cooled by liquid nitrogen. The torque required to break the inner cylinder loose was then an estimate of the yield shear strength of the material. The data are shown in **Table 4**. These results suggest that yield behavior of the material in the glassy state should be studied in conjunction with the study of material behavior in EHD contacts.

5 Discussion of Results

5.1 Pressure Dependence of Glass Transition Temperatures in Lubricants

The glass transition results presented suggest that glass transition phenomena and rheological behavior in the glassy state are important for some lubricants in some EHD applications.

The volumetric experiments covered the widest range of pressure and temperature. As seen in **Fig. 12** for N1 at low formation pressures (up to about 0.45 GPa), the transition temperature is a linear function of pressure with a slope of about 190 °C/GPa. Above 0.45 GPa, the slope decreased gradually and the glass transition relation became linear again above 0.55 GPa with a slope of about 100 °C/GPa. **Fig. 12** also includes the light scattering transition data obtained by history A for fluid N1 (slope=120°C/GPa).

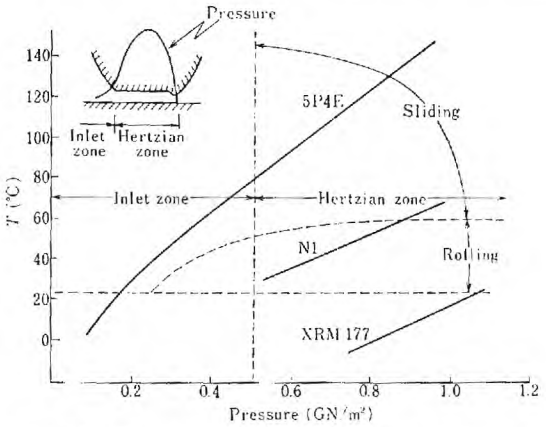

Fig. 18 Heuristic Estimates of the Relationship between Conditions in an EHD Contact and Glass-Liquid Phase Diagram of Some Lubricants (Lubricant Supply Temperature about 20°C)

The glass transition temperature for N1 at atmospheric pressure was also determined by the volumetric measurements and has a value of −81°C. This value is lower than that obtained by the DSC measurements by about 22°C. The decrease in T_g is due to the different cooling rates (28°C/hr for the volumetric measurements and 1,220°C/hr for the DSC measurements) and the different formation history used in each technique.

The volumetric and light scattering transition data for 5P4E are shown in **Fig. 11** and have behavior similar to that discussed above for N1.

5.2 Relationship of Glass Transition to EHD Conditions

To obtain an impression of the relationship between glass transition for various lubricants and conditions in EHD contacts, **Fig. 18** has been prepared. **Fig. 18** contains the liquid-glass transitions for three lubricants as measured by the volumetric technique. The three lubricants selected represent a wide range of behavior with respect to glass transition. Above and to the left of each curve is the liquid region for the material for low rate (long observation time) processes. To the right and below each curve is the glassy region. Based on limited measurements on three other hydrocarbon base oils the curve for N1 is an adequate first approximation for non-polymer containing hydrocarbon base oils. Also indicated in **Fig. 18** are the approximate ranges of pressure in the inlet and the Hertzian zones of an EHD contact. The approximate temperature ranges are also marked for an inlet temperature of about 20

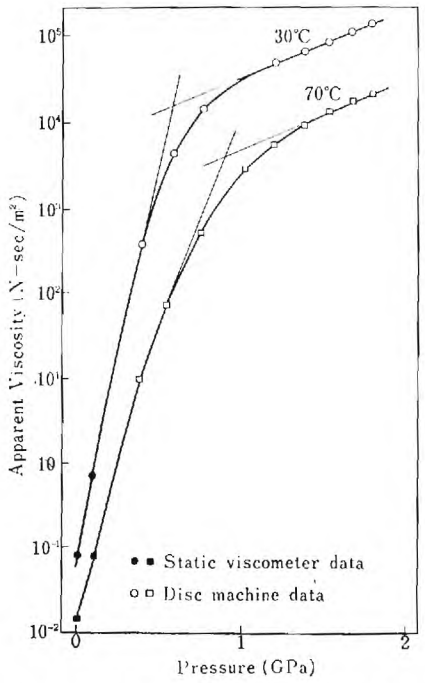

Fig. 19 The Variation of Apparent Viscosity with Pressure and Temperature[4]

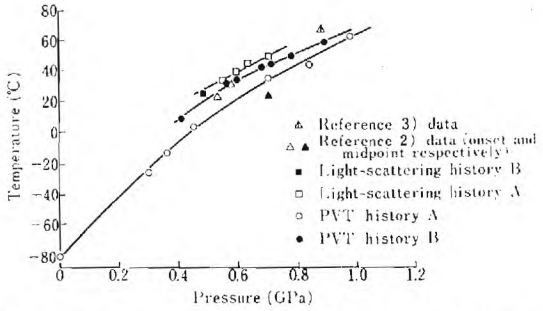

Fig. 20 Comparison of Glass Transition of Nl by Various Methods

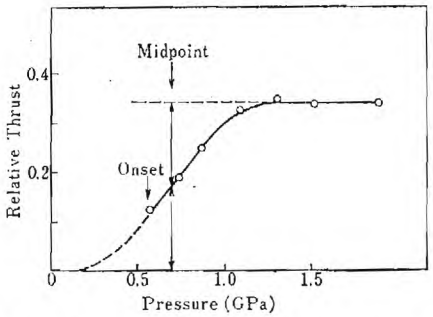

Fig. 21 Variation of the Relative Side Thrust with Contact Pressure at 23°C and 0.1 m/s[23]

°C based on the IR temperature measurements made in this laboratory[1]. What this heuristic depiction shows is that glass transition most probably occurs in many practical applications of EHD contacts with many existing lubricants. The higher the contact pressure the more likely the transition to the glassy state, particularly with rolling and low slip ratio contacts. The glass transition and glassy state behavior are most likely to effect traction but may also effect film thickness if the transition occurs in the inlet zone. The above clearly suggests the phenomena of glass transition occurs in EHD and its effects may be observable in EHD data already available.

5.2.1 EHD Traction Data

Johnson and Cameron[4] measured the traction transmitted by an elastohydrodynamic film in a rolling contact with low sliding speeds and near isothermal conditions. From the traction measurements, the variation in apparent viscosity of their oil*[2] with pressure and temperature is shown in **Fig. 19**. The variation of the apparent viscosity with pressure shows a marked change above 10^3 Pas. The authors[4] remarked that it is tempting to suppose that this change indicates a change in physical properties of the oil at high pressure. To test their remarks, the linear sections of **Fig. 19** were extrapolated to obtain an intersection. Pressures of about 0.57 and 0.88 GPa were obtained at 30 and 70°C respectively. These intersection points fall near the glass transition lines of Nl fluid as shown in **Fig. 12** which is repeated with this data in **Fig. 20**. The fact that the intersection points correspond to the measured glass transition points support the authors[4] remark.

5.2.2 EHD Side Thrust Data

Johnson and Roberts[3] devised a rolling-contact experiment with a small amount of twist. Because of certain kinematic characteristics of their contact, no side thrust will be transmitted if the lubricant behavior is that of a liquid. If the material behaves like a solid, some side thrust will be observed. **Fig. 21** is a plot of the relative side thrust as a function of contact pressure. This transition in the behavior of their oil*[3] is similar to that of specific heat or expansion coefficient of a material passing through a glass transition as discussed earlier. This observation raises the question of whether the behavior shown in **Fig. 21** is the result of a glass transition. The onset of solid like behavior occurs at about 0.5 GPa and 23°C which is plotted on **Fig. 20**. When the technique for determining the glass transition tempera-

*[2] Shell Vitra 76 similar to Nl but of higher viscosity.

*[3] Shell Vitra 76 similar to Nl but of higher viscosity.

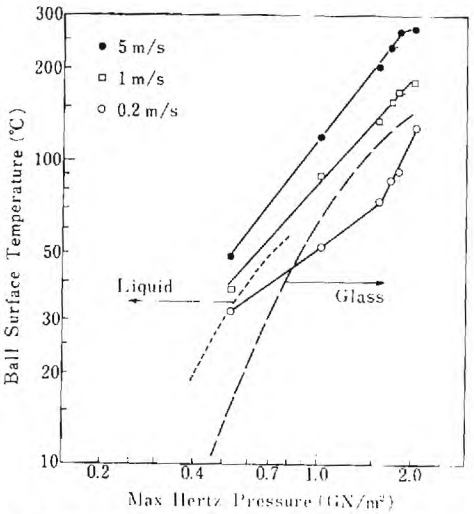

Fig. 22 The Physical State of N1 Lubricant in the Center of a Sliding Contact at Various Speeds and Hertz Pressures (Reference 9) ---- ---- and —— —— Represent the Light-Scattering and the Volumetric Glass Transition Lines Respectively

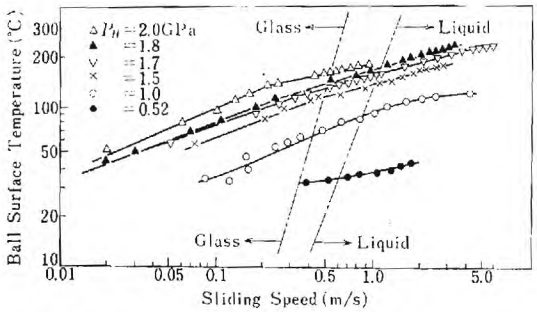

Fig. 23 The Physical State of N1 Lubricant in the Center of a Sliding Contact at Various Speeds and Hertz Pressures -·-·- and —·— Represent the Light-Scattering and the Volumetric Glass Transition Lines

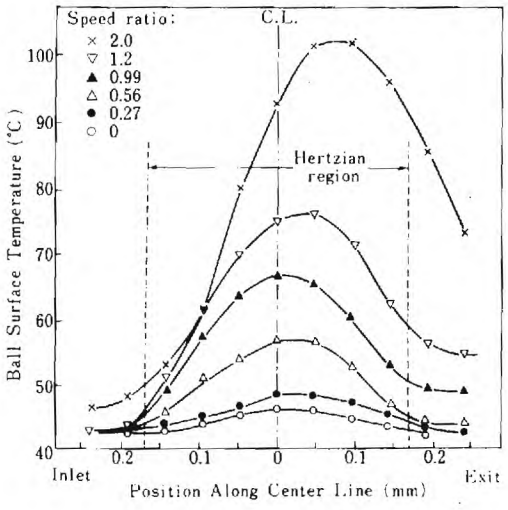

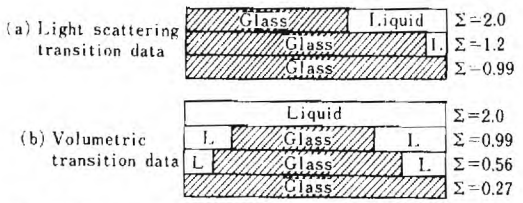

Fig. 24 Ball Surface Temperature Distribution Along the Contact Centerline at Constant Hertzian Pressure of 1.0 GPa and Constant Rolling Speed of 0.75 m/s. (a) and (b) Represent the Physical State of the Lubricant in the Contact Area as Determined by the Light-Scattering and Volumetric Transition Data Respectively

ture for such a physical behavior was used, a mid-point transition pressure (see **Fig. 20**) of about 0.7 GPa was obtained at 23°C. These values of pressure are seen to fall in the transition and glassy regions **Fig. 20**. This result agrees with Johnson and Roberts' conclusion that a transition from viscous to solid behavior occurred above a contact pressure of about 0.5 GPa.

5.2.3 EHD Temperature Measurements

Fluid and ball surface temperature distributions in a sliding and rolling contact have been measured in this laboratory[1),40),41)]. **Fig. 22** is a plot of the ball surface temperature at the contact center versus maximum Hertz pressure at three sliding speeds. **Fig. 23** shows the ball surface temperature versus sliding speed at different Hertz pressures. Because both figures have temperature and pressure plotted, we can include the glass transition lines obtained by the light-scattering and volumetric measurement techniques. As shown in these figures, the lubricant near the ball surface is in the glassy state at a sliding speed of 0.2 m/s. At higher sliding speeds, the glassy state exists only at high pressures. This result was expected since a sliding contact generates frictional heat and thus the temperature levels in the contact are relatively high.

The above discussion indicates the existence of the glassy state in sliding EHD contacts at relatively low speeds or sufficiently high pressures.

Ball surface temperature distributions for fluid N1 at different slide-to-roll ratios $\left(\Sigma=2\,\frac{(u_2-u_1)}{(u_2+u_1)}\right)$ are shown in **Fig. 24** (1). The speed ratio, Σ, ranged from zero (pure rolling) to 2.0 (simple sliding) at a constant Hertzian pressure of 1 GPa and at constant rolling speed of 0.75 m/s. Based on the measured temperatures, assumed Hertzian pressure distributions, and the glass transition data,

it can be estimated what portion of the fluid in contact with the ball surface will be in the glassy or liquid states. The portions are shown in the bar diagrams included in **Fig. 24**. The lubricant near the ball surface is in the glassy state for all speed ratios except that of $\Sigma=2.0$. At sufficiently low speed ratios, the glassy state occupies all the contact area. This result shows that the lubricant N1 is in the glassy state in a rolling/sliding contact and the glass can occupy all the contact area at low slide-to-roll speed ratios.

6 Conclusions

The glass transition temperatures of lubricants increase sufficiently with pressure to cause glass transition in EHD contacts with many typical lubricants. The glass transition behavior of lubricants of current interest varies considerably. Some, for example 5P4E, undergo glass transition at room temperature at about 0.14 GPa while bis-2-ethyl hexyl sebacate did not undergo a glass transition down to −3°C and up to 1.1 GPa.

It appears that EHD data already available in the literature are consistent with the glass transition observations reported here. Glass transition of lubricants can be expected to influence both the EHD traction and the film thickness depending on the location of the transition in the contact.

The results of the study reported here clearly suggest that further research into the glass transition of lubricants, rheological behavior of lubricants in the glassy state and further verification of glass transition in EHD contacts are needed. Analytical modeling of the mechanics of EHD contacts with glassy lubricants should be pursued. Also the study of the relationship of chemical structure to glass transition may be useful in future lubricant formulation.

Acknowledgment

The authors wish to acknowledge the support of the National Science Foundation and the National Aeronautics and Space Administration, Lewis Laboratory for supporting this program.

Appendix

Description of Experimental Fluids

The following table summarizes the oils investigated in this research and gives characteristic data for each oil.

Experimental Fluids

Symbol	Description
5P4E	Polyphenyl Ether
MCS-1218	Cycloaliphatic Hydrocarbon
MCS-460	Synthetic Hydrocarbon
Santotrac 50	Cycloaliphatic Hydrocarbon Traction Fluid plus additive
N1	Naphthenic Base Oil R-620-15
P1	Paraffinic Base Oil R-620-12
Nap 2	Napthenic Base Oil R-620-16
FN 2961	Super Refined Napthenic Mineral Oil
XRM-177-F4	Synthetic Paraffinic Hydrocarbon plus anti-wear additive
DN-600	Polyalkyl Aromatic
S1	Diester
DC-200-Blend II	Dimethylsiloxane Blend
S3-DC-200-50	Dimethylsiloxane
Advanced Ester	
S2	Polybutene LF-5193

Fluid Characterization

Symbol:	5P4E	
Type:	Five-ring Polyphenyl Ether	
Source:	Monsanto Company	
Properties:	Viscosity at 37.8°C, m^2/s	363×10^{-6}
	Viscosity at 98.9°C, m^2/s	13.1×10^{-6}
	Density at 22.2°C, Kg/m^3	1.205×10^{3}
	Density at 37.8°C, Kg/m^3	1.19×10^{3}
	Flash Point, °C	288
	Pour Point, °C	4.4
Symbol:	MCS-1218	
Source:	Monsanto Company	
Type:	Cycloaliphatic Hydrocarbon	

Properties:	It is a combination of two components each have a molecular weight less than 1,000.	
	Viscosity at 37.8°C, m^2/s	$1,418\times10^{-6}$
	Viscosity at 98.9°C, m^2/s	18.37×10^{-6}
	Density at 23.9°C, Kg/m^3	0.94×10^{3}
Symbol:	MCS-460	
Source:	Monsanto Company	
Type:	Synthetic Hydrocarbon	
Properties:	Viscosity at 37.8°C, m^2/s	37.2×10^{-6}
	Viscosity at 98.9°C, m^2/s	4.0×10^{-6}
	Viscosity at 148.9°C, m^2/s	1.9×10^{-6}
	Pour Point, °C	−29 to −32
	Density at 25°C, Kg/m^3	0.9327×10^{3}
Symbol:	Santotrac 50	
Source:	Monsanto Company	
Type:	Synthetic Cycloaliphatic Hydrocarbon Traction Fluid	
Properties:	Viscosity at 37.8°C, m^2/s	0.34×10^{-4}
	Viscosity at 98.9°C, m^2/s	0.056×10^{-4}
	Pour Point, °C	−37
	Density at 37.8°C, Kg/m^3	0.889×10^{3}
	Flash Point, °C	163
	Fire Point, °C	174
	Specific Heat at 37.8°C, J/Kg·K	0.51
	Additive package includes: Antiwear (zinc dialkyl dithiophosphate), Oxidation inhibitor, Antifoam, VI Improver (Polymethacrylate).	
Symbol:	N1	
Source:	Sun Oil Company	
Type:	Naphthenic Base Oil R-620-15	
Properties:	Viscosity at 37.8°C, m^2/s	24×10^{-6}
	Viscosity at 98.9°C, m^2/s	3.728×10^{-6}
	Viscosity Index (ASTM D-2270)	−13
	Flash Point, °C	157
	Pour Point, °C	−43
	Density at 20°C, Kg/m^3	0.9157×10^{3}
	Average Molecular Weight	305
Symbol:	P1	
Source:	Sun Oil Company	
Type:	Paraffinic Base Oil	
Properties:	Viscosity at 37.8°C, m^2/s	33.74×10^{-6}
	Viscosity at 98.9°C, m^2/s	5.402×10^{-6}
	Density at 25°C, Kg/m^3	0.8602×10^{3}
	Viscosity Index (ASTM D-2270)	103
	Pour Point, °C	−15
	Average Molecular Weight	404
Symbol:	Nap 2	
Source:	Sun Oil Company	
Type:	Napthenic Base Oil R-620-16	
Properties:	Viscosity at 37.8°C, m^2/s	114.2×10^{-6}
	Viscosity at 98.9°C, m^2/s	8.076×10^{-6}
	Viscosity Index (ASTM D-2270)	<0
	Density at 20°C, Kg/m^3	0.9303×10^{3}
	Average Molecular Weight	357
	Refractive Index	1.5173
	Pour Point, °C	−23
Symbol:	FN 2961	
Source:	Humble Oil and Refining Company	
Type:	Super Refined Napthenic Mineral Oil	
Properties:	Viscosity at 37.8°C, m^2/s	78.08×10^{-6}
	Viscosity at 98.9°C, m^2/s	8.238×10^{-6}
	Viscosity at 148.9°C, m^2/s	3.3×10^{-6}

	Density at 15.6°C, Kg/m³	0.887×10^3
	Pour Point, °C	−34
Symbol:	XRM-177-F4	
Source:	Mobil	
Type:	Synthetic Paraffinic Hydrocarbon plus antiwear additive	
Properties:	Viscosity at 37.8°C, Ns/m²	376×10^{-3}
	Viscosity at 98.9°C, Ns/m²	31.6×10^{-3}
	Pour Point, °C	< -40
	Density at 37.8°C, Kg/m³	0.8389×10^{-3}
Symbol:	DN-600	
Source:	Continental Oil Company	
Type:	Polyalkyl Aromatic	
Properties:	Viscosity at 37.8°C, m²/s	30×10^{-6}
	Viscosity at 98.9°C, m²/s	5.0×10^{-6}
	Viscosity at 148.9°C, m²/s	2.3×10^{-6}
	Density at 37.8°C, Kg/m³	0.851×10^3
	Pour Point, °C	−60
	Specific Heat at 37.8°C, J/Kg °K	1,624
Symbol:	S1-Diester	
Source:	Rohm and Hass Company	
Type:	Diester-Plexol 201 bis-2-ethyl hexyl sebecate (PL 5159)	
Properties:	Viscosity at −53.9°C, m²/s	$7,988 \times 10^{-6}$
	Viscosity at 37.8°C, m²/s	12.75×10^{-6}
	Viscosity at 98.9°C, m²/s	3.32×10^{-6}
	Cloud Point (ASTM D-2500), °C	−54
Symbol:	DC-200-Blend II	
Source:	Dow Corning Corporation	
Type:	Dimethylsiloxane Blend E1923-49	
Properties:	Viscosity at 25°C, m²/s	$1,060 \times 10^{-6}$
	Molecular Weight (GPC)	160,000
	Component Viscosities: 50×10^{-6} m²/s	75%
	$11,000 \times 10^{-6}$ m²/s	12%
	$330,000 \times 10^{-6}$ m²/s	13%
Symbol:	S3-DC-200-Blend II	
Source:	Dow Corning Corporation	
Type:	Dimethylsiloxane DC-200	
Properties:	Viscosity at 37.8°C, m²/s	82.6×10^{-6}
	Viscosity at 98.9°C, m²/s	33.1×10^{-6}
	Density at 25°C, Kg/m³	0.968×10^3
	Average Molecular Weight	7,000
Symbol:	Advanced Ester	
Source:	Shell Oil Company	
Type:	Based on Pentaerythritol (Aeroshell Turbine Oil 555 Base Oil)	
Properties:	Viscosity at 37.8°C, m²/s	25.8×10^{-6}
	Viscosity at 98.9°C, m²/s	5.1×10^{-6}
	Viscosity at 148.9°C, m²/s	2.3×10^{-6}
	Density at 37.8°C, Kg/m³	0.979×10^3
Symbol:	S2	
Source:	American Oil Company	
Type:	Polybutene LF-5193	
Properties:	Viscosity at −17.8°C, m²/s	$18,836 \times 10^{-6}$
	Viscosity at 37.8°C, m²/s	109×10^{-6}
	Viscosity at 98.9°C, m²/s	10.6×10^{-6}
	Density at 25°C, Kg/m³	0.8443×10^3
	Viscosity Index (ASTM D-2270)	87
	Polymer Number Average Molecular Weight	409

References

1) Sanborn, D. M., Winer, W. O., Rentzepis, G. M., Bair, S., Alsaad, M. A., Kunz, R. K., Nagaraj. H. S., "Investigations of Lubricant Rheology as Applied to Elastohydrodynamic Lubrication", NASA Grant No. 11-002-133, September, (1976).
2) Smith, F. W., "Lubricant Behavior in Concentrated Contact-Some Rheological Problems", *ASLE Transaction*, **3**, 18, (1960).
3) Johnson, K. L., Roberts, A. D., "Observation of Viscoelastic Behavior of an EHD Lubricant Film", *Proc. Roy. Soc. Lond.*, **A-337**, **217**, (1974).
4) Johnson, K. L., Cameron, R., "Shear Behavior of Elastohydrodynamic Oil Films at High Rolling Contact Pressures", *Proc. Inst. Mech. Engrs.*, **182**, Pt. 1, 307, (1967～1968).
5) Noel, F., "Thermal Analysis of Lubricating Oils", *Thermonica Act.*, **4**, 377, (1972).
6) Walker, D. L., Sanborn, D. M., Winer, W. O., "Molecular Degradation of Lubricants in Sliding Elastohydrodynamic Contacts", *Trans. ASME, J. Lubrication Technology*, **97**, (3), pp. 390～397.
7) Sanborn, D. M., Winer, W. O., "Lubricant Properties in Thin Lubricating Films", *Am. Chem. Soc. Div. Petrol. Chem. Preprints*, **21**, (1), pp. 57～67, (1976).
8) Lamb, John, "Experimental Linear Viscoelastic Measurements for Liquids", ACS Symposium on Lubricant Properties in Thin Lubricating Films, April (1976) (to be published).
9) Dill, J. F., Drake, P. W., Litovitz, T. A., "The Study of Viscoelastic Properties of Lubricants Using High Pressure Optical Techniques", *ASLE*, **18** (3), 202, (1975).
10) ASME, Pressure-Viscosity Report, I, II, A Report Prepared by the ASME Research Committee on Lubrication, New York, ASME, (1953).
11) McKinny, J. E., Goldstein, M., "PVT Relationships for Liquid and Glassy Poly(Vinyl Acetate)", *J. Research NBS-Phys. and Chem.*, **78A**, 331, (1974).
12) Turnbull, D., *Contemp. Phys.*, **10**, 473, (1969).
13) Gee, G., "The Glassy State in Polymers", *Contemp. Phys.*, **11**, (4).
14) Harrison, G., The Dynamic Properties of Supercooled Liquids, Academic Press, New York (1976).
15) Ferry, J. D., Viscoelastic Properties of Polymers, New York, Wiley and Sons, Inc., (1961).
16) Haward, R. N., "The Physics of Glassy Polymers," New York, Wiley and Sons, Inc.
17) Kovacs, A. J., *J. Polym. Sci.*, **30**, 131, (1958).
18) Matsuoka, S., Maxwell, B., *J. Poly. Sci.*, **32**, 131, (1958).
19) Yourtee, J. B., Cooper, S. L., "Properties of Densified Amorphous Polystyrene", *J. Appl. Poly. Sci.*, **18**, 897, (1974).
20) Greet, R. J., Turnbull, D., "Glass Transition in O-Terphenyl", *J. Chem. Phys.*, **46**, (4), (1967).
21) Barrall, E. M., II, Porter, R. S., Johnson, J. F., "Heat of Transition for Some Cholesteryl Esters by Differential Scanning Calorimetry", *J. Phys. Chem.*, **71**, (5), 1224, (1967).
22) Johari, G. P., Goldstein, M., "Viscous Liquids and the Glass Transition", *J. Chem. Phys.*, **55**, (9), 4245, (1971).
23) Yano, O., Wada, Y., "Dynamic and Dielectric Relaxations of Polystyrene Below the Glass Temperature", *J. Poly. Sci.*, **9**, (A2), 669, (1971).
24) Rank, D. H., Kiess, E. M., Fink, U., "Brillouin Spectra of Viscous Liquids", *J. Opt. Soc. Am.*, **56**, (2), 103, (1966).
25) Pinnow, D. A., Candau, S. J., LaMacchia, I. T., Litovitz, T. A., "Brillouin Scattering: Viscoelastic Measurements in Liquids", *J. Acoust. Soc. Am.*, **43**, 13, (1968).
26) Rank, D. H., Kiess, E. M., Find, U., Wiggins, T. A., *J. Opt. Soc. Am.*, **54**, 1286, (1964).
27) Cummins, H. Z., Gammon, R. W., "Rayleigh and Brillouin Scattering in Liquids: The Landau-Placzek Ratio", *J. Chem. Phys.*, **44**, (7), 2785, (1966).
28) Stevens, J. R., Jackson, D. A., Champion, J. V., "Evidence for Ordered Regions in Poly(n-butyl) Methacrylate from Light Scattering Studies", *Molecular Physics*, **29**, (6), 1893, (1975).
29) Coakley, R. W., Mitchel, R. S., Stevens, J. R., Hunt, J. L., "Rayleigh-Brillouin Light Scattering Studies on Atactic Polystrene", A paper presented at the American Physical Society Conference, Atlanta, Georgia, April, (1976).
30) Jackson, D. A., Pentecost, H. T. A., Powels, J. G., "Hypersonic Absorption in Amorphous Polymers by Light Scattering", *Molecular Physics*, **23**, (2), 425, (1972).
31) Romberger, A. B., Eastman, D. P., Hunt, J. L., "Evidence for Structure in Plastics from Light Scattering", *J. Chem. Phy.*, **51**, (9), 3723, (1969).
32) Work, Richard N., "On the Discontinuity in the Temperature Coefficient of the Velocity of Ultra Waves in Polymeric Materials", *J. Appl. Phys.*, **27**, (1), 69, (1956).
33) Mitchell, R. S., Guillet, J. E., "Brillouin Scattering in Amorphous Polymeric Solid", *J. Polymer Sci.: Polymer Phys. Ed.*, **12**, 713, (1974).
34) Friedman, E. A., Ritger, A. J., Andrews, R. D., "Brillouin Scattering Near the Glass Transition of Polymethyl Methacrylate", *J. Appl. Phys.*, **40**, (11), 4243, (1969).
35) Fabelinskii, I. L., "Molecular Scattering of Light", Plenum Press, New York, (1968).
36) Alsaad, M., "Light-Scattering Study of the Glass Transition and the Glassy State in Lubricating Oils", *Ph. D. Thesis*, Georgia Institute of Technology, (1976).
37) Debye, P., *Ann. Physik*, **39**, 789, (1912).
38) Brillouin, L., *Ann. Phys.* (Paris), **17**, 88, (1922).
39) Landau, L., Placzek, G., *Z. Phys. Sowjetunion*, **5**, 172, (1934).
40) Ausherman, V. K., Nagaraj, H. S., Sanborn, D. M., Winer, W. O., "Infrared Temperature Mapping in Elastohydrodynamics Lubrication", *Trans. ASME, Journal of Lubrication Technology*, Vol. 98F, (2), pp. 236～243. (1976).
41) Nagaraj, H. S., Sanborn, D. M., Winer, W. O., "Effects of Load, Speed and Surface Roughness on Sliding EHD Contact Temperatures", To be published *Trans. ASME, Journal of Lubrication Technology*, Presented at the Joint ASME-ASLE Lubrication Conference, Boston, Mass., October (1976).

6. Presented at the Eurotrib 77 World Tribology Conference
Lyon, France, September 1977
(to be published in WEAR)

DIRECT SURFACE TEMPERATURE MEASUREMENT BY INFRARED RADIATION IN EHD, AND THE CORRELATION WITH THE BLOK FLASH TEMPERATURE THEORY

by

H. S. Nagaraj
D. M. Sanborn
W. O. Winer

Georgia Institute of Technology
Atlanta, Georgia 30332

ABSTRACT

An infrared microdetector has been employed to measure surface temperatures in EHD contacts with Hertz pressures to 2 GPa, sliding velocities to 6.0 m/s, rolling velocities to 1.25 m/s with slide-roll ratios from -2 to +2. Different surface roughnesses have also been employed. The lambda ratio (mean film thickness to composite surface roughness) has been varied from 20 to considerably less than 1. The surfaces employed were AISI 52100 steel against Al_2O_3 and the lubricant a typical naphthenic hydrocarbon. High maximum surface temperatures have been observed (to 300C). Analysis of the data shows very good correlation with the Blok Flash Temperature Theory, for simple sliding ($\Sigma = \pm 2$). An extension of this theory to include two moving surfaces at unequal temperatures, predicts the ball surface temperature quite accurately.

INTRODUCTION

Elastohydrodynamic lubrication has been recognized as an important mode of lubrication especially for nonconformal machine elements. Considering both the present and anticipated design requirements for operating speeds and loads, a deeper and a more complete knowledge of EHD contact behavior is needed. Whereas most of the previous investigations in EHD lubrication were concerned with the formation of an adequate fluid film, more studies are needed into the mechanisms causing a breakdown of this protective film.

The transition from an adequately lubricated system to an inadequately lubricated one is well defined and provides the experimental basis of Blok's [1] critical temperature hypothesis. All transitions from one lubrication regime to another are not necessarily detrimental. As was found in both the work being presented, and that by Hirst and Stafford [2], transitions from EHD to boundary lubrication usually do not result in severe wear and high traction. This transition is characterized primarily by asperity interaction rather than gross amounts of material removal or transfer.

The frictional energy dissipation resulting from this transition causes high temperature levels in the vicinity of the contacting surfaces. These temperatures are referred to as flash temperatures. On the other hand, the overall heat transfer characteristics of the system primarily influence the bulk temperatures. Several theories exist for predicting the flash temperatures of rubbing solids. The theory was first presented by Blok [3] in 1937 and again by Jaeger [4] in 1942. More recently, Archard [5] has given a graphical procedure for determining flash

temperatures. Recognizing the importance of such a failure criteria, the AGMA [6] recommended a gear scoring criteria in 1964.

It was the purpose of the work reported in this paper to use an available infrared temperature measurement technique to measure peak surface temperatures of EHD contacts as the operating conditions became more severe. The severity of the conditions is controlled by increasing load, speed and surface roughness. The validity of the flash temperature concept and Λ (the ratio of film thickness to composite surface roughness) as failure criteria is checked by comparison with experimental results.

EXPERIMENTAL APPARATUS AND TECHNIQUE

The EHD equipment used in the following measurements is shown in Figure 1. The EHD contact is formed using a 31.8 mm diameter ball loaded against a sapphire disk 89 mm diameter by 3 mm thick with a surface roughness of 6 nm Ra. Chromium steel balls (AISI 52100) of three different roughness values have been used to study the effects of surface roughness. The values of 0.011, 0.075, and 0.38 μm Ra and are referred to as smooth, medium rough and rough, respectively. any preferred orientation of the roughness pattern. Two drive systems allow the contact surface speeds to be varied independently.

A metallurgical microscope is used to obtain film thickness measurements by means of dichromatic interferometry. The infrared radiation emitted at the contact is measured with an infrared radiometric detector having a spot size resolution of 38 μm. The contact temperatures deduced from these readings are time averaged values since a large number of surface asperities will pass through the field of view during one sampling interval.

Traction was obtained from a strain gauge load cell as shown in Figure 1. The lubricant bath temperature was monitored with a thermocouple and maintained at a desired level with a constant temperature bath.

The fluid used in this investigation is a naphthenic base oil having a peak in the emission spectra at 3.4 μm, with significant emission in the band 3.0 to 3.7 μm. The ball surface on the other hand emits as a grey body. The detector with the sapphire surface at the EHD contact will only respond to radiation in the band 1.8 to 5.5 μm.

An optical filter referred to as the wide band filter (pass band of 3.7 to 5.2 μm) has been used to eliminate the oil emission peak and allow only grey body ball surface radiation to reach the detector. The attenuation of the wide band filter was determined using a standard black body calibration source.

Figure 2 shows the radiation contributions and the signal attenuation before passing through the filter. The total radiation N is, therefore,

$$N = \eta_b N_b + \eta_F N_F + \eta_s N_s + \eta_0 N_0 \qquad (2)$$

where the attenuation factors include losses due to reflection and absorption.

There are four contributions to the radiant energy collected by the micro-detector; (1) from the ball surface N_b, (2) from the lubricant film N_F, (3) from the sapphire N_s and (4) from reflected ambient radiation N_0. Contribution (3) from the sapphire has been neglected [7] and contribution (4) can be accounted for knowing the optical properties of the system and the ambient temperature. The sapphire contribution is neglected because the sapphire emissivity is only .018 and the contributions $\eta_s N_s$ would be less than 2 percent of the ball contribution $\eta_b N_b$. Throughout the analysis the secondary reflections are neglected by an order of magnitude analysis. The radiation emitted by the ball surface, N_b, is only a function of ball emissivity ε_b and ball surface temperature T_b since the ball is a grey body. The relation between N_b, ε_b and T_b was obtained in a separate experiment in which T_b was known.

The ball radiation attenuation is determined by reflection losses

at the sapphire-air and sapphire-oil interfaces and absorption in the sapphire and lubricant films. The lubricant film contribution (2) has been eliminated by the wide band filter. The total radiation received therefore consists of only the reflected ambient radiation and the ball surface radiation. Since the ambient term can be calculated knowing the ambient temperature, the ball radiation can be found and finally after suitable calibration the surface temperature can be deduced.

Ball surface temperature measurements are made only at the center for the case of smooth and medium rough balls. The center of the EHD contact is easy to locate and also, the temperature at this location is quite close to the maximum [7.8]. In the experiments with the rough ball, the temperature measured is the maximum in the contact, whether or not it occurs at the contact center. It was necessary to make this procedural change because the contact center could not be located when the rough ball was used. This is due to the disappearance of the interference fringe pattern because of light scattering at the relatively large surface asperities. Therefore the contact was scanned for the maximum surface temperature in each case.

EXPERIMENTAL RESULTS

A. Smooth Surface Temperatures

The variation of ball surface temperature rise along the contact centerline is shown in Figures 3, 4 and 5. Figure 3 gives temperatures as a function of contact position, Hertz pressure and velocity for the case of pure sliding (sapphire surface stationary). This condition corresponds to a slide/roll ratio $\Sigma = 2$. The slide/roll ratio is defined as the slip speed (ball surface velocity minus sapphire surface velocity) divided by the rolling speed (average of the two surface velocities). The basic shape of the curves in Figure 3 are all similar, showing a maximum just downstream of the contact center. The influence of inlet heating can also be seen since the surface is as much as 50C above the bath temperature at the inlet of the Hertzian contact boundary.

Figures 4 and 5 show the variation in surface temperature along the contact centerline for the case of 1.0 m/s rolling speed and 1.02 GPa peak Hertz pressure. The temperatures are shown for various slide/roll ratios. In Figure 4 the range of Σ is $0 \leq \Sigma \leq 2$. The zero value indicates equal ball and sapphire surface speeds and is therefore considered pure rolling. In all cases shown in Figure 4 $V_b \geq V_{sa}$. Figure 5 shows the results for negative slide/roll ratios at the same conditions of pressure and rolling velocity. The values $\Sigma \leq 0$ imply that $V_{sa} \geq V_b$ with the simple sliding case ($\Sigma = -2$) representing a stationary ball and a rotating sapphire disk. The results shown in Figures 4 and 5 should not be identical because in both cases it is the ball surface temperature which is measured. Therefore, $\Sigma = +2$ corresponds to the temperature of

a moving surface passing through a given heat flux whereas $\Sigma = -2$ corresponds to the temperature of a surface stationary in the heat flux. The temperature profiles of Figure 5 should, therefore, be greater than their counterparts in Figure 4.

Figure 6 shows the ball surface temperature at the contact center and its maximum value along the center line as a function of slide-roll ratio for a Hertz pressure level of 1.02 GPa and a constant rolling velocity of 1.0 m/s.

Figure 7 shows the temperature rise for the case of pure rolling ($\Sigma = 0$) as a function of rolling speed. In comparing the results of Figures 3, 4, 5 and 7, it is apparent that pure rolling results in both greatly reduced temperatures and more symmetrical temperature profiles. When an appreciable amount of sliding is present, the profiles peak closer to the contact exit.

B. The Effects of Roughness on Surface Temperatures

The effect of surface roughness has been studied for the case of pure sliding only. Figures 8, 9 and 10 show ball surface temperature rise at the center of the EHD contact as a function of speed and load for the smooth, medium rough and rough balls, respectively. In addition, Figure 11 shows the temperature data replotted as temperature rise as a function of peak Hertz pressure and sliding speed.

The temperatures reported here are time averaged values, since the infrared detector was operated in the DC mode during these experiments. Under certain operating conditions when asperity interactions are taking place, the instantaneous temperatures developed at the individual asperities

may be significantly different from the average values. This subject has been studied by the authors and been reported elsewhere [9].

In the case of the smooth ball (Figure 8), the log-log plot of temperature rise vs. sliding speed shows the data falling on one straight line up to a certain velocity (dependent on Hertz pressure) and then on a second straight line of lower slope at higher velocities. The results of the experiments using the medium rough and rough ball do not show this characteristics as distinctly (Figures 9 and 10). The temperatures for the smooth and medium rough balls are only slightly different throughout the range of operating conditions. The surface temperatures for the rough ball appear to be significantly higher than those of the smoother balls.

The parameter Λ, which is the ratio of EHD film thickness h to the composite surface roughness σ, is a recognized parameter for predicting EHD contact performance [10]. For values greater than 2, no asperity interactions are expected. At Λ less than 1, severe asperity interaction is anticipated. The range $1 < \Lambda < 2$ is a transition region. Also, in computing the parameter Λ, the film thickness value used is that measured for the smooth ball. This is necessitated for two reasons. First of all the interference fringe pattern used to determine film thickness disappears as the roughness is increased. Secondly, the meaning of film thickness is ambiguous at significantly high roughness levels, since the local thickness changes greatly from point to point. The appropriate Λ values are shown in Figures 8, 9 and 10.

In the case of the smooth ball, Λ is greater than 2 for Hertz

pressures up to 1.81 GN/m^2, suggesting no asperity interaction. At P_H = 2.03 GN/m^2, Λ is in the range 1 to 2. However, a subsequent measurement of the surface profile did not reveal any surface alteration. Experiments using the medium rough ball resulted in $\Lambda <$ for $P_H > 1.5$ GN/m^2 and $1 < \Lambda < 2$ at lower pressures. Moderate to severe asperity interaction is therefore expected at all speeds and loads investigated. For the rough ball, Λ is less than one for all operating conditions. Subsequent relocation surface profile measurements [9,11,12] showed asperities had been removed in cases where $\Lambda < 1$.

PREDICTION OF FLASH TEMPERATURES

The flash temperature of a bearing contact refers to the temperature obtained by a surface moving through a heat source due to local frictional energy dissipation. However, in calculating such a value, the bulk temperature (surface temperatures far away from the heat source) must be specified. The oil bath temperature as measured by a thermocouple in the reservoir can be considered as the bulk temperature in the present case. The amount of time the ball surface is in contact with the oil bath is typically more than 500 times the thermal diffusion time of the material of the steel ball (defined as the time required for heat to penetrate one Hertzian radius below the surface). The bulk temperature for the ball surface should, therefore, be close to the oil bath temperature.

The trends shown in Figure 8 can be predicted using the techniques of Blok [1], Jaeger [4], and Archard [5]. The energy dissipation rate in the contact is equal to the product $(W \cdot TC \cdot V_s)$. The heat flux to each surface is then proportional to the dissipation rate divided by the area of the contact, or

$$\bar{q} \propto \frac{W \cdot TC \cdot V_s}{\pi a^2} \propto TC \cdot P_H \cdot V_s \qquad (1)$$

where the constant of proportionality includes the portion of the total heat flux transferred to the ball. According to Jaeger [4] and Archard [5] the temperature rise on the surface of a solid moving at velocity V_b and subjected to heat flux $\bar{q}$ can also be described in terms of a non-dimensional parameter $L = t_1/t_2$ (2L is called Peclet number by many

authors). The term $t_1 = a^2/2\alpha_b$ represents the time required for the effect of $\bar{q}$ to penetrate a distance a below the surface, whereas $t_2 = a/V_b$ represents the time required for a point in the contact to move a distance a. Therefore, for a given fluid and ball, L is proportional to $(P_H \cdot V_b)$. The variation in ΔT_b for simple sliding is given as

$$\Delta T_b \propto TC \cdot P_H \cdot L \tag{2}$$

or

$$\propto TC \cdot P_H^2 \cdot V_b \quad \text{for} \quad L < 0.1$$

and

$$\Delta T_b \propto TC \cdot P_H \cdot L^{1/2} \tag{3}$$

or

$$\propto TC \cdot P_H^{3/2} V_b^{1/2} \quad \text{for} \quad L > 5$$

The parameter L has been plotted in Figure 8 for the case of $P_H = 1.70$ GPa. The values 0.1 and 5 represent points for which the full solution is in good agreement with the limiting cases of equation (2) (stationary heat source solution) and equation (3) (fast moving heat source solution) respectively.

In order to compare the experimental data with equations 2 and 3, a multiple regression analysis of the data shown in Figure 8 was performed. For each Hertz pressure level the data was divided into two regions separated by the break-point velocity.

This break-point velocity is a function of Hertz pressure and can be described by

$$V_{BP} = .53\ P_H^{-1} \tag{4}$$

with a correlation coefficient r = .95. This corresponds to a value of L equal to 3.4 at the break point, which is of the same order as the theoretical break point value of 1.0 [5]. The apparent discrepancy between the theoretical and experimental values of L at the break point is perhaps due to the unavailability of data for very small values of L. For sliding velocities below V_{BP},

$$\Delta T_b = 46.99\ P_H^{2.02} V_b^{0.53} \tag{5}$$

with $r^2 = .978$. For velocities above V_{BP},

$$\Delta T_b = 53.52\ P_H^{1.34} V_b^{0.34} \tag{6}$$

with $r^2 = .985$.

These relations were obtained assuming a constant traction coefficient. However, from equations (2) and (3) it is apparent that the influence of change in traction coefficient must be included. Based on data available elsewhere [13], the traction coefficient has only a slight positive dependence on P_H in the pressure ranges studied and is dependent on sliding velocity to the power -0.29 with r = .994. The traction data used were for $3 \leq L \leq 22$. Including this dependence in equations (2) and (3) results in

$$\Delta T_b \propto P_H^{2.0} V^{.71} \quad \text{for} \quad L < 0.1 \tag{7}$$

and

$$\Delta T_b \propto P_H^{1.5} V^{.21} \quad \text{for} \quad L > 5 \ . \tag{8}$$

Recalling that equations 7 and 8 represent limiting cases (stationary and fast moving heat source solutions), the experimental results (equations 5 and 6) appear to be in reasonable agreement with the theory.

In addition to a comparison of trends with P_H and V_b, a comparison of ball surface temperatures, calculated using the method outlined by Archard [5], and the experimental results has been made. The results are summarized in Figure 12. The measured values are either the temperature at the contact center, when only those temperatures were recorded, or the average of the temperatures in the Hertzian contact area. The measured values should be somewhat higher than the calculated values since both the lubricant and surface temperatures just outside the EHD Contact are significantly higher than the bath oil temperature due to conduction and inlet heating. Because it considers conduction as the only heat transfer mechanism, the flash temperature theory should best agree with experimental results at high pressures [9,14]. In these cases, the ratio of contact length to film thickness is the greatest thereby making conduction more significant. This trend is supported by the data for P_H = 1.51 GPa and 1.05 GP, in which contact average measured temperatures have been determined. The average deviation between calculated and measured temperatures was 4.8% for the 1.51 GPa data and 17% for the 1.05 GPa data.

The above comparison has been extended to cases in which neither surface is stationary, i.e. $|\Sigma|<2$. The smooth ball center temperature data shown in Figure 6 plus a similar data set for 0.75 m/s rolling speed was found to follow the relation

$$\Delta T_b = 30.3\ \Sigma + 1.2\ ,\ ^{o}C \qquad (9)$$

for $0 \leq \Sigma \leq 2$ with a correlation coefficient of 0.99. Similarly, the data shown in Figure 7 ($\Sigma = 0$) was fit to

$$\Delta T_b = 5.2\bar{V} \ , \ ^oC \tag{10}$$

with a correlation coefficient of 0.99. The formulation by Archard [5] is followed except that the influence of a second surface must be taken into account. Also, since most of the data represented by equations 9 and 10 corresponds to $L > 5$, the fast moving heat source limit is applied. It is also assumed that the viscous dissipation takes place in a single plane since the dissipation is inversely proportional to viscosity and the shear stress is constant through the film [5]. It was further assumed that this adiabatic plane occurred at the center of the film.

The total heat flux $\bar{q}$ is the sum of that transferred to each surface (assuming convection can be neglected). Therefore

$$\bar{q} = \bar{q}_b + \bar{q}_{sa} = \frac{TC \cdot W \cdot V_s}{\pi a^2} \tag{11}$$

Since the dissipation is assumed to occur only on the midplane, the remaining fluid merely conducts the heat to the adjoining surface. This allows a linear temperature profile to be imposed between the midplane and boundary. If T_{max} is the midplane film temperature (maximum through the thickness) and T_b and T_{sa} are the surface temperatures at the same position in the contact, then the conduction equation reduces to

$$T_{max} - T_{sa} = \frac{h}{2k_f} \bar{q}_{sa} \tag{12}$$

$$T_{max} - T_b = \frac{h}{2k_f} \bar{q}_b \tag{13}$$

The average surface temperatures can be obtained from the flash temperature theory of Archard [5]. It should be noted that the location of viscous dissipation is fixed with respect to the IR detector. Therefore, the heat source is moving with respect to points on the two surfaces with velocities equal in magnitude to the absolute surface velocities.

For $L > 5$,

$$T_{sa} - T_{osa} = \frac{K_{sa}}{V_{sa}^{1/2}} \bar{q}_{sa} \tag{14}$$

$$T_b - T_{ob} = \frac{K_b}{V_b^{1/2}} \bar{q}_b \tag{15}$$

where T_o is the bulk temperature assigned to each surface and $K = .968a^{1/2}\alpha^{1/2}/k$. Equations 11-15 can be combined to yield

$$\Delta T_b = \frac{\left(\frac{TC \cdot W \cdot V_s}{\pi a^2}\right)\left(\frac{h}{2k_f} + \frac{K_{sa}}{V_{sa}^{1/2}}\right) + (T_{osa} - T_{ob})}{1 + \frac{V_b^{1/2}}{K_b}\left(\frac{K_{sa}}{V_{sa}^{1/2}} + \frac{h}{k_f}\right)} \tag{16}$$

For the conditions used in this study, $(T_{osa} - T_{ob})$ is small compared to the first term in the numerator. Using an average film thickness of 0.16 μm [12] and W = 67N, equation 16 can be evaluated for the materials used.

The ball surface temperature rise given in equation 16 assumes

only viscous shear as a heat generation mechanism. However, Figure 7 shows that even when $V_s = 0$, $\Delta T_b \neq 0$. In order to account for this additional mechanism, the temperature rise given in equation 10 ($V_s = 0$) has been added to the viscous shear component of equation 16. Excluding the pure sliding data (L = 0 for one of the surfaces), equation 16 has been applied to the remaining experiments. Figure 13 shows the predicted and measured ball surface temperatures.

It should be remembered that the predicted temperature rise is the average over the contact area whereas the measured temperature rise is the maximum along the contact centerline. It is therefore clear that the predicted values of temperature rise are higher than the measured values. There are also a number of differences in the development of flash temperature theory and the conditions found in the experiments. First of all, the theory is based on a uniform heat flux over the contact area. The heat flux distribution in the EHD contact is probably non-uniform with the maximum occurring near the center. Also because of differences in thermal diffusivities of the materials of the contact, the adiabatic plane of the fluid film may not occur at the film center. Finally, the theory assumes a semiinfinite solid with the free surface being adiabatic except under the concentrated heat flux. This is not consistent with the conditions of the experiment. The ball and sapphire surfaces outside the contact area are constantly flooded with lubricant. The agreement shown in Figure 13 should therefore be viewed cautiously. Because of the apparent agreement shown in this Figure, equation 16 can be considered as a predictive equation for the maximum ball surface temperature.

Surface roughness effects have been considered in the flash temperature

formulas recommended by the American Gear Manufacturer's Association (AGMA) in their gear scoring criterion [6]. A multiplicative factor of $1/(1 - .8Ra)$ has been used for this purpose with the range of Ra being from .25 μm to .75 μm. In the literature [15-17], factors similar to the one mentioned above have been used with the coefficient accompanying Ra varying from .62 to .89. The percent increase in flash temperature predicted by these factors versus Ra is shown plotted in Figure 14. The applicable range for the AGMA factor is indicated in this figure. Three values of Ra corresponding to the three different types of balls used, are marked in the same figure. It can be seen that up to 40 percent increase is predicted for the rough ball whereas about 7% is predicted for the medium rough ball. 0.7 to 1% increase is predicted for the smooth ball (.011 μm Ra) as compared to an ideally smooth one. An approximate comparison of the measured values with the predicted percent increases reveals a satisfactory agreement.

In order to determine an expression for the measured ball surface temperature at contact center, a surface roughness factor of the form $1/(1 - a_1 Ra)$ discussed above, is used. A multiple regression analysis of the data (181 data points) yielded the following expression for the ball surface temperature at contact center

$$\Delta T_b = 41.6\, P_H^{1.73} V_s^{.42} \left(\frac{1}{1 - .7Ra}\right) \qquad (17)$$

It is interesting to note that the surface roughness factor $1/(1 - .7Ra)$ obtained from the experimental data (equation 17) is in good agreement with the factor recommended by AGMA (Curve (2) of Figure 14). In fact,

the surface roughness factor of equation (17) lies in between curves (3) and (4). For the case of the smooth ball (Ra = .011 μm), the surface roughness factor is close to unity and the expression for ΔT_b from equation (17) can be compared with the similar expression for ΔT_b given in equation (6).

CONCLUSION

A method for measuring the temperature of one of the surfaces of an EHD contact has been developed and used to study the effects of load, rolling speed, slip and surface roughness on flash temperatures. Using a relatively simple analysis the flash temperatures have also been predicted and compared with measured values. The correlation is quite good regardless of the fact that certain assumptions made in the analysis are not valid in the experiments. This implies that either the effects of these assumptions have cancelled one another out or that the solution is not sensitive to them.

ACKNOWLEDGMENTS

This research was supported by NASA-Lewis (NGR-11-002-133) and the National Science Foundation (ENG 74-21002). The continuing encouragement of and helpful discussions with Dr. L. Wedeven of NASA-Lewis are greatly appreciated. Finally, the authors also wish to thank Mr. Scott Bair of Georgia Tech for the design and construction of much of the necessary equipment.

REFERENCES

1. Blok, H., "The Postulate about the Constancy of Scoring Temperature", Interdisciplinary Approach to the Lubrication of Concentrated Contacts (Ed. P. M. Ku), NASA SP-237 (1970).

2. Hirst, W. and Stafford, J. V., "Transition Temperatures in Boundary Lubrication", Proc. I. Mech. Eng., Vol. 186, pp. 179-192 (1972).

3. Blok, H., "Surface Temperatures under Extreme-Pressure Lubricating Conditions", Second World Petroleum Conference, Paris, Vol. 3, Section 4 (June 1937).

4. Jaeger, J. C., "Moving Surfaces of Heat and the Temperature at Sliding Contacts", Proc. Roy. Soc. N.S.W., Vol. 56, p. 203 (1942).

5. Archard, J. F., "The Temperature of Rubbing Surfaces", Wear, Vol. 2, No. 6, pp. 438-455 (October 1959).

6. American Gear Manufacturers Association (AGMA), "Gear Scoring Deisgn Guide for Aerospace Spur and Helical Power Gears", AGMA Information Sheet 217.01 (October 1965).

7. Ausherman, V. K., Nagaraj, H. S., Sanborn, D. M., and Winer, W. O., "Infrared Temperature Mapping in Elastohydrodynamic Lubrication", Trans. ASME, Journal of Lubrication Technology, Vol. 98, No. 2, pp. 236-243 (April 1976).

8. Kunz, R. K., Nagaraj, H. S., Sanborn, D. M. and Winer, W. O., "Investigations of Lubricant Rheology as Applied to Elastohydrodynamic Lubrication", NASA CR-134882, August 1975.

9. Nagaraj, H. S., Sanborn, D. M. and Winer, W. O., "Effects of Load, Speed, and Surface Roughness on Sliding EHD Contact Temperatures", Journal of Lubrication Technology, Trans. ASME, Vol. 99F, No. 2, pp. 254-263 (1977).

10. Bamberg, E. N., et al., "Life Adjustment Factors for Ball and Roller Bearings - An Engineering Design Guide", ASME, New York, (1971).

11. Jones, W. R., Nagaraj, H. S., and Winer, W. O., "Ferrographic Analysis of Wear Debris Generated in a Sliding EHD Contact", to be published in ASLE Transactions, (ASLE Preprint 77-AM-1A-1) (1977).

12. Sanborn, D. M. and Winer, W. O., "Investigations of Lubricant Rheology as Applied to Elastohydrodynamic Lubrication", NASA CR-2837, (1977).

13. Sanborn, D. M., and Winer, W. O., "Fluid Rheological Effects in Sliding Elastohydrodynamic Contacts with Transient Loading: II -

Traction", Trans. ASME, Journal of Lubrication Technology, Vol. 93F, No. 3, pp. 342-348, 1971.

14. Kunz, R. K., Nagaraj, H. S., Sanborn, D. M., and Winer, W. O., "Investigations of Lubricant Rheology as Applied to Elastohydrodynamic Lubrication", NASA CR-134882, (1975).

15. Dudley, Darle W., "Practical Gear Design", McGraw-Hill Book Company, Inc., New York (1954).

16. Kelley, B. W., "A New Look at the Scoring Phenomena of Gears", Trans. Soc. Automotive Engineers, Vol. 61, pp. 175-188 (1953).

17. Kelley, B. W., and Lemanski, A. J., "Lubrication of Involute Gearing", Proc. Inst. Mech. Engineers, Vol. 182, Pt. 3A, pp. 173-184, (1967-1968).

H.S. Nagaraj, D.M. Sanborn, W.O. Winer
School of Mechanical Engineering
Georgia Institute of Technology, Atlanta, Georgia 30332

7. Presented at the Leeds-Lyons Conference
Lyon, France, September 1977
(to be published in Proceedings of Leeds-Lyon Conference)

Infrared temperature measurements, Ferrographic analysis and surface profilometry were used to monitor asperity interactions in a sliding EHD point contact. The contact temperature and surface profile signals obtained both before and after a run-in period are compared in the frequency domain by means of a Fourier analyzer. The interaction of surface asperities is accompanied by the presence of a high frequency component in the infrared signal. It is also shown that only a relatively narrow band of wavelengths of the surface profile spectrum are relevant in the interaction process.

1. INTRODUCTION.

Because of imposed changes in operating load and speed, machine elements designed to run under full EHD lubrication usually experience some operation in the partial EHD regime. In this mode of lubrication the total load is shared between the EHD fluid film and the contacting asperities. Depending on operating conditions and surface characteristics, the partial EHD lubrication may be stable, resulting in an improved surface, or unstable resulting in a surface which can no longer be used.

This paper examines the stable situation. Its purpose is to show the usefulness of the infrared signal emitted from the EHD contact in detecting asperity interaction.

2. EXPERIMENTAL EQUIPMENT AND TECHNIQUE.

A schematic diagram of the apparatus used in the EHD simulation is shown in Fig. 1. The equipment has capabilities for measuring the lubricant film thickness, traction force and both contact surface and film temperatures. The EHD contact was formed using a 31.8 mm diameter AISI 52100 steel ball rotating and loaded against a flat stationary sapphire disk.

Steel balls of two different roughness values (.075 and .38 μm Ra) have been used to study the effects of surface roughness. The balls have no preferential roughness pattern. A relatively smooth ball (.011 μm Ra) has also been used extensively in this laboratory. However, because of limitations in load and speed available in the EHD simulator, it was not possible to produce noticeable surface alteration with this surface even to Hertz pressures and sliding velocities of 1.5 GPa and 12.7 m/s.

A consequence of requiring relatively rough surfaces for this investigation is the absence of an optical interference fringe pattern. This makes optical film thickness data impossible to obtain, which in turn precludes the determination of an average film temperature. Thus only ball surface temperatures are measured. However, this is not a major limitation of the study since the surface temperature is of primary importance in predicting contact failure.

The ball surface temperatures are deduced from the output of an infrared microdetector having a spot size resolution of 38 μm and a time response of 8 μs (1-3). In order to improve the temperature resolution of the detector the lubricant reservoir was maintained at about 15°C above ambient by circulating the test lubricant through a heat exchanger. In all results reported here, the temperatures are the maximum moving surface temperature values in the EHD contact.

A typical experiment involved taking a new ball cemented to a drive shaft and placing it in a surface profilometer to obtain an initial surface profile. The analog voltage signal was recorded on magnetic tape. The specimen was then placed in the EHD simulator and subjected to the desired operating conditions. The AC signal from the infrared detector was recorded during running both at the beginning and end of the run-in experiment. The ball was then removed and another surface profile recording was made. The magnetic tape recordings of the temperature and surface profile data were used as input to a Fourier Analyzer to transform the signals from the time domain to the frequency domain.

During some of the experiments, a fresh lubricant sample was used and a Ferrogram was obtained of the lubricant sample taken after run-in (4). The purpose of the Ferrographic analysis was to determine the concentration and size distribution of debris in the lubricant sample.

The fluid used throughout this investigation is a naphthenic base oil designated N1 in previous studies (1-5). A complete description is given in the appendix of reference (5).

3. EXPERIMENTAL RESULTS.

The recording of the profilometer trace was transferred to a Fourier Analyzer. The first step in an analysis performed by this instrument is an A/D conversion. After analysis of the digital representation of the input signal, the results may be printed and/or a D/A conversion can be made and the results plotted or displayed on a CRT.

Fig. 2a shows the surface profile of the unused ball having an initial surface roughness

of 0.38 μm Ra obtained using the 0.76 mm cut-off wavelength of the instrument. The trace represents the signal after the A/D and D/A conversions and is an excellent replica of the original signal plotted by the profilometer. The distance along the ball surface is shown in terms of the Hertzian contact diameter, d. For the conditions of steel on sapphire at 1.24 GPa peak Hertz pressure, the calculated contact diameter is 0.43 mm.

Fig. 2b shows the same ball after running for 24 minutes in the simulator. The profile traces shown in Fig. 2 were taken in the direction of the sliding motion. No attempt was made to measure the profile at precisely the same location on the ball surface. The traces taken are of sufficient length that they should be representative of any position within the wear trace. On the basis of previous results (3), the conditions of 1.24 GPa and V_s = 1.02 m/s should result in a value of $\Lambda < 1$ based on the unused ball surface roughness and the film thickness for a .011 μm Ra operating at the same conditions. The parameter Λ is the ratio of contact film thickness to composite surface roughness with the value $\Lambda < 1$ indicating that asperity interaction should be expected. Comparing the two traces in Fig. 2, it is apparent that the 24 minute run-in period has resulted in a smoother surface. The final roughness is .25 μm Ra which results in $\Lambda \simeq .4$. The 15.9 mm radius of curvature of the ball surface can also be seen.

The primary function of the Fourier Analyzer is to perform the Fast Fourier Transform (FFT) on the time varying input signal. A convenient way of displaying the amplitudes of the component terms in Fourier series is through the power spectrum. The input to the analyzer is a time varying voltage. After the A/D conversion, the FFT results in a complex amplitude for each of the 127 (plus a constant) terms used in the series for this equipment. Each of these terms is assigned a pair of channels in the analyzer. The frequency range, and therefore, frequency increment can be selected. The frequency assigned to two adjacent pairs of channels differs by a constant. The resulting plot of the power spectrum is linear in the independent variable frequency. The value of the ordinate at each center frequency (channel) is the product of the complex amplitude for that frequency and its conjugate. The units are, therefore, V^2 versus Hz. The D/A conversion makes the plotted results appear to be continuous, but all of the data processing was done digitally in terms of the coefficients of the first 127 terms of the Fourier series.

Although the results are plotted on a linear frequency scale, this is not a convenient representation for this study. This is due to the fact that the frequency is influenced by the profilometer stylus scanning speed and differences between magnetic tape recording and playback speeds. In order to remove these effects, the abscissa has been changed to read wavelength. The unit of wavelength selected is d, the Hertz contact diameter of 0.43 mm. The power spectra of the profiles shown in Fig. 2 are given in Fig. 3.

The first four channels (0-3) were cleared prior to plotting. This is because these are related to gross ball curvature and waviness. These values are so large compared to the values in higher channels (see insert), that a plot would show only the very low frequency components. Therefore, only components having wavelengths <3d have been plotted. In comparing the power spectra for the unused and run-in ball surface profiles, note the factor of two change of scale in Fig. 3a versus 3b. The most apparent contrast is the reduction of the components having wavelengths <2d. Comparing the tabular data in Fig. 3, it appears that roughness components having wavelengths >2d remain essentially unchanged after the 24 minute run-in period. The nine percent difference in DC level can be attributed to slight differences in signal amplification in obtaining the two surface profiles. The most drastic change occurs for a wavelength of one Hertz diameter. This component has been reduced by more than a factor of eight.

It has been shown previously (3) that asperity interaction can significantly alter the DC level of the ball surface temperature. In the DC mode of operation, the frequency response of the detector is 400 Hz. From surface profile measurements it has been determined that only a single asperity occupies the detector's field of view (~38 μm diameter) at any one time. However, at 1.0 m/s sliding velocity the asperity resident time in the field of view is only 40 μs. The DC mode, therefore, yields only a time averaged value. In the AC mode of operation the system can detect such temperature transients since it has a response time of 8 μs. An important consequence of operating in the AC mode, however, is that the reference signal is absent. Instead, the instrument will produce a voltage difference proportional to the variation in target radiation emitted. Through an independent experiment, using an external chopper, it has been determined that the variation indicated in the AC mode is centered on the signal received in the DC mode. From this information a plot of time-averaged surface temperature along with the maximum and minimum values can be obtained.

Fig. 4 shows a plot of the ball surface temperature at the contact center as a function of Hertz pressure. The plot shown was constructed using the DC mode data at five different Hertz pressures. In addition, the AC mode was used at the four highest Hertz pressure levels. As is shown in Fig. 4, the AC data shows no fluctuation about the DC level at P_H = 1.05 GN/m^2, but shows an increasing amount of fluctuation as the pressure is increased. The upper and lower curves represent the range of temperatures detected. It is believed that the peak values represent individual asperity interactions. Fig. 4 also shows the significance of the parameter Λ in predicting the onset of asperity interaction. Fig. 5 shows the range of temperature fluctuation about the DC level as a function of sliding speed and Hertz pressure level. Fig. 5 also shows the appropriate Λ range for each experiment. It can be seen that the AC signal contribution only occurs when Λ is approximately 1 or less.

The fact that local radiation peaks are observed both above and below the DC level supports the argument advanced previously (3) that the peak in the temperature fluctuation signal is due to local heating at an asperity; whereas the minimum signal occurs directly after this maximum and is due to the relatively low local pressure in the region following an asperity.

The AC signal from the infrared detector recorded during the run-in process was also subjected to Fourier analysis. However, in order to eliminate noise in the detector signal, a 20 KHz, 3dB filter was used during data acquisition. The noise remaining below 20 GHz had a peak power of about $5 \times 10^{-6} V^2$ whereas the detector signal had a power content on the order of $10^{-4} V^2$. Furthermore, the sampling technique used by the Fourier Analyzer tends to average out the random noise while enhancing the signal.

Fig. 6 shows the power spectra for the same IR detector signals as used for Fig. 5. The abscissa has been replotted in terms of wavelength in units of d (Hertz diameters). It is apparent from Fig. 6 that the run-in process results in a significant reduction in power at all wavelengths. In both spectra, the peak occurs near $\lambda = 2d$, although the run-in process has reduced the peak magnitude by more than a factor of three. It should be noted that the detector signal was also filtered to remove frequency components less than 500 Hz. This corresponds to wavelengths which are greater than 5d (See Fig. 6). The power spectrum decreases very rapidly for $2 < \lambda \leq 5d$, therefore, the reduction shown in Fig. 6a is not due to filtering.

A Ferrographic analysis of the lubricant sample was made following selected experiments (4). The purpose of the analysis was to independently show a correlation between wear debris in the lubricant and the presence of the AC temperature fluctuations. The correlation was confirmed by the analysis. Also, the reliability of the parameter Λ in predicting the onset of interaction was confirmed.

In Ferrographic analysis, solid particles are precipitated from the lubricant by a magnetic field as it flows slowly over a substrate. Particles are precipitated from the oil at a rate depending on size and magnetic permeability. The resulting Ferrogram yields the size distribution and concentrations of particles in the oil sample. Thirty mℓ samples were taken for experiments at various Hertz pressures and 1 m/s sliding. Knowing the approximate film thickness and surface roughnesses for each of these conditions, the Ferrogram results can be interpreted in terms of the Λ parameter.

A plot of composite Ferrogram density for each test as a function of initial Λ ratio appears in Fig. 7. The large and very rapid increase in particle density at low Λ values is evident. The transition to the high wear regime occurs as the Λ ratio approaches 1. This is in agreement with the findings of other investigators. Tallian (6) has shown that the onset of surface distress occurs at a Λ value of about 1.5. Czichos (7) reports that the change from a full EHD film to continuous asperity contact occurs as Λ decreases from 2.5 to 0.7. In Fig. 7, at Λ values greater than 2, a composite particle density of between 1 and 2 percent is observed. Since a full film should be present at these higher Λ ratios, little wear should take place. Therefore, these density readings represent the background or contaminant particle density for this set of experiments.

The importance of the parameter Λ in predicting asperity interaction is clearly shown in Fig. 7. The onset of asperity interactions predicted by the occurrence of surface temperature fluctuations correlates very well with the results of the Ferrographic analysis. The calculation of the Λ value was based on a profilometer roughness cut-off of 0.76 mm, which is reasonably close to 2d recommended value (discussed below.

Microscopic examination of the wear debris generated during these studies showed that essentially all of the metallic wear particles, regardless of the initial surface roughness, were composed of small asymmetric thin (metallic) flakes. These flakes were typically less than 10 μm in major dimension and no more than 1.5 μm thick. On the ferrograms, these particles are typically arranged in strings due to the magnetic field generated by the ferrograph.

4. DISCUSSION OF RESULTS.

An autocorrelation function of the surface profile data shown in Figs. 2 and 3 was obtained using the Fourier Analyzer. In addition to the power spectrum, the autocorrelation function can be useful in describing the surface profile. In fact, Whitehouse and Archard (8) and Peklenik(9) suggest the description of a real surface in terms of only σ, the rms roughness, and β^*, the correlation distance. Briefly, the autocorrelation function is obtained by comparing a time varying signal, in this case the surface profile measurement, with a replica of itself where the replica is shifted an amount $\beta (0 \leq \beta \leq \infty)$ along the surface. The autocorrelation function $C(\beta)$ therefore, depends on β and is obtained from

$$C(\beta) = \frac{1}{\ell} \int_0^{\ell} a(x)a(x + \beta)dx \qquad (1)$$

where $a(x)$ is the amplitude of the surface profile trace at a distance x along the surface. For a truly random signal, $C(\beta)$ will be a maximum at $\beta = 0$. If the signal is periodic, $C(\beta)$ will peak whenever β is a multiple of the wavelength. If a Gaussian distribution of surface roughness amplitudes is considered, equation 1 results in an exponential autocorrelation function when normalized such that $C(0) = 1.0$,

$$C(\beta) = \exp(-\beta/\beta^*) \qquad (2)$$

Therefore, when $\beta = 2.3\beta^*$, $C(\beta) = 0.10$. The value 0.10 has been arbitrarily set by Whitehouse and Archard as being sufficiently small that two points on the surface may be regarded as being independent. This follows from the fact that when the autocorrelation function $C(\beta)$ is close to unity, two points on the surface β distance apart are strongly interdependent. However, when $C(\beta)$ attains values close to zero, two points on the surface β distance apart are weakly correlated and therefore essentially independent. The correlation distance $2.3\beta^*$ can also be viewed as roughly being equal to the spacing between equal sized asperities. The power spectrum is the inverse Fourier transform of the autocorrelation function, or

$$P(\omega) = \int_{-\infty}^{\infty} C(t)e^{-i\omega t}dt \qquad (3)$$

Substituting equation (2) into (3) results in

$$P(\omega) = 0.5 \quad \text{for} \quad \lambda_s = 1/\omega = \beta^*$$

$$P(\omega) \simeq 0 \quad \text{for} \quad \lambda_s = 1/\omega < 0.1\beta^* \qquad (4)$$

$$P(\omega) \simeq 1 \quad \text{for} \quad \lambda_s = 1/\omega > 10\beta^*$$

The wavelength β^* can therefore be thought of as a dividing point between those surface wavelength components having significant amplitudes and the shorter wavelengths which do not. Whitehouse and Archard have shown the model to be in good agreement with a large number of real surface profiles.

Fig. 8 shows the autocorrelation function for the unused and run-in ball surfaces shown in Fig. 2. The position shift β is shown in terms of the Hertz diameter d. If the Whitehouse-Archard model is applied to the data in Fig. 8, the value of β^* can be found from $C(2.3\beta^*) = 0.1\ C(0)$. The correlation distance β^* is .17d (74μm) for the unused ball and .33d (142μm) for the run-in surface. It is apparent that the exponential model of equation (2) can only be used for $\beta \leq 2.3\beta^*$. The further increase in $C(\beta)$ implies that the profile is not truly random, but has strong periodic components with wavelengths > d. This can also be seen from the power spectra shown in Fig. 3.

Fig. 8 shows that the correlation distance has doubled as a result of the run-in process. From equation (2), a doubling of β^* implies that two points on the surface must be taken twice as far apart after run-in to be considered independent. Because of the interrelationship between the power spectra and autocorrelation function, if the surfaces were in fact random, the half power point would be shifted to a wavelength twice the value of that for the unused surface. This is the case when the high frequency components are reduced much more than the low frequency components (See Fig. 3). This is also consistent with the notion of independent points. Consider, for example, a surface comprised of only two wavelength components 2d and 0.2d. When the 0.2d wavelength component is present, the autocorrelation function would have a value of 1.0 for β = 2nd where n is an integer. However, it would also have sizeable peaks for β = 0.2nd (with drops to near zero midway between). After run-in, however, the 0.2d wavelength component will be substantially reduced. Assuming it to be eliminated, the $C(\beta)$ now peaks only once every β = 2nd and reaches zero half way between the peaks. If the correlation distance is defined as the ten percent point, it is apparent that this distance must be increased if high frequency components are reduced or eliminated. The change in the autocorrelation function as shown in Fig. 8 is what would be expected as a result of the run-in process.

Based on the results shown in Figs. 3 and 6, the authors believe that the methods presently used to determine acceptable levels of the R_a or rms surface roughness may not be the most appropriate. For example, the true rms value of the surface shown in Fig. 2a (unused rough ball) is equal to the square root of the integral of the power spectrum (Fig. 3a) over all wave lengths ($0 \leq \lambda \leq \infty$). However, the finite limits of integration must be chosen. The profilometer uses an upper limit of .76 mm (through electrical filtering) for averaging purposes and has a lower limit set by the stylus radius of 13 μm. If one assumes that the absence of surface temperature fluctuations is indicative of negligible asperity interaction then as far as asperity interaction is concerned, one can determine the significant wavelengths of the surface profile. For example, Fig. 6a shows that the temperature spectral power content during asperity interaction drops to less than ten percent of its peak value for the wavelengths $\lambda \leq d/4$. However, Fig. 3a shows that there are significant roughness components down to at least λ = .08d (the power content is essentially the square of the amplitude). The same figures show that the major components for both the roughness profile and the temperature signal are in the range $\frac{1}{2}d \leq \lambda \leq 3d$. Therefore, whereas the roughness wavelength in the range $\frac{1}{2}d \leq \lambda \leq 3d$ are obviously important in causing temperature fluctuations, wavelengths shorter than d/4 appear to have little or no effect. Based on the power reduction to ten percent of its maximum value, the lower bound for rms determination should be $\lambda \simeq d/4$. The upper limit is set at $\lambda \simeq 2d$ because the temperature signal drops off rapidly for $\lambda > 2d$ even though there are roughness components present with wavelengths greater than 2d (See Fig. 3).

On the basis of the data taken, it appears that the rms surface roughness to be used in a calculation of $\Lambda(\Lambda = h/\sigma)$ should consider only wavelengths in the range $d/4 \leq \lambda \leq 2d$. For this experiment, d = 0.43 mm the applicable range is then .11 $\leq \lambda \leq$ .86 mm. A roughness of about .38 μm Ra was obtained using the profilometer with limits of about .013 $\leq \lambda \leq$ .76 mm. By integrating the power spectrum of surface profile between the limits of .11 $\leq \lambda \leq$ .86 mm, and taking the square root, the rms value was .53 μm. This higher rms value is believed to be due to significant power in the range .76 $\leq \lambda \leq$ .86 mm and the natural difference between rms and Ra roughness measurements. The profilometer also has available cutoffs at .25 mm and .067 mm. The use of either of these values would correspond to rms integration limits of $.030d \leq \lambda \leq .58d$ and $.030d \leq \lambda \leq .18d$ respectively. Since the desired range is $.25d \leq \lambda \leq 2d$, the resulting rms values would not be reliable in predicting surface interaction.

In addition to the possibility of getting a value of surface roughness which cannot reliably predict performance, the fact that wavelengths shorter than 0.25d do not appear to be significant might have an economic impact. For example, under conditions in which the Hertz diameter is relatively large, the final stages in a lapping or polishing process may not be important.

5. CONCLUSIONS

Changes in the surface profile and EHD contact temperatures have been measured and analyzed. The existence of high frequency temperature fluctuations is found to be due to surface asperity interactions. Ferrographic analysis of the lubricant sample supports this argument.

It appears that the EHD contact behaves like a mechanical filter. Only a relatively narrow band of surface roughness wavelengths appears to be important in the process of asperity interaction. The size of the EHD contact, therefore, has a direct influence on the selection of the optimum surface finishing technique for a machine element.

The experimental results of the roughness,

temperature and Ferrographic measurements support one another and theoretical predictions. In addition, the transition from full to partial EHD as monitored by these measurements can be accurately predicted using a properly evaluated Λ value.

6. ACKNOWLEDGMENTS

This research was supported by NASA-Lewis (NGR-11-002-133) and the National Science Foundation (ENG 74-21002). The continuing encouragement of and helpful discussions with Dr. L. Wedeven of NASA-Lewis are greatly appreciated. Also, the efforts of Mr. William Jones of NASA-Lewis in obtaining the Ferrograms of the lubricant samples is appreciated. Finally, the authors also wish to thank Mr. Scott Bair of Georgia Tech for the design and construction of much of the necessary equipment.

REFERENCES

(1) TURCHINA, V., SANBORN, D.M., and WINER, W.O., 'Temperature measurements in sliding elasto-hydrodynamic point contacts', Trans. ASME, J. Lubr. Tech., 1974 96 464-471.

(2) AUSHERMAN, V.K., NAGARAJ, H.S., SANBORN, D.M., and WINER, W.O., 'Infrared temperature mapping in elastohydrodynamic lubrication', Trans. ASME, J. Lubr. Tech., April 1976, 98F 236-243.

(3) NAGARAJ, H.S., SANBORN, D.M., and WINER, W.O., 'Effect of load, speed and surface roughness on sliding EHD contact temperatures', Trans. ASME, J. Lubr. Tech., October 1976, 99, 2 254-263.

(4) JONES, W.R., and NAGARAJ, H.S., and WINER, W.O., 'Ferrographic analysis of wear debris generated in a sliding EHD contact', to be published in ASLE Trans 1977.

(5) SANBORN, D.M., WINER, W.O., 'Fluid rheological effects in sliding elastohydrodynamic point contacts with transient loading: I - film thickness', Trans. ASME, J. Lubr. Tech., 1971, 93, 262-271.

(6) TALLIAN, T.E., 'On competing failure modes in rolling contacts', ASLE Trans., 1967, 10, 418-439.

(7) CZICHOS, H., 'Influence of asperity contact conditions on failure of sliding elasto-hydrodynamic contacts', to be published in Wear Magazine, 1976.

(8) WHITEHOUSE, D.J. and ARCHARD, J.F., 'The asperities of random surfaces of significance in their contact', Proc. Roy. Soc Lond. A., 1970, 316, 97-121.

(9) PEKLENIK, J., 'New developments in surface characterization and measurements by means of random process analysis', Proc. Inst. Mech. Engr., 1967-1968, 182, 3K.

NOMENCLATURE

C	Autocorrelation function
d	Hertzian Contact diameter, m
h_c	Film thickness at Contact Center, m
ℓ	Length, m
P_H	Peak Hertz pressure, N/m^2
T_b	Ball Surface temperature, C
V_s	Sliding velocity, m/s
x	Distance along surface, m
β	Length shift in computing autocorrelation function, m
β^*	Correlation distance, m
Λ	h_c/σ
λ	wavelength, m
σ	Surface roughness, rms or Ra, m

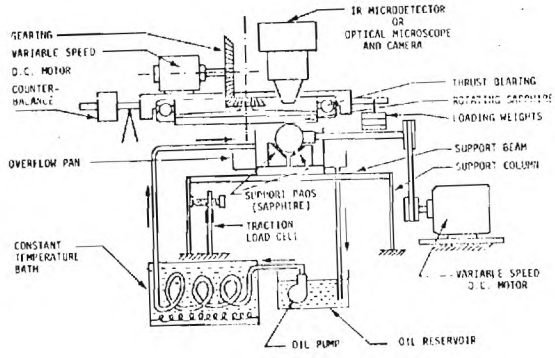

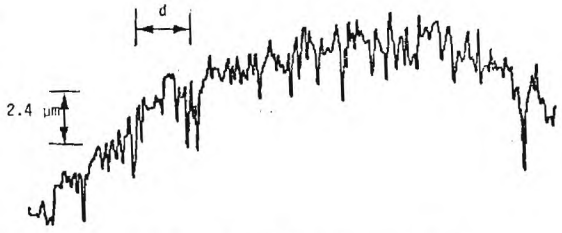

a) Unused ball surface (.38 μm Ra roughness).

b) Ball surface after running 24 minutes (.25 μm Ra roughness

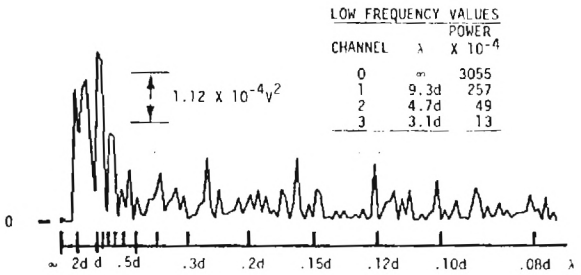

a) Unused ball surface.

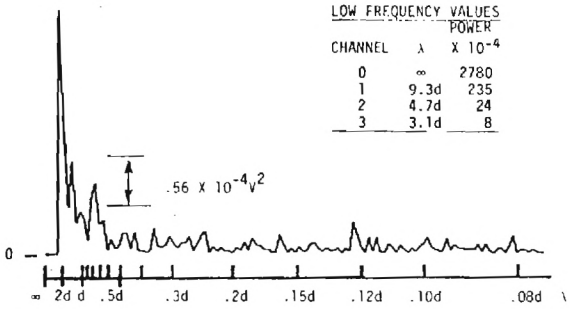

b) Ball surface after running 24 minutes.

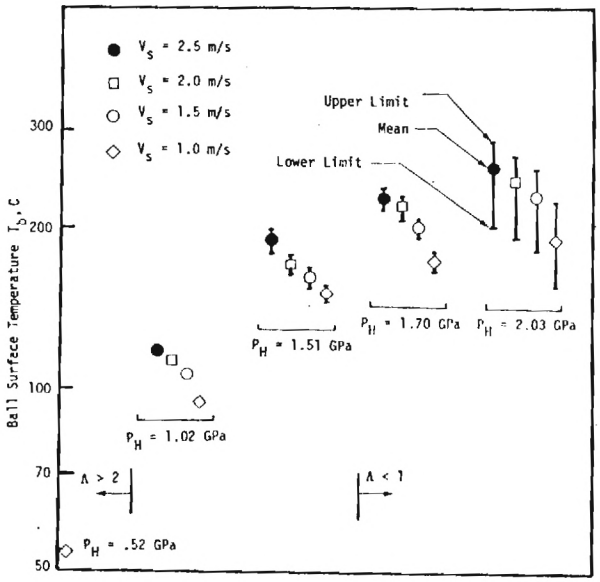

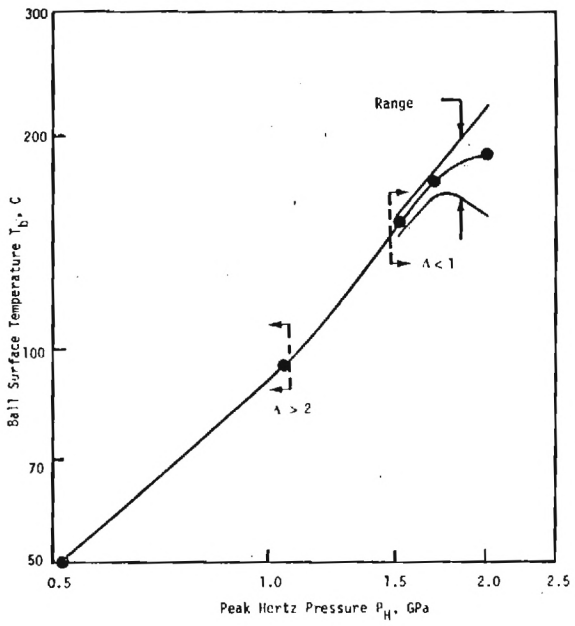

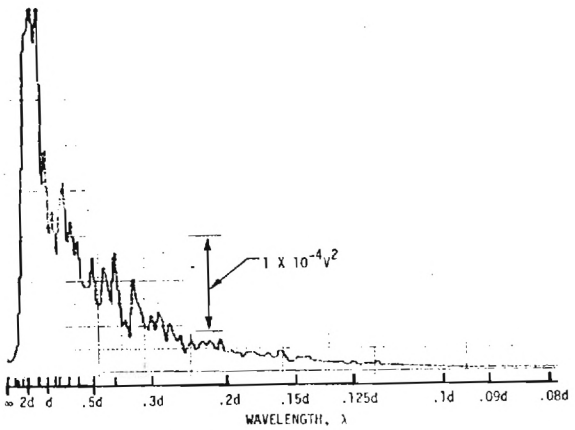

a) Ball Surface Temperature Fluctuations at Start of Run-in.

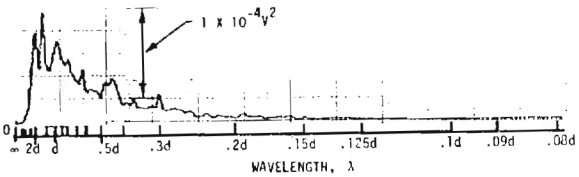

b) Ball Surface Temperature Fluctuations after 8 Minutes Run-in.

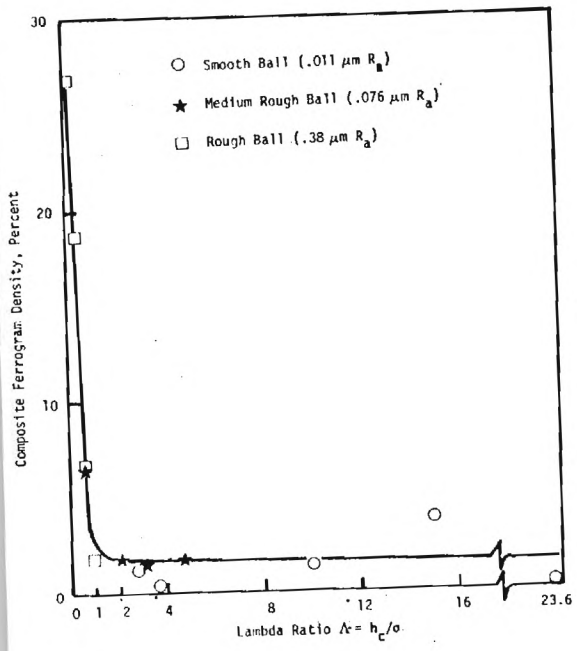

Fig. 1: Schematic of the combined rolling and sliding EHD contact simulator.

Fig. 2: Surface profiles in the direction of sliding (P_H = 1.24 GN/m^2, V_s = 1.02 m/s, Hertz diameter d = 0.43 mm, pure sliding).
a) Unused ball surface (.38 μm R_a roughness).
b) Ball surface after running 24 minutes (.25 μm R_a roughness).

Fig. 3: Power spectra of the surface profiles (P_H = 1.24 GN/m^2, V_s = 1.02 m/s, Hertz diameter d = 0.43 mm, pure sliding).
a) Unused ball surface (.38 μm R_a roughness).
b) Ball surface after running 24 minutes (.25 μm R_a roughness).

Fig. 4: Average value and range of ball surface temperature fluctuation versus peak Hertz pressure (medium rough ball: .076 μm R_a, fluid N1, V_s = 1.0 m/s, V_{sa} = 0).

Fig. 5: Average value and range of ball surface temperature fluctuations (medium rough ball: .076 μm R_a, fluid N1, V_{sa} = 0).

Fig. 6: Power spectra of ball surface radiation fluctuations (.38 μm R_a initial roughness, P_H = 1.24 GN/m^2, V_s = 1.02 m/s, Hertz diameter = 0.43 mm, pure sliding).
a) Ball surface radiation fluctuations at start of run-in.
b) Ball surface radiation fluctuations after 8 minutes run-in.

Fig. 7: Composite ferrogram density versus Lambda ratio.

Fig. 8: Autocorrelation functions of the surface profiles. (λ > 3d not included, P_H = 1.24 GN/m^2, V_s = 1.02 m/s, Hertz diameter d = 0.43 mm, pure sliding).
a) Unused ball surface (.38 μm R_a roughness).
b) Ball surface after running 24 minutes (.25 μm R_a roughness).

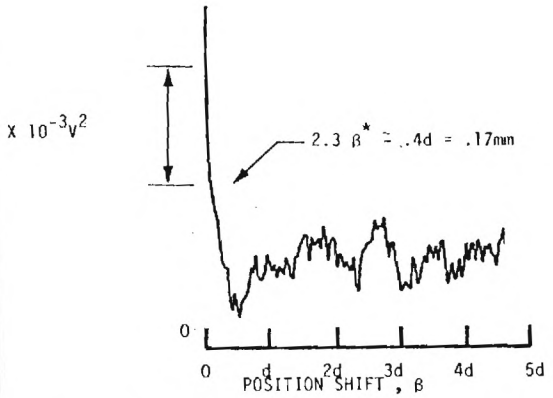

) Unused ball surface (.38 μm Ra roughness).

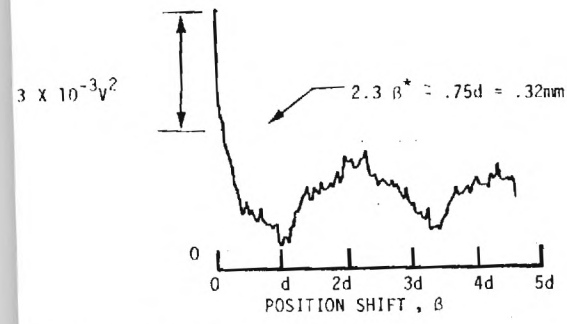

Ball surface after running 24 minutes.

8. Presented at the 1978 ASLE Annual Meeting
Dearborn, Michigan, April 1978
(to be published in Trans, ASLE)

Surface Temperature Measurements in Rolling and Sliding EHD Contacts

by

H. S. Nagaraj

Mechanical Technology Incorporated
968 Albany-Shaker Road
Latham, New York 12110

and

D. M. Sanborn

W. O. Winer

Georgia Institute of Technology
School of Mechanical Engineering
Atlanta, Georgia 30332

To be presented at
1978 ASLE Annual Mtg.
Dearborn, Mich. April '78
& published in Trans ASLE

September, 1977

(Revised December 1977)

Surface Temperature Measurements in Rolling and Sliding EHD Contacts

ABSTRACT

A number of devices in which concentrated contact conditions occur, have relatively small amounts of slip or none at all. A knowledge of contact temperatures developed under these conditions is essential to understanding the lubricant rheology and also the fluid film failure.

In this study, moving surface temperature measurements in rolling and sliding EHD point contacts were made using an available infrared technique. Film thickness and traction have also been measured. Slide to roll ratios of -2 to +2 have been studied. By using a different kinematic configuration stationary surface temperatures have also been measured. It has been shown that while surface temperature rises in the low slip region are relatively small, stationary surface temperatures are significantly higher than the moving surface temperatures. Flash temperature theory has been extended to cover the combined rolling and sliding conditions. Correlation between the predicted and the measured values has also been performed.

NOMENCLATURE

a	Hertzian contact radius, m
c	specific heat, J/(kg·K)
h	Average film thickness, m
h_c	Film thickness at contact center, m
h_m	Minimum film thickness, m
k	Thermal conductivity, W/(mK)
L	Non-dimensional time parameter $= t_1/t_2 = \frac{Va}{2\alpha}$, $(2L = \frac{Va}{\alpha}$ Peclet number)
P_H	Peak Hertz contact pressure, Pa
t_1	Thermal diffusion time $= a^2/2\alpha$, s
t_2	Characteristic resident time $= a/V$, s
T	Temperature, C
T_{bath}	Bath Temperature, C
ΔT	Temperature rise, C
T_o	Upstream (bulk) temperature, C
TC	Traction coefficient
V	Surface Velocity, m/s
$\bar{V}$	Rolling velocity $= (V_b + V_{sa})/2$, m/s
V_s	Sliding velocity $= V_b - V_{sa}$, m/s
W	Normal load, N
α	$= k/\gamma c$, thermal diffusivity, m^2/s
γ	density, kg/m^3
K	A constant $= .968\ a^{1/2}\alpha^{1/2}/k$, $m^{3/2}s^{1/2}C/N$

Λ	h_c/σ
Σ	Slide roll ratio = $V_s/\bar{V}$
σ	$=\sqrt{\sigma_b^2 + \sigma_{sa}^2}$, composite surface roughness, rms or R_a, m
σ_b	Ball surface roughness, rms or R_a, m
σ_{sa}	Sapphire surface roughness, rms or R_a, m

Subscripts

b	ball
f	fluid
sa	sapphire

INTRODUCTION

Elastohydrodynamic lubrication (EHD) commonly refers to the hydrodynamic lubrication of elastically deformable surfaces. The bearing surfaces draw the lubricant in between them because of their motion and thereby generate high hydrodynamic pressures to support the load. If the speeds of the bearing surfaces are unequal, relative slip occurs. A number of devices in which EHD contact conditions occur, have relatively small slip or none at all. A study of the influence of slip on some important parameters in the EHD conjunction forms the subject of this paper.

Very often a combination of rolling and sliding is kinematically described by a parameter referred to as the slide-roll ratio and denoted by Σ. Σ is the ratio of the slip speed (difference between the surface velocities) to the rolling speed (average or one-half the sum of the two surface velocities). Thus, Σ is given by $(V_b - V_{sa})/\frac{1}{2}(V_b + V_{sa})$. Σ can vary between $-\infty$ and $+\infty$. The value of Σ equal to 0 corresponds to conditions of pure rolling, when the two surfaces are moving at the same speed in the same direction. Values of Σ equal to ± 2 correspond to the cases when one of the surfaces is moving and the other is stationary. Σ equals $\pm\infty$ refer to conditions where the rolling component is zero, when the two surfaces move at the same speed but in opposite directions. The range of practical interest is however, Σ equal to -2 to +2, and only this range is investigated in the present work. Σ equal to ± 2 is referred to as simple sliding in this work.

Slip or relative sliding between the bearing surfaces produces shearing of the viscous fluid film and thereby generates a large amount of heat. A knowledge of the temperatures developed in the conjunction zone is required in studying the failure of the lubricant film and also in understanding the lubricant rheology under severe conditions of pressure, shear stress and shear rate. Recent studies [1] have indicated a possibility of the lubricant going into a glassy state in ordinary EHD situations. Temperature measurements under these conditions can help in ascertaining whether the lubricant is in a glassy state or in a liquid state.

Temperature measurements in EHD contacts in simple sliding have been reported

earlier by the authors [2, 3, 4]. The objective of the present paper has been to study the influence of slip on surface temperatures in EHD contacts. The influence of slip on lubricant film thickness and traction have also been studied in order to support the temperature measurements.

EXPERIMENTAL APPARATUS AND TECHNIQUE

A schematic of the combined rolling and sliding EHD contact simulator used in the present study is shown in Figure 1. The rolling and sliding EHD point contact is formed between a 31.8 mm diameter AISI 52100 steel ball and a 88.9 mm diameter sapphire disk. The steel ball and the sapphire disk are rotated about mutually perpendicular axes at varying speeds to produce any desired combination of rolling and sliding. For purposes of clarity, in Figure 1, the axis of rotation of the steel ball is shown in the plane of the paper, while in the actual apparatus it is perpendicular to the plane of the figure. The radial position of the ball on the sapphire disk can also be varied to produce the required combination of rolling and sliding. A mechanical brake, however, had to be used to control the speed of the sapphire disk at large values of positive slip (ball speed greater than the sapphire disk speed).

Slide to roll ratio could be determined to within .02 of the reported values. This accuracy was found sufficient for the purposes of the study reported in this paper.

The equipment has capabilities for a simultaneous measurement of film thickness and traction. The temperatures of both the surface and the fluid could be measured simultaneously with traction. The film thickness and temperatures however were determined in two separate experiments.

Fully flooded conditions were maintained in all the experiments. Sufficient amount of the lubricant was automatically carried into the contact by the moving ball. But when the ball was stationary and only the sapphire disk was rotating, the lubricant had to be introduced directly into the contact zone by a separate jet. The lubricant bath temperature was maintained approximately constant (to within 2°C) in order to have a common reference temperature for all the experiments.

Film thickness was measured using both the monochromatic optical interference technique described in reference 5 and the dichromatic technique of Foord, Wedeven, et al [6, 7]. Tractive force was measured by noting the output of a carefully calibrated strain gage load cell (shown in Figure 1). The

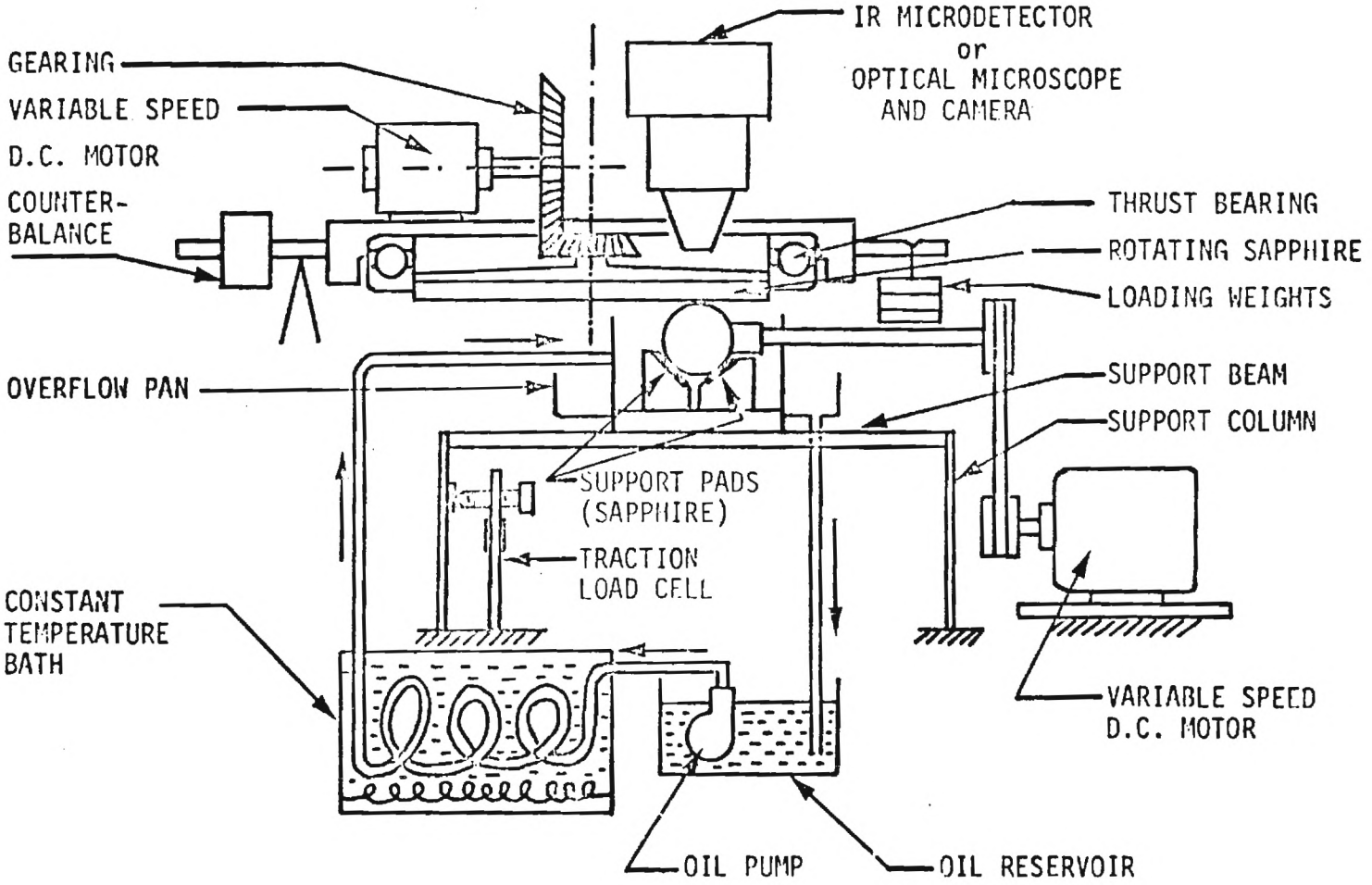

Figure 1. Schematic of the Combined Rolling and Sliding EHD Contact Simulator.

temperatures in the EHD contact were determined using an available infrared technique described in References 3 and 4. The spot size resolution of the infrared microdetector used was 36 μm and, therefore, the temperature distributions within the EHD contact could be measured with a sufficient resolution.

The fluid used throughout this investigation is a naphthenic base mineral oil designated N1 in previous studies [1-5]. A complete description of this fluid is given in reference 5. A smooth steel ball (.011 μm R_a) was used in this study in order to avoid any possible asperity interactions. In fact, in all the experiments reported in this paper, Λ was maintained considerably greater than 1.

EXPERIMENTAL RESULTS AND DISCUSSION

Film Thickness and Traction Measurements

Table 1 is a summary of the film thickness and traction experiments. Rolling velocity, slide-roll ratio and peak Hertz pressure were all varied.

Photomicrographs of the optical interference fringes for one set of operating conditions are shown in Figure 2. Figure 2 contains data for slide-roll ratio ranging from -.10 to 2.00. It can be seen from Figure 2 that the film thickness at contact center is essentially constant over the entire range of slide-roll ratio. Photomicrographs similar to the ones shown in Figure 2 were taken for other operating conditions also. Eventhough the film thickness over the entire contact region could be determined using these pictures only minimum film thickness and center film thickness values were recorded. By noting the color of the fringe appearing at the desired location and referring to the calibration chart for the dichromatic fringe system [8], the film thickness values were directly determined.

Film thickness and traction have been plotted as a function of Σ in Figures 3 and 4 respectively. The effect of the slide/roll ratio on film thickness is small. It is apparent from Figure 4 that the peak normally obtained in TC vs. Σ experiments in nominal line contacts is not present here. Wedeven's traction data for point contacts [6] also lacks such a peak. The influence of rolling velocity on film thickness and traction under conditions of zero slip is shown in Figure 5.

Table 1. Summary of Rolling Experiments: Film Thickness and Traction

(Smooth ball: .011 μm R_a, Fluid N1)

$\bar{V}$	Σ	V_s	P_H	T_{BATH}	h_c	h_m	TC
m/s	-	m/s	GPa	°C	μm	μm	--
0.5	2.00	1.00	0.81	34	.18	.076	.061
"	0.60	0.30	"	37	"	"	.056
"	0.40	0.20	"	38	"	"	.055
"	0.20	0.10	"	38	"	"	.050
"	0.00	0.00	"	39	"	"	.017
"	-.20	-.10	"	38	"	"	--
"	-.40	-.20	"	40	"	"	--
"	-.88	-.44	"	41	"	"	--
0.75	2.00	1.50	"	39	.19	.089	.058
"	1.20	0.90	"	"	.20	"	.058
"	0.67	0.50	"	"	.20	"	.055
"	0.13	0.10	"	"	.22	"	.049
"	0.00	0.00	"	38	.22	"	.024
"	2.00	1.50	0.66	33	.22	.15	.051
"	1.20	0.90	"	34	.24	.18	.051
"	0.67	0.50	"	34	"	"	.051
"	0.19	0.14	"	35	"	"	.051
"	0.00	0.00	"	"	"	"	.014
"	-.13	-.10	"	"	"	"	.041
"	2.00	1.50	1.02	40	.15	.064	.061
"	.27	-.20	"	38	.18	.076	.059
"	0.00	0.00	"	37	.22	"	.020
"	-.27	-.20	"	"	.17	"	.057
0.51	0.00	0.00	"	"	.18	"	.020
0.72	0.00	0.00	"	"	.22	"	.023
1.00	0.00	0.00	"	"	.24	.127	.023
1.25	0.00	0.00	"	"	.28	.178	.027

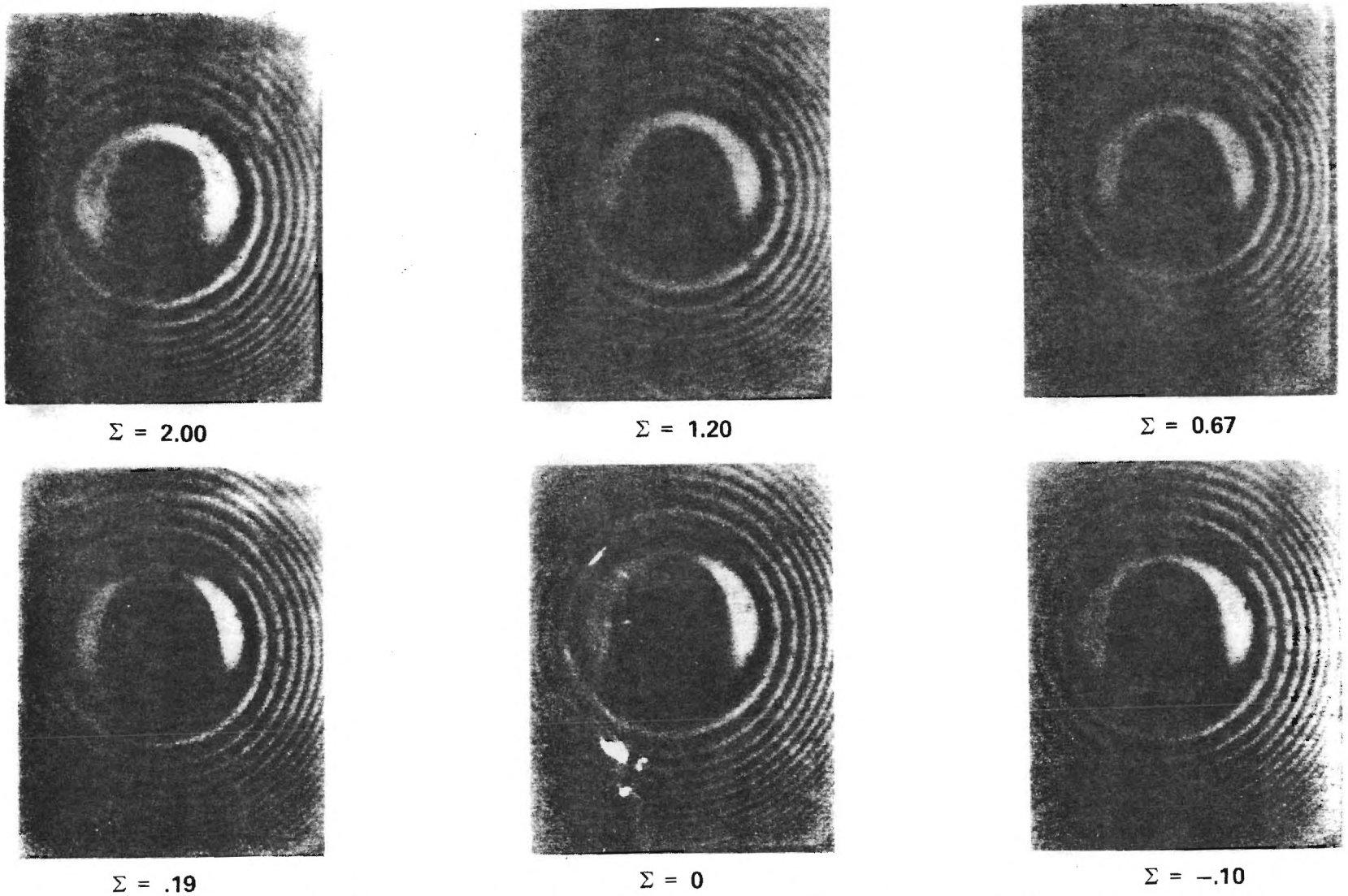

Figure 2. Photomicrographs of optical interference fringes representing film thickness (Smooth ball ⇒ .011 μm R_a, Fluid N1, P_H = .66 GPa, $\bar{V}$ = .75 m/s).

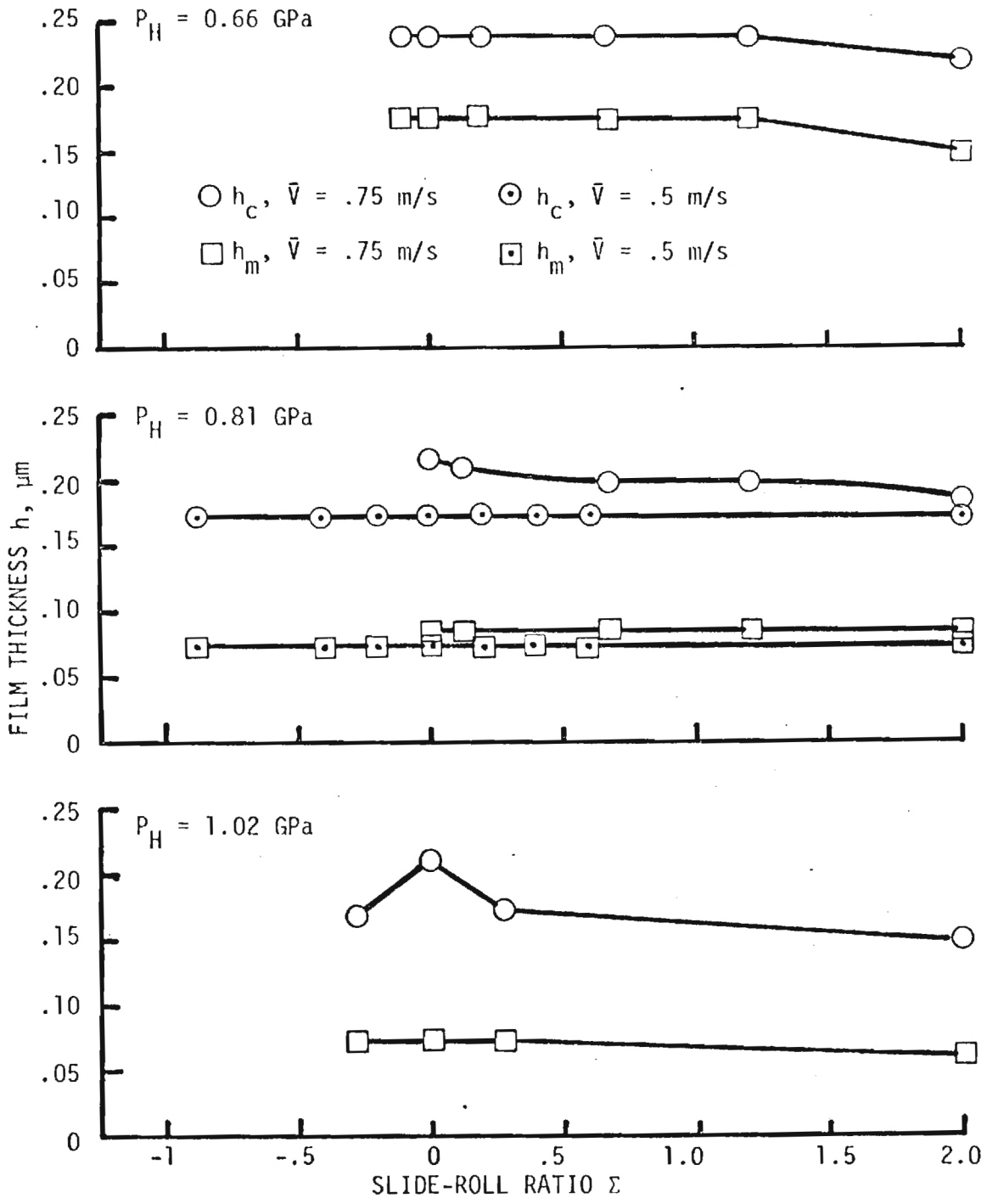

Figure 3. Film Thickness as a Function of Slide-Roll Ratio (.011 μm R_a roughness).

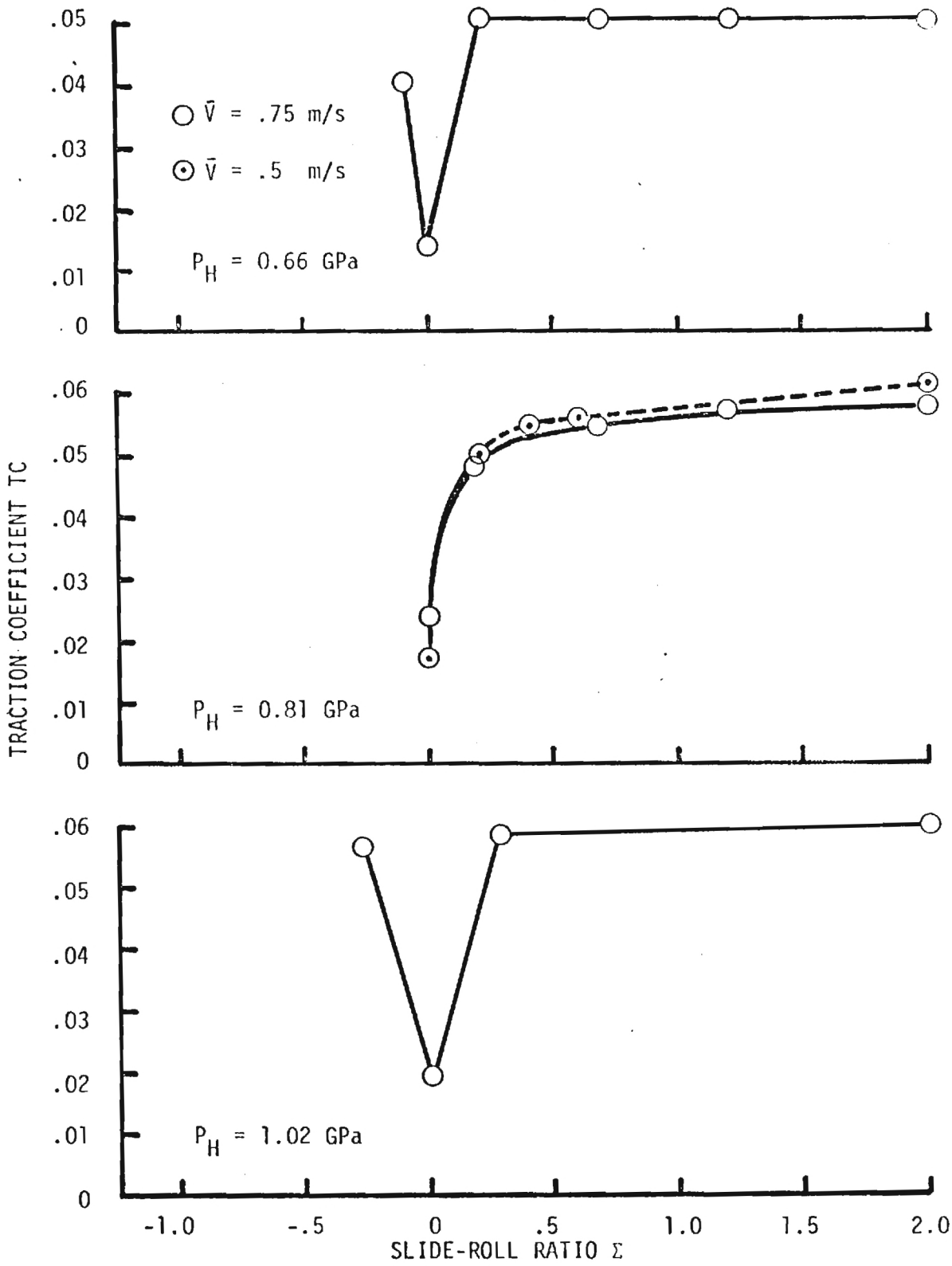

Figure 4. Traction Coefficient as a Function of Slide-Roll Ratio (.011 μm R_a roughness).

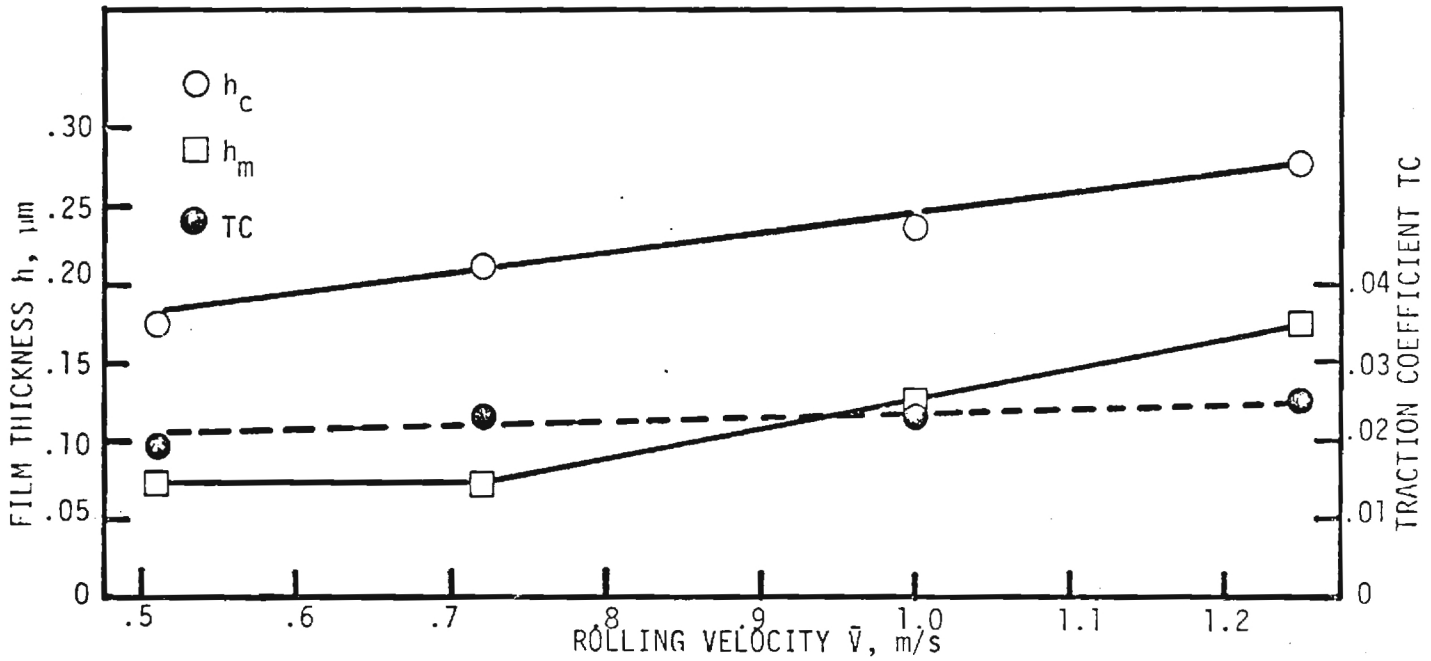

Figure 5. Film Thickness and Traction Coefficient as a Function of Rolling Velocity (Σ = 0, .011 μm R_a Roughness, P_H = 1.02 GPa).

Temperature Measurements for Positive Slide-roll Ratios

Table 2 shows the results of the ball surface temperature measurements. Because of small changes in the lubricant bath temperature during the course of the experiments, the temperature rise $\Delta T(\Delta T = T_b - T_{bath})$ has been tabulated instead of the absolute temperature of the surface. Also, due to the relatively low infrared detector signal level under conditions of small amounts of sliding only the more severe conditions of these listed in Table 1 were used in the temperature measurement experiments. However, these conditions are closer to those found in normal practice.

The data from Table 2 has also been plotted and is shown in Figures 6 - 8. Figures 6 and 7 show the dependence of temperature rise on slide-roll ratio Σ for rolling velocities of 0.75 and 1.00 m/s respectively. A linear regression analysis of the maximum temperature rise data for both the rolling velocities resulted in

$$\Delta T_b = 30.3\Sigma + 1.2, \ ^\circ C \qquad (1)$$

with a correlation coefficient of 0.99.

Figure 8 shows the temperature rise as a function of rolling velocity for the case of pure rolling ($\Sigma = 0$). The data fit the straight line

$$\Delta T_b = 5.2\bar{V}, \ ^\circ C \qquad (2)$$

with a correlation coefficient of 0.99.

Table 2. Summary of Rolling Experiments: Ball Surface Temperature Rises

(Smooth ball: .011 μm R_a, P_H = 1.02 GPa, Fluid N1)

$\bar{V}$	Σ	V_s	V_b	V_{sa}	T_{BATH}	CENTER ΔT_b	MAX. ΔT_b
m/s		m/s	m/s	m/s	°C	°C	°C
0.75	2.00	1.50	1.50	0.00	42	54	64
0.75	1.20	0.90	1.20	0.30	42	35	36
0.75	0.99	0.74	1.12	0.38	43	26	26
0.75	0.56	0.42	0.95	0.54	42	14.5	15
0.75	0.27	0.20	0.85	0.65	40	6	6
0.75	0.13	0.10	0.80	0.70	41	4.5	4.5
0.75	0.00	0.00	0.75	0.75	41	4	4
1.00	2.00	2.00	2.00	0.00	44	53	62.5
1.00	1.50	1.50	1.75	0.25	45	42	46.5
1.00	1.30	1.30	1.65	0.35	45	37.5	39
1.00	1.04	1.04	1.52	0.48	44	36	37.5
1.00	0.60	0.60	1.30	0.70	43	21	21.5
1.00	0.40	0.40	1.20	0.80	43	10.5	10.5
1.00	0.12	0.12	1.06	0.94	42	6	6
1.00	0.00	0.00	1.00	1.00	41	5	5
0.50	0.00	0.00	0.50	0.50	41	2	2
1.25	0.00	0.00	1.25	1.25	41	7	7
0.75	-2.00	-1.50	0.00	1.50	28	76	76
0.75	-1.28	-0.96	0.27	1.23	39.5	32	36.5
0.75	-0.80	-0.60	0.45	1.05	38.5	22.5	25
0.75	-0.45	-0.34	0.58	0.92	38	14.5	15
0.75	-0.27	-0.20	0.65	0.85	39	14	14
1.00	-2.00	-2.00	0.00	2.00	26	89	89
1.00	-1.52	-1.52	0.24	1.76	39.5	45	49.5
1.00	-0.90	-0.90	0.55	1.45	34	27.5	31
1.00	-0.40	-0.40	0.80	1.20	38.5	18	19.5
1.00	-0.12	-0.12	0.94	1.06	37.5	10.5	11

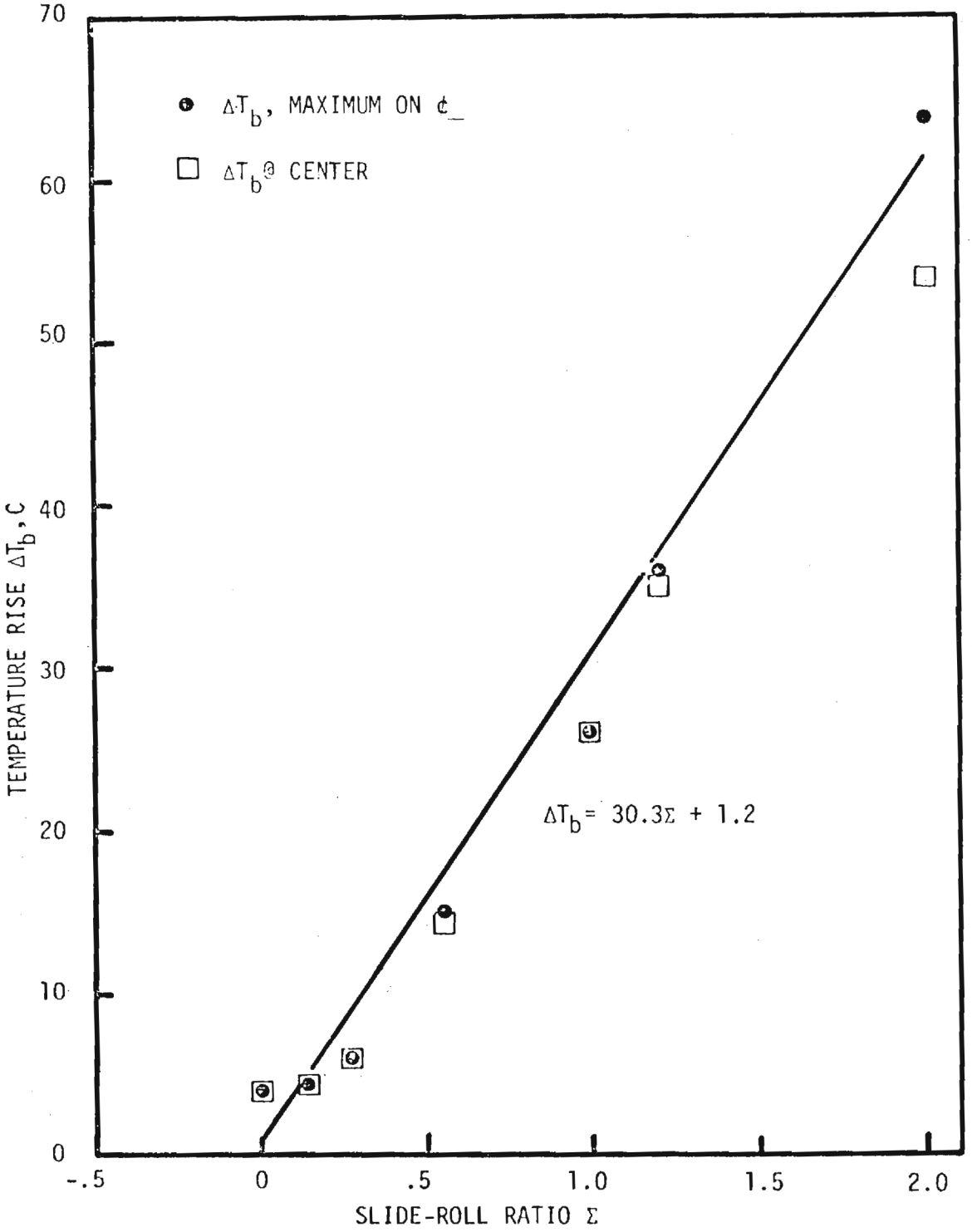

Figure 6. Ball Surface Temperature Rise as a Function of Slide-Roll Ratio (.011 μm R_a Roughness, P_H = 1.02 GPa, $\bar{V}$ = 0.75 m/s).

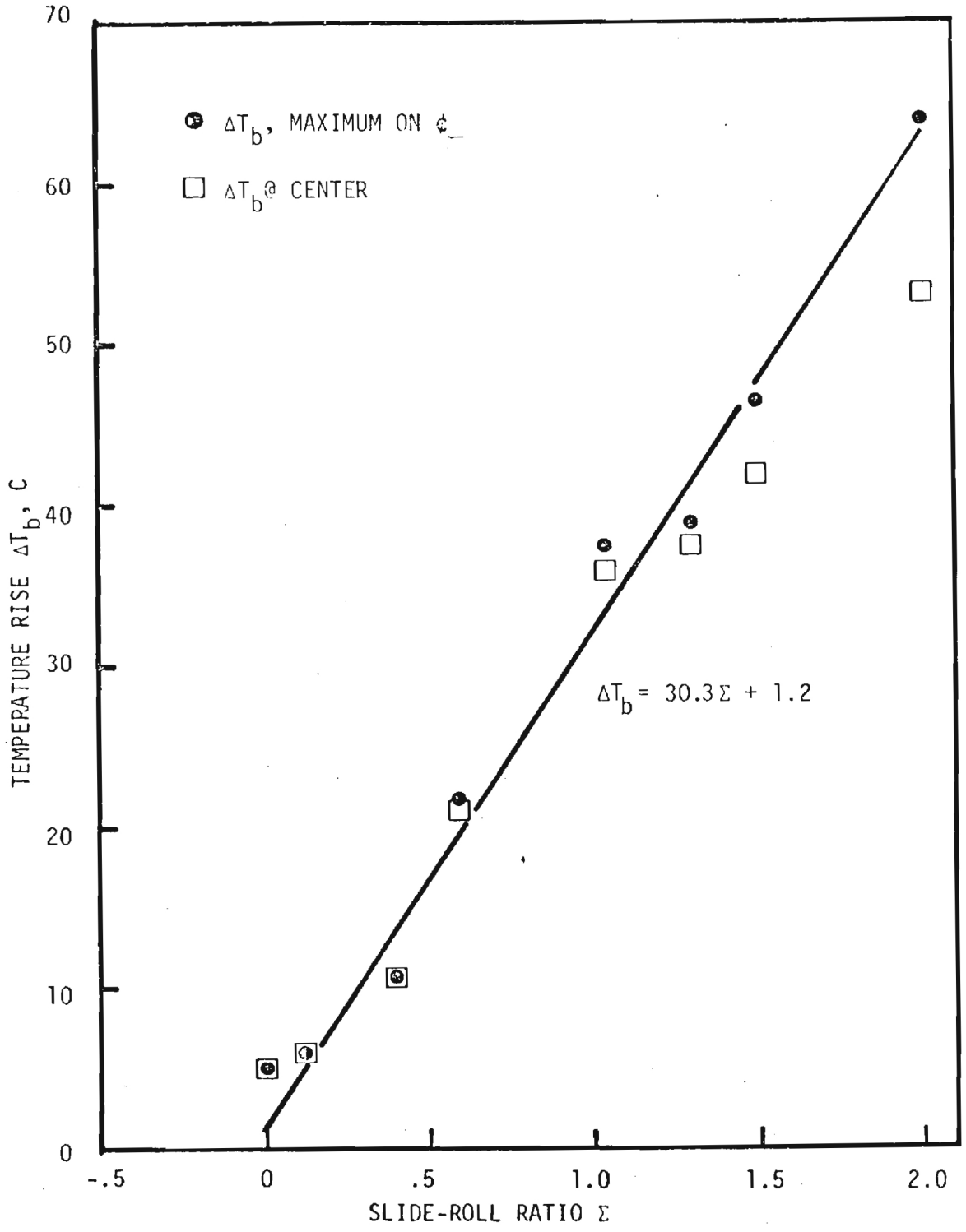

Figure 7. Ball Surface Temperature Rise as a Function of Slide-Roll Ratio (.011 μm R_a Roughness, P_H = 1.02 GPa, $\bar{V}$ = 1.0 m/s).

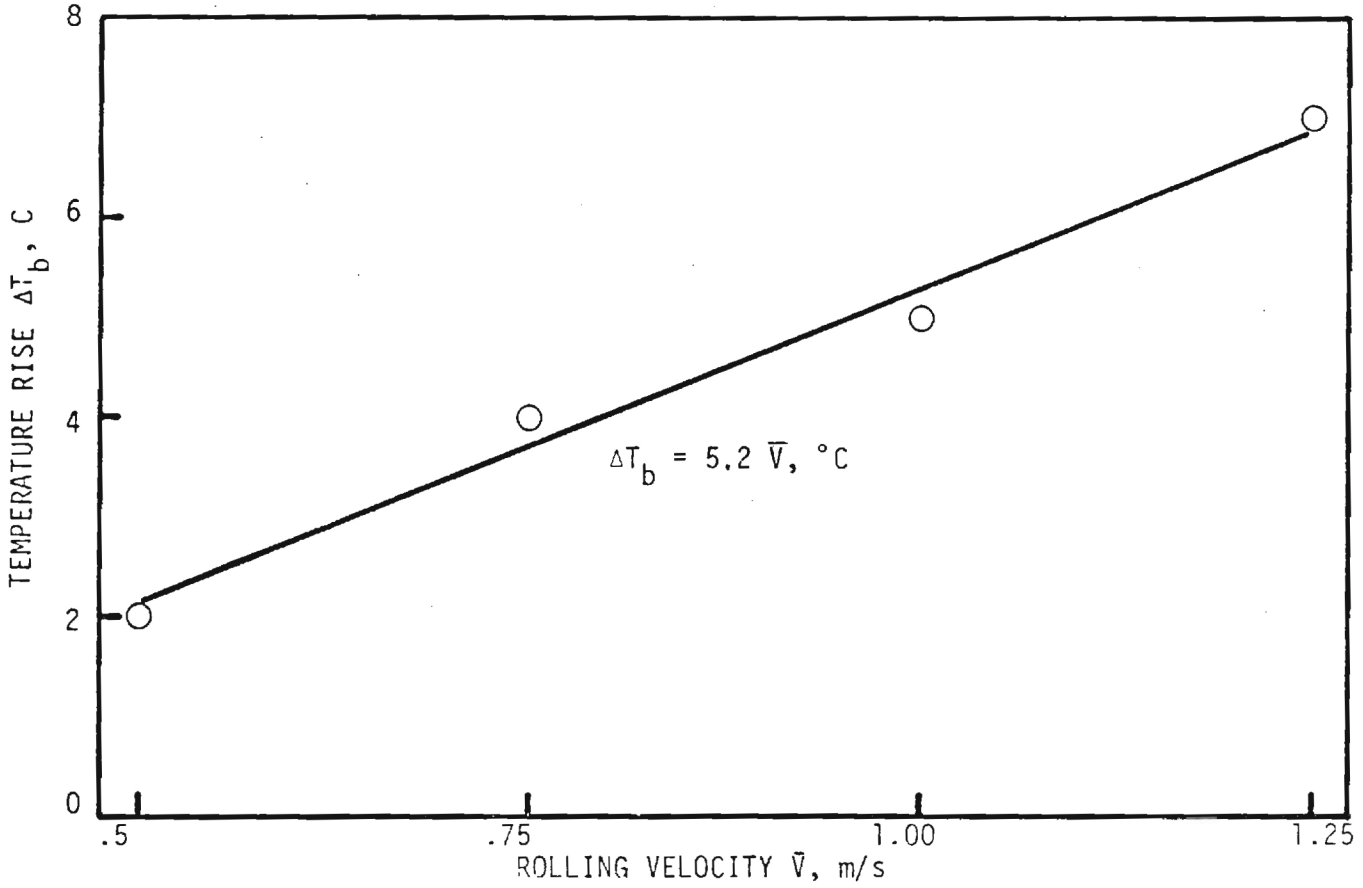

Figure 8. Ball Surface Temperature Rise as a Function of Rolling Velocity (.011 μm R_a Roughness, P_H = 1.02 GPa, Σ = 0, Maximum ΔT Occurs at Contact Center).

The variation of surface temperature rise with position in the EHD contact is shown in Figures 9 through 11 for slide-roll ratios in the range 0 to 2.0. The data for $\overline{V}$ = .75 m/s (Figure 9) and $\overline{V}$ = 1.00 m/s (Figure 10) are quite similar and the sliding results (Σ = 2.0) are in good agreement with the data reported in previous publications [3, 4]. It is interesting to note the small amount of inlet heating present under these conditions. For example, at 1.5 Hertz radii upstream of the contact center, the surface temperature is less than 5 C above the bath temperature. This relatively low value is consistent with the film temperature rise in the inlet predicted by Greenwood and Kauzlarich [9].

A second observation from Figures 9 and 10 is the movement of the peak in the temperature profile toward the exit as Σ is increased. Also, Figure 11, which contains only zero slip data, shows that the peak occurs near the contact center and the temperature at the inlet and exit contact boundaries are nearly equal. The trend toward a symmetric temperature distribution as Σ approaches zero is a result of the primary mechanism of heat generation changing from viscous shear when appreciable slip is present, to compression heating at $\Sigma \simeq 0$. Viscous shear results in a heat flux present throughout the contact region. If this flux were uniform, the ball surface temperature would continue to rise as it passed through the contact. The fact that the heat flux is very much greater at the contact center results in a temperature reduction as the exit boundary is approached. The faster the heat flux falls off, the lower the exit temperature should be. In the case of pure rolling, the viscous shear component is absent and the temperature rise is due to shear in the inlet and compressional heating. The latter term is a function of the pressure profile, which is nearly symmetric in the contact. The film and surface temperature should, therefore, rise and fall with pressure. Therefore, the trends shown in Figures 9 through 11 appear to be reasonable.

The flash temperature analysis of Blok [10], Jaeger [11], and Archard [12] discussed elsewhere [4], has been extended by Sanborn [1] to consider the influence of rolling by assuming that the viscous dissipation takes place in the fluid midplane, and that the remaining fluid merely conducts the heat to the adjoining surfaces. Sanborn has derived the following expression for the ball surface temperature rise

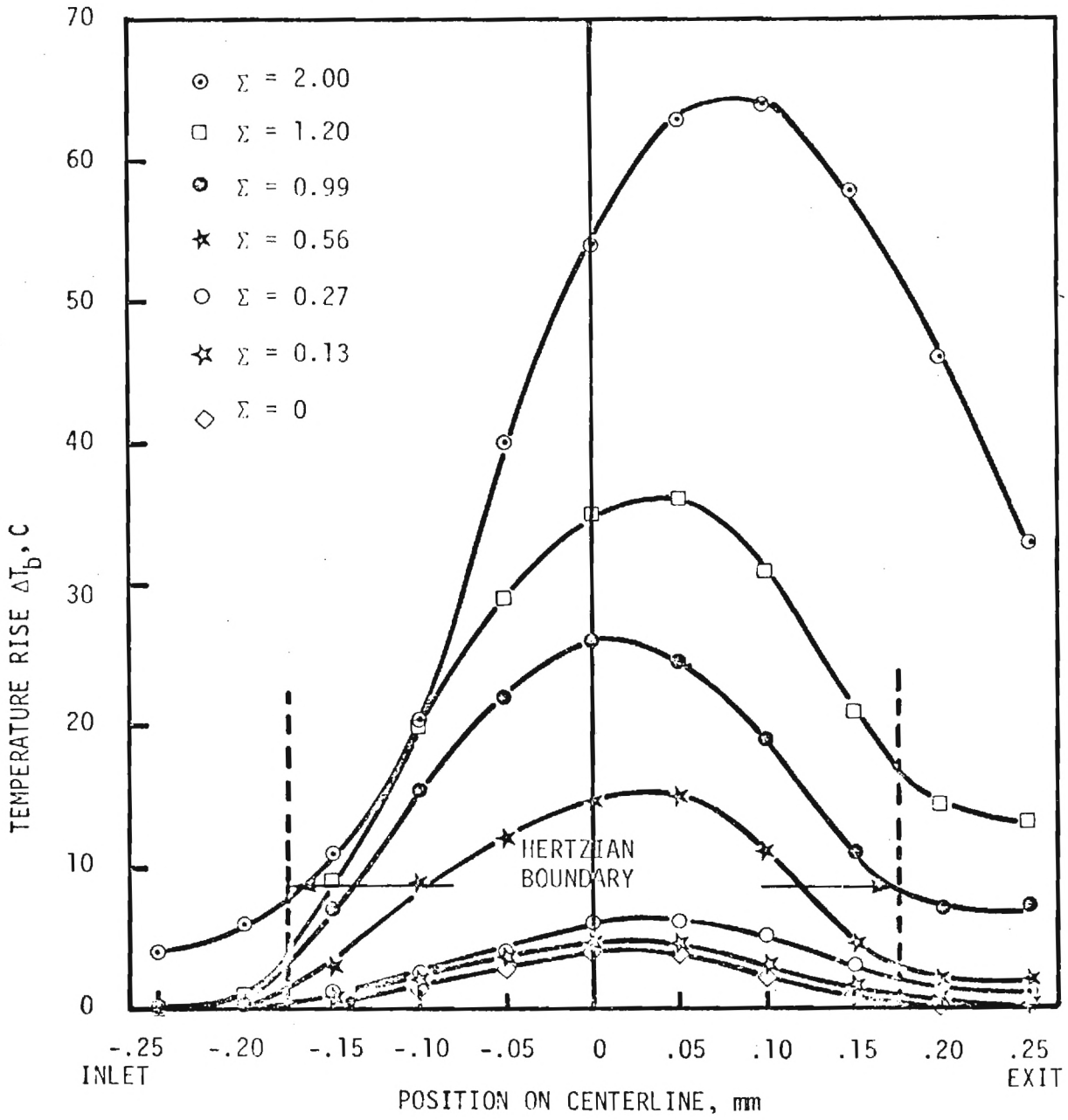

Figure 9. Ball Surface Temperature Rise Along the Contact Centerline (.011 μm R_a Roughness, P_H = 1.02 GPa, $\bar{V}$ = .75 m/s).

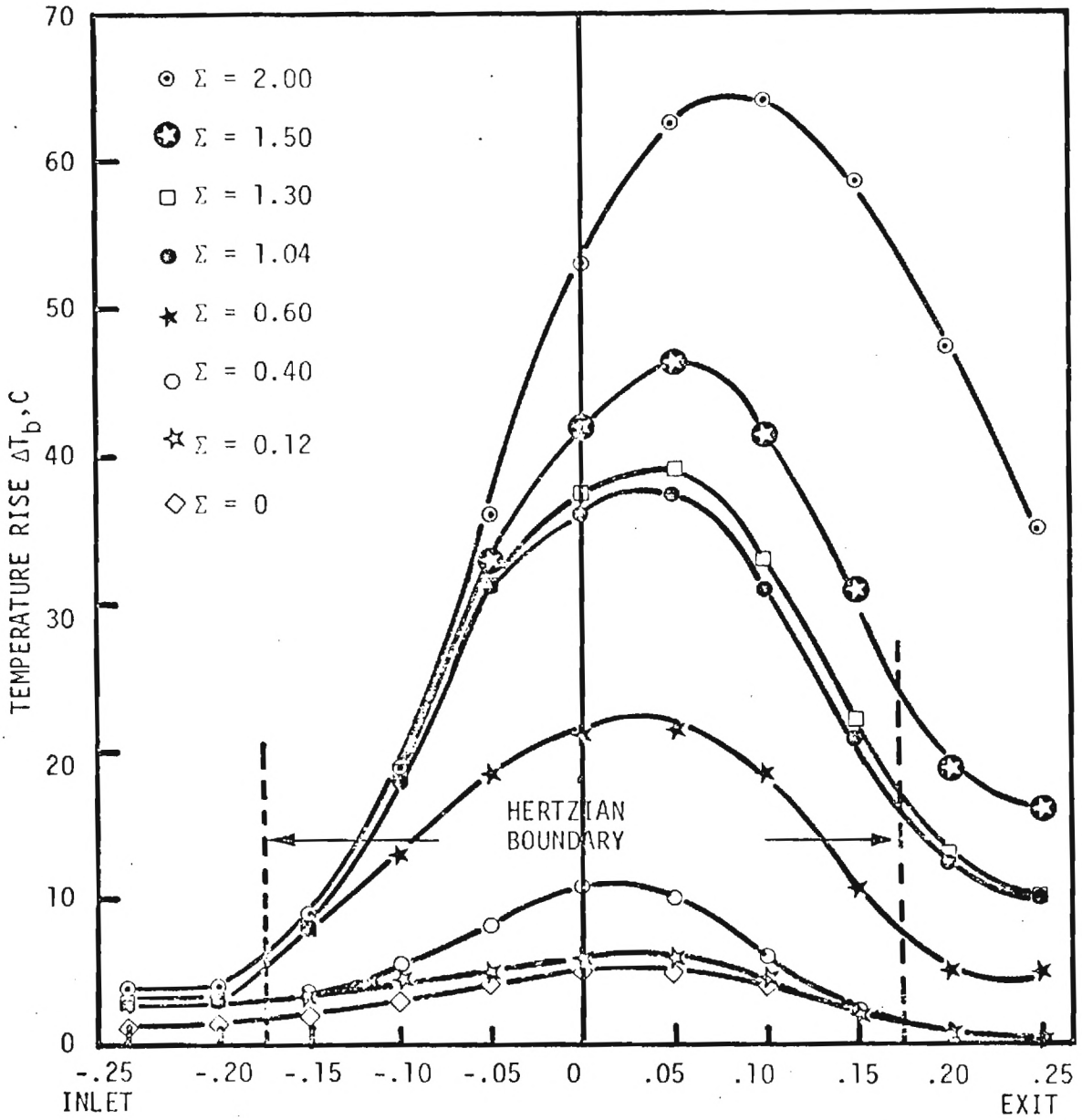

Figure 10. Ball Surface Temperature Rise Along the Contact Centerline (.011 μm R_a Roughness, P_H = 1.02 GPa, $\bar{V}$ = 1.00 m/s).

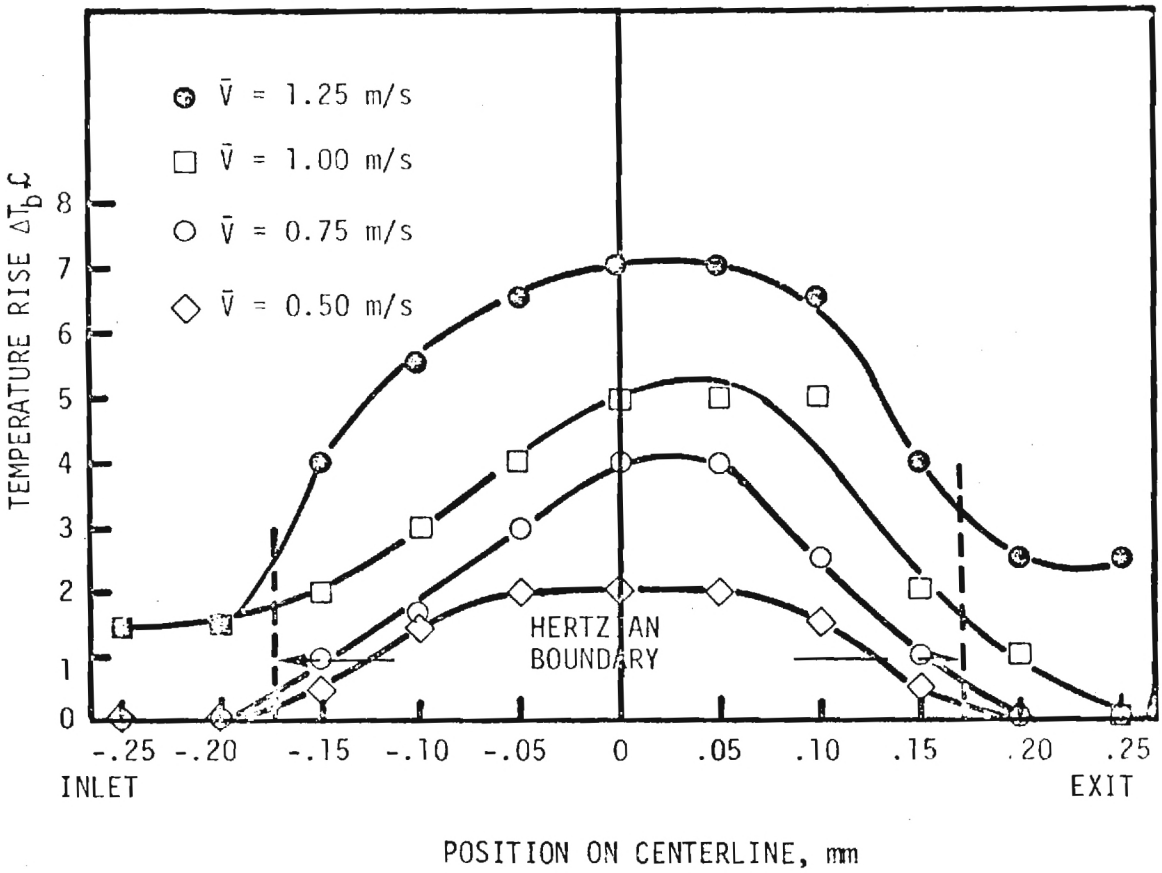

Figure 11. Ball Surface Temperature Rise Along Contact Centerline (.011 μm R_a Roughness, P_H = 1.02 GPa, Σ = 0).

$$\Delta T_b = \frac{\left(\frac{TC \cdot W \cdot V_s}{\pi a^2}\right)\left(\frac{h}{2k_f} + \frac{K_{sa}}{V_{sa}^{1/2}}\right) + (T_{osa} - T_{ob})}{1 + \frac{V_b^{1/2}}{K_b}\left(\frac{K_{sa}}{V_{sa}^{1/2}} + \frac{h}{2k_f}\right)} \qquad (3)$$

Reference [1] contains the derivation of equation (3).

Equation (3) has been evaluated for the materials used, and by using an average film thickness of 0.16 μm (Figure 2) at a load of 67 N. Considering the temperature rise during pure rolling (equation (2)), the ball surface temperature rise is given by

$$\Delta T_b = 5.2\,\bar{V} + \frac{66.7\ TC \cdot V_s}{\frac{V_{sa}^{1/2}}{5.8\,V_{sa}^{1/2} + 14.9} + \frac{V_b^{1/2}}{11.8}} \qquad (4)$$

Equation (4) has been evaluated using the conditions shown in Table 2 except for the conditions of simple sliding ($\Sigma = 2$, $V_{sa} = 0$). The simple sliding data was excluded because $L_{sa} = 0$, and therefore T_b and T_{sa} are likely to be considerably different resulting in the assumption of the adiabatic plane being at the center of the film being in error. The results are shown in Figure 12.

It should be remembered that the predicted temperature rise is the average over the contact area whereas the measured temperature rise is the maximum. From Figure 12, it is, therefore, clear that the predicted values of temperature rise are higher than the measured values.

There are a number of differences in the development of flash temperature theory and the conditions found in the experiments. First of all, the theory is based on a uniform heat flux over the contact area. The

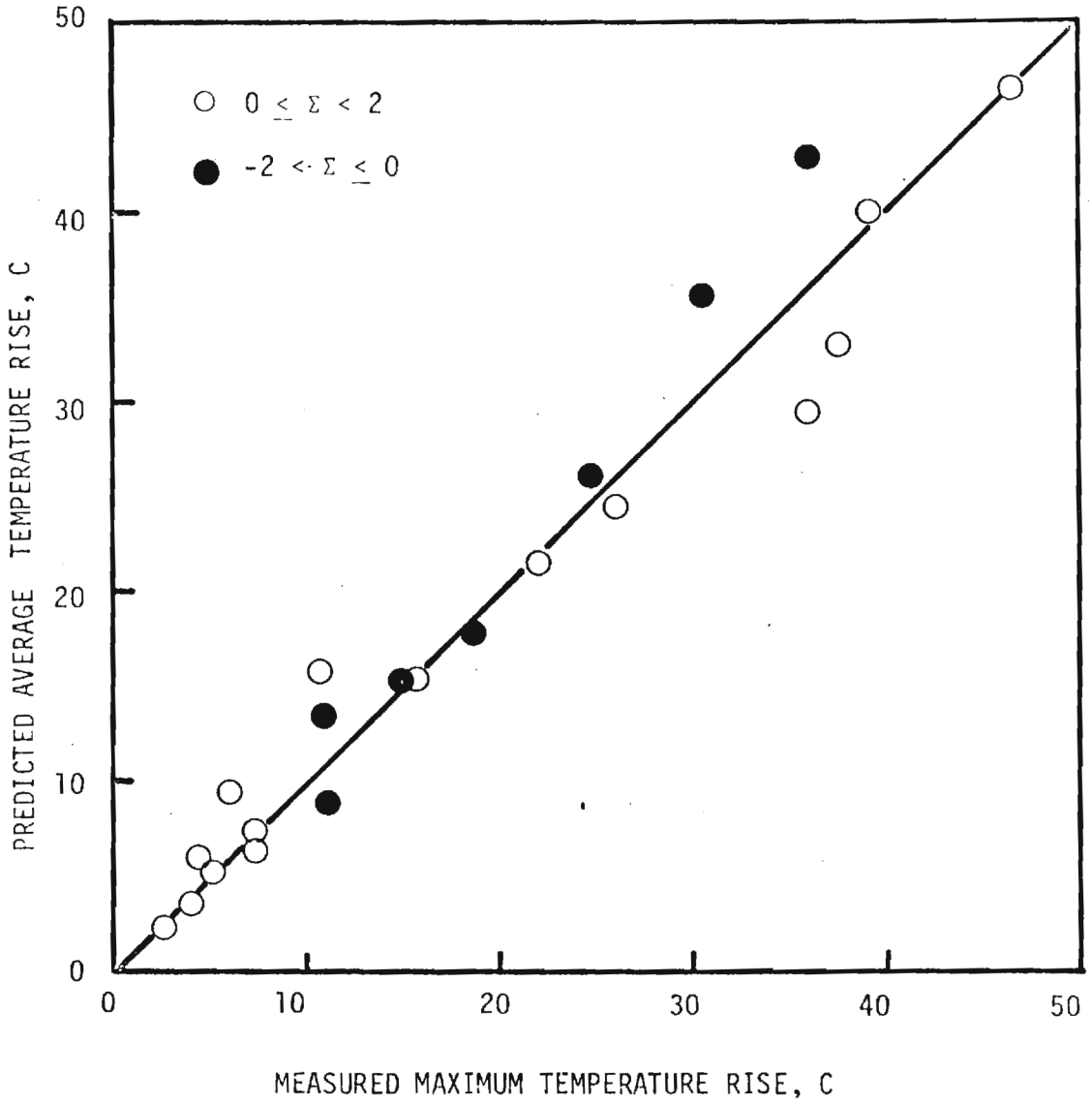

Figure 12. Comparison of Predicted Average and Actual Maximum Ball Surface Temperature Rises for L > 5.

heat flux distribution in the EHD contact is probably non-uniform with the maximum occurring near the center. Also because of differences in thermal diffusivities of the materials of the contact, the adiabatic plane of the fluid film may not occur at the film center. Finally, the theory assumes a semifinite solid with the free surface being adiabatic except under the concentrated heat flux. This is not consistent with the conditions of the experiment. The ball and sapphire surfaces outside the contact area are constantly flooded with lubricant. The agreement shown in Figure 12 should, therefore, be viewed cautiously.

Temperature Measurements for Negative Slide-roll Ratios

Ball surface temperatures for negative slide-roll ratio are discussed in this section. When the slide-roll ratio is -2, only the sapphire is moving and the ball surface is stationary and, therefore, the measured ball surface temperature corresponds to the stationary surface temperature. This technique, therefore, offers a way to measure stationary surface temperature. In the work reported previously [3, 4], the stationary surface temperature (i.e. sapphire surface temperature) was not measured because of the low emissivity of sapphire. However, since the thermal conductivity of the ball material is close to that of sapphire a knowledge of the stationary ball surface temperature will aid in estimating the stationary sapphire surface temperature.

Figure 13 shows the ball surface temperature at the contact center and its maximum value along the center line as a function of slide-roll ratio for a Hertz pressure level of 1.02 GPa and a constant rolling velocity of .75 m/s. The results for positive slide-roll ratio have been included in this figure for comparison. Asymmetry in the ball surface temperature about $\Sigma = 0$ can be observed. The slightly higher temperatures for negative slide-roll ratios are due to lower values of the ball speed. Similar data for a higher rolling speed of 1.0 m/s is shown in Figure 14. It can be noticed in both the figures that the stationary ball surface temperature ($\Sigma = -2$) is significantly higher than the moving ball surface temperature ($\Sigma = 2$).

Figure 15 shows the ball surface temperature distribution as a function of position on centerline at various negative slide-roll ratios, including the one for pure rolling. A constant load yielding a peak Hertz pressure of 1.02 GPa is used and the rolling velocity is held constant at .75 m/s. Figure 16 shows similar data but for a higher rolling speed of 1.0 m/s. Figures 9 and 10 can be compared with Figures 15 and 16. Even though the temperature distributions are similar, the values are slightly higher for negative slide-roll ratios. It is rather interesting to note the movement of the position of peak temperature as the slide-roll ratio is varied. The peak is at the center for pure rolling. For slide-roll ratios increasing

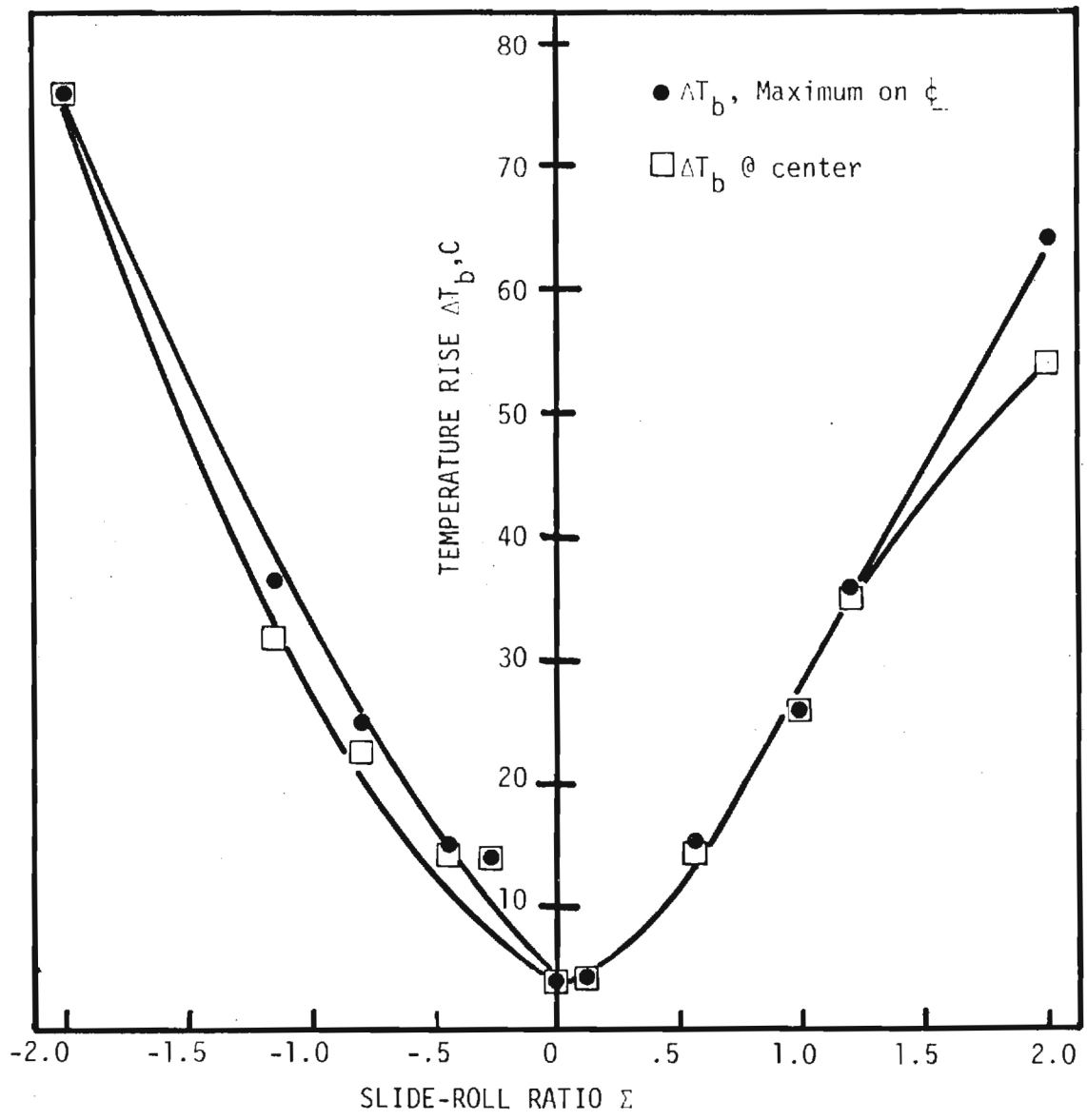

Figure 13. Ball Surface Temperature Rise as a Function of SLIDE-ROLL RATIO (-2 to +2) (Smooth ball ⇒ .011 μm Ra, P_H = 1.02 GPa, $\bar{V}$ = .75 m/s).

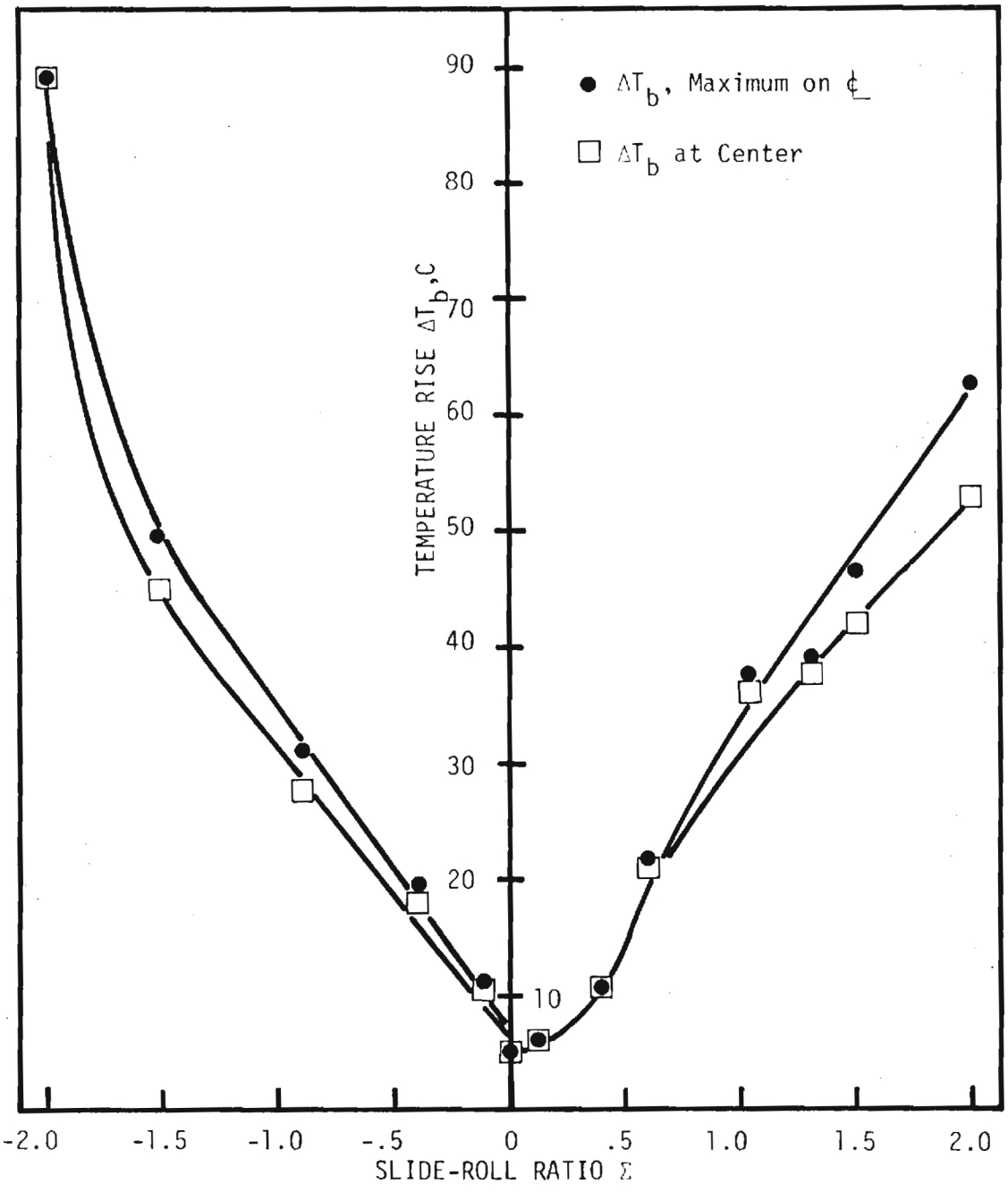

Figure 14. Ball Surface Temperature Rise as a Function of Slide-Roll Ratio (Smooth ball ⇒ .011 μm Ra, P_H = 1.02 GPa, $\bar{V}$ = 1.0 m/s).

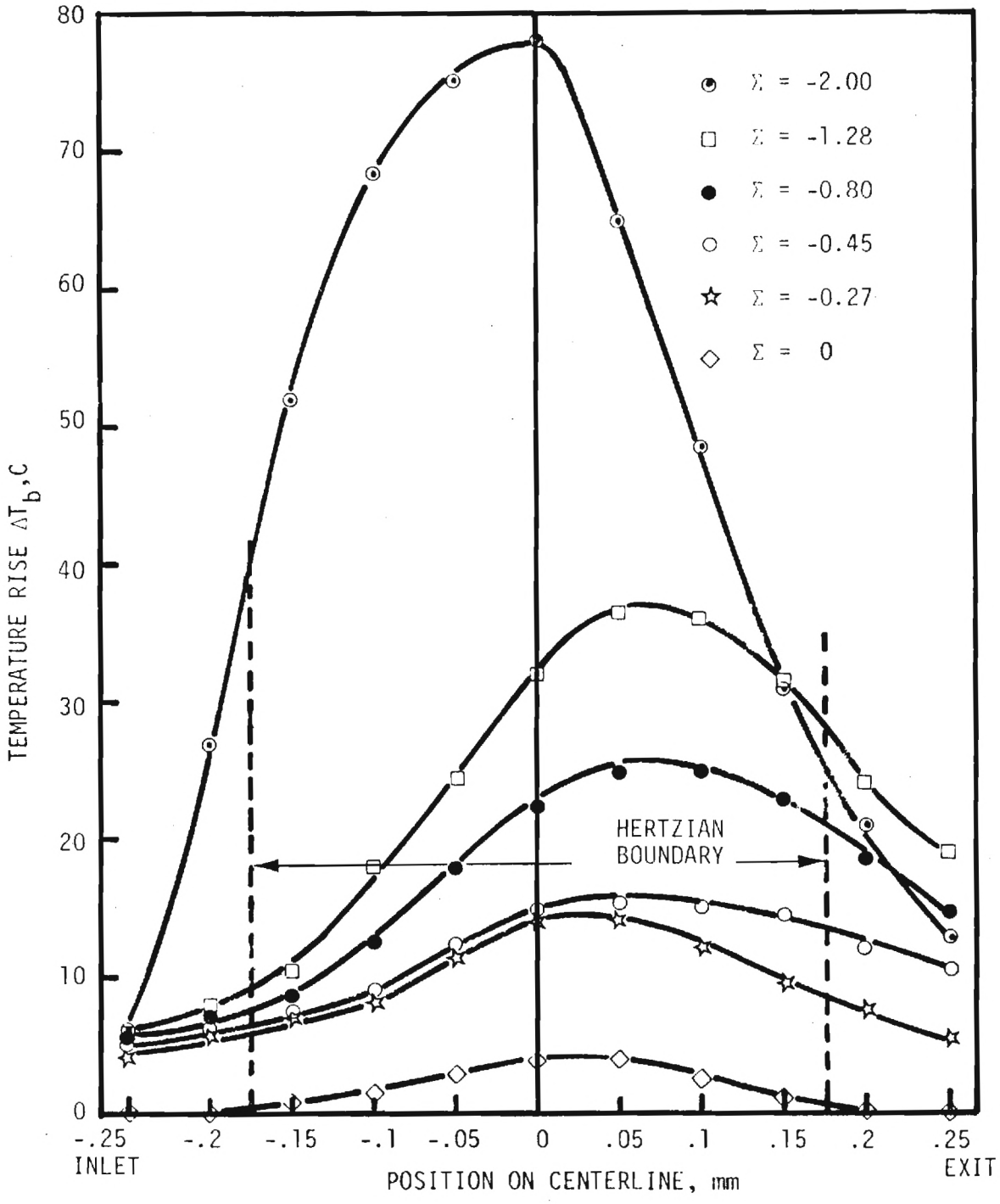

Figure 15. Ball Surface Temperature Rise along the Contact Centerline (Smooth ball => .011 μm Ra, P_H = 1.02 GPa, $\bar{V}$ = .75 m/s.)

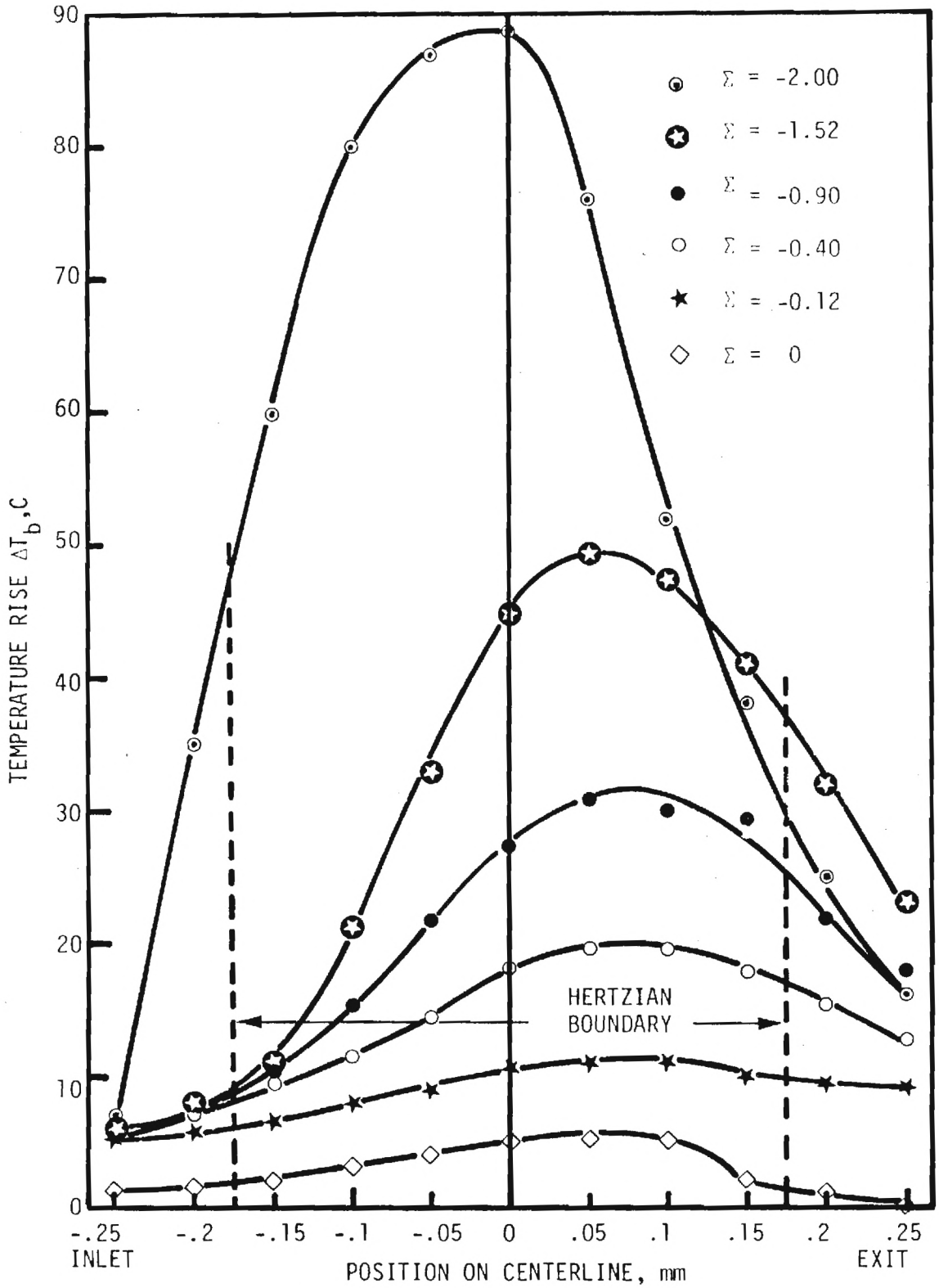

Figure 16. Ball Surface Temperature Rise along the Contact Centerline (Smooth ball ⇒ .011 μm Ra, P_H = 1.02 GN/m^2, $\bar{V}$ = 1.0 m/s).

negatively, the peak occurs slightly beyond the center towards the exit. This behavior is because of a change in the heat generation mechanism from compressional heating at pure rolling to significant viscous heating at higher values of slip. This is similar to the trend observed for positive slide-roll ratios. However, the position of peak temperature for $\Sigma = -2$, is at the center of the contact. Ball surface being stationary in this case, has a maximum temperature rise at contact center where the heat flux has a maximum intensity.

In addition to the results shown above, stationary ball surface temperature was measured at a peak Hertz pressure level of 1.02 GPa, for speeds ranging from 0.82 to 2.58 m/s. The results are summarized in Table 3. A linear regression analysis of the temperature rise with speed yielded

$$\Delta T_b = 58.6\ V_{sa}^{0.62} \tag{5}$$

with a correlation coefficient of 1.0.

It is interesting to note that the exponent 0.62 on V_{sa} in equation (5) compares well with the exponent on speed in the low speed case given in equation (8) of reference [4]. This means that the stationary heat source theory applicable for $L < .1$, can also predict the trend in stationary surface temperatures. The bath temperature does not represent the bulk temperature in the present case, since the ball is not rotating. However, the bulk temperature for this case was determined by measuring the ball surface temperature two to three Hertzian diameters before the contact.

The flash temperature analysis discussed earlier can also be applied to negative slide-roll ratios, because individual surface velocities were used. This analysis however, cannot be applied to stationary

Table 3 Summary of Stationary Ball Surface Temperature Measurement

(Smooth ball: .011 μm R_a, Fluid N1, P_H = 1.02 GPa)

V_b	V_{sa} (= V_s)	T_{bath}	T_b @ Center (= $T_{b,max}$)	ΔT_b ($T_b - T_{bulk}$)*
m/s	m/s	C	C	C
0	.82	28	92.5	50.5
0	1.20	28	108	66
0	1.24	28	109.5	67.5
0	1.50	28	118	76
0	1.70	28	125	83
0	1.85	26	128	86
0	1.98	26	131	89
0	2.58	28	146	104

*T_{bulk} ≈ 42 C for all the experiments (T_{bulk} = T_b two to three Hertzian diameters before the contact).

surface temperature calculation since the assumption of mid-plane film temperature being the maximum is not valid in this case. This situation is similar to the case when $\Sigma = 2$, where again a similar assumption was not valid. The ball surface temperature rise calculated using equation (4) for negative slide-roll ratios is shown plotted (as shaded circles) versus measured temperature rise in Figure 12. The predicted values are again higher than the measured values. Probable reasons for this discrepancy have already been cited.

CONCLUSIONS

Moving surface temperature measurements in rolling and sliding EHD contacts have been made using an available infrared technique. Film thickness and traction have also been measured. Slide to roll ratios of -2 to +2 have been studied. By using a different kinematic configuration (ball stationary and only the sapphire moving), stationary surface temperatures have also been measured. It has been shown that while surface temperature rises in the low slip region are relatively small, stationary surface temperatures are significantly higher than the moving surface temperatures.

Flash temperature theory has been extended to cover the combined rolling and sliding conditions. Measured surface temperatures are lower than the predicted values. The reasons for the apparent discrepancy are believed to be due to a number of differences in the development of flash temperature theory and the conditions found in the experiments.

ACKNOWLEDGMENTS

This research was supported by NASA-Lewis (NGR-11-002-133) and the National Science Foundation (ENG 74-21002). The continuing encouragement of and helpful discussions with Dr. L. Wedeven of NASA-Lewis are greatly appreciated. The authors also wish to thank Mr. Scott Bair of Georgia Tech for the design and construction of much of the necessary equipment.

REFERENCES

1. Alsaad, M. A., Kunz, R. K., Nagaraj, H. S., Bair, S. S., Rentzepis, G. M., Sanborn, D. M., and Winer, W. O., "Investigations of Lubricant Rheology as Applied to Elastohydrodynamic Lubrication," NASA CR-2837, May 1977.

2. Turchina, V., Sanborn, D. M., and Winer, W. O., "Temperature Measurements in Sliding Elastohydrodynamic Point Contacts," Trans. ASME, Journal of Lubrication Technology, Vol. 96, Ser. F, No. 3, July 1976, pp. 464-671.

3. Ausherman, V. K., Nagaraj, H. S., Sanborn, D. M., and Winer, W. O., "Infrared Temperature Mapping in Elastohydrodynamic Lubrication," Trans. ASME, Journal of Lubrication Technology, Vol. 98, Ser. F, No. 2, April 1976, pp. 236-243.

4. Nagaraj, H. S., Sanborn, D. M., and Winer, W. O., "Effect of Load, Speed and Surface Roughness on Sliding EHD Contact Temperatures," Trans. ASME, Journal of Lubrication Technology, Vol. 99, Ser. F, No. 2, April 1977 pp. 254-263.

5. Sanborn, D. M., and Winer, W. O., "Fluid Rheological Effects in Sliding Elastohydrodynamic Point Contacts with Transient Loading: I - Film Thickness," Trans. ASME, Journal of Lubrication Technology, Vol. 96, Ser. F, No. 3, July 1971, pp. 464-471.

6. Wedeven, L. D., "Traction and Film Thickness Measurements under Starved Elastohydrodynamic Conditions," Trans. ASME, Journal of Lubrication Technology, Vol. 97, Ser. F, No. 2, April 1975, pp. 321-329.

7. Foord, C. A., Wedeven, L. D., Westlake, F. J., and Cameron, A., "Optical Elastohydrodynamics," Proceedings of the Institution of Mechanical Engineers, Vol. 184, Part 1, 1969-70.

8. Nagaraj, H. S., "Investigation of Some Temperature Related Phenomena in Elastohydrodynamic Contacts Including Surface Roughness Effects," Doctoral Dissertation, Georgia Institute of Technology, Dec. 1976. and University Microfilms, Ann Arbor, Michigan 1977.

9. Greenwood, J. A., and Kauzlarich, J. J., "Inlet Shear Heating in Elastohydrodynamic Lubrication," Trans. ASME, Journal of Lubrication Technology, Vol. 95, Ser. F, No. 4, Oct. 1973, pp. 417-426.

10. Blok, H., "Surface Temperatures Under Extreme-Pressure Lubricating Conditions," Second World Petroleum Conference, Paris, June, 1937, Vol. 3, Section 4.

11. Jaeger, J. C., "Moving Sources of Heat and the Temperature at Sliding Contacts," Proc. Roy. Soc. N.S.W., Vol. 56, 1942, p. 203.

12. Archard, J. F., "The Temperature of Rubbing Surfaces," Wear, Vol. 2, No. 6, Oct. 1959, pp. 438-455.

. Presented at the ASME/ASLE Lubrication Conference
Boston, Massachusetts, 5-7 October 1976
(JOLT, Vol. 99, No. 2, April 1977)

Reprinted from the JOURNAL OF LUBRICATION TECHNOLOGY, *Vol. 99, No. 2, April 1977*

H. S. Nagaraj[1]
Graduate Student.

D. M. Sanborn
Associate Professor.

W. O. Winer
Professor.

Georgia Institute of Technology,
School of Mechanical Engineering, Atlanta, Ga.

Effects of Load, Speed, and Surface Roughness on Sliding EHD Contact Temperatures

An infrared technique has been used to determine the effects of load, speed and surface roughness on temperature in a sliding EHD point contact. Ball surface temperatures are reported for sliding speeds of 0.35 to 5.08 m/s at 0.52 to 2.03 GN/m² maximum pressure with surface roughness in the range 0.01 to 0.38 μm c.l.a. The relationship between asperity interaction, as measured by relocation surface profilimetry and high frequency temperature measurements, and the ratio of film thickness to surface roughness has also been studied.

Introduction

Elastohydrodynamic lubrication has been recognized as an important mode of lubrication especially for nonconformal machine elements. Considering both the present and anticipated design requirements for operating speeds and loads, a deeper and a more complete knowledge of EHD contact behavior is needed. Whereas most of the previous investigations in EHD lubrication were concerned with the formation of an adequate fluid film, more studies are needed into the mechanisms causing a break down of this protective film.

The transition from an adequately lubricated system to an inadequately lubricated one is well defined and provides the experimental basis of Blok's [1][2] critical temperature hypothesis. All transitions from one lubrication regime to another are not necessarily detrimental. As was found in both the work being presented, and that by Hirst and Stafford [2], transitions from EHD to boundary lubrication usually do not result in severe wear and high traction. This transition is characterized primarily by asperity interaction rather than gross amounts of material removal or transfer.

The frictional energy dissipation resulting from this transition causes high temperature levels in the vicinity of the contacting surfaces. These temperatures are referred to as flash temperatures. On the other hand, the overall heat transfer characteristics of the system primarily influence the bulk temperatures. Several theories exist for predicting the flash temperatures of rubbing solids. The early theory of Blok [3] in 1937 has been put on a rigorous basis by Jaeger [4] in 1942. More recently, Archard [5] has given a graphical procedure for determining flash temperatures. Recognizing the importance of such a failure criteria, the AGMA [6] recommended a gear scoring criteria in 1964.

[1] Presently, Mechanical Technology Inc., Latham, N.Y.

Contributed by the Lubrication Division and presented at the Joint Lubrication Conference, Boston, Mass., October 5-7, 1976, of THE AMERICAN SOCIETY OF MECHANICAL ENGINEERS. Manuscript received by the Lubrication Division, March 15, 1976; revised manuscript received June 14, 1976. Paper No. 76-Lub-23.

[2] Numbers in brackets designate References at end of paper.

Nomenclature

a = Hertzian contact radius, m
c = specific heat, $J/(kg\,K)$
h = film thickness, m
k = thermal conductivity $W/(mK)$
$L = t_1/t_2$, nondimensional time parameter
P = pressure, N/m^2
q = heat flux, $W/(sm^2)$
R^2 = coefficient of determination in regression analysis
T = temperature, C
TC = traction coefficient
t_1 = thermal diffusion time, s
t_2 = characteristic resident time, s
V_{Hp} = sliding velocity at break-point for $\Delta T = f(P_H)$, m/s
V = sliding velocity, m/s
W = normal load, N
$\alpha = k/\rho c$, thermal diffusivity, m^2/s
ΔT = temperature rise above bulk oil temperature, C
η = viscosity, Ns/m^2
Λ = ratio of film thickness to composite surface roughness
ρ = density, kg/m^3
$\sigma = \sqrt{\sigma_b^2 + \sigma_s^2}$, composite surface roughness, m

Subscripts

b = ball surface
c = contact center value
f = fluid
H = Hertzian conditions
s = sapphire
st = steel

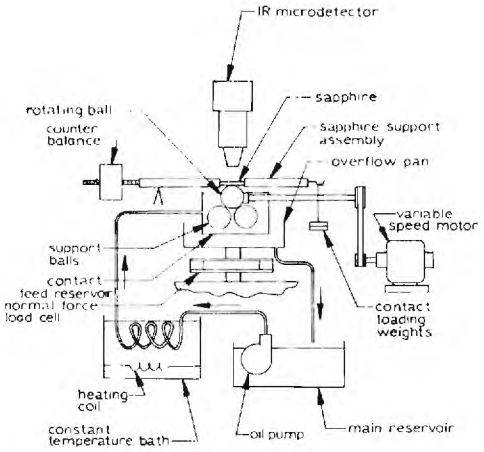

Fig. 1 Sliding EHD test apparatus

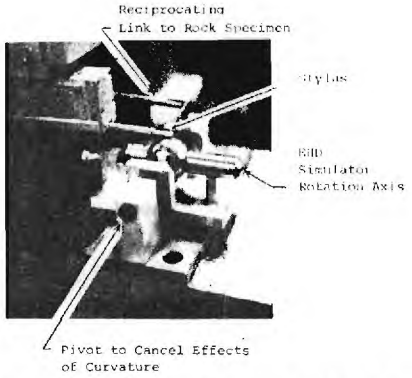

Fig. 2. Surface profilimeter and specimen relocation apparatus

It was the purpose of the work reported in this paper to use an available infrared temperature measurement technique to measure peak surface temperatures of sliding EHD contacts as the operating conditions became more severe. The severity of the conditions is controlled by increasing load, speed and surface roughness. The validity of the flash temperature concept and Λ (the ratio of film thickness to composite surface roughness) as failure criteria is checked by comparison with experimental results.

Experimental Apparatus and Technique

The EHD equipment (Fig. 1) used in all the following measurements is basically the same as reported previously [7, 8, 9]. The sliding EHD contact is formed using a 31.8 mm diameter chrome steel (AISI 52100) ball rotating and loaded against a sapphire flat 1.6 mm thick. The infrared radiation emitted at this contact is measured with an infrared radiometric detector having a spot size resolution of 38 μm with a 15x objective and a response time of 8 μ-s in the A.C. mode of operation. It was necessary to monitor the oil reservoir temperature with a thermocouple and to hold it constant with a constant temperature bath and an oil circulation system.

The measuring system used for surface profile measurements is shown in Fig. 2 with a specimen rotation attachment and a relocation stage fitted to the instrument. Because of the curvature of the ball surface, it was necessary to modify the standard system to allow measurements over an adequate arc length at high vertical magnification. This has been accomplished by rotating the ball about its axis under a fixed stylus.

A relocation mechanism is incorporated in the rotation attachment. In order to detect any change in the surface profile, it is necessary to measure the profile at precisely the same point on the ball surface before and after being used in the EHD contact. Four of the possible six degrees of freedom are removed by using a pair of V-blocks to support the ball by two cylindrical collars cemented to the ball surface. The centerlines of the collars and ball are made as nearly coincident as possible. Since one of the collars is used to rotate the ball in the EHD contact simulator, the plane containing the wear track will be normal to this center line. The other two degrees of freedom are removed by providing stops to limit motion along the axis of rotation and the amount of rotation about this axis.

Chromium steel balls (AISI 52100) of three different roughness values have been used to study the effects of surface roughness. The c.l.a. values are 0.011, 0.075 and 0.381 μm and are referred to as smooth, medium rough and rough, respectively. These balls were finished by the standard grinding process and did not have any preferred orientation of the roughness pattern. Because of the high loads and relatively rough surfaces used in this study, it was not possible to accurately measure film thickness by an optical technique. Unfortunately, the fluid temperature can not be obtained without an accurate film thickness distribution and it can not be assumed that the film thickness values for the smooth ball are the same as those for

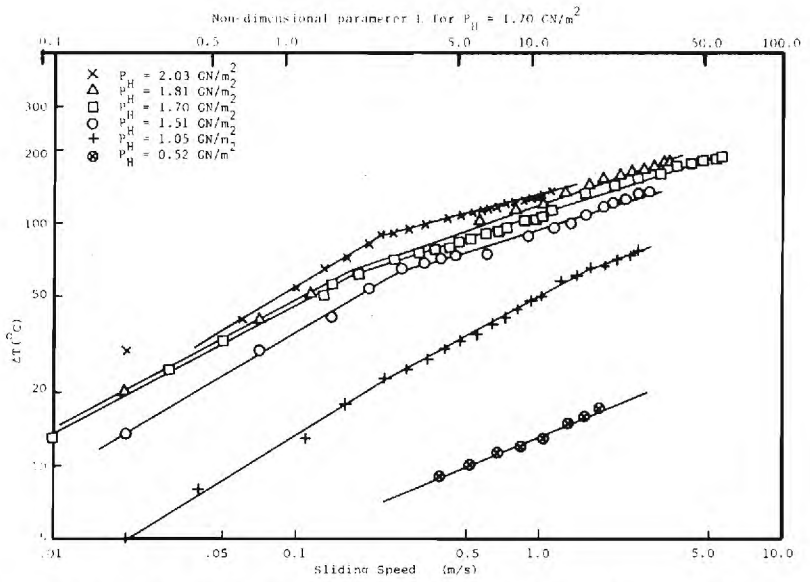

Fig. 3. Ball surface temperature rise at contact center, smooth ball (0.011 μm c.l.a.) $1 < \Lambda$ for $P_H = 2.03$ GN/m^2, otherwise $\Lambda > 2$

the rough ball under such severe conditions. Therefore only ball surface temperatures were measured.

The technique for measuring the ball surface temperature distribution in the contact has been described earlier [8]. Ball surface temperature measurements are made only at the center for the case of smooth and medium rough balls. The center of the EHD contact is easy to locate and also, the temperature at this location is quite close to the maximum [8, 9]. In the experiments with the rough ball, the temperature measured is the maximum in the contact, whether or not it occurs at the contact center. It was necessary to make this procedural change because the contact center could not be located when the rough ball was used. This is due to the disappearance of the interference fringe pattern because of light scattering at the relatively large surface asperities. Therefore the contact was scanned for the maximum surface temperature in each case.

The fluid used throughout this investigation is a naphthenic base oil designated N1 in previous studies. A complete description of the fluid is given in appendix of reference [10].

Ball Surface Temperature Measurements Under Severe Conditions

As mentioned above, temperature measurements were taken only or near the center of the Hertzian contact. This temperature is near the maximum and is, therefore, representative of the most severe conditions in the EHD contact.

Fig. 3 shows a plot of the ball temperature rise at the contact center above the bath temperature, as a function of sliding velocity for peak Hertz pressures ranging from 0.52 to 2.03 GN/m^2. For a given Hertz pressure, the data plotted on log-log coordinates falls on one straight line for velocities up to a break-point value and then on another line, of lower slope, for higher velocities. This same data has been replotted at selected velocities as a function of Hertz pressure in Fig. 4. The temperature rise is the difference between the ball surface temperature at the contact center and the lubricant bath temperature as measured with a thermocouple. Fig. 4 shows that except for the combined conditions of relatively high velocity and Hertz pressure, the data for a given speed follows a power law model with an exponent on Hertz pressure of approximately 2.

The trends shown in Figs. 3 and 4 can be predicted using the techniques of Jaeger [4] and Archard [5]. The energy dissipation rate in the contact is equal to the product (W·TC·V). The heat flux to each surface is then proportional to the dissipation rate divided by the area of the contact, or

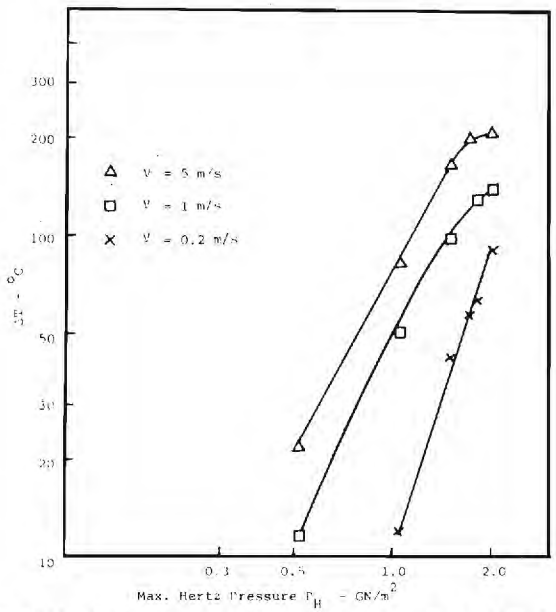

Fig. 4 Surface temperature use at contact center versus maximum Hertz pressure, smooth ball (0.011 μm c.l.a.)

Table 1 Summary of comparison of measured temperatures and those predicted by the Blok-Jaeger-Archard theory for the smooth ball (0.011 μm c.l.a.).

P_H (GN/m^2)	V (m/s)	Traction coefficient	Avg. calculated temperature (°C)	Measured center temperature (°C)	Avg. measured temperature (°C)
2.03	1.0	0.07[a]	158	172	—
1.81	1.0	0.07[a]	137	167	—
1.70	0.05	0.07[a]	40	60	—
	1.0	0.07[a]	129	154	—
	2.54	0.07[a]	198	202	—
1.51	0.70	0.07	98	124	109
	1.0	0.07[a]	111	136	—
	1.39	0.07	128	147	131
	2.54	0.06	156	175	156
1.05	0.35	0.16	77	65	58
	0.70	0.13	98	81	68
	1.39	0.07	92	100	81
	2.54	0.06	101	118	90
	5.08	0.04	104	120	93

[a] Assumed value based on similar conditions

$$\bar{q} \propto \frac{W \cdot TC \cdot V}{\pi a^2} \propto TC \cdot P_H \cdot V \tag{1}$$

However, for Hertz pressures ≥ 1.5 GN/m^2, the traction coefficient is essentially constant as shown in Table 1.

$$\bar{q} \propto P_H \cdot V \tag{2}$$

According to Jaeger [4] and Archard [5] the temperature rise on the surface of a solid moving at velocity V and subjected to heat flux $\bar{q}$ can be described in terms of a nondimensional parameter $L = t_1/t_2$. The term $t_1 = a^2/2\alpha_b$ represents the time required for the effect of $\bar{q}$ to penetrate a distance a below the surface, whereas $t_2 = a/V$ represents the time required for a point in the contact to move a distance a. Therefore, for a given fluid, L is proportional to (P_H·V). The variation in ΔT (ball surface temperature—bulk oil temperature) is given as [4, 5]

$$\Delta T \propto P_H L \text{ for } L < 0.1 \tag{3}$$

and

$$\Delta \propto P_H L^{1/2} \text{ for } L > 100 \tag{4}$$

or that

$$\Delta T \propto P_H{}^2 V \text{ for } L < 0.1 \tag{5}$$

and

$$\Delta T \propto P_H{}^{3/2} V^{1/2} \text{ for } L > 100 \tag{6}$$

The conditions during the experiment were such that L is somewhere near the middle of these two extremes. From Figs. 3 and 4 it can be seen that the predicted trends agree favorably with experimental results. For $P_H = 1.70$ GN/m^2, the parameter L is also shown in Fig. 3.

In order to determine how well the data fits the Jaeger-Archard predictions of equations (5) and (6), a multiple regression analysis of the data shown in Fig. 3 was performed. For each Hertz pressure level, the data were divided into two regions separated by a break-point velocity. This break-point velocity is a function of Hertz pressure and can be described by

$$V_{BP} = 1.564\, P_H{}^{-3.22} \tag{7}$$

with a coefficient of determination $R^2 = 0.87$. For sliding velocities below V_{BP},

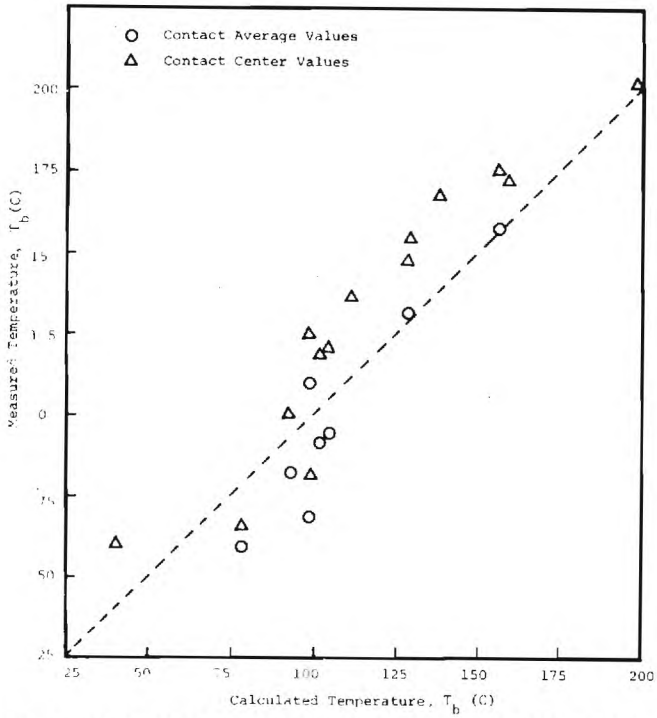

Fig. 5 Comparison of average contact temperatures calculated using the Blok-Jaeger-Archad theory and measured temperatures, smooth ball (0.011 μm c.l.a.)

$$\Delta T = 46.99\, P_H^{2.02} V^{0.53} \tag{8}$$

with $R^2 = 0.978$. For velocities above V_{BP},

$$\Delta T = 53.52\, P_H^{1.34} V^{0.34} \tag{9}$$

with $R^2 = 0.985$. In terms of normal load, equations (8) and (9) may be approximated by

$$\Delta T \simeq 3W^{2/3} V^{1/2} \text{ for } V \leq V_{BP} \tag{10}$$

and

$$\Delta T \simeq 8.5 W^{4/9} V^{1/3} \text{ for } V \geq V_{BP} \tag{11}$$

From Fig. 3, it can be seen that the measurements lie in the region from $L = 0.13$ to 50, which corresponds to the intermediate region mentioned by Archard [5]. It would be reasonable to expect, therefore, from equations (5–6) that the theoretical exponent of P_H should be in the range 2 to ⅔ and that of velocity should be in the range 1 to ½ (with increasing L).

For both the low speed and high speed regimes, the agreement with respect to load dependence is very good, whereas the dependence on velocity is not in satisfactory agreement. It should be noted, however, that the exponents in Archard's model were determined assuming a constant traction coefficient. Previous experiments with the same fluid [11] show that when all of the data of Fig. 3 are considered, the traction coefficient varies considerably. If the traction coefficient itself were dependent on velocity to the power − ½ to − ⅙, as speed increases, the agreement between the experimental results and Archard's theory would be excellent. Previous measurements [11] show almost no dependence of TC on W, but a dependence on velocity to the power −0.40 at $L = 5$ and −.28 at $L = 20$. It must be concluded, therefore, that if the variation in traction coefficient is taken into account, that the trends predicted by flash temperature theory are in good agreement with the experimental results obtained. It should be noted, however, that the measurements are of contact center values, whereas the theoretical values are average temperatures in the contact. Since the relative shape of the ball surface temperature distribution does not change appreciably with load and speed, this difference is not likely to be significant.

In addition to a comparison of trends with P_H and V, a comparison of ball surface temperatures, calculated using the method outlined by Archard [5], and the experimental results has been made and the results are summarized in Fig. 5. The measured values are either the temperature at the contact center, when only those temperatures were recorded, or the average of the temperatures in the Hertzian contact area. A regression analysis of measured temperatures on calculated temperatures resulted in a coefficient of determination of 0.85. Table 1 shows these temperatures as functions of peak Hertz pressure and sliding velocity.

It should be noted that the calculated temperatures were obtained by adding the bath temperature, as measured with a thermocouple, to the calculated temperature rise. The measured values, however, whether the center line or contact average temperatures, are the values which result directly from the experimental data reduction for the cases where traction measurements were made. The measured values should be somewhat higher than the calculated values since both the

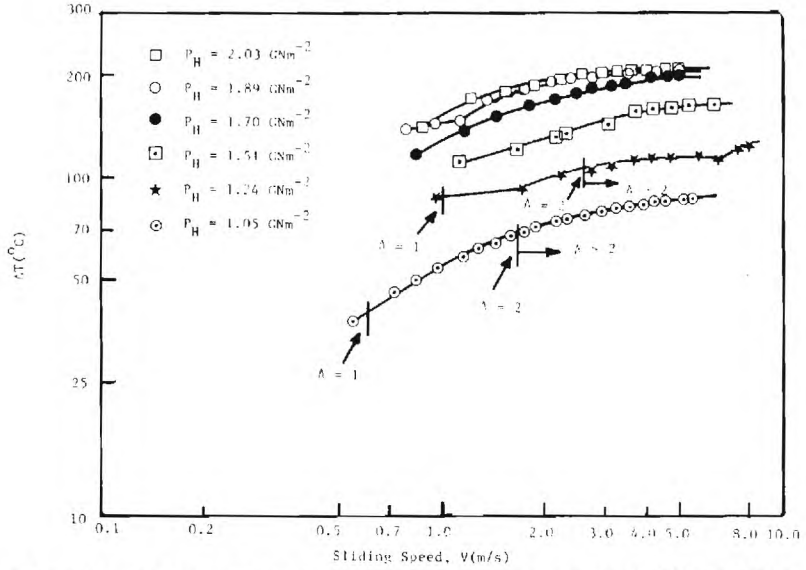

Fig. 6 Ball surface temperatures rise at contact center, medium rough ball (0.076 μm c.l.a.), (Λ < 1, except as noted)

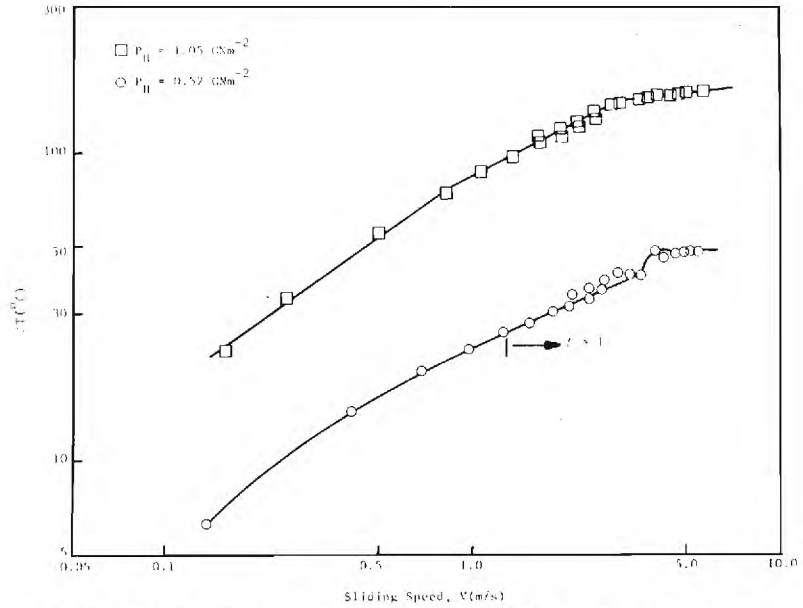

Fig. 7 Maximum ball surface temperature rise, rough ball (0.381 μm c.l.a.) ($\Lambda < 1$ except as noted)

lubricant and surface temperatures just outside the EHD contact are significantly higher than the bath oil temperature due to conduction and inlet heating.

Because it considers conduction as the only heat transfer mechanism, the flash temperature theory should best agree with experimental results at high pressures. In these cases, the ratio of contact length to film thickness is the greatest thereby making conduction more significant. This trend is supported by the data for $P_H = 1.51$ GN/m^2 and 1.05 GN/m^2, in which contact average measured temperatures have been determined. The average deviation between calculated and measured temperatures was 4.8 percent for the 1.51 GN/m^2 data and 17 percent for the 1.05 GN/m^2 data using a Celsius temperature scale.

Surface Roughness Effects

To study the effect of ball surface roughness on surface temperature, AISI 52100 steel balls of various roughness values were used in the EHD contact simulator. In previous studies [7, 8] the center line average roughness of the balls was 0.011 μm. The surface finish of the sapphire in all cases was approximately 0.006 μm c.l.a. Surface profiles of both the ball and sapphire were measured on the profilimeter as described previously.

Figs. 3, 6, and 7 show ball surface temperature rise (difference between ball surface and bulk oil temperature) at the center of the EHD contact as a function of speed and load for the smooth, medium rough and rough balls, respectively. In addition, Fig. 8 shows the temperature data replotted as temperature rise as a function of peak Hertz pressure and sliding speed. In the experiments with the rough ball, the temperature reported is the maximum in the contact, whether or not it occurs at the contact center. It was necessary to make this procedural change because the contact center could not be located when the rough ball was used.

The temperatures reported in Figs. 3–8 are time averaged values, since the infrared detector was operated in the DC mode during these experiments. Under certain operating conditions when asperity interactions are taking place, the instantaneous temperatures developed at the individual asperities may be significantly different from the average values. This subject will be treated in detail in the next section.

The temperatures for the smooth and medium rough balls are only slightly different throughout the range of operating conditions. The surface temperatures for the rough ball appear to be significantly higher than those of the smoother balls. To put all temperatures on an equivalent basis, the rough ball data in Figs. 7 and 8 should be reduced by approximately 10°C. This is the difference between the maximum and center surface temperatures for the smooth ball [9].

The parameter Λ, which is the ratio of EHD film thickness h to the composite surface roughness σ, is a recognized parameter for predicting EHD contact performance [12]. For values greater than 2, no asperity interactions are expected. At Λ less than 1, severe asperity interaction is anticipated. The range $1 < \Lambda < 2$ is a transition region. Surface roughness measurements made on the sapphire and ball

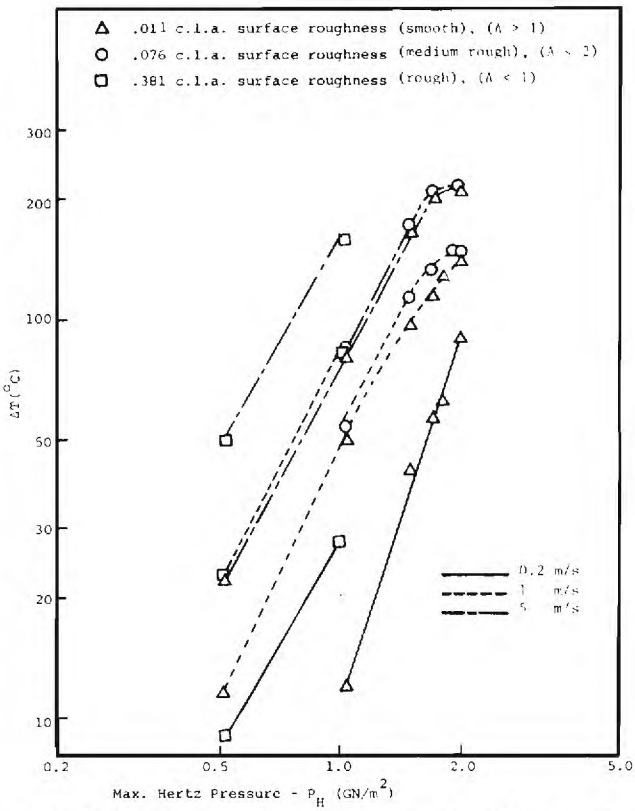

Fig. 8 Ball surface temperature rise versus maximum Hertz pressure

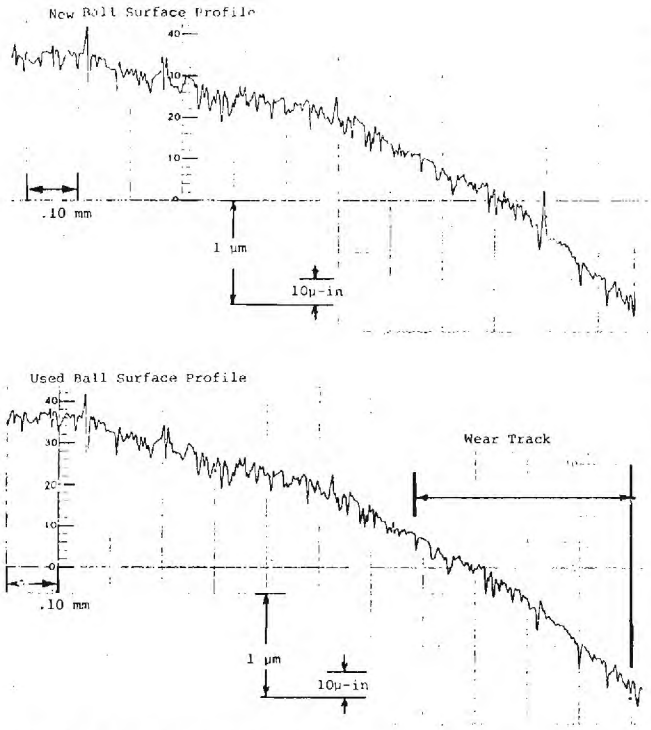

Fig. 9 Relocation profile for the medium rough ball (0.076 μm c.l.a.), P_H = 1.70 GN/m², 0.83 ≤ V ≤ 5.0 m/s)

surfaces in this laboratory are c.l.a. values. The values of Λ obtained using c.l.a. rather than r.m.s. roughness are not sufficiently different that the transition values noted above are significantly altered [12]. Also, in computing the parameter Λ, the film thickness value used is that measured for the smooth ball. This is necessitated for two reasons. First of all the interference fringe pattern used to determine film thickness disappears as the roughness is increased. Secondly, the meaning of film thickness is ambiguous at significantly high roughness levels, since the local thickness changes greatly from point to point. The appropriate Λ values are shown in Figs. 3, 6–8.

In the case of the smooth ball, Λ is greater than 2 for Hertz pressures up to 1.81 GN/m², suggesting no asperity interaction. At P_H = 2.03 GN/m², Λ is in the range 1 to 2. However, a subsequent measurement of the surface profile did not reveal any surface alteration. Experiments using the medium rough ball resulted in $\Lambda < 1$ for $P_H > 1.5$ GN/m² and $1 < \Lambda < 2$ at lower pressures. Moderate to severe asperity interaction is therefore expected at all speeds and loads investigated. A relocation surface profile measurement was obtained and is shown in Fig. 9. At a Hertz pressure of 1.70 GN/m² it can be seen that peaks have been removed in the wear track. For the rough ball, Λ is less than one for all operating conditions. A profile measurement for P_H = 1.24 GN/m² and $V = 5$ m/s is shown in Fig. 10. The removal of asperities is clearly visible on the trace. In addition, the alteration of the surface in the wear track could be visually detected.

The above observations reinforce the importance of the parameter Λ in describing the extent of asperity interaction. In addition, it is now apparent that significant asperity interaction will result in increased surface temperatures. As can be seen from Fig. 9, the method has been successful in relocating the same area on the ball surface for re-examination. However, since it is not practical to obtain profiles of the entire wear tract region before and after running in the EHD contact, an indication of no asperity interaction is inconclusive. Asperity interaction may have taken place at locations other than those measured.

High Frequency Temperature Fluctuations

It has been shown above that asperity interaction can significantly alter the ball surface temperature level. The results given thus far, however, are time-averaged temperatures obtained with the infrared detector in the DC mode. In this mode of operation, the frequency response is 400 Hertz. From the surface profile measurements (Figs.

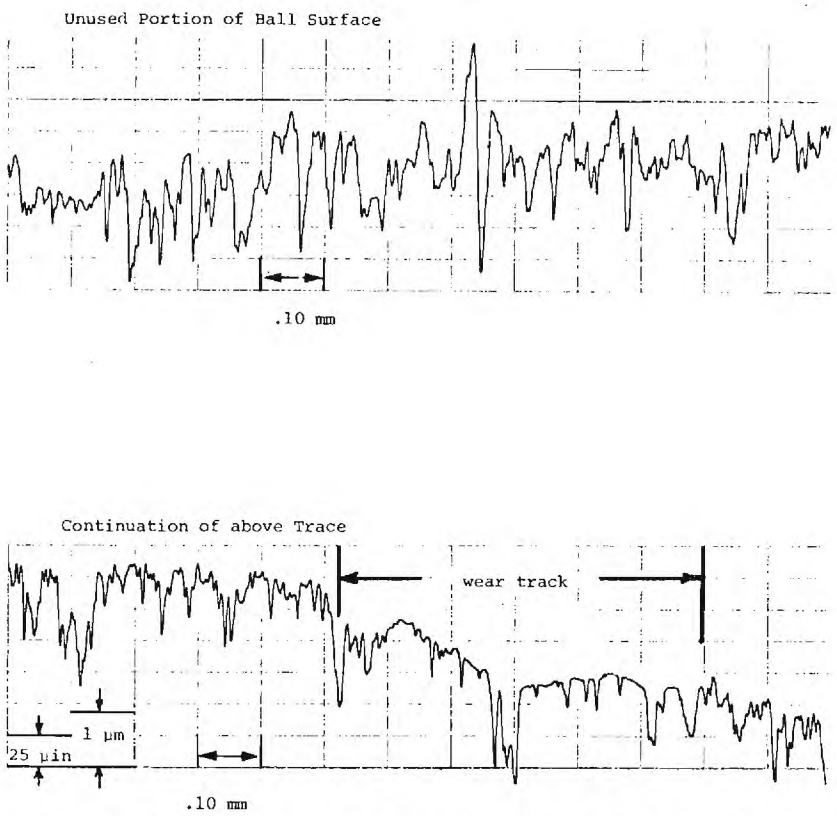

Fig. 10 Surface profile showing severe wear, rough ball (0.38 μm c.l.a.), 1.24 GN/m², 0.5 to 5.0 m/s sliding speed

9, 10) it has been determined that only a single asperity can occupy the detector's field of view (.04 mm diameter) at any one time. However, at 1.0 m/s sliding velocity the asperity resident time in the field of view is only about 40 μs. The DC mode, therefore, cannot respond to a temperature rise caused by a single asperity interaction. The available AC mode of operation, however, can detect such temperature transients. The liquid nitrogen cooled detector has a response time of 8 μs. An important consequence of operating in the AC mode, however, is that the reference signal is absent. Instead, the instrument will produce a voltage difference proportional to the variation in target radiation emitted. Through an independent experiment, using an external chopper, it has been determined that the variation indicated in the AC mode is centered on the signal received in the DC mode. From this information a plot of time-averaged surface temperature along with the maximum and minimum values can be obtained.

Because electrical noise problems were encountered when using the AC mode, a variable frequency electrical band pass filter was also used. Although the noise and signal could not be entirely separated due to the closeness of their frequencies, a pass band of 1.0 to 20 KHz proved effective, since the high peaks in the signal are within 20 KHz for most of the sliding speeds.

Fig. 11 shows a plot of the ball surface temperature at the contact center as a function of Hertz pressure. The .076 μm c.l.a. surface roughness ball was used at a sliding speed of 1.0 m/s. The plot shown was constructed using the DC mode data at five different Hertz pressures. In addition, the AC mode was used at the four highest Hertz pressure levels. As is shown in Fig. 11, the AC data shows no fluctuation about the DC level at $P_H = 1.05$ GN/m^2, but shows an increasing amount of fluctuation as the pressure is increased. The upper and lower curves represent the range of temperatures detected. It is believed that the peak values represent individual asperity interactions. Fig. 11 also shows the significance of the parameter Λ in predicting the onset of asperity interaction.

Upon examination of the AC radiation signal over a time interval of about one ball revolution it was found that the highest radiation emitted from the contact surface was immediately followed by a very low radiation value. This suggests that the high pressure and local energy dissipation at the asperity is causing the high temperature, while the region immediately behind the asperity is a relatively low pressure thick oil film in which the energy dissipation is low, resulting in a lower surface temperature. This reasoning depends on the assumption that the surface emissivity is constant over the region of interest, since radiation fluctuations have been interpreted as temperature fluctuations.

This seems reasonable because even though fresh metal surface is being formed at the asperity tip due to wear. The surface film formation on a fresh surface in an oil environment, which has absorbed oxygen present, occurs in the order of nanoseconds. Therefore, the surface emissivity would not be observably changed on the time scale of the measurements. The radiation fluctuations observed are therefore not affected by fluctuations in emissivity and are in fact due to temperature fluctuations. The generation of wear particles under such operating conditions has been confirmed through a Ferrographic analysis of the used oil samples [9].

Fig. 12 is a graph of the same data, along with data from higher sliding speeds. In all cases, the center value represents the DC (time averaged value). From this data it appears that the range of temperatures detected in the AC mode of operation increases significantly as more of the normal load is supported by individual asperities. This corresponds to a condition of decreasing Λ values. Similar results have been obtained for the case of the rough ball (.38 μm c.l.a.), where the Λ values are much smaller and the magnitude of radiation fluctuations is much greater. For the cae of the smooth ball, where Λ is never less than one, no high frequency temperature fluctuations have been observed.

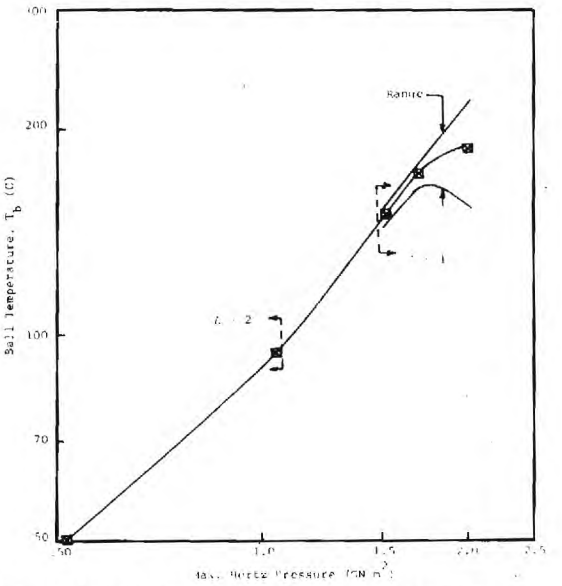

Fig. 11 Average value and range of ball surface temperature fluctuation—medium rough ball (0.076 μm c.l.a.), 1.0 m/s sliding velocity

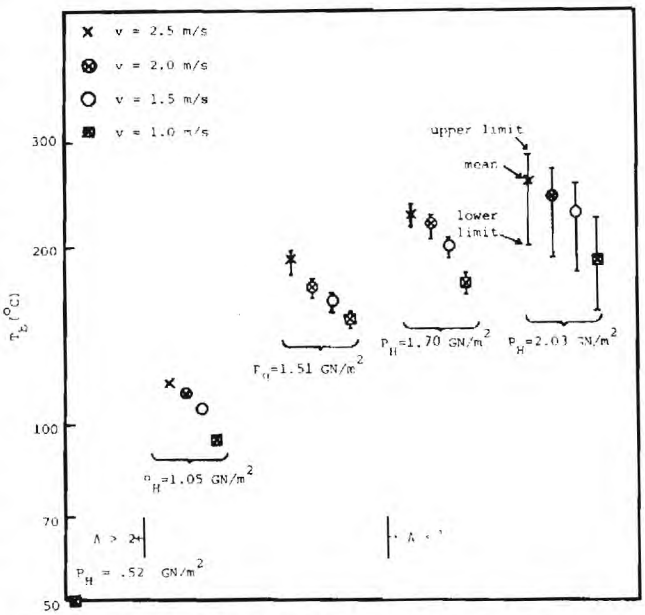

Fig. 12 Average value at range of ball surface temperature fluctuations —medium rough ball (0.076 μm c.l.a.)

Conclusion

Ball surface temperatures, both time averaged and instantaneous, have been measured in a sliding EHD point contact. The temperature levels are in good agreement with those predicted by Jaeger [4] and Archard [5] over a wide range of operating speeds, loads. The validity of the parameter Λ in predicting the onset of asperity interaction has been confirmed through the use of relocation profilimetry and Ferrographic analysis of the oil sample. High frequency flucutations in temperature also accompanied the beginning of this interaction.

Acknowledgments

This research was supported by NASA-Lewis (NGR-11-002-133) and the National Science Foundation (ENG 74-21002). The continuing encouragement of and helpful discussions with Mr. Wm. Jones and Dr. L. Wedeven of NASA-Lewis are greatly appreciated.

References

1 Blok, H., "The Postulate about the Constancy of Scoring Temperature," Interdisciplinary Approach to the Lubrication of Concentrated Contacts (Ed. P. M. Ku), NASA SP-237, 1970.

2 Hirst, W., and Stafford, J. V., "Transition Temperatures in Boundary Lubrication," *Proc. I. Mech. Eng.*, 1972, Vol. 186, pp. 179–192.

3 Blok, H., "Surface Temperatures under Extreme-Pressure Lubricating Conditions," Second World Petroleum Conference, Paris, June, 1937, Vol. 3, Section 4.

4 Jaeger, J. C., "Moving Surfaces of Heat and the Temperature at Sliding Contacts," *Proc. Roy. Soc.* N.S.W., Vol. 56, 1942, p. 203.

5 Archard, J. F., "The Temperature of Rubbing Surfaces," *Wear*, Vol. 2, No. 6, Oct. 1959, pp. 438–455.

6 American Gear Manufacturers Association (AGMA), "Gear Scoring Design Guide for Aerospace Spur and Helical Power Gears," AGMA Information Sheet 217.01 (presented by A. J. Lemanski), Oct. 1965.

7 Carlson, S., Jakobsen, J., Nagaraj, H. S., Molina-C, M. A., Sanborn, D. M., and Winer, W. O., "Investigations of Lubricant Rheology as Applied to Elastohydrodynamic Lubrication," NASA CR-134730, Sept. 1974.

8 Ausherman, V. K., Nagaraj, H. S., Sanborn, D. M., and Winer, W. O., "Infrared Temperature Mapping in Elastohydrodynamic Lubrication," ASME Paper presented at Joint ASME-ASLE Lubrication Conference, Miami Beach, Fla, Oct. 1975, Paper No. 75-Lub-13.

9 Kunz, R. K., Nagaraj, H. S., Sanborn, D. M., and Winer, W. O., "Investigations of Lubricant Rheology as Applied to Elastohydrodynamic Lubrication," NASA CR-134882, Aug. 1975.

10 Sanborn, D. M., and Winer, W. O., "Fluid Rheological Effects in Sliding Elastohydrodynamic Point Contacts with Transient Loading: I—Film Thickness," JOURNAL OF LUBRICATION TECHNOLOGY, TRANS. ASME, Series F, Vol. 93, No. 2, Apr. 1971, pp. 262–271.

11 Sanborn, D. M., and Winer, W. O., "Fluid Rheological Effects in Sliding Elastohydrodynamic Point Contacts with Transient Loading: II—Traction," JOURNAL OF LUBRICATION TECHNOLOGY, TRANS. ASME, Series F, Vol. 93, No. 3, July 1971, pp. 342–348.

12 Bamberger, E. N., et al., "Life Adjustment Factors for Ball and Roller Bearings—An Engineering Design Guide," ASME, New York, 1971.

DISCUSSION

F. F. Ling[3]

I have read the authors' papers with the greatest interest. As usual, this paper contains much valuable experimental information. There are two points which I would like very much to call attention to, however.

The first has to do with the statement in the third paragraph, ". . . The early theory of Blok [3] in 1937 has been put on a rigorous basis . . .". Blok's theory is on a sound foundation, i.e., as much as Jaeger [4]. In other words, it is the straight application of the heat equation.

The second point is that, while there is nothing wrong with equations (3)–(6), it is not necessary to use two sets of equations. (Incidentally, Archard [5] used Blok's work to give the summary paper for the kind of calculations which the authors did.) In other words, there is one equation for the heat partition calculation which is valid for all Peclet numbers.[4,5]

I have done a calculation for the case of $P_H = 1.7\ \mathrm{GN/m^2}$, $v = 1$ m/s and T.C. = .07. ΔT at the center from Fig. 3, as near as I can gather, is 110°C. Pursuing the calculation, and using the average value of P_H, I got 115°C. This, of course, led to a calculated temperature (i.e., with bulk temperature added) at the center of 159°C.

P. M. Ku[6]

The authors have shown that their observed variations of the maximum surface temperature rise, ΔT, with respect to load and sliding speed can be accounted for by the known theoretical behavior of flash temperature. Considering the difficulties of the temperature measurements, the results are certainly gratifying.

The reported effects of surface roughness on ΔT are most welcome and are indeed qualitatively expected. As surface roughness is increased, one expects the friction coefficient, f, to increase, and likewise the frictional power loss, $\phi = fWV$. It is therefore pertinent to ask whether the surface roughness effect shown in Fig. 8, for example, could be quantitatively related to the changes in friction coefficient.

As a matter of some interest, this discusser and associates have examined the behaviors of the quasi-steady surface temperature, T_s (i. e., Blok's "bulk temperature") and the conjuction-inlet oil temperature, T_0, with respect to the frictional power loss, ϕ, of several sliding-rolling systems [13, 14, 15].[7] It has been found that

$$T_s - T_j = C\phi^n$$

and

$$T_0 - T_j = C_0\phi^n$$

where T_j = oil-jet temperature (which is akin to the bath temperature within the context of this paper), and C, C_0, and n are fitting constants. The above relationships appear to hold quite well regardless of disk material, oil type, surface topography, and most operating variables, as long as the actual values of $\phi = fWV$ are used. However, the constants C and C_0 are quite sensitive to system design and the oil flow rate, i.e., they are dependent on the details of the heat transfer process.

Additional References

Carper, H. J., and Ku, P. M., "Thermal and Scuffing Behavior of Disks in Sliding-Rolling Contact," *ASLE Trans.*, Vol. 18, 1975, pp. 39–47.

Ku, P. M., Staph, H. E., and Carper, H. J., "Gear Tooth Scoring Investigation," *USAAMRDL Tech. Rept. 75-33*, July 1975.

Ku, P. M., Staph, H. E., Carper, H. J., and Anderson, E. L., "Lubricant/Metallurgy Interaction Effects on Turbine Engine Lubricant Load Rating," *AFAPL Tech. Rept. 76-27*, Mar. 1976.

G. Paul,[8] A. Cameron,[9] and E. P. Shuttleworth[10]

We have read this paper with interest as it is very similar to work

[3] Professor and Chairman, Department of Mechanical Engineering, Rensselaer Polytechnic Institute, Troy, N. Y. Fellow ASME.

[4] Ling, F. F., and E. A. Saibel, "Thermal Aspects of Galling of Dry Metallic Surfaces in Sliding Contact," *Wear*, Vol. 1, 1957, pp.80–91.

[5] F. F. Ling, *Surface Mechanics*, Wiley-Interscience, Vol. 68, 1973.

[6] Southwest Research Institute, San Antonio, Texas.

[7] Numbers 13–15 in brackets designate Additional References at end of discussion.

[8] Lubrication Laboratory, Imperial College, London, England.

[9] Professor, Lubrication Laboratory, Dept. of Mechanical Engineering, Imperial College, London.

[10] Lubrication Laboratory, Dept. of Mechanical Engineering, Imperial College, London.

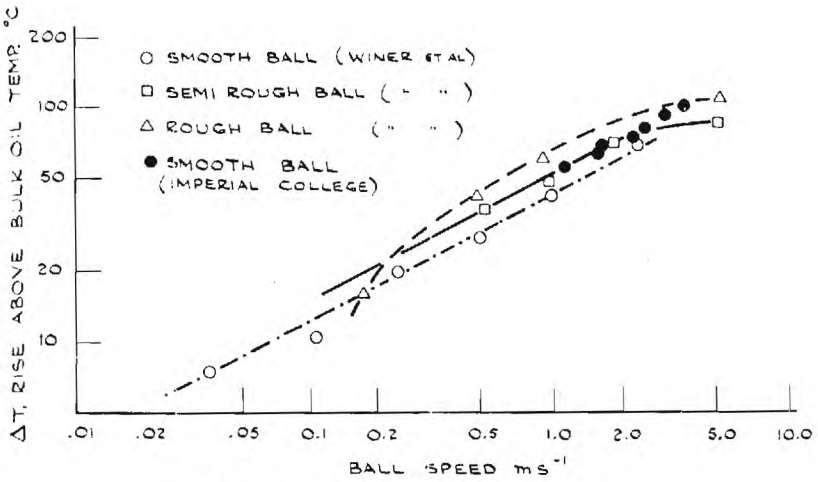

Fig. 13 Ball surface temperature versus sliding speed

that we have been doing. It is found in the paper that the experimental results for the variation of temperature rise with velocity do not correlate with predictions made from Archard's model. This is explained as being due to a variation in traction coefficient with sliding speed and yet, as stated in the text, Table 1 shows that for Hertz pressures above 1.5 G N/m^2 the traction coefficient is essentially constant. We do not understand this apparent contradiction.

In Fig. 13 we have replotted some of the results presented in this paper to compare them with some made at Imperial College. We have subtracted 10°C from the rough ball temperature to get the contact centre temperature. It was stated that over the range of operating conditions the rough ball had a significantly higher temperature than the other two which were essentially the same. The plot does not appear to support this statement. It can be seen that our results fall nicely in the range given in the paper. The oil was a similar type and the reservoir temperature was about 45°C. The ball was optically smooth. It is reassuring that using this difficult technique there is such close agreement between the results.

The high frequency temperature variations are very interesting. We do not quite understand what causes a significant reduction in temperature after an asperity contact. If it were purely an elastohydrodynamic effect leading to a lower pressure it would be present whether or not there had actually been an asperity contact immediately before it. In this case there would be temperature falls at all values of Λ. In practice the temperature troughs shown an even more marked sensitivity to the load than the peaks. Have the authors considered whether or not the emmissivity of these troughs is significantly altered, perhaps by debris deposition or the formation of some form of oxide layer?

Authors' Closure

The authors would like to thank the discussers for their valuable discussion.

The authors agree with Professor Ling that Blok's theory is on a sound foundation. The comment in the paper was to indicate that we felt Jaeger's approach was more systematic. While the equations (3) and (4) can be replaced with a single equation, it was found convenient to represent the trends in the two regimes separately. The sample calculations reported by Dr. Ling are certainly encouraging.

The probable reason for the effect of surface roughness on ΔT is the corresponding change in friction coefficient as suggested by Mr. Ku. However, since the friction coefficients were the experimentally measured values, no attempt was made to include the variation of TC with roughness in the expressions for ΔT. The authors would like to note that the traction coefficient increased appreciably (up to 50 percent) for lambda ratios less than 1 where the asperity interactions are rather severe.

The range .70 to 1.39 m/s for the sliding velocity at 1.51 GN/m^2 peak Hertz pressure in Table 1, is indeed a small fraction of the range indicated in Fig. 13, and therefore the constant value for TC reported in Table 1 should not be misunderstood. In fact, over the full range of speed indicated in Fig. 13, measurements (not reported in the present paper) show an appreciable decrease in traction coefficient with sliding speed.

Paul, et al. in their discussion have indicated that ΔT is not substantially different for different roughness balls with reference to Fig. 13 drawn by them. The authors would like to point out that the dashed line in Fig. 13 for the rough ball (the basis for their conclusion) was plotted incorrectly by them. The ΔT values for the rough ball (at P_H = 1.05 GN/m^2) used in Fig. 13 drawn by the discussers are up to 40C in error. This kind of plotting error invalidates the conclusion made by the discussers. Keeping in mind that the ΔT values are plotted on a log scale in Fig. 13, the correct values of ΔT for rough ball obviously

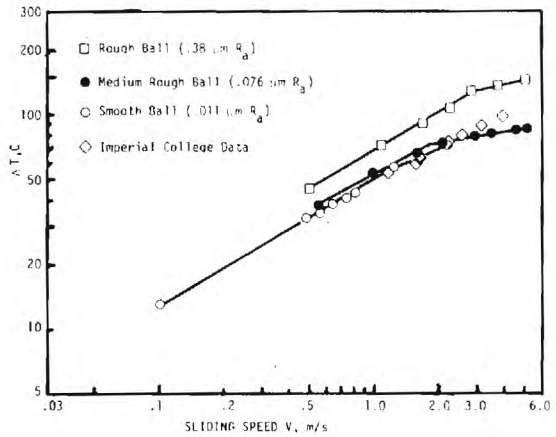

Fig. 14 Ball surface temperature rise at contact center versus sliding speed (P_H = 1.05 GN/m^2)

indicate the effect of surface roughness. Fig. 14 has been prepared using the correct values for ΔT, which shows clearly the effect of surface roughness. Also an earlier figure, Fig. 8 in the paper, indicates that ΔT increases substantially with surface roughness. In fact, in a later work the authors have made correlations of ΔT with the c.l.a. value of surface roughness, and the results are seen to be in excellent agreement with surface roughness factors of the form $1/(1 - .8\sigma)$, where σ is the composite roughness in μm.

Further, it was determined that emissivity fluctuations were not present in the time scale corresponding to the temperature fluctuations. The reasons for this have already been cited in the paper. Similarly, the emissivity of troughs does not change in the time scale of measurements. In the case of a thick elastohydrodynamic film, the local pressure variations are negligible and therefore no temperature fluctuations are observed. However, when the surface asperities touch one another, large local pressure variations and local traction variations do exist and therefore give rise to temperature fluctuations. Calculations of the portion of load carried by fluid pockets were made[11] based on surface statistics, which clearly indicated that a significant load is carried by the asperities at sufficiently low lambda values.

[11] Nagaraj, H. S., Sanborn, D. M., and Winer, W. O., "Asperity Interactions in Partial EHD Contacts," to be published.